FORMATION OF NITRIC OXIDE IN FLAMES

A thesis submitted by

ISABEL MARIA PALMA ALEIXO CABRITA

to the

University of Sheffield

for the

Degree of Doctor of Philosophy

Department of Chemical Engineering
and Fuel Technology,
University of Sheffield.

SHEFFIELD - ENGLAND
- 1 9 8 1 -

PAGE NUMBERS CLOSE TO THE EDGE OF THE PAGE.

SOME ARE CUT OFF

To the memory of my father, whose constant encouragement and support has enabled me to get this far with my education.

SUMMARY

The aim of this work was the investigation of the production of the important pollutant nitric oxide in hydrogen-rich flames in the presence of both nitrogenous compounds and hydrocarbons, and also the effect of the type of hydrocarbon on the mechanism of disappearance of these nitrogenous compounds. The project is thus related to that of ascertaining the mechanism and rate with which a nitrogen compound in a fuel such as coal ultimately ends up as NO or N_2 on combustion. A variety of laminar flames were burned with different $[H_2]/[O_2]$ ratios in the burner supplies, and argon as diluent in such an amount that an adiabatic temperature of 1900 K was reached. Nitric oxide was added to the unburnt gases of these flames in varying amounts. Concentrations of NO were measured with a chemiluminescent NO_x Analyser, whereas those of the cyanides and NH_i species formed were measured with ion-specific electrodes. Disappearance of NO was only observed when hydrocarbons were added to a flame together with the NO, and this decay of NO only took place in the reaction zone, in contrast to the cyano and NH_i species, which were at their highest concentrations in the reaction zone. Nitric oxide was then re-formed downstream with the highest rate of production being near the reaction zone. The initial loss of NO in the reaction zone appeared to be proportional to the number of carbon atoms in a molecule of the hydrocarbon. Downstream, both the cyano pool and NH_i pool decayed; the cyano pool disappeared via $HCN + OH \rightarrow HOCN + H$ or $CN + H_2O \rightarrow HOCN + N$ as the rate-determining steps.

Since NH_i species were formed in flames to which NO and a hydrocarbon were added, in order to have a better understanding of the mechanism of production of NO from NH_i, flames were studied with various $[H_2]/[O_2]$ ratios, temperatures and quantities of added ammonia. The reactions which appeared to determine the production of NO from the various NH_i species formed from NH_3 were

$$N + OH \rightarrow NO + H \quad \ldots\ldots \quad (A)$$

in the reaction zone, and

$$NH_2 + OH \dashrightarrow NO + H_2 + H \quad \ldots\ldots \quad (B)$$

downstream. In addition, NO reacted to form N_2 in:

$$N + NO \rightarrow N_2 + O \quad \ldots\ldots \quad (C)$$

in the reaction zone, and subsequently downstream in one or other of

$$NH_2 + NO \dashrightarrow N_2 + H_2O \quad \ldots\ldots \quad (D)$$

$$NH + NO \dashrightarrow N_2 + OH \quad \ldots\ldots \quad (E)$$

The extent to which reactions (D) and (E) occur depends upon $[H_2]/[O_2]$ ratio in the unburnt gases and the temperature of the flame. The addition of a hydrocarbon to a flame with ammonia in the burner supplies, only seemed to affect the reaction zone, where again a cyano pool was observed.

From the experimental observations, rate constants for reaction (B), which produces NO, were determined. In addition, velocity constants were measured for (D) and (E) as well as for the oxidation of HCN by OH and, CN by H_2O.

ACKNOWLEDGEMENTS

I would like to express my gratitude to my supervisor, Dr. A.N. Hayhurst who has always shown so much understanding and has given me constant encouragement throughout my work.

This study is original unless otherwise stated. I would like to acknowledge the assistance of Professor J. Goodings, particularly with respect to computing problems which arose in my work.

My thanks also go to all the technical staff for their assistance and their "entertainment" in those hours of experimental work. In particular, my sincere thanks are due to Mr. M. Wilde for his photographic work, to Mr. Reynolds for ensuring that I received my equipment when I needed it, and to Mrs. Czerny for typing my thesis.

My sincere gratitude is expressed to the University of Sheffield, which made this work possible by providing me with a Styring Scholarship for two years and three months.

Finally, I would like to acknowledge my husband and my mother who both worked so much that I could devote all my time to this dissertation.

CONTENTS

LIST OF SYMBOLS

$[X]$	-	concentration of X (ppm).
$[X]_0$	-	concentration of X in the unburnt gases (ppm).
$[NH_i]_t$	-	total concentration of NH_i species, (i.e., N, NH, NH_2 and NH_3) (ppm).
$[X]_e$	-	concentration of X at equilibrium (molecules ml^{-1}).
γ	- and γ_H -	ratio of $[H]/[H]_e$.
γ_{OH}	-	ratio of $[OH]/[OH]_e$
t	-	time (ms).
T	-	temperature (K).
T_{ad}	-	adiabatic temperature (K).
u.g.	-	unburnt gases.
b.g.	-	burnt gases.
v	-	velocity (m/s).
Q	-	flow rate (m^3/s).
ρ	-	density (kg/m^3)
D_f	-	diameter of the flame (mm).
x	-	distance from the reaction zone (mm).
R.Z.	-	reaction zone.
K_a	-	equilibrium constant of reaction (a).
k_a	-	rate constant of reaction (a) (molecule, ml, s units).
I	-	intermediate.
NI	-	nitrogenous intermediate.
O_x	-	oxidant.

Remarks:- concentrations which appear in expressions for rate constants, are expressed in molecules per ml.

LIST OF FIGURES

List of Additional Figures Which Appear in Appendix A.

LIST OF TABLES

List of Additional Tables Which Appear in the Appendices.

Table No.

Appendix D.

LIST OF PHOTOGRAPHIC PLATES.

Chapter 1.

Introduction.

There are different classes of pollutants emitted from combustion devices. The levels of such emissions depend upon physical and chemical processes which occur during combustion, as well as the kinetics of formation of these pollutants.

Nitrogen oxides, denoted as NO_x (*i.e.* NO and NO_2)are discharged to the atmosphere from combustion systems. However, their concentrations are quite low. These species are also produced in small quantities in forest fires and lightning; however, high local concentrations are produced by nitric acid plants, *etc.* and can be quite harmful to the environment. Nitric oxide is not known to cause damage directly, but in the atmosphere is converted to NO_2, which is considered a nuisance. For instance, NO_2 has been shown to increase the incidence of respiratory diseases (Shy *et al.* 1970). Some studies have been carried out on the effect of NO_x on plants and animals (Perkins 1974; Enrich & Henry 1968) with the result that NO_x has been blamed partly for lung cancer and the weakness of some mammalian species to resist bacterial infections. One of the dangers of emissions of NO to the atmosphere, is the depletion of ozone in the stratosphere (Sawyer 1972), which allows enhanced penetration by U.V. radiation, thereby raising the occurrence of skin cancer. This extra penetration of U.V. radiation in turn can also affect agriculture, since alterations of surface temperatures might be expected. In fact, NO_x is blamed along with SO_x, for increasing the acidity of rain in North-Eastern U.S.A. and in Scandinavia. Also, once NO_2 is formed, it may react in the atmosphere with hydrocarbons, producing peroxoacyl nitrates (known as PAN) which are lachrymatory.

More attention has been paid recently to NO_x emissions from combustion devices; however, the mechanism of formation of such species is not well understood yet. Reactions involving NO_x take place in an environment established by combustion reactions, although these reactions are not part of the combustion process itself. The two principal sources of NO in the combustion of conventional fuels are:

1. Oxidation of molecular nitrogen in the air supply.
2. Oxidation of nitrogen-containing compounds in the fuel.

The fixation of molecular nitrogen in air occurs at relatively high temperatures, i.e. above 1200^{o} C. Whereas, at temperatures below 1000^{o} C the contribution of fuel-nitrogen to the formation of NO becomes significant. In combustion devices burning crude oil or coal, fuel-nitrogen can be an important source of NO, since significant amounts of organic nitrogen compounds are often present. Mathematical models to explain the formation of NO_x have proved satisfactory in some cases, but they cannot predict its formation in all situations.

Before Lyon and Benn (1973) studied the removal of NO_x from flue gases by reaction with NH_3, no commercial process was used to decrease the quantity of NO_x emitted. The usual way of reducing NO_x in flue gases is either through modifications of the combustion process or alterations of the combustor.

A study of the formation of nitric oxide from fuel-nitrogen in flames was the purpose of this work. Different amounts of NO, NH_3 and hydrocarbons were added to hydrogen-oxygen-argon flames and the concentrations of NO, NH_3 and cyanides were measured along a flame axis. The flames had temperatures in the range 1822-2635 K and were burnt at atmospheric pressure on a Padley-Sugden burner (Padley & Sugden 1958). The reaction zone was flat, and the composition, temperature and velocity profiles in the burnt gases were close to those for plug-flow. Flames were sampled through a water-cooled quartz

probe into a chemiluminescent analyser to determine NO concentrations, and also into aqueous KOH solutions to measure the concentrations of cyano-and NH_i-species, using specific ion electrodes.

Chapter 2.

Formation of NO_x in flames.

2.1 Introduction.

At the present time, of the various atmospheric pollutants, NO_x emissions are increasingly becoming more effective in provoking disturbances and alterations to the environment. As a result, particular attention has been paid to the formation of NO, which is the oxide of nitrogen emitted in greatest quantities at high temperatures. Several workers have studied its formation under varying conditions (Bowman 1975, Hayhurst & Maclean 1974, Iverach & Kirov 1973, Fenimore 1970). There are two sources for the nitrogen in NO emissions from combustion systems: N_2 in the combustion air and nitrogenous species present in the fuel, either in impurities or in the fuel itself, like nitrogenous rocket fuels. The formation and survival of NO depend upon combustion conditions, such as the temperature profile of a flame, the supply of oxygen, rate of quenching, etc. The conversion of fuel-nitrogen to NO was found by Martin & Berkau (Shaw 1973) to be less sensitive to a rise in temperature than the oxidation of molecular nitrogen. Formation of NO appears to be encouraged by high flame temperatures, high oxygen concentrations and high nitrogen-content of the fuel. Survival of NO seems to be encouraged by rapid quenching of the gas to about 1300° C (Shaw 1973). Emission levels in turbulent diffusion flames are also strongly influenced by combustion aerodynamics. This chapter owes much to a review by Hayhurst and Vince (1980).

2.2 Some previous studies of the mechanism of formation of NO.

The mechanism of formation of NO from atmospheric nitrogen has been extensively studied. It is accepted that in the combustion of lean and near-stoichiometric fuel-air mixtures, the Zel'dovich mechanism is important. However, numerous investigators (Fenimore 1971, Iverach *et al.* 1973,

Sarofim 1973, Bachmaier 1973; Iverach 1973, Homer 1973, de Soete 1973, Morley 1975, Haynes 1975) have reported that in the combustion zone, measured rates of formation of NO are significantly larger than that predicted by the Zel'dovich scheme. Near the reaction zone, the rates of formation of NO are considerably greater than in the post-flame zone, with the amount of NO formed in the reaction zone increasing as fuel-air ratio increases. The largest discrepancies between the measured rate of formation of NO and that predicted by Zel'dovich are accordingly observed in fuel-rich flames. In fuel-rich flames a rapid rate of formation of NO by the so-called "prompt NO" route has excited controversial discussions and is discussed below.

2.2.1 The Zel'dovich mechanism.

Molecular nitrogen has a dissociation energy of 941 kJ mol^{-1}, and according to Zel'dovich (1946) it reacts via the following chain mechanism:

$$O + N_2 \rightarrow NO + N \qquad (1)$$

$$N + O_2 \rightarrow NO + O. \qquad (2)$$

Step (1) is universally accepted as the rate-determining step in the formation of NO in the post-flame gases, with a rate constant quoted (Wray 1962, Bachmaier et al. 1973) as approximately $5 \times 10^{13} \exp(-37{,}890/T)$ ml mol^{-1} s^{-1}, correct to a factor of 2. Fenimore & Jones (1957), because of kinetic inconsistencies in N_2O/H_2 flames with additives, suggested that step (2) might be bypassed by the reaction

$$N + OH \rightarrow NO + H \qquad (3)$$

especially in rich flames. Actually the reverse of reaction (3) can become quite important in flames, when the concentration of NO is very high. Steps leading also to the formation of N_2O and HNO have also been discussed (Albers et al. 1975, Duxbury & Pratt 1975), and these have been found quite important in cold, lean, well-stirred flames (Malte & Pratt 1974).

Although measures to minimize emissions of NO_x based on the Zel'dovich mechanism have proved satisfactory, not much success in quantitative predictions of rates of formation of NO has been obtained.

Thomson et al. (1972) were the first in pointing out the importance of supra-equilibrium concentrations of radicals when measuring rates of formation of NO_x in and near the primary reaction zone. These and other workers (Ay & Sichel 1976, Sarofim & Pohl 1973) were able to account for observed rates of formation of NO in a variety of flames, within experimental accuracy, by assuming rapid balancing of radical inter-conversions (Bulewicz et al. 1956). Huller et al. (1973) and Malte & Pratt (1975) have also validated the extended Zel'dovich mechanism; however, levels of NO have been consistently found in excess of such predictions (Fenimore 1971, Iverach et al. 1973, Bowman et al. 1973, Malte et al. 1974, Vince 1974, Malte & Pratt 1975). In turbulent diffusion flames, the excess levels of NO have been attributed to temperature fluctuations (Gouldin 1974, Moss & Bray 1975), because the rate-determining step of the Zel'dovich mechanism is highly sensitive to temperature. Also in studies carried out of a swirling turbulent diffusion flame of methane in air, Sadakata and Beér (1977) observed the rate of formation of NO in the main reaction zone to be faster than that provided by the Zel'dovich mechanism.

Recently, amounts of NO_2 representing as much as 30% of NO_x emissions have been found from gas turbines (Cernansky & Sawyer 1975, Schefer & Sawyer 1977). Cernansky & Sawyer (1975) suggested a plausible scheme for NO_2 production from NO in turbulent diffusion flames, based on a temporary co-existence of high radical concentrations, high $[O_2]$ and relatively cold conditions. Also Fenimore (1975) found in the reaction zone values for $[NO_2]/[NO]$ greater than the equilibrium ratio, when adding NO to lean premixed flames of CO and/or H_2 in air. However, this ratio fell to

approximately the equilibrium one in the post-flame gases. Any reasonable scheme leading to the formation of NO_2, involves NO molecules as reactant. However, it now seems clear that in most flames, the NO_2 found in the gases is formed during sampling.

The Zel'dovich mechanism so far, has been found frequently unsatisfactory in predicting the high rates of formation of NO in the reaction zone and the final emissions of NO from hydrocarbon flames.

2.2.2 Prompt NO.

The Zel'dovich mechanism often predicts lower NO-formation rates than those observed, and extensions of the basic system allowing for supra-equilibrium [O], temperature fluctuations and various nitroxy compounds do not always explain the experimental observations. This was discussed in the previous section. Fenimore (1971) observed that extrapolating linear or almost linear experimental [NO] profiles to a time zero, for hydrocarbon-air flames burned on a flat burner, produced a positive intercept. This led to the idea of a rapid formation of NO in the reaction zone, in addition to that of the Zel'dovich mechanism. This rapid formation of NO he labelled as "prompt NO". The Zel'dovich mechanism alone could not account for variations of the above-mentioned intercept with the type of fuel, temperature, pressure and stoichiometry. Since this was not observed in flames without hydrocarbons, Fenimore (1971) postulated that NO arises from an attack by a hydrocarbon fragment on molecular nitrogen. Many investigators (Burdett & Hayhurst 1977, Malte & Pratt 1975, Takagi et al. 1975, Iverach et al. 1973) have confirmed the distinction between flames with and without hydrocarbon. Reaction (1) is highly endothermic and Fenimore found prompt NO weakly temperature dependent. This was also confirmed by studies made by De Soete (1975) and Hayhurst & Vince (1977). In addition Fenimore (1971), Eberius et al.

(1977) and Heberling (1975), studying the dependence of prompt NO levels upon pressure, found that the Zel'dovich mechanism alone could not explain the experimental observations. At the same temperature, the levels of prompt NO in fuel-rich flames have been found higher than those in lean or stoichiometric flames (Ay & Sichel 1976, Malte et al. 1974, Iverach et al. 1973, Fenimore 1971).

Some of the assumptions made by Fenimore when studying "prompt NO" may not be correct: first he considered that the tips of the flame-lets of the flat-flame burner corresponded to the flame front, and this can be a source of error in the determination of residence times. This error will be more significant close to the flame front and the concentration of NO can then be greatly overestimated. Secondly, he considered oxygen atoms to be in equilibrium. Near the reaction zone this is clearly doubtful; it leads to a significant curvature in the [NO] profile near the reaction zone if only the Zel'dovich mechanism operates and in part it will account for the intercept observed by Fenimore (1971). However, the above information from studies carried out by other investigators supports the evidence that a pathway, distinct from the Zel'dovich reactions for the formation of NO, is the attack of a hydrocarbon fragment on a nitrogen molecule in the flame front. How much of the intercept is truly prompt is a question which can be put forward; Sarofim & Pohl (1973) studying premixed methane flames concluded that supra-equilibrium O atom concentrations could account for all the intercept, except possibly in very rich flames. However, several workers have measured both local temperatures and [O] and concluded that the Zel'dovich mechanism was inadequate. This same conclusion was drawn by Blauwens et al. (1977) in studies made on lean ethylene flames. Bowman & Seery (1971) did not find any evidence for prompt NO in shock tube studies; however, as

Iverach et al. (1973) quote, the high temperatures in such studies could have a masking effect. Bowman et al. (1973) have found evidence for prompt NO in a jet-stirred reactor. Studies carried out by Eberius et al. (1970), Blauwens (1977), Miyauchi (1977), Peeters (1973) and Hayhurst and coworkers (1974, 1977) led to the elucidation of the kinetics of various reactions, which could be involved in the formation of "prompt NO". Actually, the response of prompt NO to variations in temperature and stoichiometry in the work carried out by Hayhurst and co-workers was as expected from Fenimore's work (1971).

In various studies (Bachmaier et al. 1973, Haynes et al. 1975, Morley 1976, Takagi et al. 1975, Peeters & Vinckier 1975, Miyauchi et al. 1977, Blauwens et al. 1977) cyano-species like CN and HCN, believed to be intermediates, were actually identified and measured in flames. These investigations only revealed cyano-species in hydrocarbon flames. Haynes (1975) observed that the maximum [NO] intercept actually coincided with the highest initial rate of decay of HCN. The amount of HCN, corrected for N_2 and hydrocarbon concentration, was found by Morley (1976) to be nearly independent of temperature and fuel type. However, there is some controversy about the mechanism of formation of HCN from N_2, due to there being so many short-lived hydrocarbon radicals which could attack N_2 with incompletely known kinetics and the fact, that $CH_i + H \rightarrow CH_{i-1} + H_2$ is possibly in equilibrium in the reaction zone in a hydrocarbon flame. This last point is illustrated by the study made by Peeters & Vinckier (1975). Hayhurst & Vince (1977) observed in their work that the amounts of prompt NO formed were proportional to $[N_2]$, the quantity of hydrocarbon added and number of atoms of carbon in a molecule of the hydrocarbon additive. Consequently, Hayhurst & Vince (1977) concluded that CH and CH_2 were the only plausible candidates for reaction with N_2. Morley

(1976) opted for CH and obtained a rate constant for $CH + N_2 \rightarrow HCN + N$ ($\Delta H = 9$ kJ mol^{-1}) of the same order of magnitude as that obtained from room temperature flash photolysis (Braun *et al.* 1967), *i.e.* 2.4×10^{-14} ml $molecule^{-1}$ s^{-1} at *ca.* 2400 K. However, Miyauchi *et al.* (1977), in their study, found an almost quantitative agreement between predictions and results, by considering HCN to be formed in $CH_2 + N_2 \rightarrow HCN + NH$ ($\Delta H^{o} = 88$ kJ mol^{-1}). No distinction between the above two reactions was reported by Blauwens *et al.* (1977), but Benson (1977) has argued for a predominance of CH radicals attacking N_2. Eberius *et al.* (1975), adding HCN to low pressure flames, found that this compound disappeared and reappeared again. They suggested that such behaviour could be due to the formation of an intermediate before HCN is formed, but HCN could well be suffering pyrolysis before entering the reaction zone.

2.2.3 The production of NO from fuel-nitrogen.

In several recent experimental investigations of NO from combustion devices, nitrogen-containing compounds in the fuel were found to be an important source of NO. The nitrogen content of fossil fuels can vary considerably. During distillation, the fuel-nitrogen is concentrated in the higher boiling fractions, and it is for these fuels that fuel-nitrogen is most important as a potential source of NO. In distillate fuels, the fuel-nitrogen can exist as amines and ring compounds (*e.g.*, pyridine, quinoline and carbazoles). The nitrogen content of most coals ranges from 1 to 2% by weight. During combustion of distillate fuels or coal, organic compounds present in the fuel will very likely undergo thermal decomposition before entering the combustion zone. Consequently, the intermediates for NO formation will, in general, be low molecular weight nitrogen-containing compounds (e.g., NH_3, NH_2, HCN, CN, *etc.*) (Bowman 1975).

Although experimental studies have been made of the combustion of many nitrogen-containing compounds, very little detailed information on the kinetics of formation of NO from these compounds has been obtained. Existing data indicate that the oxidation of many nitrogen-containing compounds to NO is rapid, occurring in a time scale comparable to that of combustion reactions.

In the vicinity of the reaction zone, observed NO concentrations from fuel-N_2 significantly exceed their equilibrium values. In the post-combustion zone, the NO concentration decreases, relatively slowly for fuel-lean mixtures and very rapidly for fuel-rich mixtures as found by Haynes (1977), Fisher (1977), Fenimore (1978),Fenimore &Jones (1961), Fenimore (1976), Cernansky & Sawyer (1975), Haynes et al. (1975) and Hayhurst & Vince (1977). The amount of fuel-nitrogen converted to NO is particularly sensitive to the fuel-air ratio. Relatively high NO yields are found for rich mixtures, these being only slightly dependent upon temperature, contrasting with the strong dependence upon temperature of NO formation from molecular nitrogen in the air supply. Several investigators have proposed mechanisms (Fenimore 1976, De Soete 1975, Haynes, Iverach & Kirov 1975). Fenimore and De Soete have proposed one, in which the primary fuel-nitrogen compound reacts to form an intermediate (e.g., HCN, CN, NH_2, NH, N). The initial step may involve pyrolysis of the compound or reaction with the fuel or even with a fuel fragment. Then the nitrogen intermediate reacts via two competitive reaction paths. If the intermediate reacts with oxygen-containing species, it will form NO, and, if it reacts with NO or another nitrogenous intermediate will give N_2. Based on experimental observations, NO formation and the combustion process occur on a similar time scale and it is usually assumed that reactions involving nitrogen-containing radicals are sufficiently rapid,

for their concentrations to be in equilibrium relative to one another very early in the reaction scheme. This partial equilibrium assumption simplifies greatly the calculation of NO yields, since the number of kinetic equations required to describe the fuel-nitrogen conversion process is greatly reduced.

A typical plot for [NO] and [HCN] profiles along a flame without additive is shown in Fig.2.1 (Haynes et al. 1974). The concentration of NO increases sharply near the reaction zone and then is approximately constant, whereas [HCN] has its maximum also near the reaction zone, decaying downstream, in contrast with [NO]. The amount of hydrocarbons in the flame decays along the flame. Flagan, Galant and Appleton (1974) have studied NO formation in lean mixtures. They assumed the fuel-nitrogen to be distributed in equilibrium proportions amongst all the possible single N-atom - containing species, except that they excluded N atoms and oxidised N, i.e., NO, HNO, NO_2, etc. denoted as RNO. They considered the following reactions:

$$NH + O \rightleftharpoons N + OH \quad (4)$$

$$NH + H \rightleftharpoons N + H_2 \quad (5)$$

$$NH + OH \rightleftharpoons N + H_2O \quad (6)$$

$$NH + O \rightarrow NO + H \quad (7)$$

$$N + O_2 \rightarrow NO + O \quad (8)$$

$$N + OH \rightarrow NO + H \quad (9)$$

Reactions which could also affect the production of NO are those yielding N_2, N_2O, N_2H, such as:

$$N + NO \rightarrow N_2 + O \quad (10)$$

$$NH + NO \rightarrow N_2O + H \quad (11)$$

$$N + NH \rightarrow N_2 + H \quad (12)$$

$$NO + NO \rightarrow N_2O + O \quad (13)$$

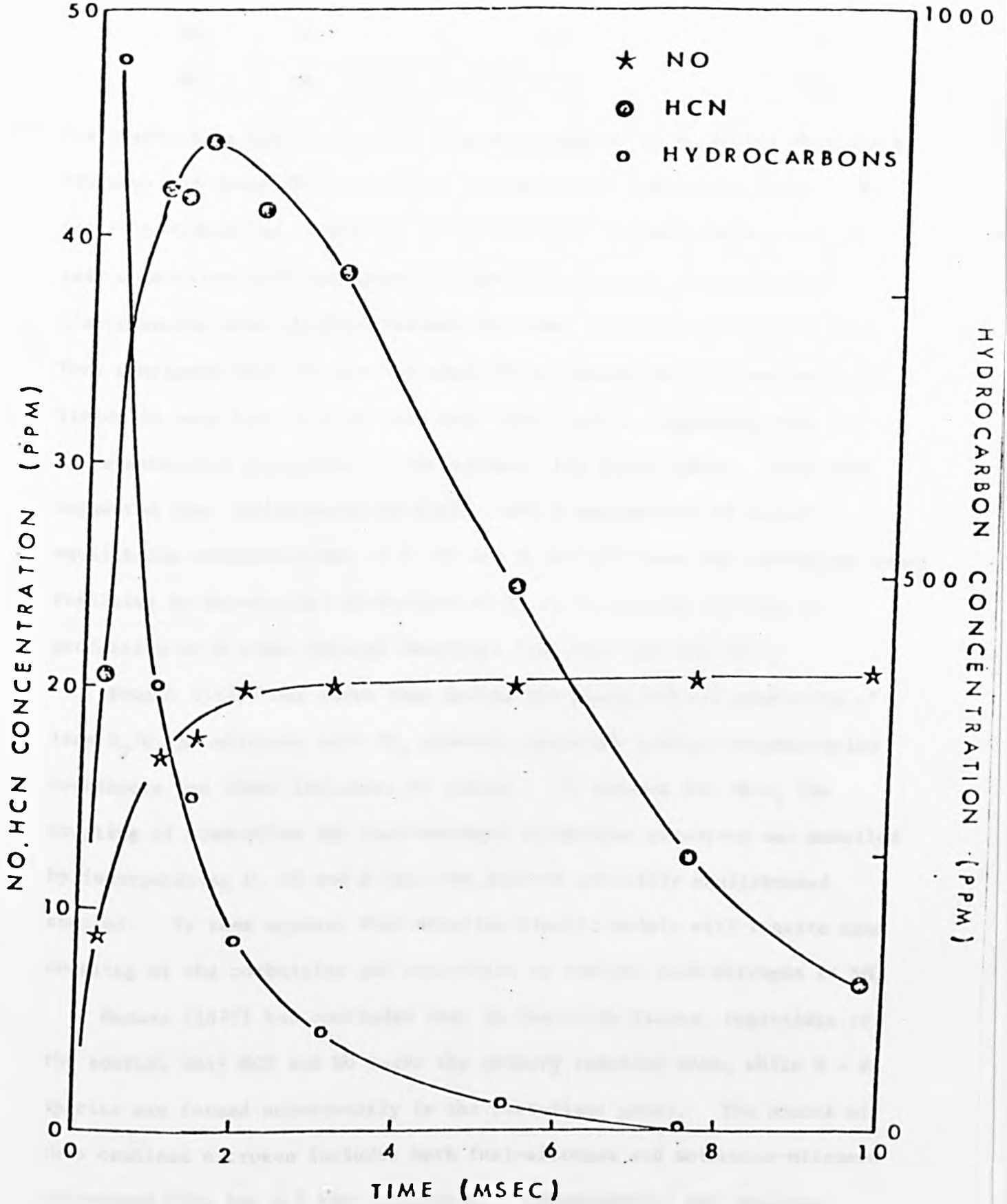

Figure 2.1 : Measured profiles of NO, HCN and hydrocarbons in an ethylene-air flame, ϕ = 1.64, T = 2040K. (Haynes et al. 1974).

$$NH_2 + NO \rightarrow N_2 + H_2O \qquad (14)$$

$$NH + NH \rightarrow N_2H + H \; . \qquad (15)$$

The predictions appear to agree with measurements of NO yields obtained by Fenimore and Jones (Fenimore 1972, Flagan, Galant & Appleton 1974). But for rich combustion conditions at artificially reduced temperatures or lean combustion with excessively large fuel-nitrogen concentrations, discrepancies were obtained between the model and the experimental data. They concluded that the partial equilibrium assumption over-estimates NO yields in very fuel-rich or very fuel-lean flames, suggesting that the above-mentioned assumption is not adequate for these cases. They also suggested that the measured NO yields were a consequence of supra-equilibrium concentrations of O, OH and H radicals near the combustion zone, resulting in accelerated production of NO by increasing the rate of production of N atoms through reactions like (4), (5) and (6).

Bowman (1975) has shown that during the shock-induced combustion of lean $H_2/O_2/Ar$ mixtures with NH_3 present, there are radical concentration overshoots and these influence NO yields. To account for this, the coupling of combustion and fuel-nitrogen conversion processes was modelled by incorporating O, OH and H into the pool of partially equilibrated species. It then appears that detailed kinetic models will require some coupling of the combustion and conversion to convert fuel-nitrogen to NO.

Haynes (1977) has concluded that in fuel-rich flames, regardless of the source, only HCN and NO leave the primary reaction zone, while N - H species are formed subsequently in the post-flame gases. The source of this combined nitrogen includes both fuel-nitrogen and molecular-nitrogen introduced with the air for combustion. Consequently, the reaction scheme is the following:

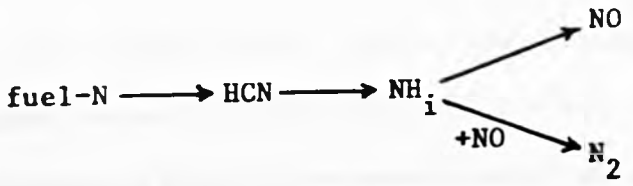

The general veracity of this reaction scheme has been supported by Fenimore (1976) but there is disagreement about the mechanism of N-H bond formation from HCN. Of all the reactions involving NH_i (i.e. N, NH, NH_2, NH_3) which lead to the formation of NO, the best known is: $N + OH \rightarrow NO + H$. Reactions of NH and NH_2 with O atoms have been proposed, but the low concentration of O atoms makes these reactions relatively unimportant. Also, interactions between NO and NH_i were proved to be fast, e.g. in (10), (14) and $NH + NO \rightarrow N_2 + OH$. Having more than one NH_i species, it is important to consider them in some detail.

Kaskan and co-workers (1973) reported that the following reactions can be important:

$$NH_3 + OH \rightleftharpoons NH_2 + H_2O \qquad (16)$$

$$NH_3 + H \rightleftharpoons NH_2 + H_2 \qquad (17)$$

$$NH_2 + OH \rightleftharpoons NH + H_2O \qquad (18)$$

$$NH_2 + H \rightleftharpoons NH + H_2 \qquad (19)$$

which they thought to be rapidly equilibrated in the burnt gases. Also, reactions can be established involving NH species such as the following ones:

$$NH + OH \rightleftharpoons N + H_2O$$

$$NH + H \rightleftharpoons N + H_2$$

A possible complication for this scheme would be reactions between NO and hydrocarbon radicals, as well as NH_i species with the same radicals. The occurrence of this would invalidate the mechanism discussed above, so that in the presence of hydrocarbons, further modifications may be required to allow for reactions of these hydrocarbon species with NO and NH_i.

Mulvihill and Phillips (1975) studied the breakdown of cyanogen in a flame of unburnt composition $[H_2]/[N_2]/[O_2] = 4.5 / 8 / 1$. They found that C_2N_2 was converted into approximately equal amounts of HCN and a mixture of CO and CO_2 during its passage through the reaction zone. As a result the main primary reaction

$$H + C_2N_2 \rightarrow HCN + CN \qquad (20)$$

is considered to be followed by reaction (21) rather than (22)

$$CN + O_2 \rightarrow NCO + O \qquad (21)$$

$$CN + H_2 \rightarrow HCN + H \qquad (22)$$

and NCO reacts further to give:

$$NCO + O \rightarrow CO + NO \qquad (23)$$

$$NCO + H \rightarrow CO + NH \qquad (24)$$

In this study a low yield of NO was observed when C_2N_2 was introduced alone, and a consumption of NO in the reaction zone when C_2N_2 and NO were introduced together. This was attributed to : NH + NO → products, because the main alternative:

$$CN + NO \rightarrow N_2 + CO \qquad (25)$$

was proved to be too slow to account for the removal of NO at the operating temperature. They also found theoretical concentration profiles agreeing with the experimental observations.

Morley (1975) concluded in his study that the amount of HCN formed did not depend upon the source of nitrogen and that it varied linearly with the amount of fuel-nitrogen. The amount of NO converted from fuel-nitrogen was found to fall with increasing nitrogen concentration, decreasing temperature and increasing fuel-air equivalence ratio, and the rate of disappearance of HCN was independent of the amount of fuel nitrogen added to the flame.

For flames above 2530 K and 2 or 3 mm after the burner exit, the disappearance of HCN was first order, this rate being faster for cooler flames, closer to the reaction zone. Morley's proposed mechanism is:

$$HCN + H \rightleftharpoons CN + H_2 \quad (26)$$

$$CN + CO_2 \rightleftharpoons NCO + CO \quad (27)$$

$$NCO + H \rightleftharpoons CO + NH$$

$$NCO + H_2 \rightleftharpoons CO + NH_2 \quad (28)$$

$$CN + OH \rightleftharpoons NCO + H \quad (29)$$

with reaction (29) fitting the results much better than the alternative process (27), which was rejected.

Merryman and Levy (1975) studied methane flames with and without nitrogen-containing compounds, and their data, based on detailed NO and NO_2 profiles, indicated the following reactions:

$$NH + O_2 \rightarrow NO + OH \quad (30)$$

$$CH + O_2 \rightarrow CO + OH \quad (31)$$

$$NO + HO_2 \rightarrow NO_2 + OH \quad (32)$$

$$NO_2 + O \rightarrow NO + O_2 \quad (33)$$

They detected NH and CH, with NO being rapidly consumed in the visible flame by HO_2 radicals, and NO_2 being formed. They found in their flames that reaction (33) could not account for all the NO produced, so that other reactions, such as those in the Zel'dovich scheme and Fenimore's prompt NO mechanism take place. The same investigators measured the amount of NO_2 consumed in (33) and found that in fuel-rich flames a 100% conversion to NO was observed, whereas for oxygen-rich only 60% of NO_2 was converted to NO. They could not explain this possibly odd observation, attributing it, amongst other things, to an equilibrium condition.

Tagaki et al. (1979) have recently studied the formation of nitric oxide from fuel-nitrogen in staged combustion. Apart from the formation of NO, HCN and NH_i in the first stage, these workers also investigated the effects of operating conditions (equivalence ratio, temperature, types and amounts of fuel nitrogen) on the production of NO. Takagi et al. (1979) concluded that HCN was not formed in non-hydrocarbon flames, in contrast with those with hydrocarbon. This seems to agree with what Fenimore (1971) observed in the formation of prompt NO. The conversion of HCN into NO was much larger in the second stage of combustion than that of NH_3. Fig.2.2 shows the effect of the equivalence ratio on the formation of NO, HCN and NH_3 in the first stage of combustion. In fuel-lean flames the main nitrogen compound formed is NO, and its amount increases with the addition of fuel nitrogen; in richer mixtures, [HCN] and [NH_3] increase and lower [NO] is found, until [NO] becomes independent of the content of fuel-nitrogen. However, HCN and NH_i do not reach a saturation point, as does nitric oxide. The effect of temperature is shown in Fig.2.3 for the first stage of combustion. With both stages of combustion, NO emission was significantly less than with the single-stage combustor, for the same total equivalence ratio of 0.8. The formation of NO was minimized at ϕ = 1.3 - 1.4 for the first stage; this same value for ϕ was found by Martin et al. (1977). Above that value for ϕ, the increase in [NO] was suggested as being due to the high conversion of HCN and NH_3 in the first stage of combustion. These investigators also observed that [NO] decreased with temperature after the second stage of combustion, which is due to lower rates of conversion of HCN and NH_3 to NO. In two-stage combustion, compared with a single stage combustor, no saturation in [NO] was observed for increasing amounts of fuel-nitrogen. Tagaki et al. (1979) believed that this was due to the fact that more HCN

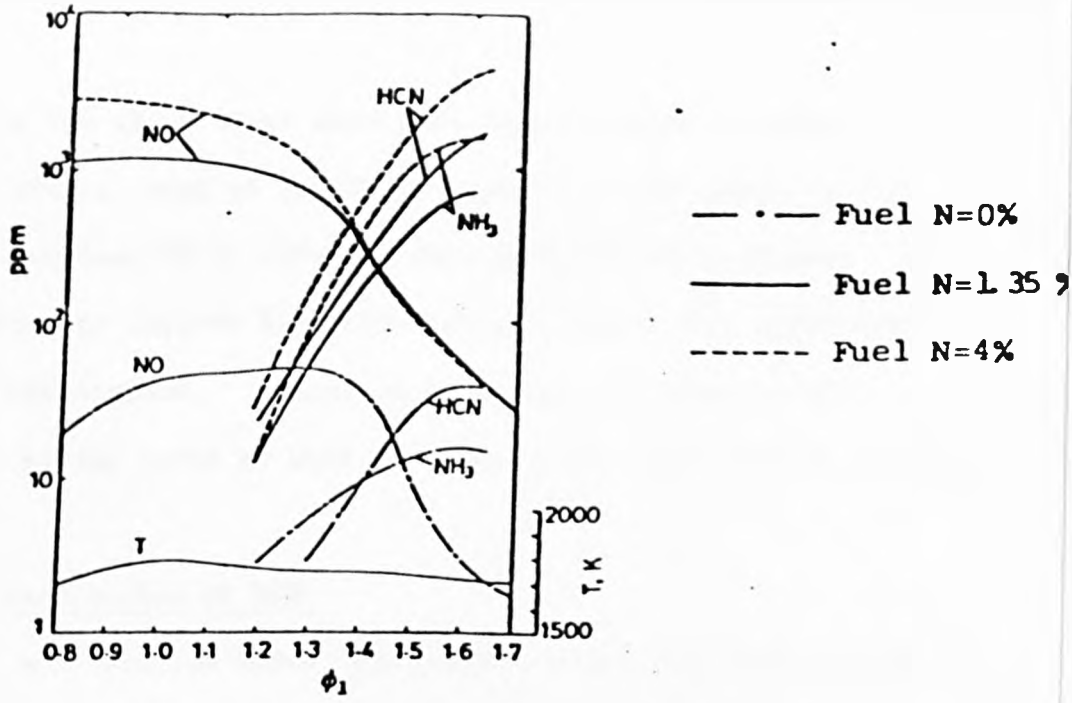

Fig.2.2 Concentrations of NO, HCN and NH_3 vs. equivalence ratio in first stage combustion (burning velocity = 14.7 cms^{-1}) from Takagi et al. (1979).

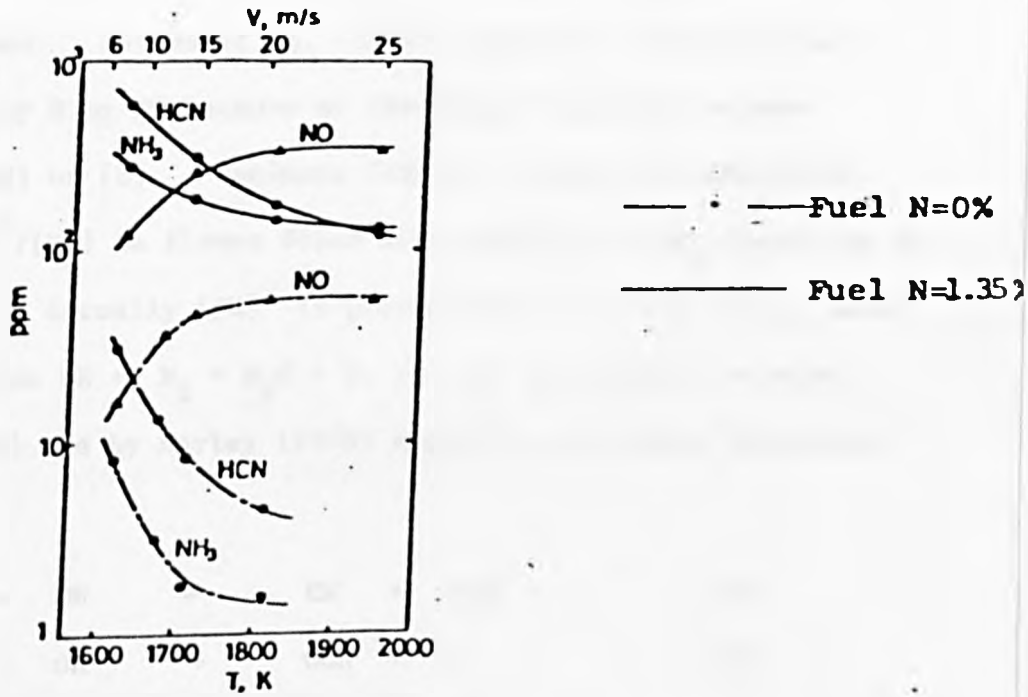

Fig.2.3 Concentrations of NO, HCN and NH_3 against temperature of the burnt gases in first stage combustion from Takagi et al. (1979).

and NH_3 is formed in the first stage when more fuel-nitrogen is added. In non-hydrocarbon flames, most of the NO is formed from NH_3 added in the second stage and a lot less NO is obtained than in hydrocarbon flames. This is the main difference in fuel-NO formation between flames with hydrocarbon and flames without hydrocarbon. Mixing of secondary air promotes NO formation. Higher mixing rates as well as higher temperature result in more NO.

2.2.4 The destruction of HCN.

Cyano species, as discussed above, are always formed when hydrocarbons and any nitrogenous species, either molecular nitrogen from air or compounds containing chemically bonded nitrogen, are present in flames. Cyano species do not seem to form NO directly under flame conditions, although $CN + O_2 \rightarrow NO + CO$ has been documented (Basco 1965) after room-temperature flash photolysis. HCN and CN are usually assumed balanced in a flame (Boden *et al.* 1968), so that both could be plausible routes of disappearance of cyano species and they are the only likely ones, since C_2N_2 involves termolecular collisions. Haynes *et al.* (1975) suggested a direct attack on HCN or CN, either by H or OH because of the proportionality between $-d(\ln[HCN])/dt$ and [OH] or [H]. Fenimore (1976), finding $-d(\ln[HCN])/dt$ proportional to $[H_2O]^2/[H_2]$ in flames doped with pyridine or NH_3 opted for an attack by H_2O on HCN. Actually $[OH]^2$ is proportional to $[H_2O]^2/[H_2]$, owing to the balanced reaction $OH + H_2 = H_2O + H$, so that the results obtained both by Fenimore (1976) and by Morley (1976) might be considered indistinguishable, *i.e.*

$$HCN + OH \rightleftharpoons CN + H_2O \qquad (34)$$

$$CN + OH \rightarrow OCN + H \qquad (35)$$

$$OCN + H_i \rightarrow CO + NH_i$$

with reaction (35) as the rate-determining step. Considering various studies (Hayhurst & McLean 1974, Davies & Thrush 1968, Bullock & Cooper 1972, Mulvihill & Phillips 1975, Rentzepis 1964), it appears that temperature is possibly the main factor deciding which species attacks the cyano pool. In Mulvihill and Phillips' work (1975), at 1500 K the oxidant reacting with CN is O_2, Morley's (1976) is OH at 2500 K, and Haynes et al. (1975) found CO_2 as the most likely candidate within the temperature range (ca. 1300 - 2400 K). However, Haynes[2](1977) subsequently proposed an alternative scheme for fuel-rich flames: HCN + OH → HOCN + H, or a kinetically equivalent process, for 1950 - 2300 K. Fenimore (1978) concluded also that the disappearance of HCN was first order in both HCN and OH. According to Haynes (1977) and Morley (1976), possible sequences for the disappearance of cyanates formed from the cyano-pool decay, are:

$$\begin{aligned} &OCN + H_2 = HCNO + H \\ &HNCO + H \rightarrow NH_2 + CO \qquad (36) \\ &HOCN \rightarrow HNCO \xrightarrow{+H} NH_2 + CO \\ &OCN + H \rightarrow NH + CO \end{aligned}$$

so that NH_i species are formed.

2.2.5 The role of NH_i species in the post-flame gases.

NH_i species may react either with hydrocarbon fragments (Safrany 1964, 1969) or with an oxidant, forming NO, or even with NO itself, forming N_2. In the absence of hydrocarbons, NH_i species alone account for the formation of NO and N_2, via the following scheme (Haynes et al. 1975, Morley 1976, Fenimore 1976):

$$NI + O_x \rightarrow NO + \ldots \qquad (37)$$

$$NI' + NO \rightarrow N_2 + \ldots \qquad (38)$$

where O_x is an oxygen-containing species and NI and NI' are nitrogenous intermediates, which can consist of one or more of the NH_i species. NI and NI' need not be identical (Seery 1977, Haynes 1977), since NH_i species are interconvertible by reactions like

$$NH_i + (O)H = NH_{i-1} + H_2(O).$$

The rates of these reactions in the NH_i - pool are comparable to those of ammonia (Kaskan & Hughes 1973). Reaction (38) is notable in being the only one which yields a reduction in pollutant levels.

2.2.6 Final considerations in the production of NO in flames.

Cyano species, as well as NH_i species, have been found in the burnt gases of flames with hydrocarbons and, since cyanides are as noxious as NO_x, rich hydrocarbon flames should be avoided. Nitric oxide can also undergo destruction reactions in flames, especially if CH_i and NH_i species are present. The following list includes several possible reactions with reasonably low activation energies.

CH	+	NO	→	HCO	+	N	(39)
CH	+	NO	→	HCN	+	O	(40)
HCN	+	N	→	N_2	+	CH	(41)
HCN	+	NO	→	N_2	+	HCO	(42)
NH	+	NO	→	N_2	+	OH	
NH_2	+	NO	→	N_2	+	H_2O	
N	+	NO	→	N_2	+	O	
NH_i	+	CH	→	HCN	+	H_i	(43)
NH_i	+	NH_i	→	N_2	+	H/H_2.	(44)

Myerson (1975), using a flowing system of simulated combustion effluents succeeded in destroying up to 90% of the NO present by adding controlled

amounts of mixtures of hydrocarbon and oxygen. The most critical parameter was the hydrocarbon/oxygen ratio. Yamagishi et al. (1975) studied the dependence of ([NO] + [HCN] + [NH_3]) on equivalence ratio (Ø), reducing it from 50 ppm for Ø = 1.4 to 3 ppm for Ø = 2.0. The peak concentration of HCN occurred at Ø = 1.7. Iverach et al. (1973) achieved a decline in [NO], in the post flame gases entirely through the NH_i-pool. When [HCN] is greater than [NO], it has been shown (Bachmaier 1973) that HCN survives far into the post flame region of premixed hydrocarbon flames of Ø = 1.5, where high [NH_i] and supra-equilibrium [OH] are present. However, for Ø = 1.5 or 2.0 none of this axial decline was observed by Vince (1977). Actually, the observations made by this worker, did not fall in line with the description given by Iverach et al. (1973). Vince observed a very sudden and large drop in [NO], occurring within the reaction zone. In addition to Iverach et al.'s scheme (1973), another sink for NO had to be postulated. The most likely candidate was Myerson's (1975), i.e. CH + NO → HCO + N $\xrightarrow{NO}$ N_2 + O, with CH_2 and CH_3 also as possible candidates for attacking NO. The presence of hydrocarbon radicals increases in importance in richer flames, since they manage to survive long enough even to attack NO. Very little information about the behaviour of hydrocarbons in fuel-rich flames is available, and consequently it is difficult to discuss the attack of nitrogenous compounds by a hydrocarbon. Experiments with fuel-nitrogen (Hayhurst & Vince 1980) supported the idea that CH_i + NO → products is very fast at 1900 K. Halstead et al. (1973) found the rate constant for CN + NO → CO + N_2 to be 5×10^{11} ml $mol^{-1}s^{-1}$ at 2000 K, which is quite high. So far, there is no evidence of HCN reacting with NO in extremely rich flames. However, de Soete (1975) suggested a rate constant for HCN + NO → N_2 + HCO of 3×10^{12} exp(-30000/T) ml $mol^{-1}s^{-1}$.

2.2.7 General Conclusions after an Analysis of Previous Studies.

Analysing the previous work discussed above enables some conclusions to be drawn on a mechanism for the production of NO in flames:

1. The Zel'dovich mechanism is accepted as valid for fuel-lean and near-stoichiometric fuel-air mixtures.

2. The chemistry of nitrogen species in fuel-rich hydrocarbon flames, even in the absence of fuel-nitrogen, is far more complicated than the mechanism predicted by Zel'dovich. Concentrations of NO, HCN and NH_i species appear well above their values for equilibrium.

3. Formation of cyano species is related to the decay of hydrocarbons and, in very fuel-rich flames also occurs downstream of the reaction zone. Even in the absence of hydrocarbons, there is some controversy on the mechanism for the disappearance of the cyano-pool. However, either one of the following reactions is believed to occur:

$$HCN + OH \rightarrow OCN + H_2$$

$$CN + OH \rightarrow OCN + H \text{ ,}$$

with formation of CN from:

$$HCN + H \rightleftharpoons CN + H_2$$

$$HCN + OH \rightleftharpoons CN + H_2O$$

4. Formation of NO in the post-flame gases appears to be related to the initial decay of HCN (Haynes *et al.* 1975).

5. If fuel-nitrogen is added in sufficient quantities, the concentration of NO is thought to be high when leaving the reaction zone and then decays in the post-flame to a value which is characteristic of the flame (Haynes *et al.* 1975).

6. NH_i species are observed in some flames; their behaviour is not very clear and is possibly related to HCN decay.

A very brief description of possibilities for controlling NO_x emissions is given below. To reduce emissions of NO_x, either its formation is prevented, or, once it is formed, catalytic removal from the exhaust is applied. Reductions by about 20% of NO_x emissions in the course of SO_x removal by gas washing have been observed (Perkins, 1974). However, this technique has not been studied as a means of removing NO, since NO is highly insoluble and its conversion to NO_2 is small. So far, combustion modifications to reduce the levels of NO_x in exhaust gases have been designed considering only the formation of thermal NO, i.e. in reaction (1). Reaction (1) can be retarded by reducing peak temperature, or residence time at or near peak temperature or O atom concentration. Reductions of up to 30% in [NO] from some boilers have proved possible using low excess air (Bartock et al. 1972). Actually, low excess-air combustion was observed to be more effective in reducing fuel-NO rather than thermal NO. Also, two-stage combustion has been proving successful. This technique uses sub-stoichiometric air in the first stage and heat is removed before the remainder of the air is admitted in the second stage. However, some reductions lead sometimes to a decrease in efficiency (Tabaczynski 1974). Turner and Siegmund (1972) found that fuel-NO could be diminished as much as thermal NO by staging. Yamagishi et al. (1975) showed that total nitrogenous emissions, including NO_x, decrease with increasing ϕ in the primary stage, but HCN peaked at $\phi = 1.7$. Most of the fuel-N added to a primary flame with $\phi = 1.2$ was observed unreacted throughout the whole flame by Martin and Dederick (1977). Cooled exhaust-gas recirculation, although possible for eliminating thermal NO with high recirculation ratios, has been found not to affect fuel-NO (Turner 1972) and the effect on prompt NO is thus probably also minimal. Water injection appears promising with spark-ignition engines. The effect of water injection on prompt NO is

however negligible, since the addition of water only reduces the temperature in the NO formation zone (Greeves et al. 1977). Similarly, not much influence on prompt NO is observed by reducing air preheat or combustion intensity. A device which also reduces thermal NO_x without affecting prompt NO is the cooled porous disk burner. The use of fuel-lean conditions, as well as varying burner parameters could also lead to reduction of NO_x emissions (Schefer & Sawyer 1977, Hilliard & Weinberg 1976, Heap et al.1972, Sakai et al. 1973, Bartock et al. 1972, Jones 1973, Lefebvre 1975). Modifying the fuel might also be a way of reducing emissions of NO_x, although so far it has not attracted much attention. Shaw (1972) tested approximately 70 fuel additives to assess the feasibility of such an approach in aircraft gas turbines. The decomposition of NO in the combustion products could well be another way of reducing NO_x emissions. Muzio et al. (1977) achieved 80% reduction by adding ammonia (1:1 for initial NO) in the presence of 2% excess air. These workers also tried to use hydrocarbons instead of NH_3, but unfortunately their attempts failed, unless the addition rate yielded a fuel-rich mixture. In fact, commercial processes to remove NO_x from flue gases by reaction with NH_3 have been reported by Lyon and Benn (1978). Myerson (1975), however, presented detailed information for the reduction of nitric oxide by adding hydrocarbon and oxygen to the post-flame gases at 1200-1700 K. Finally, a technique which is spreading at present, is fluidised combustion. In spite of having long residence times, because temperatures are too low, virtually no thermal NO is generated. Most NO_x from fluidised beds is actually from fuel-N. Jonke et al. (1979) showed that there was no change in NO_x when N_2 in the combustion air was replaced by argon.

Chapter 3.

Apparatus and Experimental Techniques.

The layout of the apparatus used is shown in Plate 1. Gases from a bank of cylinders were metered by capillary flowmeters and mixed inside a pair of swirl-cans before feeding a water-cooled Padley-Sugden burner. The flames were sampled by a water-cooled quartz probe at various axial distances from the burner exit. The sampled gases passed to either a chemiluminescent analyser, which measured concentrations of NO in ppm, or, after being metered, through known amounts of KOH solutions for measurement of concentrations of cyanides and NH_i species. The description of the apparatus is divided into four sections: gas supply, burner, sampling system and gas analysis.

3.1 The supply of gas to the Burner.

The gases used were supplied in cylinders by B.O.C. Some of them were of standard purity as H_2, O_2, Ar, CH_4, C_2H_4 and C_3H_4 and others, such as mixtures of NO in argon for calibrating the chemiluminescent analyser and for fuel-NO experiments and, mixtures of ammonia in argon (also for fuel-nitrogen experiments) were supplied with its chemical analysis, correct to within 1% of the stated concentration of NO or ammonia.

Each gas, emerging from pressure-reducing cylinder heads, passed through an on/off valve and a fine control needle valve (Edwards High Vacuum, U.K., Model LB1B) before being metered by a capillary flowmeter. The gas then entered at least one brass mixing vessel and finally went to the burner. PVC tubing was used for all gases except hydrogen, for safety reasons. A chemical attack on the tubing by mixtures of NO in argon was observed from a coloration of the tubing; however, this was negligible during the time taken in one run.

Plate 1.

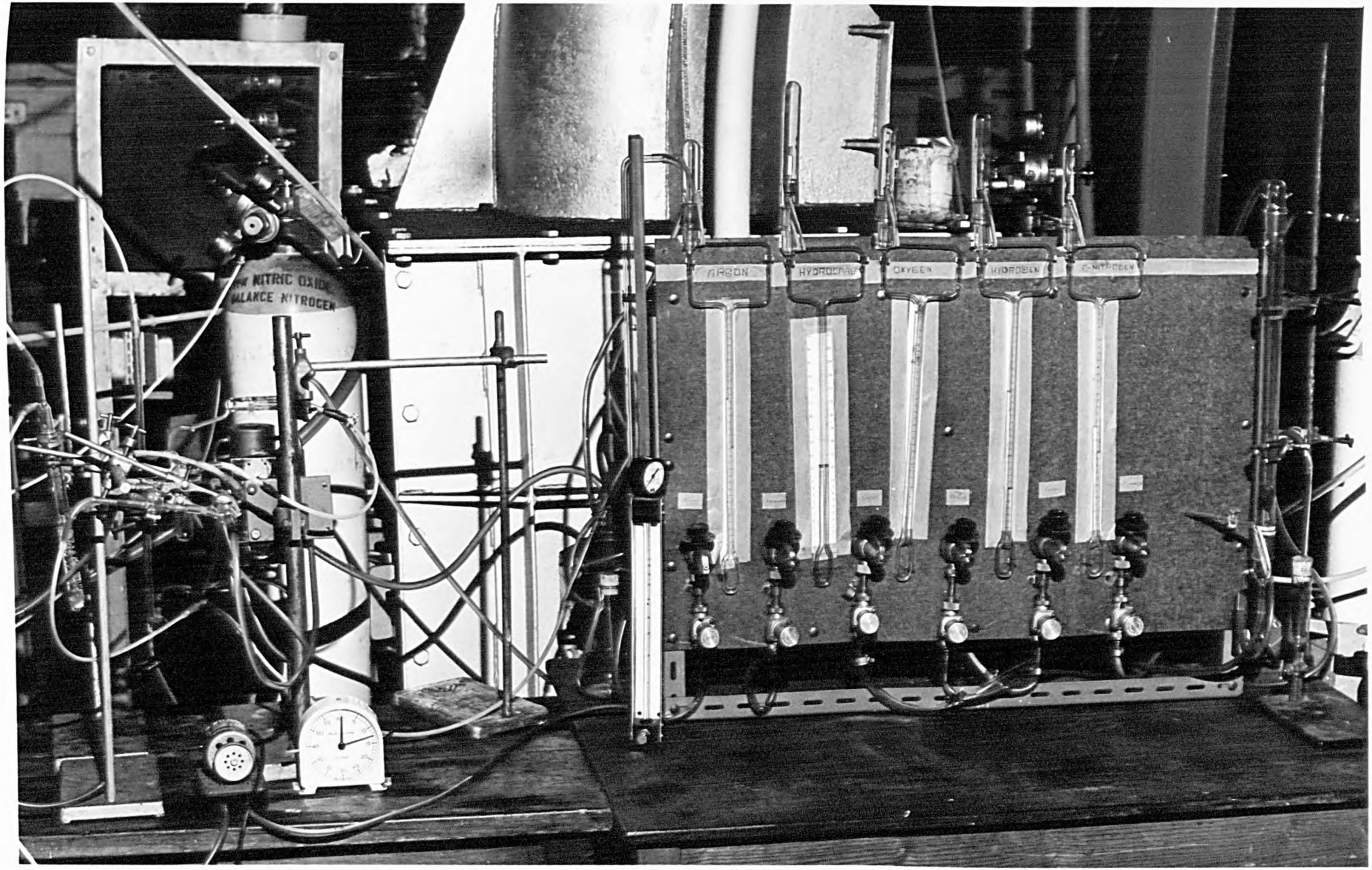
NITRIC OXIDE
BALANCE NITROGEN
ARGON
HYDROCARB
OXYGEN
HYDROGEN
NITROGEN

The basic principle used for measuring a flow rate is the relation between the pressure drop across a capillary and the flow. The pressure drop across the flow meter is indicated by the difference between two levels of a liquid in a U-tube, like the one shown in Fig.1. in Appendix A. The liquids were chosen not to interfere with the gas flow. The capillaries were calibrated using a wet-type laboratory gas meter for flows above 2 ml/s and a bubble meter for flows below that amount.

The gas mixers had three tangential entry tubes and were large enough (100 ml) to ensure thorough mixing. They also had releasable base plates in case of flashback. To have a minimum formation of NO_2 by reaction of NO with O_2, when the mixture enters the burner, NO was only added to the unburnt gases in the second mixer, just before the burner. Actually, the presence of NO_2 in the burnt gases was not detected in this experimental work.

3.2 The Burner.

The burner was like the one used by Padley and Sugden (1953), the only difference being that an outer flame shielding the central one was not used. When such shielding was necessary, as for measurements of temperature and [H], another burner of the same type was used. The burner is shown in Plate 2 and a cross-section of it is given in Fig.2. in Appendix A. The central part is constituted from a core of stainless steel hypodermic tubes "araldited" together. The internal diameter of each tube is 0.6 mm, the central core is 16 mm. in diameter. No over-heating was ever observed, even in the hottest hydrogen flame, i.e. adiabatic temperature of 2635 K. The burners were manually adjusted in the axial direction by means of a worm mechanism with little back lash. The distance from burner head to probe tip, which was read off a calibrated winding wheel, was considered accurate to within 0.1 mm.

Plate 2.

A shielded flame was not used to measure concentrations of various species present, because the gases were sampled only along the flame axis, and diffusion is not expected to be of any significance for axial distances below 2 burner diameters. Actually this rule of thumb was checked by measuring the concentration of NO in hydrogen/oxygen flames without hydrocarbons, since the amount of NO was observed to be unaltered in such flames. Only for the richest flame was the concentration of NO larger than that added to the flame at distances greater than 12 mm. from the burner exit (i.e. 0.75 flame diameters).

3.3 The sampling system.

A general layout of the sampling system is shown in Plate 3 and a schematic diagram is given in Fig.3.1. The burnt gases were sucked from the flame axis through a water-cooled quartz probe. The same probe was used in all experiments. The concentrations of NO were continuously measured in a chemiluminescent analyser, with the gas sampled by a vacuum pump in the analyser unit. To measure the concentrations of cyanides and NH_i species, the burnt gases (sampled also by a vacuum pump) were bubbled through a KOH solution after being metered by a bubble meter. The pressure at the entry of the bubbling container was read with a mercury manometer, with one end open to the atmosphere. Ion selective electrodes were used to measure the amount of cyanides and NH_i in the solutions. Separate experiments were carried out to measure the concentrations of NO and NO_x and, NH_i and cyanides, along the burnt gases. The sampled gas was diverted at point 1 in Fig.3.1 to either the chemiluminescent analyser or the system of gas bubblers. Traps were placed before the bubbling system (at 2 and 3 in Fig.3.1) for condensing water; these were not needed, however when measuring concentrations of NO_x, since a condenser already existed in the gas inlet

Plate 3.

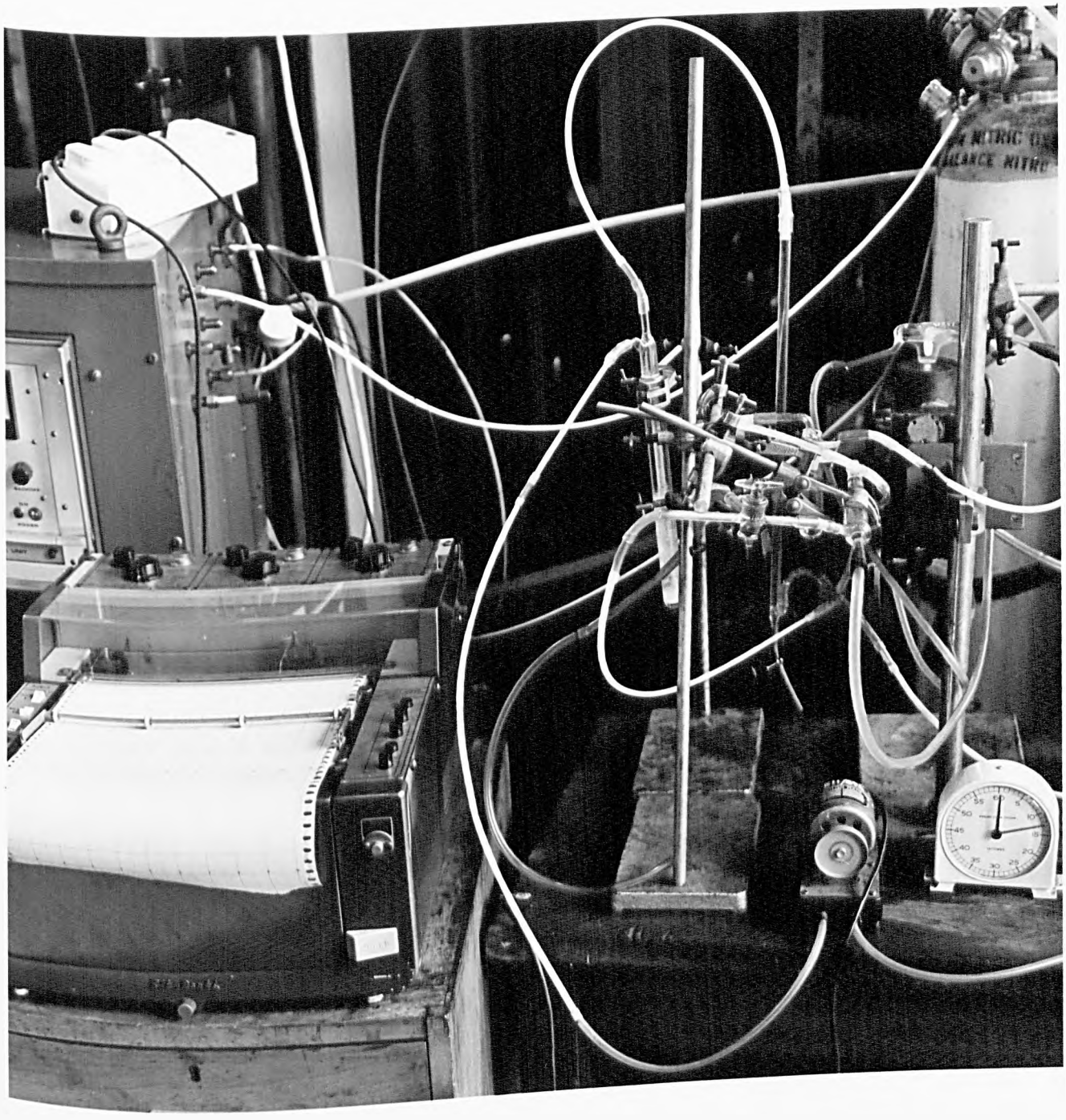

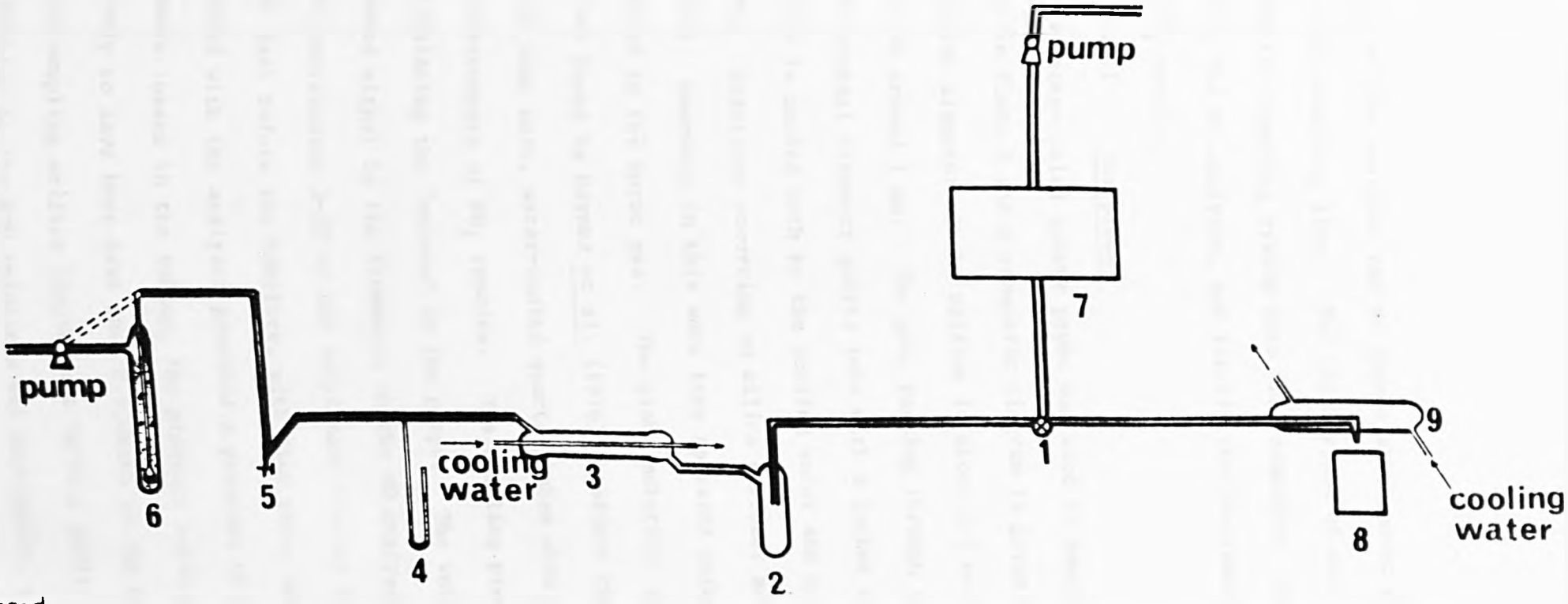

Legend

1-diversion point for the burnt gases

2-water trap

3- " " with cold water circulation

4-mercury manometer

5-bubble meter

6-sampling bottle with bubbler

7-NO+NO_x chemiluminescent analyser

8-burner

9-quartz probe

Fig.3.1 — A schematic diagram of the sampling system

system of the analyser and no appreciable amount of water condensed in the short sampling line. For the purpose of description, it is convenient to divide the sampling system into four segments: the probe, the bubbling system, the NO analyser, and finally the instruments used to measure cyanides and NH_i species.

3.3.1 The probe.

A water-cooled quartz probe was used to sample the gases. The probe is shown in Plate 4 and a schematic diagram is given in Fig. 3 in Appendix A. The inlet diameter of the orifice is about 0.2 mm with a wall thickness at entry of around 1 mm. The gas, passing through the orifice expands in a 5 mm internal diameter quartz tube with a jacket of cold water surrounding it. The gas is cooled both by the cooling water and by its expansion inside the probe. Reactions occurring on silica surfaces are mentioned by Allen (1975); however, in this work they appeared unimportant, since NO_2 was not detected in the burnt gas. The probe material, as well as tubing material, was not found by Haynes et al. (1976) to affect the concentration of cyanides. In the same work, water-cooled quartz probes also gave consistent results in measurements of NH_i species. The sampling pressure was maintained constant by regulating the "vacuum" in the pumps. The volumetric sampling rate was measured either by the flowmeter on the NO analyser panel, i.e. 10 ml/s (this represented 3-5% of the total mass flux of burnt gases) or by the bubble meter just before the bubblers, with flow rates around 2 ml/s. The pump supplied with the analyser provided a pressure of 0.57 bar; owing to pressure losses in the tubing, the pressure ratio across the probe tip was unlikely to have been less than 0.5,which is the critical ratio for sonic flow at the sampling orifice (Hayhurst & Telford 1977). The pump used when gas was bubbled in the KOH solutions was adjustable, so that the pressure was always kept around 0.6 bar.

Plate 4.

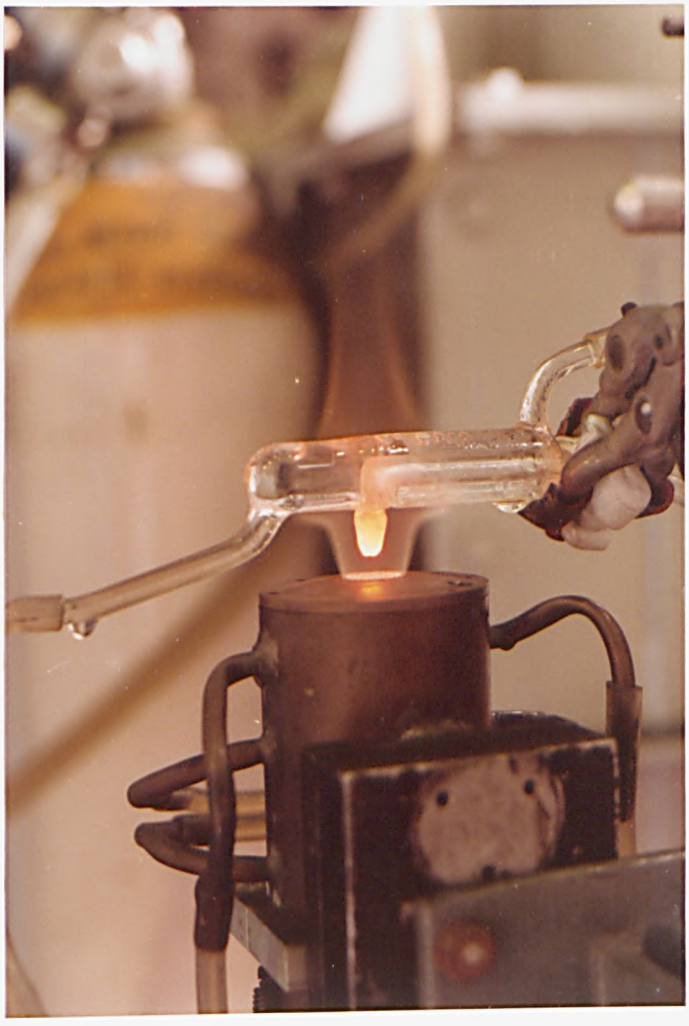

3.3.2 The system of gas bubblers.

A schematic diagram of a gas bubbler with its container is shown in Fig.4 in Appendix A. The sampled gas flows through teflon tubing to minimize reactions which could occur with PVC. The KOH solution in the container had a molarity of 10^{-2} M; this value was chosen so that the pH would be appropriate for CN^- to be produced from the pool of cyanides and NH_3 from the pool of NH_i species. The gas sparging tubes were bought from Gallenkamp and were of sintered glass type of porosity grade No. 1.

3.3.3 The NO_x Analyser.

Plate 5 shows the NO_x Analyser. Figs. 5 and 6 in Appendix A give schematic diagrams of it. Allen (1973) mentions several non-interfering methods of analysis of NO, with expensive instrumentation needed to achieve a sensitivity lower than 1 ppm. However, the concentrations of NO in the flames in this work were always above 10 ppm, which were easily detected by the chemiluminescent analyser. This had sufficient sensitivity, specificity and reliability; however, gases had to undergo a second cooling to condense the water out from the probe, since the presence of it in the analyzer's capillaries could seriously disturb its functioning. The chemiluminescent method is based on reactions between nitric oxide and ozone. The application of this photochemical reaction to measure concentrations of NO was first reported by Fontijn et al. (1970). The detailed mechanism was elucidated by Clough and Thrush (1967). The method consists of monitoring the infra-red radiation emitted when NO and O_3 are mixed in a reaction chamber. The more important reactions are:

$$NO + O_3 \rightarrow NO_2 + O_2$$

$$NO + O_3 \rightarrow NO_2^* + O_2$$

Plate 5.

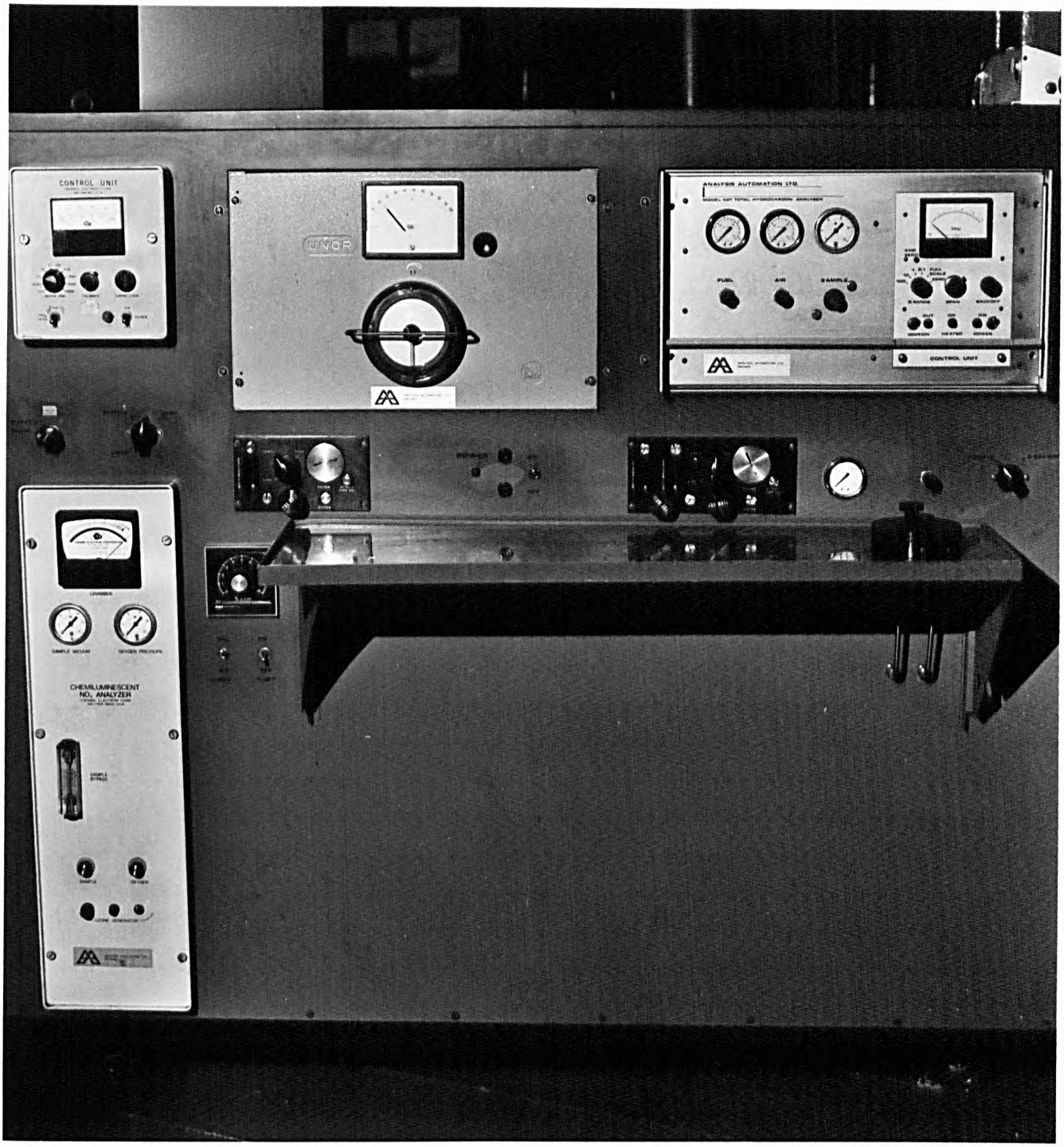
CONTROL UNIT
UNOR
ANALYSIS AUTOMATION LTD.
FUEL
AIR
SAMPLE
CONTROL UNIT
CHEMILUMINESCENT
NO, ANALYZER

$$NO_2^* \rightarrow NO_2 + h\nu \quad (\lambda = 0.6\text{-}3.0\ \mu m)$$
$$NO_2^* + M \rightarrow NO_2 + M \ .$$

where NO_2^* is the B_1 excited electronic state of NO_2. (At room temperature, ca 7% of NO_2 is in this state). The fate of NO_2^* depends upon the pressure of the gas. In the analyser, the pressure of the reaction chamber was normally above 1 Torr., so that most of the NO_2^* is quenched by collisions. The amount of chemiluminescence, although small, is enough for a very sensitive determination of [NO]. Approximately 2% of the oxygen supplied is converted into ozone by means of a silent-discharge ozone generator. The flow rates of O_2 and sample in the reaction chamber are controlled using pressure regulators and flow restricting capillaries. Chemiluminescence from the above reactions occurs near an optical glass filter and is monitored by a high-sensitivity photomultiplier with the light sensitive portion close to the optical filter, thus affording maximum utilization of the light emitted. The filter blocks out light of wavelength less than 600 nm, so that any interference from other possible chemiluminescent reactions is virtually eliminated. The amplifier converts the current from the photomultiplier into a voltage signal, amplifying it to a maximum of 10 volts for any operating range. Since the response of the photomultiplier is proportional to the concentration of NO, only one mixture is needed to calibrate the analyzer.

3.3.3.1 General operating characteristics of the TECO Model 10A Analyser.

Reaction chamber vacuum	8-12 Torr
Flow rate of ozonised O_2 to chamber	2.0 ml/s
Flow rate of gas sample to chamber	0.67 ml/s
Total flow rate of gas sample	ca. 16 ml/s

Sample vacuum	up to 430 Torr.
Sensitivity	8 scales, from 0–2.5 to 0–10 000 ppm
Linearity	± 1% of full-scale
Accuracy	derived from calib. gas ± 1% full-scale
Response time	ca. 0.7 s to full-scale deflection
Zero drift	negligible after ½ h. warm up

Owing to the exigencies of laboratory space, 1 m of PTFE tubing had to be inserted between probe and analyser, giving rise to a lag time of ca. 15s, compared with which the instrument response time is negligible. Despite the linearity of the instrument and the certified guarantees of B.O.C., it is wise to use at least two cylinders of calibration gas; the calibration of the NO_x - analyser was made with 900 ppm of NO in argon and occasionally 100 ppm of NO in argon was used.

3.4 Instrument and ion selective electrodes for cyanides and ammonia.

The burnt gases were bubbled through a KOH solution with pH = 12, so that HCN and CN yield CN^- but N, NH, NH_2 and NH_3 in the NH_i pool yield NH_3. The gas passed through a known volume of solution during a known time, and volumetric flow rate and pressure at the bubbler inlet were noted. To measure the cyanides, a selective cyanide-sensitive electrode was used, developed by Activion Glass Limited. The total amount of ammonia also present in the solution, was measured with an ammonia electrode, supplied by Orion. The electrodes were connected to the measuring instrument, which is in fact a pH meter, produced by Corning Limited. The description of this instrument and electrodes is given in the following sections. Using the electrodes, the concentrations displayed on the measuring instrument are those in the solutions prepared; consequently, calculations have to be made to convert these into either [HCN + CN] or $[NH_i]$ in the burnt gases. Examples of these calculations from raw data are shown in Appendix B.

3.4.1 Model 12 pH Meter.

This instrument was used to measure the concentrations of both the cyanide and NH_3 species. The Model 12 pH Meter is a high-impedance voltmeter which permits the comparison of unknown solutions with solutions of known concentration. The concentrations of unknown solutions may be presented directly as pH units or in mV. This instrument is shown in Plate 6. The 173 mm. scale length has two linear and two log scales. The lower linear scale, depending on the setting of the FUNCTION switch, allows measurements in the range 0 to ± 1400 mV. The upper linear scale permits readings of any 100 mV in the range 0 to ± 1400 mV. The upper log scale allows cation activity to be measured directly and the lower log scale anion activity.

Table 3.1

Technical Specification of the Model 12 pH Meter.

Readout

173 mm scale length meter, mirror backed, knife edge pointer with taut band suspension.

Operating ranges

pH	0 to 14
mV	0 to ± 1400

Manual and automatic temperature compensation 0 to 100° C (for ATC operation an optional ATC probe is required).

Accuracy

		pH	Rel mV
Reproducibility	Normal	± 0.02	± 2
	Expand	± 0.002	± 0.2
Linearity	Normal	± 0.05	± 5
	Expand	± 0.005	± 0.5

		pH	Rel mV
Resolution	Normal	0.1	10
	Expand	0.005	0.5

Circuit Details

Input current	Less than 5 pA
Input Impedance	Greater than 10 ohms
Polarizing current (KF) -	10 A

Recorder Output Mode	Recorder Output (mV)	Meter Reading
pH	0	0.000
	+ 50	7.00
	+ 100	14.00
mV	+ 100	- 1400
	- 100	+ 1400

3.4.2 Ammonia electrode - Model 95 - 10.

The model 95-10 Ammonia Electrode allows fast, simple and accurate measurements of ammonia in aqueous solutions. All the solutions had to fall within pH 11 to 14 range and have a total level of dissolved species below 1 M and not to have interference from other species present in the solution. This electrode uses a hydrophobic gas-permeable membrane separating the sample solution from the electrode internal solution. Dissolved ammonia in the sample solution diffuses through the membrane until the partial pressure of ammonia is the same on both sides of the membrane. The partial pressure of the ammonia present will be proportional to its concentration. Ammonia diffuses through the membrane in the internal filling solution, and, to a small extent, reacts reversibly with water in the filling solution:

$$NH_3 + H_2O \rightleftharpoons NH_4^+ + OH^-$$

Plate 6.

CORNING
pH METER MODEL 12
FUNCTION
STDBY
TEMP °C
LOCK
CAL
assembly instructions
ORION
RESEARCH

The relationship between ammonium ion and hydroxide is:

$[NH_4^+]\ [OH^-]/[NH_3]$ = constant. The internal filling solution contains ammonium chloride at a sufficiently high level for the ammonium ion concentration to be considered fixed. Thus, $[OH^-] = [NH_3] \times \text{constant}$. The potential of the electrode sensing element with respect to the internal reference element varies according to the Nernst equation, i.e.

$$E = E_o - S \log [OH^-]$$

where S is the "electrode slope". Since the hydroxide concentration is proportional to ammonia concentration, the electrode response to ammonia will also be according to the Nernst equation, i.e.

$$E' = E_o - S \log [NH_3]$$

where E' (reference potential) is partly determined by the internal reference element, which responds to the fixed level of chloride in the internal filling solution.

The slope of the electrode is determined with two ammonium chloride solutions of known concentrations. A schematic diagram of the electrode is shown in Fig. 7 in Appendix A.

Table 3.2

Specifications of the Ammonia Electrode- Model 95-10.

Concentration range	- 10^{-6} to 1M (0.02 to 17,000 ppm NH_3 or 0.01 to 14,000 ppm N)
Temperature range	- 0^o to 50^o C.
Electrode resistance	- 200 to 600 megohms
pH range	- samples and standards must be adjusted to above pH 11.

Life	- when used to normal operating conditions, the electrode membrane and filling solution must be replaced about every 30 days.
Minimum sample size.	- 2½ ml in a 30 ml beaker.
Size	- length - 151 mm body diameter - 17 mm cap diameter - 22 mm cable - 75 mm

3.4.3 The cyanide-sensitive Electrode (Activion type 003 15 005).

The cyanide sensitive electrode responds in a selective manner in a wide range, so that the concentration of cyanides can be determined even in the presence of other ions. The electrode potential can also be described by the Nernst equation:

$E = E_o + S \log [CN^-]$ where S is the "electrode slope".

It is apparent that the relation E vs. (log $[CN^-]$) is a linear one at constant temperature. The activity coefficient can be maintained constant by having solutions with constant ionic strengths. A pH higher than 12 was essential in order to suppress hydrolysis of the cyanide salts. The electrode was originally calibrated with KCN solutions of known concentrations. For safety reasons, the same electrode was calibrated subsequently with KI solutions with the same ionic strength of 1M as those of cyanides. The calibration curves were parallel, so that for further calibrations iodide solutions were used.

Table 3.3

Specifications for the Activion cyanide-sensitive electrode.

Selectivity	$K_{sel.}[CN^-]/[OH^-] = 10^{-8}$
Response time	30 s in 10^{-2} to 10^{-3} M aqueous solutions. In more dilute solutions can take up to a few

	minutes. Response time becomes shorter with increasing ionic strength.
Resistance against chemicals	The electrode body does not undergo any change in aqueous solutions of strong acids, inorganic salts, bases, chlorine, phenol, formaldehyde further in various alcohols; other organic solvents may attack the electrode body.
Measuring range	10^{2} - 10^{-6} M 260 - 0.026 ppm
Reproducibility	± 2 mV
Resistance at 25° C	1 Mohm

3.5 Sources of error in the experimental measurements.

When a probe is inserted into a flame, the flame is usually disturbed, due to changes in the flow field. Even if no distortion of the flow-field takes place, a diffusional flux in front of the probe is converted into a convective flux at the probe inlet. In the case of non-isokinetic sampling, when the sampling velocity exceeds the unperturbed-flow velocity, invasion of species in the vicinity of the probe occurs. This means that the apparent concentration of a certain species in isokinetic sampling increases whilst in non-isokinetic sampling it decreases. The probe walls could also lead to errors in sampling: 1 - their thickness could alter the pattern of streamlines; 2 - their temperature could alter the rates of diffusion and convection; 3 - the occurrence of a velocity boundary layer near the probe wall, which is important in laminar flames. Yanagi (1977) has studied in detail the effect of aerodynamics and concentration-gradients on the gas composition during sampling. However, the probe used in this work had a very narrow inlet (ca. 0.2 mm) which could be considered as a microprobe, so that concentrations would not be altered appreciably (Westenberg,1957).

Apart from physical alterations, chemical ones can take place, where species can either be formed or destroyed during sampling. Chemical reactions which could take place in the probe to alter the apparent [NO] have been studed by Bilger (1975). They are typically:

1. Catalytic effects of surfaces of both the probe and sampling line on the thermal equilibration between NO_2 and NO.
2. Oxidation of NO to NO_2 by supra-equilibrium species such as OH and HO_2.
3. Homogeneous reduction of NO to N_2.
4. Oxidation of cyano and amine species to NO.

The last step might be important in very rich flames, and this is the only step yielding NO, since the first three consume it. In rich premixed flames, like those in this work, $[NO_2]/[NO]$ is generally accepted to be small. Actually in the flames studied here, NO_2 was not detected in the burnt gases. However, Amin (1977) has shown analytically that without wall effects, NO_2 would be converted almost quantitatively to NO in less than 1 ms, and stainless steel and quartz probes do not possess sufficient activity to prevent this. These losses of NO can be significant, as discussed by Siewert (1975), Cernansky (1976), England et al. (1973), Bilger (1975), Cernansky and Sawyer (1975) and Allen (1973). However, the flames studied in this work were too rich to expect any significant formation of NO_2 (see discussion in the following chapters), as was found to be the case in practice. Blyholder and Allen (1965) found that NO is adsorbed on various catalytic surfaces whereas Shelef et al. (1968) have studied the surface catalysed reaction of NO by CO. In addition, England et al. (1973) have investigated the effects of using different probe materials and cooling the probe. Their cooled stainless steel probes gave lower readings for

[NO] than quartz ones. Cooling is not crucial for quartz probes, except in very rich flames (i.e., $\phi > 1.4$). An extensive list of reactions involving NO that might occur during sampling to falsify its measured concentration is given below:

$$NO + H_2 \rightarrow HNO + H$$

$$NO + H \rightarrow N + OH$$

$$NO + H + M \rightarrow N + OH + M$$

$$NO + O \rightarrow N + O_2$$

$$NO + OH \rightarrow HNO + O$$

$$NO + NO \rightarrow N_2 + O_2$$

$$NO + CN \rightarrow \text{products}$$

$$NO + HCN \rightarrow \text{products}$$

$$NO + NH_i \rightarrow \text{products}$$

$$NO + CH_i \rightarrow \text{products}$$

$$N + O_2 \rightarrow NO + O$$

$$NH_i + OH \rightarrow NO + \text{products}$$

$$N_2 + O \rightarrow NO + N$$

If hydrocarbon radicals are present, they are likely to react with NO at temperatures as low as 1200 K (Fenimore & Jones 1961, Myerson 1975). However, the gases inside the probe are likely to be at temperatures much less than 1200 K, and so reactions such as $CH_i + NO \rightarrow$ products are likely to be important only at the very tip of the probe. Because the probe is cooled, rate constants of some of the above reactions will be relatively low, so that only reactions of the type $NH_i + OH \rightarrow NO +$ products and $NH_i + NO \rightarrow N_2 +$ products are likely to be important. Vince (1978) found little variation in the measured concentrations of NO obtained by using different probes. One of Vince's probes was the one used in this investigation.

Additional confirmation that the measurements of [NO] with it are genuine came from the fact that when NO was added to different flames free of hydrocarbons, the concentration of nitric oxide measured along the flame axis was constant and equal to the quantity added. This confirms that all those reactions which did not involve CH_i, CN or HCN are quite unimportant in this sampling system.

In the determination of concentrations of ammonia and cyanides, errors might occur due to dissolution of the above species in the water condensed in the sampling line. However, no significant amounts of NH_3 and cyanides were ever found in the water removed from the condensers. The concentration of NO, plus that of NH_i, in flames with 50 ppm of ammonia added, were in fact found to be equal to the total amount of ammonia. This establishes that NH_i species in the pool when dissolved yield NH_3 which is the species measured by the electrode. In flames containing hydrocarbons, the determination of $[NH_i]_t$ has a higher degree of uncertainty, because species such as OCN and HOCN could be present in solutions which yield NH_3.

The ammonia and cyanide electrodes were checked for interferences from the presence of other species, which might be detected by the electrodes. According to the instructions for the cyanide-specific electrode, the KOH aqueous solutions with CN^- present have to be diluted with an equal volume of 0.1 M Na OH. Ions of sodium may alter the performance of the same electrode if they are present in significant amounts. However, this was checked by using a NaOH solution free of cyanides, and the cyanide electrode was found to be unresponsive to the presence of Na^+ in the levels of concentration used in the present work. The cyanide electrode was also checked for interference by cyanate ions. This electrode did not detect the presence of cyanate even when its concentration was very high compared to

the amounts which might be formed in a flame. However, in the case of the ammonia electrode, although unresponsive to Na^+ ions, a slight response was observed when cyanates were added to the solution. To check the sensitivity of the ammonia electrode to cyanates, two different amounts (0.5 and 1.0 g) of potassium cyanate were added to 20 ml of NaOH, with pH = 12.0 and 0.5 g of NH_4 Cl added. The ammonia electrode indicated $[NH_4^+]$ = 0.45 M, agreeing well with the expected value of 0.467 M. When 0.5 g of KCNO was also added to the above solution, the electrode's response changed to 0.5 M. The concentration of CNO^- was 0.3 M. This means that for 0.3 moles/ℓ of CNO^- the electrode registered 0.05 moles/ℓ. No further change was observed in the ammonia electrode's response when 1 g of KCNO was present in the same solution of ammonium chloride. Accordingly, measurements of $[NH_i]_t$ in flames with hydrocarbons present were considered to have a maximum error of 17%,due to the presence of cyanates. Consequently, there is a higher degree of uncertainty than with flames without hydrocarbons.

The reactions of CN and HCN with hot quartz surface have been studied by Blair et al. (1977). It turns out that they are only likely to take place at the probe tip. The sum $\{[NO] + [NH_i]_t + [HCN + CN]\}$ in flames with 90 ppm of NO added and with 0.05% of hydrocarbon in the unburnt gas, was measured and found to equal the total concentration of NO added. This proves that reactions e.g. forming N_2 during sampling are not important in flames with low amounts of additives (although they might become more important with higher $[NO]_0$),and also that ions like CNO^- are not interfering with the measurements, which appear to be generally unaffected by sampling effects.

Other sources of errors are the calibration of capillaries, manometer readings, volumetric flow readings and even the time and velocity of bubbling, in that they all affect measurements of [HCN] and $[NH_i]_t$. Errors associated with the calibration of capillaries have been shown by Vince (1978) to be

relatively unimportant. Several experiments were carried out to determine which values of bubbling time and velocity through the KOH solutions led to smallest errors. Increasing the bubbling time and decreasing the velocity led to an increase in the measured values of $[NH_i]_t$ and [cyanides]; however, above certain values for the bubbling time and with the minimum flow of gas with the pump available, the measured concentrations of the above species became constant. In fact, when using short bubbling times, the amounts of NH_i and cyanides absorbed by the KOH solutions were too low to be measured. Hence a bubbling time, which could lead to measurements with the electrodes to be as accurate as possible, was chosen. Actually, errors in these measurements were believed to be the most significant in this work, although they are very difficult to quantify precisely, and consequently both $[NH_i]_t$ and [HCN + CN] may well be slightly low.

Another error is that associated with the use of the chemiluminescent analyser. This was calibrated with a mixture of nitric oxide in molecular nitrogen. However, the gas used as diluent in the flames is argon, with the result that chemiluminescence is increased (Pereira 1975), because of the different quenching efficiencies of Ar and N_2. Consequently, higher levels of NO than those present in the flames are measured, expecially in flames with low additions of nitrogenous species (i.e. high amounts of Ar). The concentrations of NO given by the analyser were accordingly corrected by decreasing the measured [NO] by 30 percent (Pereira 1975).

3.6 Studies on methods to determine [NO], $[NH_i]_t$ and [HCN + CN] and estimates of error.

The chemiluminescent analyser has been widely used and accepted as giving satisfactory results (Allen 1973, Hayhurst & Vince 1977, 1980, Myerson 1974, Takagi 1979). Ion selective electrodes also have been utilized by other investigators and compared to alternative methods for determining the amounts of NH_i species and cyanides (Haynes et al. 1975, Takagi et al. 1977,

Haynes 1977, Takagi et al. 1979). Takagi et al. (1977) measured the same quantity of cyanides (to within 30%) with the ion selective electrode and silver nitrate titrations. In addition, Haynes et al. (1975) has measured and compared the values of $[NH_i]_t$ obtained with the specific ion electrode and a colorimetric method. The agreement was satisfactory and the absolute errors quoted were also 30 percent.

The reproducibility of concentrations measured in this study was of the order of 95 percent for [NO] and 70 percent for $[NH_i]_t$ and [HCN + CN]. This agrees with the values obtained by other investigators quoted above. To estimate errors for any particular measurement, one has to consider both systematic and random errors, as well as the accuracy of the data. Taking into account all errors, the following uncertainties were estimated for [NO], $[NH_i]_t$ and [cyanides]:

Concentration	Uncertainty factor (%)
[NO]	± 10
$[NH_i]_t$ (flames with hydrocarbons)	± 30
$[NH_i]_t$ (flames without hydrocarbons)	± 20
[HCN + CN]	± 20

Chapter 4.

Measurement of flame properties.

4.1 Introduction.

Premixed hydrogen-oxygen mixtures, with argon as diluent were burned. For this study, several flames with different $[H_2]/[O_2]$ ratios were used. Ammonia, nitric oxide and hydrocarbons were added to them and [NO], $[NH_i]_t$ and [HCN + CN] were measured along the burnt gases, as discussed in the previous chapter. All the flames were fuel-rich and argon was chosen as diluent, rather than nitrogen, because it does not interfere with the NO-NH_i-N_2 system. Equilibrium concentrations and adiabatic temperatures of every flame were computed by Dr. N.A. Burdett. Recent values for equilibrium constants were taken from Jensen & Jones (1978). This program is based on the method outlined by Gaydon & Wolfhard (1970). The equilibrium concentrations of H, OH, H_2, H_2O and Ar in the burnt gases, along with the temperature and velocity for the different flames burned are presented in Table 4.1. Table C1 in Appendix C presents all the flames studied, with additives and compositions.

4.2 Temperature measurements.

Temperature was measured by the Na D-line reversal method (Gaydon & Wolfhard 1970) using a shielded flame on a burner similar to the one used in the experimental work. This was done with the kind assistance of Dr. J. Ogden. Two different sodium concentrations were atomised into the burner supplies and both gave very similar values for the temperature. The observations near the reaction zone are falsified by chemiluminescence of Na atoms and, therefore, the temperature at that point had to be extrapolated (Padley & Sugden 1958). Fig. 4.1 shows temperature profiles for various flames. Only flames 1 and 2 are practically isothermal. All the others

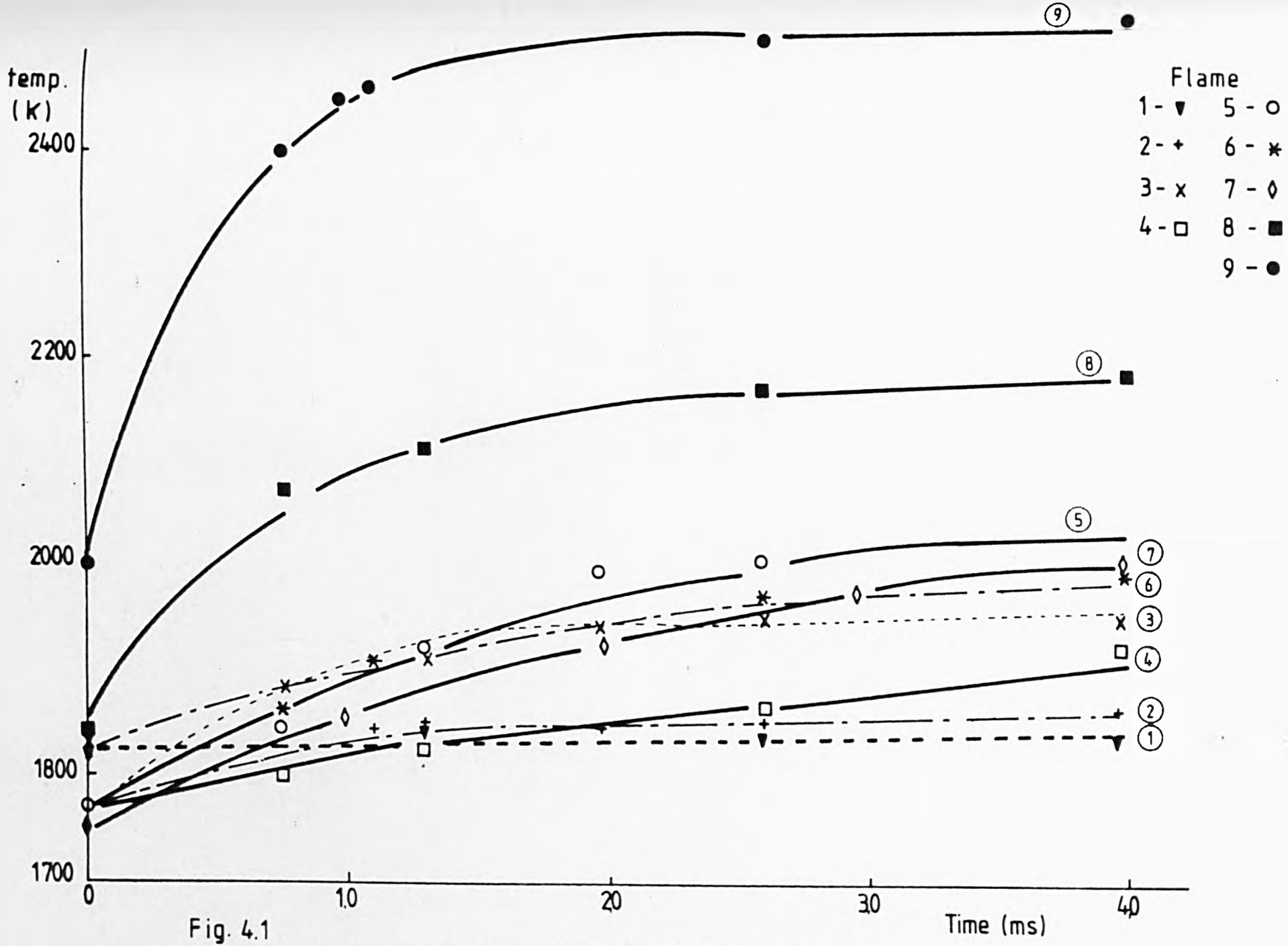

Fig. 4.1

Temperature profiles along the flame axis.

have a temperature difference of at least 130 K between the reaction zone and a point 30 mm downstream. The flames with the greatest temperature variations are those richest in hydrogen. The temperature profiles were considered to remain unchanged by additions of various hydrocarbons and nitrogenous substances, such as NO and NH_3, described in Table C1 in Appendix C. This assumption was made because the highest addition of a nitrogenous species was 5000 ppm (i.e. 0.5 vol.%) and these additions always replaced the same amount of argon, and consequently the total flow rate was unaltered. Only hydrocarbons were added as extra volumes to these flames, but the amount was never greater than 1 vol.%, so that according to Padley (1958) the temperature profile is not expected to be appreciably altered.

4.3 Velocity of the burnt gases.

The velocity of the burnt gas was calculated assuming plug flow and complete combustion, so that

$$v = Q_{u.g.} \frac{T_{ad}}{288} \frac{4\rho}{\pi D_f^2}$$

where

v = velocity

$Q_{u.g.}$ = volumetric flow rate of the unburnt gas

T_{ad} = adiabatic temperature

ρ = parameter which measures the contraction of volume when complete combustion takes place

D_f = diameter of a flame, which was assumed to be equal to the diameter of the hypodermic portion of the burner (i.e. 16 mm).

The velocity as derived above does not take concentration and temperature variations into account. Values for the velocity in the various flames are also presented in Table 4.1. The velocity for flames with additives was

Table 4.1

Data relating to flames used in the fuel-nitrogen study.

Flame No.	Adiabatic Temperature (K)	$[H_2]/[O_2]/[Ar]$	$Q_{u.g.}$ (10^{-6} m^3/s)	$V_{b.g.}$ (m/s)	Equilibrium gas composition (molar)				
					$[H_2O]$	$[H_2]$	[Ar]	$[H]x10^4$	$[OH]x10^5$
1	1822	2.5/ 1 / 10.5	250	7.38	0.1538	0.0384	0.8077	0.786	2.095
2	1900	2.5/ 1 / 9.7	250	7.66	0.1638	0.0409	0.7950	1.500	4.890
3	1986	2.5/ 1 / 8.9	250	9.42	0.1753	0.0438	0.7806	2.917	10.980
4	1900	3.5/ 1 / 8.2	250	7.64	0.1709	0.1281	0.7007	2.656	2.890
5	2030	3.5/ 1 / 7.0	250	9.70	0.1903	0.1425	0.6664	7.183	9.817
6	1900	4.0/ 1 / 7.43	250	7.62	0.1746	0.1745	0.6506	3.108	2.546
7	1900	5.0/ 1 / 5.97	250	7.60	0.1824	0.2735	0.5436	3.8880	2.114
8	2151	3.18/1 / 6.49	280	11.60	0.2063	0.1214	0.6706	14.59	31.50
9	2635	2.74/1 / 3.5	300	11.90	0.3037	0.1166	0.5529	154.0	961.0

considered to be the same as without them. This is because NO and NH_3 replaced the same amount of argon and in any case no more than 1% of additives was ever used.

4.4 Measurement of radical concentrations.

The concentrations of H atoms in the hydrogen-oxygen flames were obtained from measurements of the disequilibrium parameter $\gamma = [H]/[H]_e$. The determination of γ for flames at 1900 K (adiabatic temperature) was kindly done by Dr. N.A. Burdett using a mass spectrometric technique and for flames at other temperatures by Dr. J. Ogden using an optical method. In the latter case, the Na/Li comparison technique was used, from which the absolute concentrations of H atoms can be obtained (James & Sugden 1955). In the work done by Dr. N.A. Burdett, strontium was added to flames at 1900 K and the ratio $[Sr^+]/[Sr\ OH^+]$ measured with a mass spectrometer (Hayhurst & Kittelson 1974). The above ratio is governed by a balance of $Sr\ OH^+ + H = Sr^+ + H_2O$ and is therefore proportional to [H]. Absolute values of γ were obtained by matching the observed rate of disappearance of H to that computed from the known rate constants (Jensen & Jones 1978) of

$$H + H + M \rightarrow H_2 + M$$

$$H + OH + M \rightarrow H_2O + M.$$

The dependence of γ^{-1} upon time is linear and is given by the following relation:

$$1/\gamma = 1/\gamma_o + bt,$$

where γ_o is the value for $[H]/[H]_e$ in the reaction zone and b is a constant. The values of γ_o and b for the different flames are given in Table 4.2.

Table 4.2

Values of γ_o and b for different flames.

Flame No.	γ_o	b $(ms)^{-1}$
1	8.3	0.0398
2	9.4	0.0401
3	14.6	0.0771
4	15.6	0.0237
5	19.1	0.0872
6	22.5	0.0182
7	49.0	0.00263
8	19.9	0.185

The concentrations of OH radicals were not measured. In rich isothermal hydrogen flames $[H]/[H]_e \equiv [OH]/[OH]_e$, so that OH concentrations can be determined from the same γ values. However, the majority of the flames show temperature variations along their axes. The dependence of [OH] upon temperature variation along any one flame is discussed in the following section. Because [H] and [OH] always decay with time in proportion to γ, similar profiles are obtained for [H] and [OH]. Fig. 4.2 shows some typical profiles for one flame.

4.5 The effect of temperature variations and presence of additives on radical concentration.

Temperature variations along the flame axis can change the relation between $[H]/[H]_e$ and $[OH]/[OH]_e$, as well as the values for any equilibrium constant. The error in taking $[H]/[H]_e = [OH]/[OH]_e$ is greater towards the reaction zone. Here, in flames with large temperature variations, γ for OH is lower than that for H atoms by as much as 40 percent. The implications of this will be considered in the following chapters in which rate constants are determined. In subsequent chapters values for all equilibrium constants at particular distances were always obtained at the corresponding local temperature.

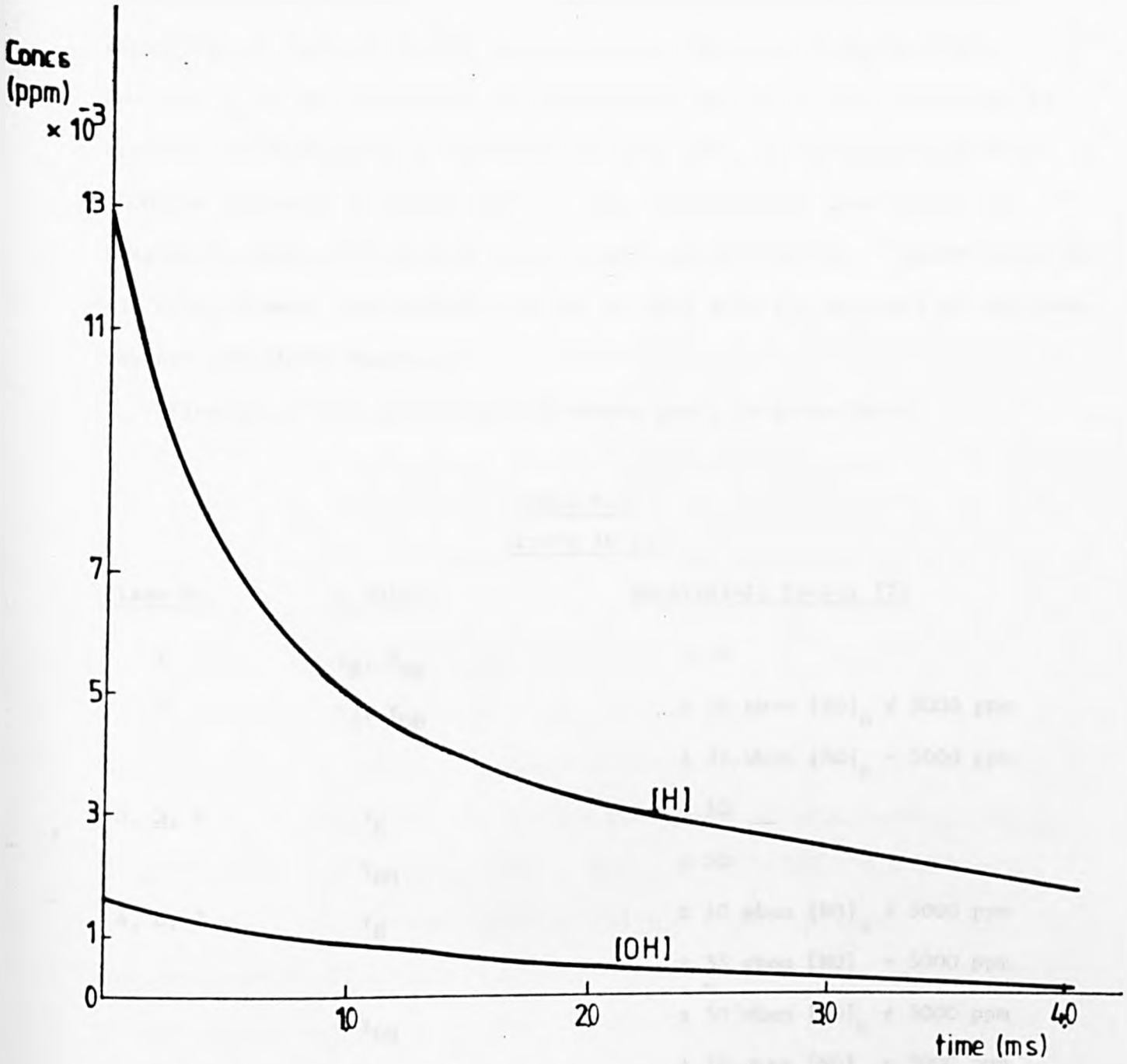

Fig. 4.2 Profiles of [OH] and [H] in the flame with $[H_2] / [O_2] = 3.5$ and $T_{ad} = 2030K$

High concentrations of added nitric oxide may also reduce radical concentrations, but only flames with 5000 ppm of NO added are expected to have significantly lowered radical concentrations (Bulewicz & Sugden 1964). However, γ_o is not altered by the presence of NO, but b (see Table 4.2) is expected to increase by a factor of 2.5 when $[NO]_o$ is increased from 0 to 5000 ppm (Bulewicz & Sugden 1964). This will be taken into account in Chapter 7, where studies with these flames are carried out. Accordingly, in all other flames, the variation of [H] or [OH] with the presence of additives, was not considered important.

Finally, a list of estimate of errors for γ is given below:

Table 4.3

Errors in γ.

Flame No.	γ values	Uncertainty Factor (%)
1	γ_H, γ_{OH}	± 10
2	γ_H, γ_{OH}	± 10 when $[NO]_o \neq 5000$ ppm
		± 35 when $[NO]_o = 5000$ ppm
3, 5, 8	γ_H	± 10
	γ_{OH}	± 50
4, 6, 7	γ_H	± 10 when $[NO]_o \neq 5000$ ppm
		± 35 when $[NO]_o = 5000$ ppm
	γ_{OH}	± 50 when $[NO]_o \neq 5000$ ppm
		± 75 when $[NO]_o = 5000$ ppm

Chapter 5.

Observations in flames with ammonia added alone.

5.1 Experimental observations in flames with ammonia at 1900 K.

5.1.1 Introduction.

Flames with $[H_2]/[O_2]/[Ar]$ equal to 2.5/1/9.7, 3.5/1/8.2 and 4.0/1/7.43 were used to study the formation of NO with ammonia as sole additive. 50 ppm and 125 ppm of ammonia were added to the unburnt gas mixture of these flames and also 615 ppm to the first, 525 ppm to the second and 515 ppm to the last flame. [NO] and $[NH_i]_t$ (which is the sum of [N], [NH], $[NH_2]$ and $[NH_3]$) were then measured along every flame axis, as described earlier. The concentration of N_2 was determined by a mass balance on nitrogenous species. The concentration profiles of the above species along the flames are described in the following section.

5.1.2 Concentration profiles.

Typical profiles of concentration of NO, NH_i and N_2 are presented in Figs. 5.1 to 5.4. These plots demonstrate the variation of concentrations for the same $[H_2]/[O_2]$ ratio of 2.5 for the amount of added ammonia, $[NH_3]_o$, being increased from 50 to 615 ppm. Also, the ratio $[H_2]/[O_2]$ was varied from 2.5 to 4.0 for the same amount of 125 ppm of ammonia added. The concentration profiles along flames with other values of $[H_2]/[O_2]$ or $[NH_3]_o$ all had similar patterns. In fact, in all flames, the majority of NO and N_2 is formed in the reaction zone, with a corresponding disappearance of the ammonia present. The fast formation of NO and N_2 and the simultaneous disappearance of ammonia continues for about 1 ms. Afterwards, with the lowest additions of NH_3, the concentrations of all these species remain almost constant, but increase slowly for higher additions, with the greatest increase corresponding to the highest amount of total NH_3 present. The

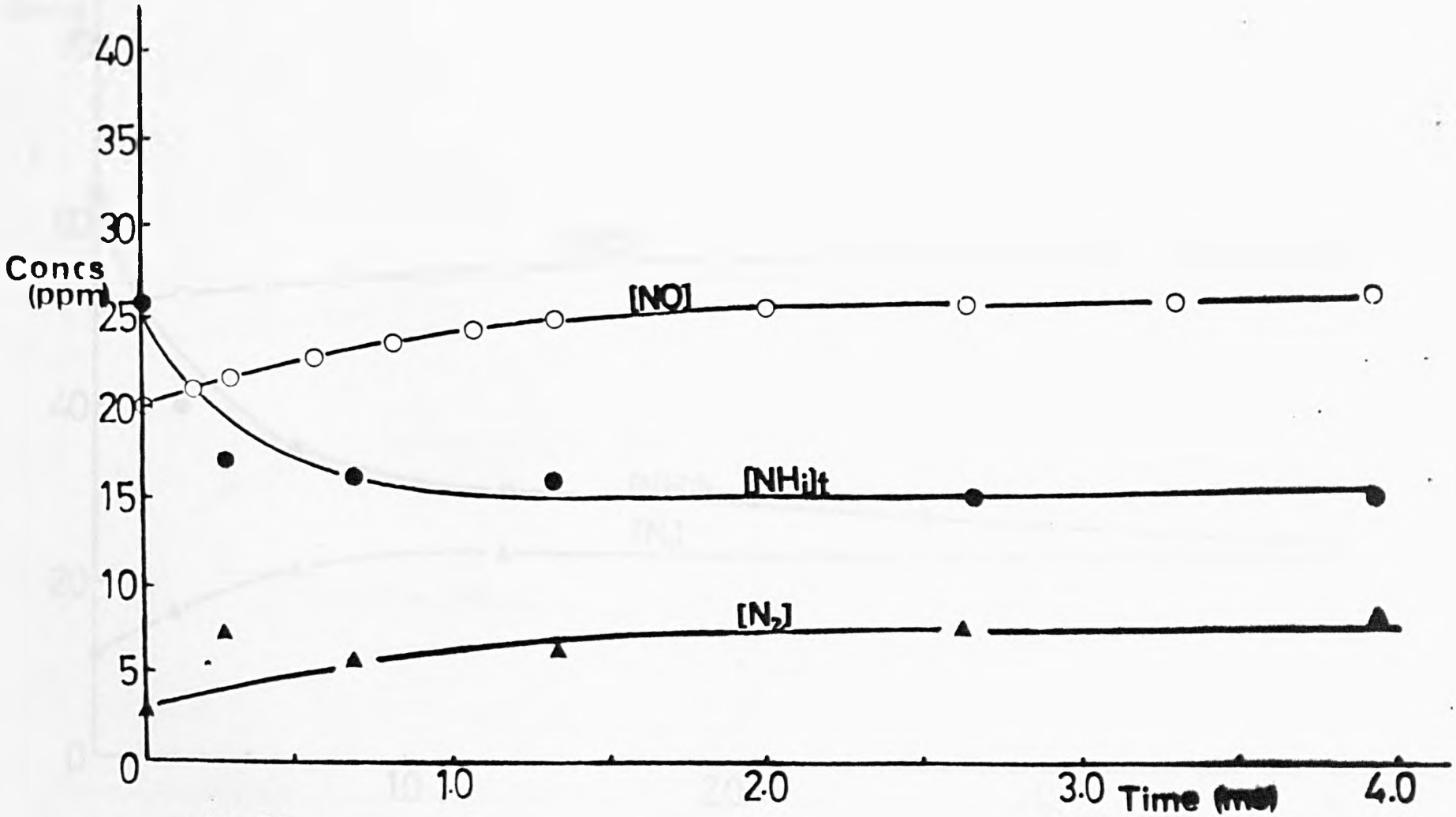

Fig. 5.1

Concentration profiles of the nitrogeneous species present in the flame with $[H_2]/[O_2]/[Ar] = 2.5/1/9.7$ and $[NH_3]_o = 50$ ppm

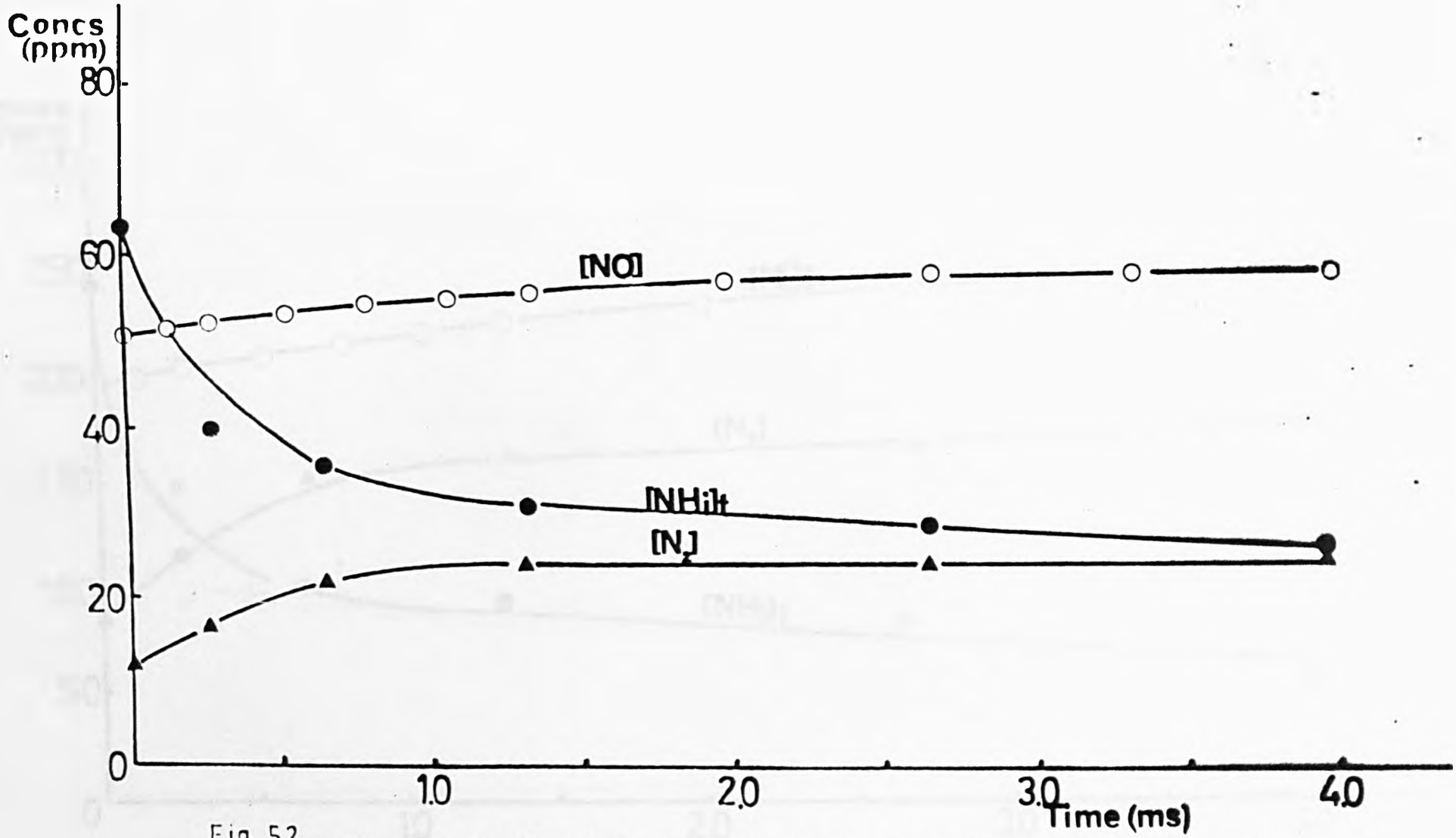

Fig. 5.2 Concentration profiles of the nitrogeneous species present in the flame with $[H_2] / [O_2] / [Ar] = 2.5 / 1. / 9.7$ and $[NH_3]_o = 12.5$ ppm

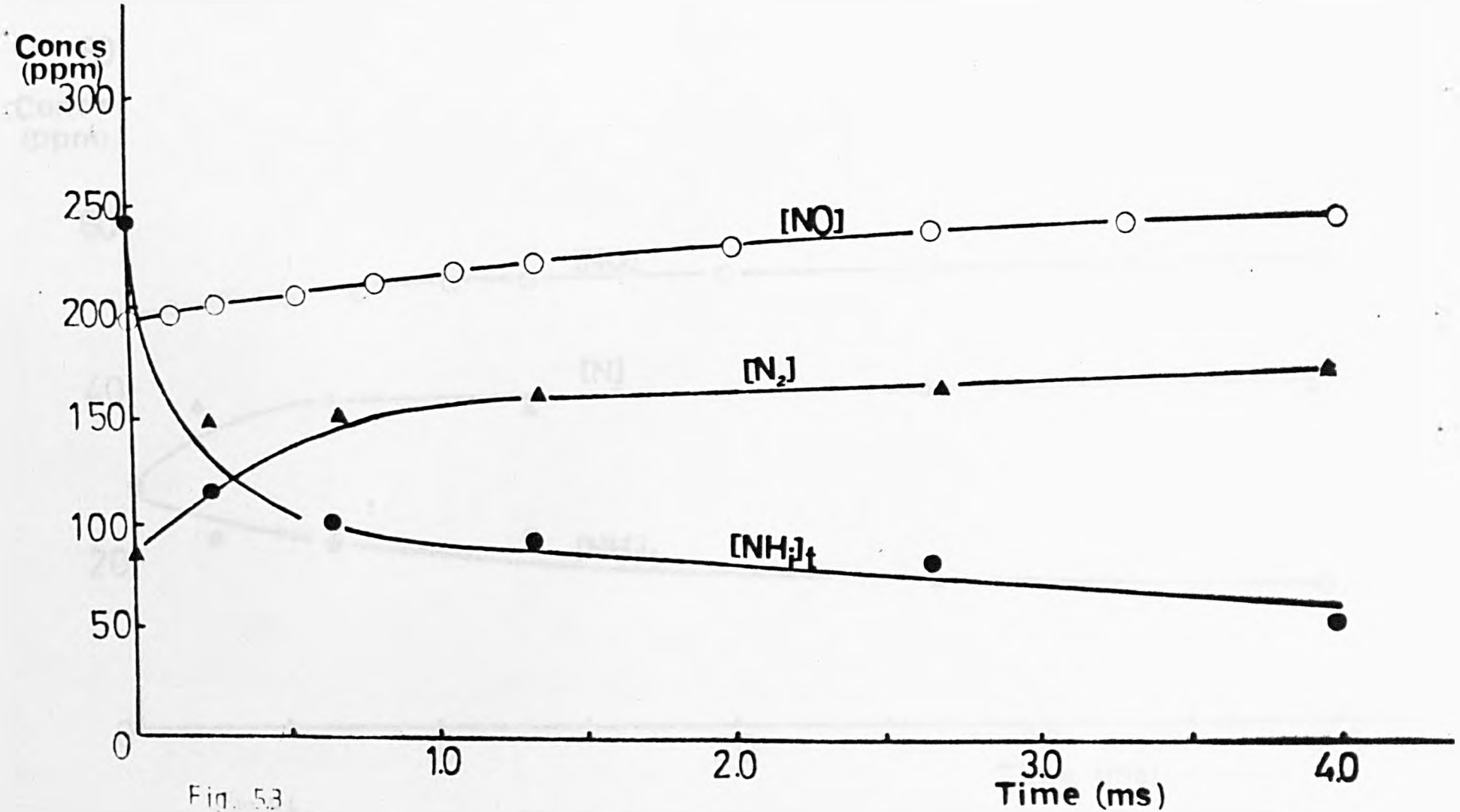

Fig. 5.3

Concentration profiles of the nitrogeneous species present in the flame with $[H_2]/[O_2]/[Ar] = 2.5/1./9.7$ and $[NH_3]_0 = 615$ ppm

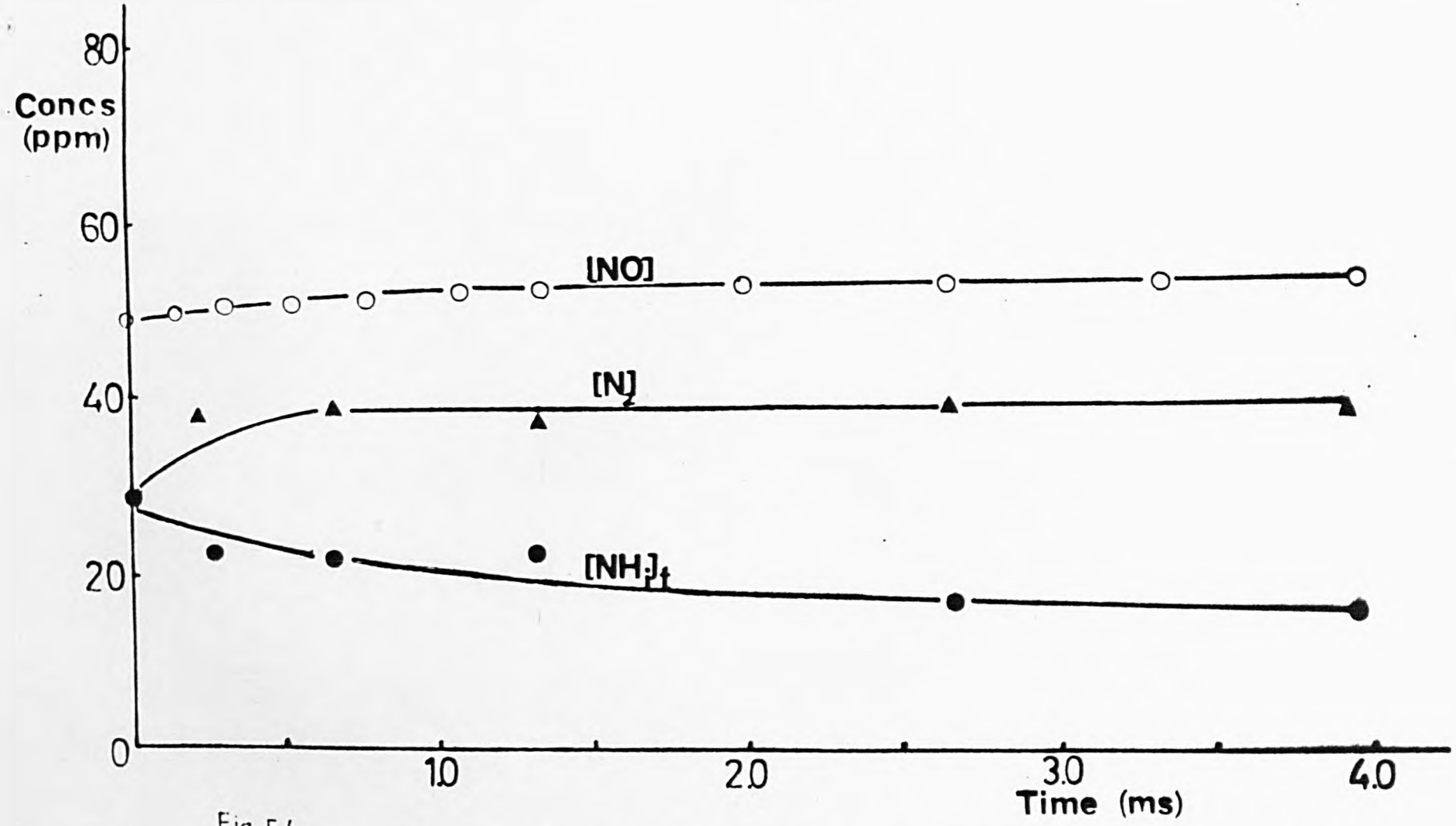

Fig. 5.4 Concentration profiles of the nitrogeneous species present in the flame with $[H_2]/[O_2]/[Ar] = 4.0/1/7.43$ and $[NH_3]_o = 125$ ppm

final amount of N_2 increases with $[NH_3]_o$. The changes observed in the concentrations of N_2, NO and of total-NH_i appear very early in the flame, i.e. by about 0.5 ms. The same behaviour is observed for richer hydrogen flames (i.e. $[H_2]/[O_2] > 2.5$). In flames with different $[H_2]/[O_2]$ ratios and the same $[NH_3]_o$, although [NO] is approximately the same, by and large more N_2 is formed in richer hydrogen flames, whilst the amount of NH_i species is bigger in the less rich flame, i.e. $[H_2]/[O_2] = 2.5$.

5.2 A mechanism of formation of NO.

5.2.1 Introduction.

As all the flames studied are hydrogen-rich, the pool of NH_i-species formed from ammonia addition is most likely to be as follows:

$$NH_3 + H = NH_2 + H_2 \qquad (1)$$

$$NH_2 + H = NH + H_2 \qquad (2)$$

$$NH + H \rightleftarrows N + H_2 \qquad (3)$$

The evidence for this state of affairs has been discussed in Chapter 2. In each case H has been chosen rather than OH, because in these flames [H] > [OH]. There is some doubt (Kaskan and Hughes 1973) as to whether reaction (3) is balanced, because of the immense reactivity of N atoms. However, assuming for the time being that all three reactions are balanced, one obtains

$$[N]/[NH]/[NH_2]/[NH_3] = K_1K_2K_3\{\gamma[H]_e/[H_2]\}^3 / K_1K_2\{\gamma[H]_e/[H_2]\}^2 / K_1\{\gamma[H]_e/[H_2]\} / 1.0$$

where the equilibrium constant K_1 refers to reaction (1), etc. Table 5.1 presents this ratio for various points along every flame studied; it should be remembered that [N] is proportional to γ^3, $[NH] \propto \gamma^2$ and $[NH_2] \propto \gamma$, if the above equilibrium formulation holds.

Table 5.1

Relative equilibrium concentration of the species present in the NH_i-pool.

$[H_2]/[O_2]$	Time (ms)	[N] / [NH] / $[NH_2]$ / $[NH_3]$
2.5	0.0	0.75 / 0.033 / 0.39 / 1.0
	1.32	0.25 / 0.017 / 0.28 / 1.0
	2.63	0.11 / 0.010 / 0.21 / 1.0
3.5	0.0	1.06 / 0.036 / 0.41 / 1.0
	0.26	0.50 / 0.027 / 0.35 / 1.0
	1.32	0.19 / 0.014 / 0.25 / 1.0
4.0	0.0	1.26 / 0.053 / 0.49 / 1.0
	0.66	0.56 / 0.029 / 0.37 / 1.0
	1.32	0.049/ 0.007 / 0.37 / 1.0

Table 5.1 shows that very near the reaction zone [N] and $[NH_3]$ are always comparable and slightly more N atoms seem to be present in richer flames. Well downstream, NH_3 becomes the most abundant species in the pool. In every flame [NH] is bordering on being negligible, particularly in the burnt gases. NH_2 is neither dominant nor unimportant. This variation in relative abundances of the various NH_i species is likely to be important in determining which one of them is e.g. reacting to produce NO at a given point in a flame.

Having dealt with equilibrium amongst the NH_i species, various reactions can be considered as possibilities for producing NO and N_2 from this pool. Altogether, those will be:

$$NH_3 + H = NH_2 + H_2 \qquad (1)$$

$$NH_3 + OH = NH_2 + H_2O \qquad (1a)$$

$$NH_2 + H = NH + H_2 \quad (2)$$

$$NH_2 + OH = NH + H_2O \quad (2a)$$

$$NH + H \rightleftharpoons N + H_2 \quad (3)$$

$$NH + OH \rightleftharpoons N + H_2O \quad (3a)$$

$$NH_i + NH_j \rightarrow N_2 + (i+j)/2\ H_2 \quad (4)$$

$$N + NH_i \rightarrow N_2 + i/2\ H_2 \quad (5)$$

$$N + OH \rightarrow NO + H \quad (6)$$

$$N + NO \rightarrow N_2 + O \quad (7)$$

$$NH_2 + OH \rightarrow NO + H + H_2 \quad (8)$$

$$NH_3 + OH \rightarrow\rightarrow NO + 2H_2 \quad (9)$$

$$NH_2 + NO \rightarrow\rightarrow N_2 + H_2O \quad (10)$$

$$NH + NO \rightarrow\rightarrow N_2 + OH \quad (11)$$

The reaction NH + OH → NO + H_2 has not been considered, because a more likely set of products is N + H_2O, which makes the reaction indistinguishable (at least as far as its dependence on γ is concerned) from the forward step of (3). Also reaction (11) has been ignored compared with (7) and (10) for producing N_2, because [NH] is relatively small, except possibly at the higher temperatures. In common with other workers (Kaskan & Hughes 1973, Iverach et al. 1973, Haynes 1977) reactions producing HNO at temperatures around 2000 K have been ignored. The reaction N + H_2O → NO + H_2 is spin forbidden and reactions of the type NH_i + H_2O → NO + $(i+2)/2 H_2$ were not considered since rate constants would be much lower than for reactions like NH_i + OH → NO + $(i+1)/2 H_2$. It is likely that the last three reactions in the above list are not simple elementary processes and this is represented by double arrows.

Before relating the above scheme of reactions to the experimental observations, it is necessary to consider the behaviour of nitrogen atoms.

Perhaps the most general procedure is to consider a steady state of affairs, so that

$$[NH]\{k_3\gamma[H]_e + k_{3a}\gamma[OH]_e\} = [N]\{k_{-3}[H_2] + k_{-3a}[H_2O] + k_5[NH_i] + k_6\gamma[OH]_e + k_7[NO]\} \quad (I)$$

The back reaction of (6) has not been included in the left hand side of eq. (I). This is because $k_{-6} = 1.3\times10^{-15}$ ml molecule^{-1}s^{-1}, so that $k_{-6}\gamma[H]_e[NO] = 1.3\times10^{-15}\times22\times1.18\times10^{15}\times7.6\times10^{14} = 2.6\times10^{6}$ molecule ml^{-1}s^{-1} at the very most. It can be deduced from the data given below in Table 5.3 that the corresponding value of the left hand side of eqn. (I) is roughly 2×10^{18} molecule ml^{-1}s^{-1}, which means that the reverse of (6) is making no contributions to the production of N atoms in the systems investigated here. Values of k_3, k_{-3}, k_5, k_6 and k_7 are given below, along with their references and degrees of uncertainty.

According to Duxbury & Pratt (1975): $k_3 = 1.0\times10^{12}\times T^{0.68}\exp(-956/T)$ ml mol^{-1}s^{-1} = $1.66\times10^{-12}\times T^{0.68}\exp(-956/T)$ ml molecule^{-1}s^{-1}, $k_{3a} = 2.66\times10^{-12}\times T^{0.56}\exp(-755/T)$ ml molecule^{-1}s^{-1}. These expressions give $k_3 = 1.7\times10^{-10}$ and $k_{3a} = 1.2\times10^{-10}$ ml molecule^{-1}s^{-1} at a temperature of 1900 K, although it has to be remembered that these are estimated values and may have very wide margins of error (Duxbury & Pratt 1975). It is instructive to compare the above k_3 with the pre-exponential factors for the rate constants of similar reactions.

Reaction	Pre-exponential factor of the rate constant (ml molecule^{-1}s^{-1})	Reference
$H + OH \rightarrow H_2 + O$	2.5×10^{-11}	Jensen & Jones 1978
$H + HF \rightarrow H_2 + F$	7.0×10^{-11}	"
$H + HCl \rightarrow H_2 + Cl$	8.1×10^{-12}	"
$H + p\text{-}H_2 \rightarrow o\text{-}H_2 + H$	8.0×10^{-11}	Schofield,1967
$H + HD \rightarrow H_2 + D$	2.3×10^{-11}	"
$H + CH_4 \rightarrow H_2 + CH_3$	6.7×10^{-11}	"
$H + HS \rightarrow H_2 + S$	2.5×10^{-11}	NBS,1977

Continued..

Reaction	Pre-exponential factor of the rate constant (ml molecule^{-1}s^{-1})	Reference
$H + HO_2 \rightarrow H_2 + O_2$	4.2×10^{-11}	McEwan & Phillips 1975
$H + CH_2O \rightarrow H_2 + CHO$	5.4×10^{-11}	"

The pre-exponential for k_3, according to the expression given above, at 1900 K is 2.8×10^{-10}, which is four times higher than the largest in the above table. On the basis that reaction (3) is similar to those in the table and also that an activation energy is not particularly expected, a reasonable estimate for k_3 would be of the order of 10^{-12} to 10^{-11} ml molecule^{-1}s^{-1} at flame temperatures. Westley (1979) quotes 5.3×10^{-12} ml molecule^{-1}s^{-1} for k_3 at 1900 K, which is lower than the values in the table. This value determined by Westley (1979) was used in the study of the kinetics of NH_3 and NO carried out by Silver et al. (1980). The same value of k_3 is also used in this study. Reaction (3a) is usually treated as kinetically similar to (3) and Duxbury & Pratt (1975), as already discussed above, estimate a slightly lower k_{3a} than k_3. However, Westley (1979) proposes a value for k_{3a} which is about 50 times bigger than his estimated k_3, i.e. 2.6×10^{-10} ml molecules^{-1}s^{-1}. The value of k_{3a} used in this work is only 4.9 times greater than k_3, i.e. 2.6×10^{-11} ml molecule^{-1}s^{-1}.

The rate constant for the reverse of reaction (3), k_{-3}, could not be found in the literature. It was therefore calculated from k_3 and the equilibrium constant K_3, which was taken from compilations (Janaf Tables 1970, 1974). Because $k_{-3} = k_3/K_3$ we have at 1900 K, $k_{-3} = 5.3 \times 10^{-12}/530 = 1.0 \times 10^{-14}$ ml molecule^{-1}s^{-1}. Also K_3 may have a high degree of uncertainty, mainly due to errors in the reported properties for NH (Janaf Tables 1975). The same holds for k_{-3a} which is $2.6 \times 10^{-11}/6.3 \times 10^{3} = 4.1 \times 10^{-15}$ ml molecule^{-1} s^{-1} at 1900 K.

NH_i in reaction (5) could be N atoms, NH, NH_2 or NH_3. Taking these in turn, we have:

i=0: the reaction is termolecular and involves a third body and in this work the most likely one is argon. Reaction (5) thus becomes $N + N + Ar \rightarrow N_2 + Ar$, for which $k_5 = 1.0 \times 10^{-33}$ $ml^2 molecule^{-2} s^{-1}$, correct to a factor of 3 (Schofield, 1967).

i=1: $k_5 = 1.7 \times 10^{-11}$ ml $molecule^{-1} s^{-1}$ (Duxbury and Pratt, 1975) at 1900 K. This is also an estimated value, so that the degree of uncertainty may be quite high.

i=2: a value for the reaction $N + NH_2 \rightarrow N_2 + H_2$ could not be found in the literature, so that, as a first approximation the same value as for i=1 is taken.

i=3: if N_2 is taken as a product, a value for the rate constant could not be found in the literature. As the reaction $N + NH_3 \rightarrow NH + NH_2$ is a hydrogen atom transfer process with $k_5 = 3.4 \times 10^{-14}$ ml $molecule^{-1} s^{-1}$ (Duxbury and Pratt 1975), it was accordingly assumed to occur. Again, the rate constant cannot be very reliable.

We are now in a position to estimate the most likely candidate for reaction (5). Table 5.2 tabulates the possibilities outlined above. Conditions in Table 5.2 refer to those at the reaction zone and the highest additions of ammonia. Concentrations are those for equilibrium. According to Table 5.2 $N + NH_2 \rightarrow 2NH$ could well be one of the candidates for reaction (5). The process $N + NH \rightarrow N_2 + H$ is about 10 times slower, but as the uncertainty associated with the first reaction is very high, both reactions will be considered for the time being in eq. (I). The other two possibilities, for which i is 0 and 3, can be rejected.

A value for k_6 at 300 K is available (NBS 1977) and is 5.3×10^{-11} ml $molecule^{-1} s^{-1}$, correct to a factor of 2. Bowman (1975) presents a value of

Table 5.2

Rates of reaction of the various possibilities for reaction (5).

i	Reaction rate in (ml molec. sec. - units)	$[H_2]/[O_2]$		
		2.5	3.5	4.0
0	$k_5[N]^2[Ar] \rightarrow$	$7.95\times10^{-34}[N]^2$	$7.01\times10^{-34}[N]^2$	$6.51\times10^{-34}[N]^2$
1	$k_5[N][NH] \rightarrow$	$1.59\times10^{-16}[N]$	$1.28\times10^{-16}[N]$	$1.66\times10^{-16}[N]$
2	$k_5[N][NH_2] \rightarrow$	$1.88\times10^{-15}[N]$	$1.46\times10^{-15}[N]$	$1.53\times10^{-15}[N]$
3	$k_5[N][NH_3] \rightarrow$	$9.62\times10^{-18}[N]$	$7.12\times10^{-18}[N]$	$6.25\times10^{-18}[N]$

1.7×10^{-10} ml molecule^{-1}s^{-1} in the range 300-2500 K, which is 3 times the above one. In studies at 1950 K by Haynes (1977), reaction (6) is referred to as forming NO, with $k_6 = 4.98 \times 10^{-11}$ ml molecule^{-1}s^{-1}. Campbell & Thrush (1968) quoted 6.8×10^{-11} ml molecule^{-1}s^{-1}, which is near the first estimate. Because of this, a value of k_6 equal to 5.3×10^{-11} ml molecule^{-1}s^{-1} was taken for the calculations in this chapter.

Between 300 K and 5000 K a value for k_7 equal to 2.7×10^{-11} ml molecule^{-1}s^{-1} was recommended by Baulch et al. (1973), correct to 30%. The above value is also assumed in this work. However, there are indications (Monat et al. 1978) that the value for the rate constant of the backward step in (7) quoted by Baulch et al. (1973) is too low by a factor of 2. In this case the value adopted here for k_7 could well be a little on the low side.

A summary of the terms in eq. (I) is presented in Table 5.3, for different flames and at various distances along them.

In calculating the above reaction rates, [NH] and [NH_2] were estimated from equilibrium concentrations. This is justified in that Kaskan and Hughes (1973) have studied the various NH_i species and have concluded that there is indeed equilibrium between NH_3, NH_2 and NH. Firstly, a comparison of the terms on the left hand side of eq. (I) will be made and then afterwards for the right hand side.

Examination of Table 5.3 reveals the higher terms on each side of eq.(I). The left hand side of eq. (I) was taken to equal $k_3[H] + k_{3a}[OH]$, since these terms are comparable. Of the terms on the right hand side of eq. (I), $k_6[OH]$ is always the biggest. The value of $k_5[NH_i]$ is always very small and negligible compared to the other terms, likewise $k_{-3a}[H_2O]$ can be ignored. The terms $k_{-3}[H_2]$ and $k_7[NO]$ are always lower than the dominant term, $k_6[OH]$. However, $k_{-3}[H_2]$ becomes more important in richer hydrogen flames and they might become comparable downstream e.g. in the flame with $[H_2]/[O_2] = 4.0$, as shown

Table 5.3

Values determined for rates of reaction and [N]/[NH] in various flames, at two distances.

Designation (s^{-1})	Time (ms)	$[H_2]/[O_2]$ = 2.5 $[NH_3]_0$		$[H_2]/[O_2]$ = 3.5 $[NH_3]_0$		$[H_2]/[O_2]$ = 4.0 $[NH_3]_0$	
		50 ppm	615 ppm	50 ppm	525 ppm	50 ppm	515 ppm
$k_{-3}[H_2]$	0.0	1.55×10^{3}	1.55×10^{3}	4.87×10^{3}	4.87×10^{3}	6.63×10^{3}	6.63×10^{3}
$k_{-3a}[H_2O]$		2.40×10^{3}	2.40×10^{3}	2.66×10^{3}	2.66×10^{3}	2.72×10^{3}	2.72×10^{3}
$k_5[NH]$		49.8	614	47.1	495	62.2	641
$k_5[NH_2]$		591	7.30×10^{3}	537	5.60×10^{3}	572	5.90×10^{3}
$k_6\gamma[OH]_e$		8.71×10^{4}	8.71×10^{4}	9.20×10^{4}	9.20×10^{4}	1.22×10^{5}	1.22×10^{5}
$k_7[NO]$		2.20×10^{3}	2.10×10^{3}	2.40×10^{3}	1.91×10^{4}	2.50×10^{3}	1.92×10^{4}
$k_3\gamma[H]_e$		2.80×10^{4}	2.80×10^{4}	8.44×10^{4}	8.44×10^{4}	1.46×10^{5}	1.46×10^{5}
$k_3\gamma[OH]_e$		4.17×10^{4}	4.17×10^{4}	4.41×10^{4}	4.41×10^{4}	5.39×10^{4}	5.39×10^{4}
[N]/[NH]		0.75	0.75	1.26	1.08	1.49	1.33
$([N]/[NH])_e$		18.1	18.1	17.3	17.3	22.0	22.0
$([N]/[N]_e)$		0.041	0.041	0.073	0.062	0.068	0.060
$k_{-3}[H_2]$	1.32	1.55×10^{3}	1.55×10^{3}	4.87×10^{3}	4.87×10^{3}	6.63×10^{3}	6.63×10^{3}
$k_{-3}[H_2O]$		2.40×10^{3}	2.40×10^{3}	2.66×10^{3}	2.66×10^{3}	2.72×10^{3}	2.72×10^{3}
$k_5[NH]$		39.4	444	34.4	332	18.0	170
$k_5[NH_2]$		645	7.30×10^{3}	614	5.90×10^{3}	437	4.10×10^{3}
$k_6\gamma[OH]_e$		6.20×10^{4}	6.20×10^{4}	6.05×10^{4}	6.05×10^{4}	7.11×10^{4}	7.11×10^{4}
$k_7[NO]$		2.91×10^{3}	2.70×10^{4}	2.90×10^{3}	2.42×10^{4}	3.11×10^{3}	2.40×10^{4}
$k_3\gamma[H]_e$		1.90×10^{4}	1.90×10^{4}	5.51×10^{4}	5.51×10^{4}	8.70×10^{4}	8.70×10^{4}
$k_{3a}\gamma[OH]_e$		3.04×10^{4}	3.04×10^{4}	2.97×10^{4}	2.97×10^{4}	3.49×10^{4}	3.49×10^{4}
[N]/[NH]		0.72	0.53	1.20	0.92	1.46	1.17
$([N]/[NH])_e$		12.3	12.3	11.3	11.3	13.1	13.1
$[N]/[N]_e$		0.059	0.043	0.1	0.081	0.11	0.089

in Table 5.3. The term $k_7[NO]$ becomes more or less important depending upon the amounts of ammonia added. Hence, the above three terms should appear as equally important in the right hand side of eq. (I). Following from this the parameter $\sigma = [N]/[NH]$ is given by:

$$\sigma = (k_3\gamma[H]_e + k_{3a}\gamma[OH]_e)/(k_6\gamma[OH]_e + k_{-3}[H_2] + k_7[NO]). \quad (II)$$

We are now in a position to investigate if there is sufficient time for a steady-state to be established between nitrogen atoms and NH radicals. The concentration of N atoms varies according to: $d[N]/dt = a[NH] - b[N]$, in the reaction zone, where a and b are constants. As NH is in equilibrium with NH_2 and NH_3, we might assume that [NH] is constant and independent of time in the reaction zone. In this case, d[N]/dt turns out to be $d[N]/dt = a'-b[N]$, with $a' = a[NH]_{R.Z.}$. If the relaxation time is defined as the time taken for [N] to reach a[NH]/be, where e is the base of Napierian logarithms, that time equals $\int_0^{a'/be} \frac{d[N]}{(a'-b[N])}$. The relaxation time is equal to $\frac{1}{b}\{1-\ell n(e-1)\}$ which is approximately 1/b. Considering the flame with $[H_2]/[O_2] = 4.0$ and $[NH_3]_0 = 50$ ppm, d[N]/dt is $5.4\times10^4[NH] - 1.3\times10^5[N]$ for conditions near the reaction zone, and the relaxation time turns out to be approximately 7.7 μs. As the residence time in the reaction zone is around 20 μs, the steady-state is indeed just established within the reaction zone. It, therefore, seems reasonable to consider such a state of affairs from the reaction zone onwards, the relaxation time will be even shorter for appreciable concentrations of NH_3. We can thus conclude that, because of the make-up of eq. (II), N atoms are governed by a steady-state, rather than a balance of reaction (3).

Kaskan & Hughes (1973) have studied the extent of equilibration in the NH_i-pool, by burning NH_3/O_2 flames at atmospheric pressure and 2010 K. They found that NH_3 and NH_2 were nearly equilibrated *via* $NH_3 + OH = NH_2 + H_2O$. The concentrations of OH in the $[H_2]/[O_2]$ flames burned in this work were

about ten times lower than in those of Kaskan & Hughes (1973), with [H] expected to be much higher here. Reactions such as (1) and (2) are known to be equilibrated (Nadler et al. 1970, Kaskan & Nadler 1973). This equilibration was assumed in mixtures of $H_2 + N_2O + N_2$ in a heated quartz vessel by Fenimore (1978) and by Haynes (1977) for fuel-rich hydrocarbon flames. Estimates of the relaxation times of reactions (1) and (2) indicate that both are balanced in times less than 20 μs for the conditions of this work.

Table 5.3 presents steady-state values for [N]/[NH] as derived from eq. (II). They can be compared with the values, (also given in Table 5.3) of this ratio if equilibrium holds between N and NH. For equilibrium we have $k_3[H][NH] = k_{-3}[H_2][N]$ or $([N]/[NH])_{eq} = K_3[H]/[H_2]$, which depends upon γ. The values of $([N]/[NH])_{eq}$ in Table 5.3 are always much larger than steady-state values of [N]/[NH]. Since, [NH] can be taken as the equilibrium concentration (Kaskan & Hughes 1973, Haynes 1977, Nadler et al. 1970, Kaskan & Nadler 1973) the ratio $([N]/[NH])/([N]/[NH])_{eq}$ is equal to $[N]/[N]_e$ where $[N]_e$ is the concentration of N atoms in the fully balanced pool. Values for $[N]/[N]_e$ are also presented in the final line in Table 5.3. It will be seen that the concentration of N atoms is always lower than the one at equilibrium. Kaskan and Hughes (1973) found the concentration of N atoms in ammonia flames to be lower than that predicted on equilibrium considerations and they reported a value of 2 to 3% for $[N]/[N]_e$. It is interesting to note that the values for $[N]/[N]_e$ given in Table 5.3 agree with those found by Kaskan & Hughes (1973). Of course, it should not be forgotten that the flames used in this work were different from theirs.

In the next section, calculations are done taking values for [N]/[NH] as described above. The concentrations of NH_i - species are determined as functions of $[NH_3]$, and this is obtained from a mass balance on the pool, i.e.,

$$[NH_i]_t = [NH_3] + [NH_2] + [NH] + [N]$$

$$= [NH_3]\{1 + K_1\gamma[H]_e/[H_2] + (1+\sigma)K_1K_2\gamma^2 \times ([H]_e/[H_2])^2\}$$

so that, $[NH_3] = [NH_i]_t/\{1 + \alpha\gamma + \beta(\sigma+1)\gamma^2\}$

$$= [NH_i]_t/\tau$$

with

$\alpha = K_1[H]_e/[H_2] = \gamma[NH_2]/[NH_3]$

$\beta = K_1K_2([H]_e/[H_2])^2 = \gamma^2[NH]/[NH_3]$

$\sigma = [N]/[NH]$

$\tau = \{1 + \alpha\gamma + \beta(\sigma+1)\gamma^2\}$.

As the amount of N atoms present is much lower than might have been expected, it is possible that NH_2 and even NH_3 play a part in the production of NO and N_2. Certainly, the above considerations show that NH_3 and NH_2 are the dominant NH_i species well downstream in a flame (where $\gamma \to 1$), but of course N atoms have their greatest concentrations in the reaction zone ($\gamma >> 1$).

5.2.2 Theoretical studies on the formation and disappearance of nitric oxide.

Equations will now be derived to ascertain whether the experimental observations fit the predictions of various mechanisms of production and disappearance of NO. Assuming first that NO is formed through NH_2 reacting with OH and disappears by reacting with NH_2 in reaction (10) to form N_2, $d[NO]/dt$ equals $k_8[NH_2][OH] - k_{10}[NH_2][NO]$, or

$$\frac{d[NO]/dt}{[NH_2][NO]} = k_8\frac{\gamma[OH]_e}{[NO]} - k_{10}. \qquad \text{(III)}$$

In the previous section, [NH], $[NH_2]$ and $[NH_3]$ were found to be in equilibrium with one another and $[N]/[NH] = \sigma$ is given by the steady state relationship

(II). Eq. (III) thus becomes:

$$([H_2]\tau\ d[NO]/dt)/(K_1\gamma[H]_e[NH_i]_t[NO]) = k_8(\gamma[OH]_e/[NO]) - k_{10}. \qquad (IV)$$

This will be checked by plotting the experimental results as the left hand side of eq. (IV) against $\gamma[OH]_e/[NO]$.

As an alternative scenario, we might assume that the net rate of production of NO is given by:

$$d[NO]/dt = k_9[NH_3][OH] - k_{10}[NH_2][NO]$$

which gives:

$$([H_2]\tau\ d[NO]/dt)/(K_1\gamma[H]_e[NH_i]_t[NO]) = k_9\{([H_2][OH])/(K_1[H][NO])\} - k_{10}. \qquad (V)$$

The left hand side of eq. (V) will be plotted against $[H_2][OH]/(K_1[H][NO])$ to check it with the experimental measurements.

As a third possibility, if the formation and disappearance of NO is assumed to be <u>via</u> N atoms:

$$d[NO]/dt = k_6[N][OH] - k_7[N][NO] \quad ,$$

with [N] given by the steady state relationship (II), leading to:

$$\frac{[NO]}{\gamma[OH]_e} \cdot \frac{[H_2]^2\tau\ d[NO]/dt}{K_1K_2\gamma^2[H]_e^2[NH_i]_t} \cdot \frac{\left(\frac{k_6}{k_7} \cdot \frac{\gamma[OH]_e}{[NO]} + 1\right) + \frac{k_{-3}}{k_7}\frac{[H_2]}{[NO]}}{\left(\frac{k_6}{k_7}\frac{\gamma[OH]_e}{[NO]} - 1\right)} =$$

$$\left(k_3\frac{[H]_e}{[OH]_e} + k_{3a}\right)[NO] \; . \qquad (VI)$$

This equation can be tested by plotting its left hand against [NO].

Other sets of combinations of the type $NH_i + OH \rightarrow NO$ + products and $NH_i' + NO \rightarrow N_2$ + products were also checked against the experimental results. However, none of these plots are presented due either to bad fits or to unreasonable values for rate constants being derived from the slope and intercept. These schemes will thus be rejected out of hand.

In the following section, eq. (IV) - (VI) will be checked against the experimental observations to determine the best fit and obtain the corresponding rate constants. It is hoped that this will reveal the reaction mechanism most consistent with the measurements obtained.

5.2.3 Discussion of the observations in flames at 1900 K with ammonia added alone.

Eq. (IV) was first checked with the experimental measurements obtained in all the flames studied for various amounts of ammonia added. Some plots are given in Fig. 5.5 which shows scatter amongst the points near the reaction zone, which are those with higher rates of reaction and Υ values. The points for 50 ppm of NH_3 present are notable in being farthest away from what might be considered a best line fit. Fig.5.6 checks the same reaction mechanism, but leaves out the points near the reaction zone, i.e. those up to 2 mm from it. There is now a tolerable fit to one straight line, which has slope and intercept yielding, respectively, $k_8 = (9.7\pm2.0)\times10^{-13}$ ml molecule^{-1} s^{-1} and $k_{10} = (4.6\pm1.0) \times 10^{-12}$ ml molecule^{-1}s^{-1}. This pair of reactions seems possible well downstream in this flame, but improbable close to the reaction zone.

Eq. (V) will now be checked against the experimental measurements and the appropriate plot is given in Fig.5.7. It is clear from Fig.5.7 that three straight lines, rather than one, have to be drawn through the experimental points. The slope of these almost parallel lines gives k_9 equal to $(4.5\pm1.4)\times10^{-12}$ ml molecule^{-1}s^{-1}; however, three different values for k_{10} are obtained, which is at variance with the model.

Next, eq. (VI) is checked in Fig. 5.8. Also in this plot it is not possible to fit one single straight line through all the points. Each amount of added ammonia defines a set of points through which lines can be fitted. If in addition, it is assumed that $k_{3a} = 5k_3$, the value of k_3 given by the slope is within the range 5×10^{-11} - 1×10^{-10} ml molecule^{-1}s^{-1}.

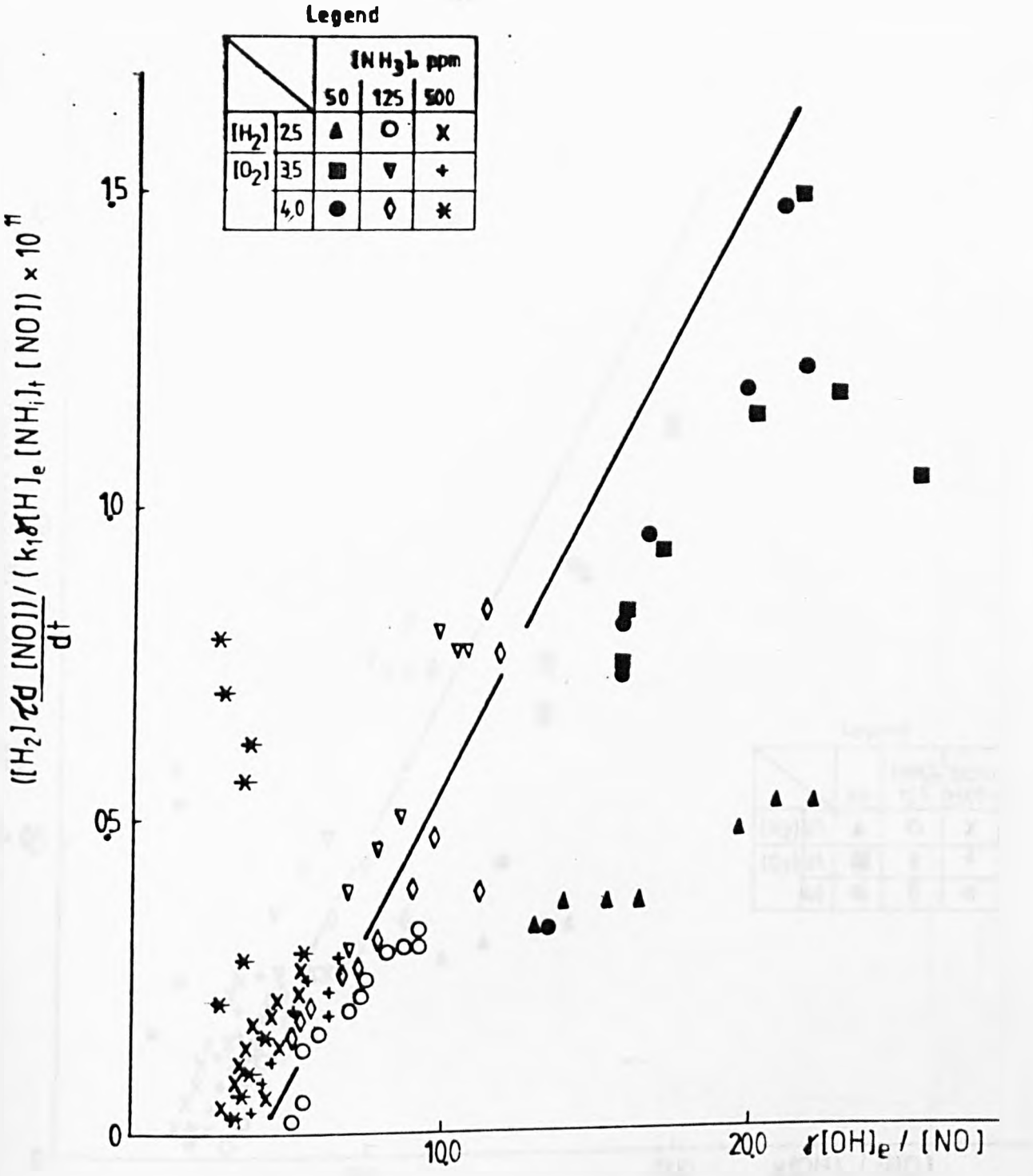

Fig 5.5 Plot to check the kinetic scheme in flames 2, 4 and 6

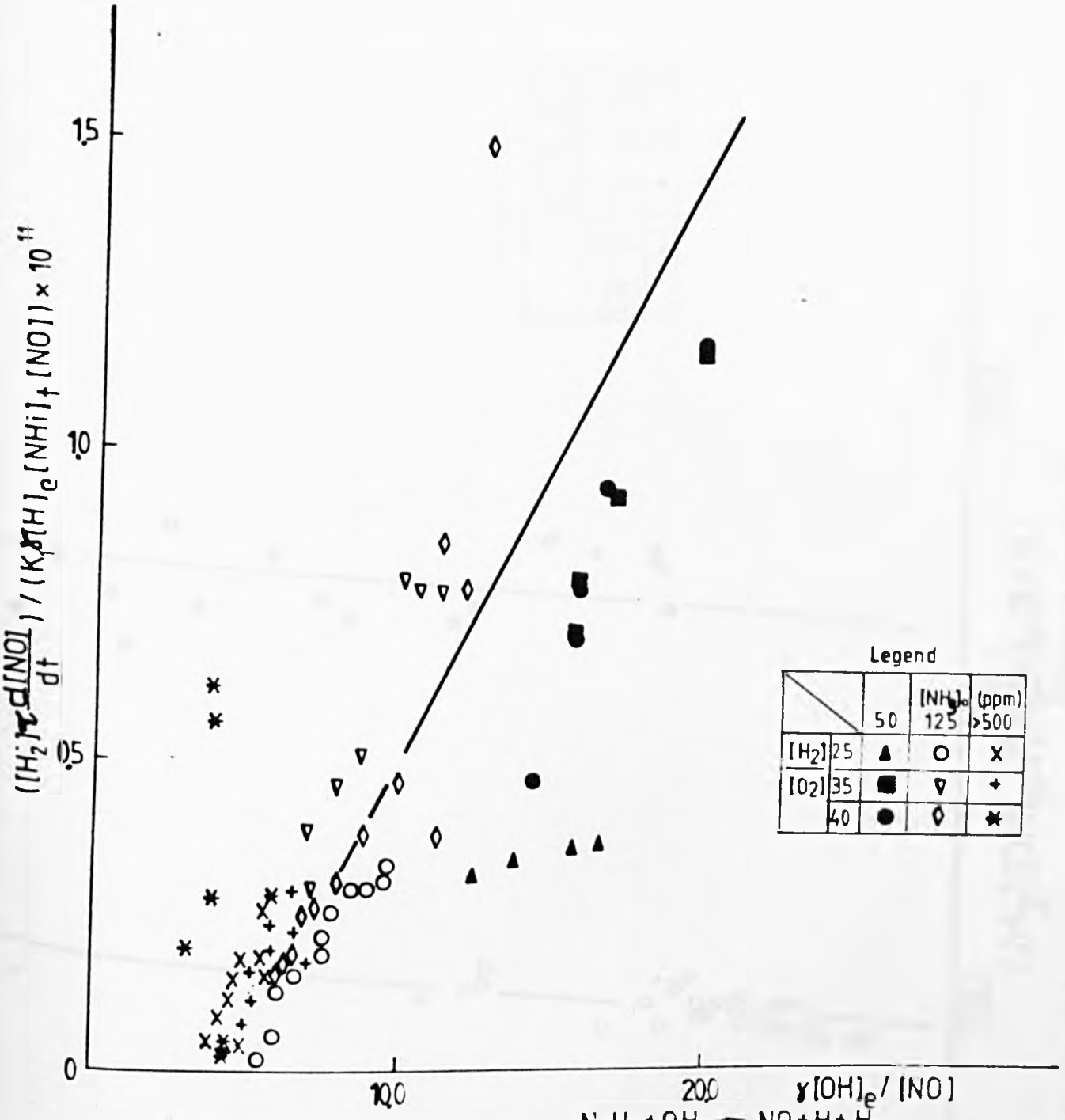

Fig. 56 Plot to check the scheme

$$N + H_2 + OH \longrightarrow NO + H + H_2$$

$$N + H_2 + NO \longrightarrow N_2 + H_2O$$

omitting points nearest the reaction zone in flames 2,4 and 6

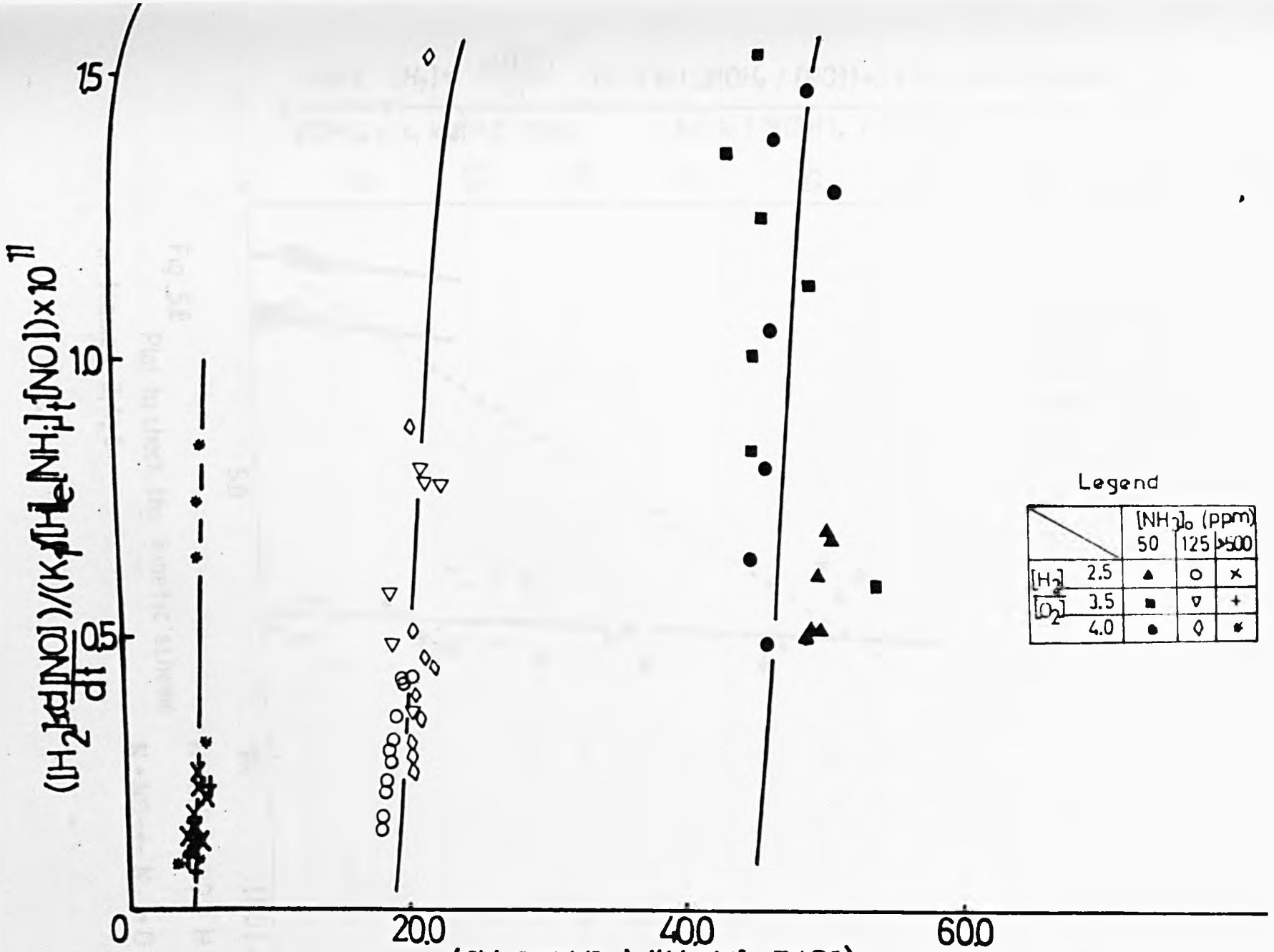

Fig. 5.7

Plot to check the kinetic scheme $\begin{cases} NH_3 + OH \rightarrow NO + 2H_2 \\ NH_3 + NO \rightarrow N_2 + H_2O \end{cases}$ in flames 2,4,6

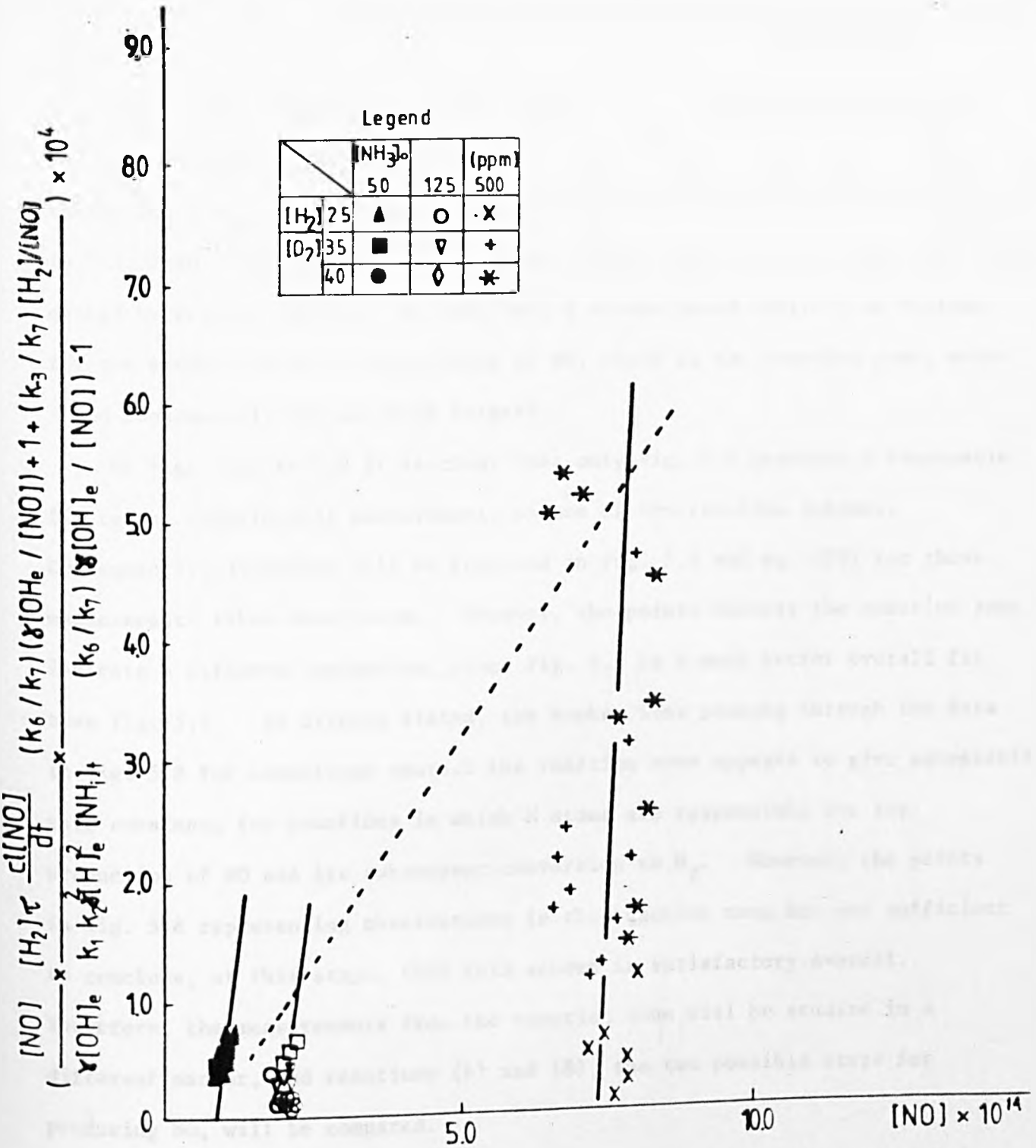

Fig 5.8 Plot to check the kinetic scheme in flames 2, 4, 6

These values are bigger than those in the literature. It thus seems likely that N atoms do not play a role throughout the whole length of the flame. However, if a line is fitted through the points measured close to the reaction zone, especially those for richer flames (the broken line in Fig.5.8), a straight line through the origin is obtained, in agreement with eq. (VI). The slope yields $(k_3[H]_e/[OH]_e + k_{3a}) = 7.5\times10^{-11}$ ml molecule^{-1}s^{-1}. Also, taking $5k_3 \simeq k_{3a}$, k_3 turns out to be $(6.2\pm5.0)\times10^{-12}$ ml molecule^{-1}s^{-1} and $k_{3a} = (3.1\pm2.0)\times10^{-11}$ ml molecule^{-1}s^{-1}. These values agree to within 50% with those quoted by Westley (1979). We thus have a scheme based entirely on N atoms for the production and disappearance of NO, close to the reaction zone, where $\dot{Y}$ and consequently [N] are both largest.

Of Figs. 5.5 to 5.8 it is clear that only Fig. 5.6 provides a reasonable fit to the experimental measurements of one of the reaction schemes. Consequently, attention will be focussed on Fig. 5.6 and eq. (IV) for those measurements taken downstream. However, the points nearest the reaction zone indicate a different mechanism, since Fig. 5.6 is a much better overall fit than Fig. 5.5. As already stated, the broken line passing through the data in Fig. 5.8 for conditions nearest the reaction zone appears to give acceptable rate constants for reactions in which N atoms are responsible for the production of NO and its subsequent conversion to N_2. However, the points in Fig. 5.8 representing observations in the reaction zone are not sufficient to conclude, at this stage, that this scheme is satisfactory overall. Therefore, the measurements from the reaction zone will be studied in a different manner, and reactions (6) and (8), the two possible steps for producing NO, will be compared.

In flames with only 50 ppm of ammonia added the amount of N_2 formed in the reaction zone is negligible so that

$$[NH_3]_0 = [NH_3] + [NH_2] + [NH] + [N] + [NO].$$

By definition

$$[NH_2]/[NH_3] = K_1 \gamma [H]_e/[H_2] = \alpha\gamma$$

$$[NH]/[NH_3] = K_1K_2 \gamma^2 [H]_e^2/[H_2]^2 = \beta\gamma^2$$

$$[N]/[NH] = \sigma = \left(k_3 \gamma [H]_e + k_{3a} \gamma [OH]_e\right) / \left(k_6\gamma[OH]_e + k_7[NO] + k_{-3}[H_2]\right)$$

or

$$[NH_3]_0 - [NO] = [NH_3]\left(1 + \alpha\gamma + \beta\gamma^2 (1+\sigma)\right),$$

i.e.

$$[NH_3] = \frac{[NH_3]_0 - [NO]}{\left(1+\alpha\gamma+\beta\gamma^2(1+\sigma)\right)}$$

and,

$$[N] = \frac{\sigma\beta\gamma^2 \left([NH_3]_0 - [NO]\right)}{\left(1 + \alpha\gamma + \beta\gamma^2 (1+\sigma)\right)}$$

$$[NH_2] = \frac{\alpha\gamma\left([NH_3]_0 - [NO]\right)}{\left(1 + \alpha\gamma + \beta\gamma^2(1+\sigma)\right)}$$

Let us consider now two possible kinetic schemes for the reaction zone:

$$N + OH \rightarrow NO + H \qquad (6)$$

$$NH_2 + OH \rightarrow NO + H + H_2 \qquad (8)$$

For (6) the rate of appearance of NO can be given by:

$$d[NO]/dt = k_6 [N] [OH]$$

$$= k_6 \frac{\sigma\beta\gamma^3 \left([NH_3]_0 - [NO]\right) [OH]_e}{\{1 + \alpha\gamma + \beta\gamma^2 (1 + \sigma)\}}$$

We shall assume that reactions in the reaction zone can be modelled as a plug flow reactor with residence time t_o and time independent or fixed γ, the above relation can be integrated, yielding:

$$\ell n \left(\frac{[NH_3]_0}{[NH_3]_0 - [NO]_{R.Z.}} \right) = \ell n \left(\frac{1}{1 - \frac{[NO]_{R.Z.}}{[NH_3]_0}} \right)$$

$$= \frac{k_6 \, \sigma \, \beta\gamma^3 \, [OH]_e \, t_o}{\{1 + \alpha\gamma + \beta\gamma^2(1+\sigma)\}} \qquad \text{(VII)}$$

Similar consideration of Reaction (8) gives:

$$d[NO]/dt = k_8 \, [NH_2] \, [OH]$$

$$= k_8 \, \frac{\alpha\gamma^2 \, \{[NH_3]_0 - [NO]\} \, [OH]_e}{\{1 + \alpha\gamma + \beta\gamma^2 \, (1 + \sigma)\}} \, ,$$

leading to:

$$\ell n \left(\frac{1}{1 - \frac{[NO]_{R.Z.}}{[NH_3]_0}} \right) = k_8 \, \frac{\alpha\gamma^2 \, [OH]_e \, t_o}{\{1 + \alpha\gamma + \beta\gamma^2(1+\sigma)\}} \, . \qquad \text{(VIII)}$$

The left hand sides of eq. (VII) and (VIII) are plotted in Figs. 5.9 and 5.10 against $(\sigma\beta\gamma^2 \, [OH]_e \, t_o)/(1 + \alpha\gamma + \beta(\sigma+1)\gamma^2)$ and $(\alpha\gamma^2 \, [OH]_e \, t_o)/(1+\alpha\gamma+\beta(\sigma+1)\gamma^2)$ respectively. Unfortunately, only three points are available. The plot in Fig.5.10 does not agree with eq. (VIII), because most probably it has a negative slope and a positive intercept, instead of a positive slope and zero intercept. However, Fig.5.9 is much more consistent with a straight line through the origin, as suggested by eq. (VII). The value of k_6 determined from the slope of that line is inevitably crude, because of all the above assumptions and a lack of knowledge of t_o. The value indicated for k_6 is $(5\pm5) \times 10^{-10}$ ml molecule^{-1} s^{-1}, which is about 1 order of magnitude higher than those quoted before (Campbell & Thrush 1968, Haynes 1977, NBS 1977). Only Bowman (1975) quotes a value for k_6 as high as 1.7×10^{-10} ml molecule^{-1}s^{-1}. Although k_6 appears on the large side, it seems that N atoms are more likely to be the species responsible for the appearance of NO in and close to the reaction zone.

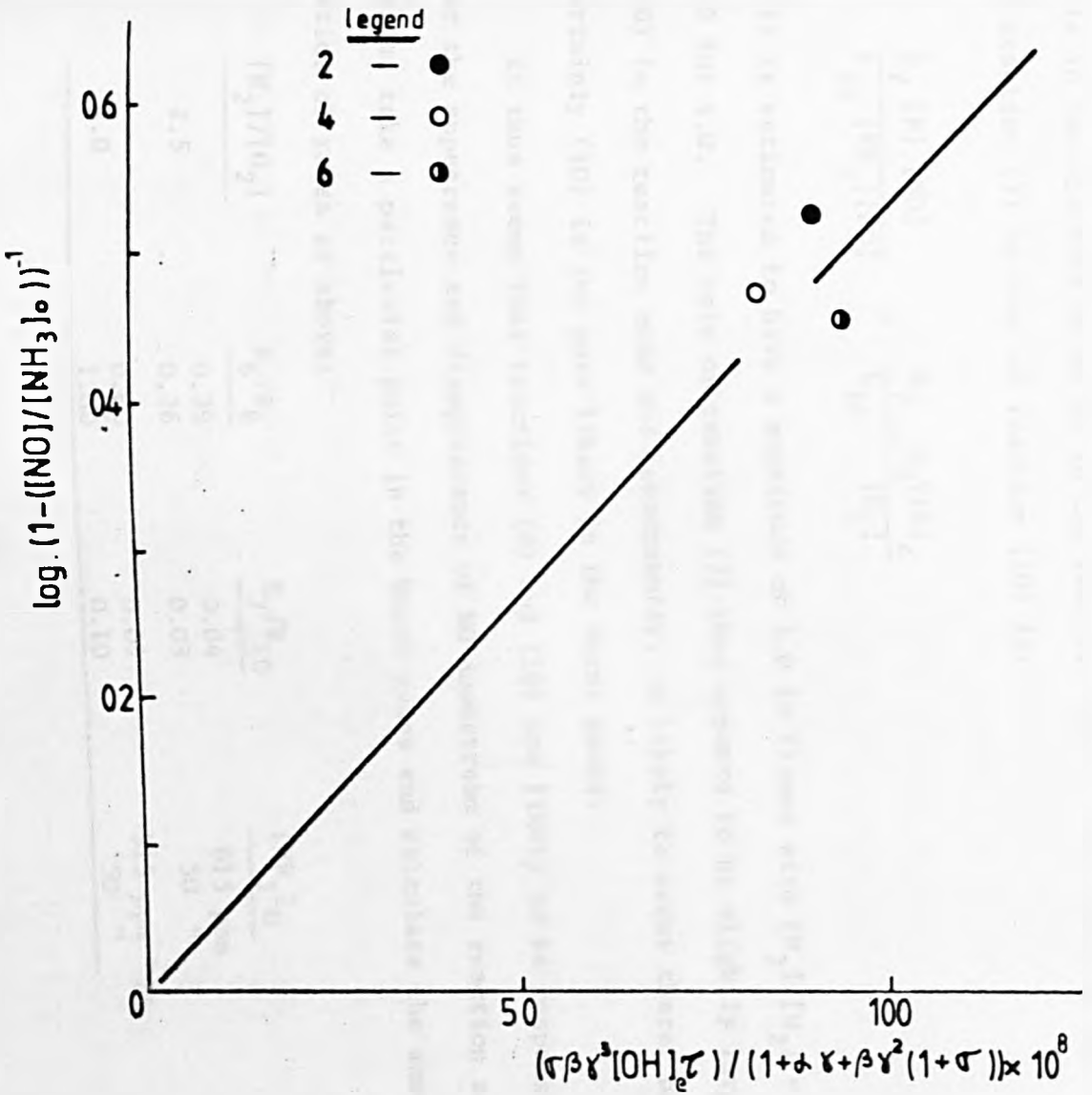

Fig. 5.9 Plot to check N + OH → NO + H with [NO] measured in the reaction zone in flames 2,4 and 6

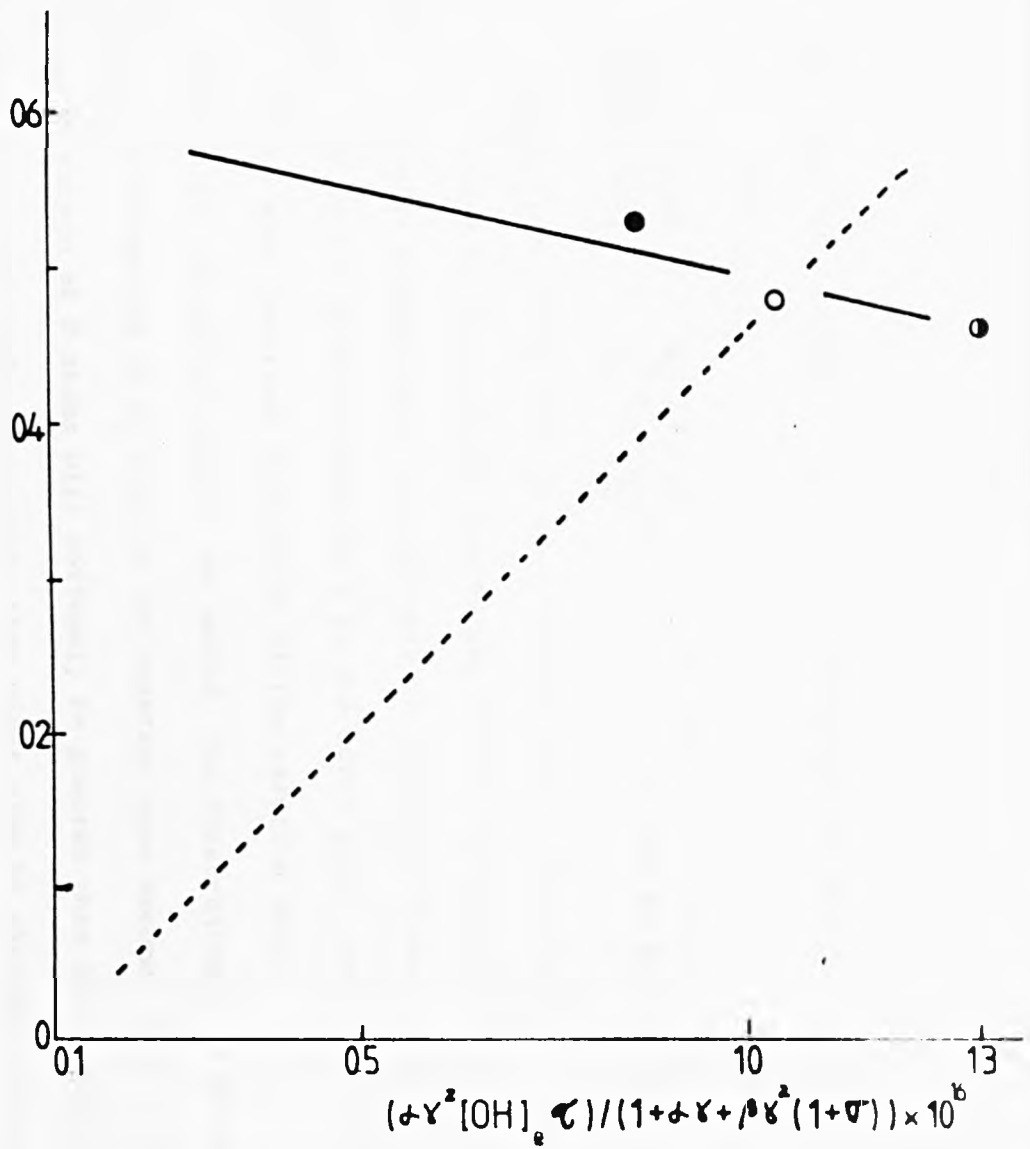

Fig. 5.10 Plot to check NH_2 + OH → NO + H + H_2 with [NO] measured in the reaction zone in flames 2,4 and 6

Finally, let us compare the rates of formation of NO via (6) and (8). Their ratio is:

$$\frac{k_6\,[N]\,[OH]}{k_8[NH_2][OH]} = \frac{k_6}{k_8}\,\sigma\,\frac{K_2\gamma[H]_e}{[H_2]}$$

, the estimatedvalue of which ranges from 5.3 to 10.3 in the reaction zone. This confirms the above conclusion of reaction (6) dominating (8) in the reaction zone. The ratio is however proportional to γ so that in a typical flame γ might decrease from say 20 in the reaction zone to 2 in the burnt gases, enabling reaction (8) to become more important downstream of the reaction zone.

When large amounts of ammonia are added, the disappearance of NO and a consequent formation of N_2 even in the reaction zone becomes more important. The concentration of N atoms will obviously be greater than in flames with 50 ppm of NH_3 added, and consequently they might also be expected to play a role in the destruction of NO in the reaction zone. The ratio of the rate of reaction (7) to that of reaction (10) is:

$$\frac{k_7\,[N]\,[NO]}{k_{10}\,[NH_2][NO]} = \frac{k_7}{k_{10}}\,\sigma\,\frac{K_2\gamma[H]_e}{[H_2]}$$

This is estimated to have a magnitude of 1.0 in flames with $[H_2]/[O_2] = 2.5$ and 1.9 for 4.0. The rate of reaction (7) thus appears to be slightly larger than (10) in the reaction zone and consequently, is likely to occur there, but certainly (10) is the more likely in the burnt gases.

It thus seems that reactions (8) and (10) are likely to be responsible for the appearance and disappearance of NO downstream of the reaction zone. Let us take a particular point in the burnt gases and calculate the same ratios of rates as above:

$[H_2]/[O_2]$	R_6/R_8	R_7/R_{10}	$[NH_3]_0$
2.5	0.39	0.04	615 ppm
	0.26	0.03	50 "
4.0	0.80	0.09	515 ppm
	1.00	0.10	50 "

The above table confirms the conclusion drawn before on the important steps in the production and destruction of nitric oxide.

5.2.4 An overall look at the observations in flames at 1900 K with ammonia added.

Chapter 2 discussed what various investigators had proposed as kinetic schemes for the formation and disappearance of NO in various flames at different temperatures (Haynes 1977, Iverach *et al.* 1975, Fenimore 1971, 1972, 1975, 1976, 1978, Kaskan & Hughes 1973). For reaction (10), Silver *et al.* (1980) found a rate constant of 2.3×10^{-12} ml molecule^{-1} s^{-1} at 1200 K. The rate coefficient was given in terms of $AT^n \exp(-E/RT)$, with $n<0$. Fenimore (1978) quoted a higher value for k_{10}, *i.e.* 8.3×10^{-12} ml molecule^{-1}s^{-1} within the range 1300 - 1400 K. In our study at 1900 K, $k_{10} = (4.6 \pm 1.0) \times 10^{-12}$ ml molecule^{-1}s^{-1} which is 0.55 of Fenimore's, twice that obtained by Silver *et al.* (1980) and consequently 'acceptable' in magnitude.

Unfortunately, a value for k_8 was not found in the literature. Fenimore (1976) concluded that reaction (8) might be responsible for the formation of NO, but in a later study he concluded (Fenimore 1978) that H_2O rather than OH attacks the NH_i-pool. The observations of this study indicate that the reaction $NH_i + H_2O \rightarrow NO +$ products is not occurring, because very poor fits of the experimental data were obtained to the predictions of the model based on NO arising from reaction between H_2O and NH_i species. The rate of the reaction reported by Fenimore (1978) as being responsible for the appearance of nitric oxide, is quoted as having the same value as its disappearance, *i.e.* $k[NH_2][H_2O] = k_{10}[NH_2][NO] = 8.3 \times 10^{-12} [NH_2][NO]$ or $k = 8.3 \times 10^{-12} [NO]/[H_2O]$. This indicates a low value for k of around 10^{-14} ml molecule^{-1}s^{-1}. Fenimore (1978) thought the generation of NO to be a multi-step scheme with the formation of hydroxylamine in:

$$NH_2 + H_2O = NH_2OH + H \quad (\Delta H = 247 \text{ kJ/mol})$$

$$NH_2OH + H \rightarrow NH_2O + H_2$$

$$NH_2O + H \rightarrow NH_2 + OH$$

$$NH_2O + H \rightarrow H_2 + HNO$$

$$HNO = H + NO$$

Emerging from our work is the proposal that OH instead of H_2O reacts with NH_2 in reaction (8). The first step could yield either NH_2OH or NHOH + H, with the above subsequent reactions. Unfortunately, the presence of species like NH_2OH, NHOH or HNO, was not investigated and consequently there is no direct evidence for the fine details of such a mechanism. However, $(9.7\pm2.3) \times 10^{-13}$ ml molecule^{-1}s^{-1} appears to be a reasonable value for the rate constant of (8), if the process does indeed involve more than one elementary step.

The occurrence of reactions (8) and (10) in the burnt gases, and (6) and (7) close to the reaction zone was discussed above and compared with others (i.e., NH_i + OH or NH_i + NO to give NO or N_2, respectively, where i = 0, 1, 2 and 3). The fast appearance of NO in and close to the reaction zone is explained by the major role played by N atoms in producing NO in that area. Values for k_6, k_3 and k_{3a} cannot be determined accurately, due to lack of sufficient data. However, they agree within a factor of 1.8 with those values in the literature (Westley 1978, Bowman 1975, Campbell & Thrush 1968).

The fact that slight temperature variations occur along the early part of most flames and that γ_{OH} has been considered equal to γ_H, alter somewhat the values derived for the rate constants k_3, k_{3a}, k_6, k_7, k_8 and k_{10}. Let us assume that γ_{OH} is about 50% of that for H atoms in richer hydrogen flames. The temperature variations will involve a shift of points in Fig. 5.6 towards zero abcissa. This yields a decrease in the derived k_{10} to a

value probably approaching that of Silver et al. (1980). The same will occur in Fig.5.7. As for Fig.5.8, although the points will be shifted in the upward direction, the slope will not be altered. This, in turn, will not cause any major change in the conclusions on the most probable mechanism, but could give rise to a lower rate constant for reaction (10).

Before flames at different temperatures are studied, the formation of molecular nitrogen will be discussed in the following section.

5.2.5 The production of N_2.

It has been shown that whatever the amount of ammonia added to a flame, the formation of N_2 downstream of the reaction zone is satisfactorily represented by reaction (10). The concentration of N_2 was not measured but was calculated by a mass balance on nitrogenous species. If (10) is the only reaction which gives rise to N_2,

$$d[N_2]/dt = k_{10} [NH_2] [NO], \text{ or}$$

$$\frac{d[N_2]}{dt} = k_{10} \frac{K_1 \gamma [H]_e [NH_i]_t [NO]}{\tau [H_2]} \quad . \qquad \text{(IX)}.$$

The left hand side of eq. (IX) is plotted against $(K_1 \gamma [H]_e [NH_i]_t [NO])/(\tau[H_2])$ in Fig.5.11. Due to lack of sufficient data, the rates of production of N_2 were determined from the slopes of the tangents at each point on the profile of $[N_2]$ versus time (see Figs. 5.1 to 5.4), described in section 5.3. The points nearest to the reaction zone are those with highest rates of reaction. The points in Fig.5.11 are very scattered. The line drawn in Fig.5.11 refers to the points well downstream, where reaction (10) is more likely to occur. This line passes through the origin which conforms with eq. (IX). The resulting value of k_{10} is $(1.2\pm0.8) \times 10^{-11}$ ml molecule^{-1}s^{-1}, which is bigger than that $(4.6\pm1.0) \times 10^{-12}$ ml molecule^{-1}s^{-1} obtained above, as well as the similar values in the literature. This plot also agrees with

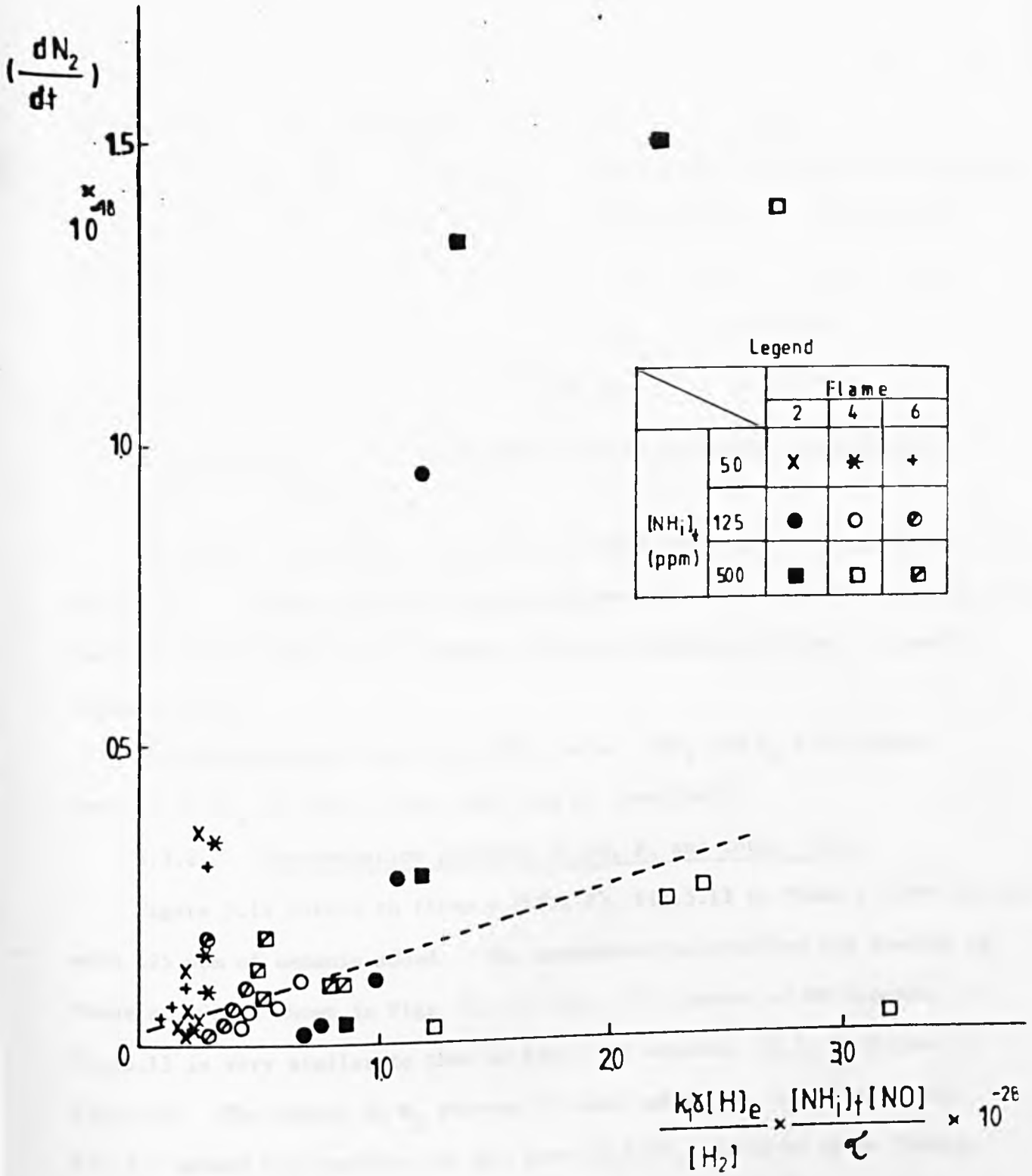

Fig 5.11 Plot to check the disappearance of NO via $NH_2 + NO \rightarrow N_2 +$ products in flames 2, 4 and 6

the conclusion drawn in the previous section that reaction (10) is not the dominant step in the disappearance of NO near the reaction zone.

Like reaction (8), (10) appears too complex to be an elementary process. As with reaction (8) the presence of intermediates was not investigated. Certainly, one could have at least two different sets of products, e.g.:

$$NH_2 + NO \rightarrow N_2 + H_2O \qquad (\Delta H^o_{298} = -52.2 \text{ kJ/mol})$$

$$NH_2 + NO \rightarrow N_2 + H + OH \qquad (\Delta H^o_{298} = -23.8 \text{ kJ/mol})$$

5.3 Observations in flames with ammonia added at various temperatures.

5.3.1 Introduction.

Up to now, observations in flames at 1900 K have been described and discussed. A range of other flames have been studied, with the same $[H_2]/[O_2]$ ratio as before, but with an amount of Argon yielding different adiabatic temperatures.

The concentration profiles of NO, total - NH_i and N_2 for various amounts of NH_3 to these flames will now be described.

5.3.2 Concentration profiles of NO, N_2 and total - NH_i.

Figure 5.12 refers to flame 1 (1822 K), Fig.5.13 to flame 3 (1986 K), both with 125 ppm of ammonia added. The concentration profiles are similar to those at 1900 K shown in Figs. 5.1 to 5.4. The amount of NO reported in Fig.5.13 is very similar to that in Fig.5.12, whereas $[NH_i]_t$ is higher in Fig.5.12. The amount of N_2 present is also smaller in the first flame. Fig.5.2 showed the profiles for the same $[H_2]/[O_2]$ ratio as these flames, the same amount of added ammonia and an adiabatic temperature of 1900 K. Denoting the concentration of each species at 1822 K by the subscript 1, at 1900 K by 2 and that at 1986 K by 3, one has:

$$[NO]_{(1)} < [NO]_{(2)} < [NO]_{(3)}$$

$$[NH_i]_{t(1)} > [NH_i]_{t(2)} > [NH_i]_{t(3)}$$

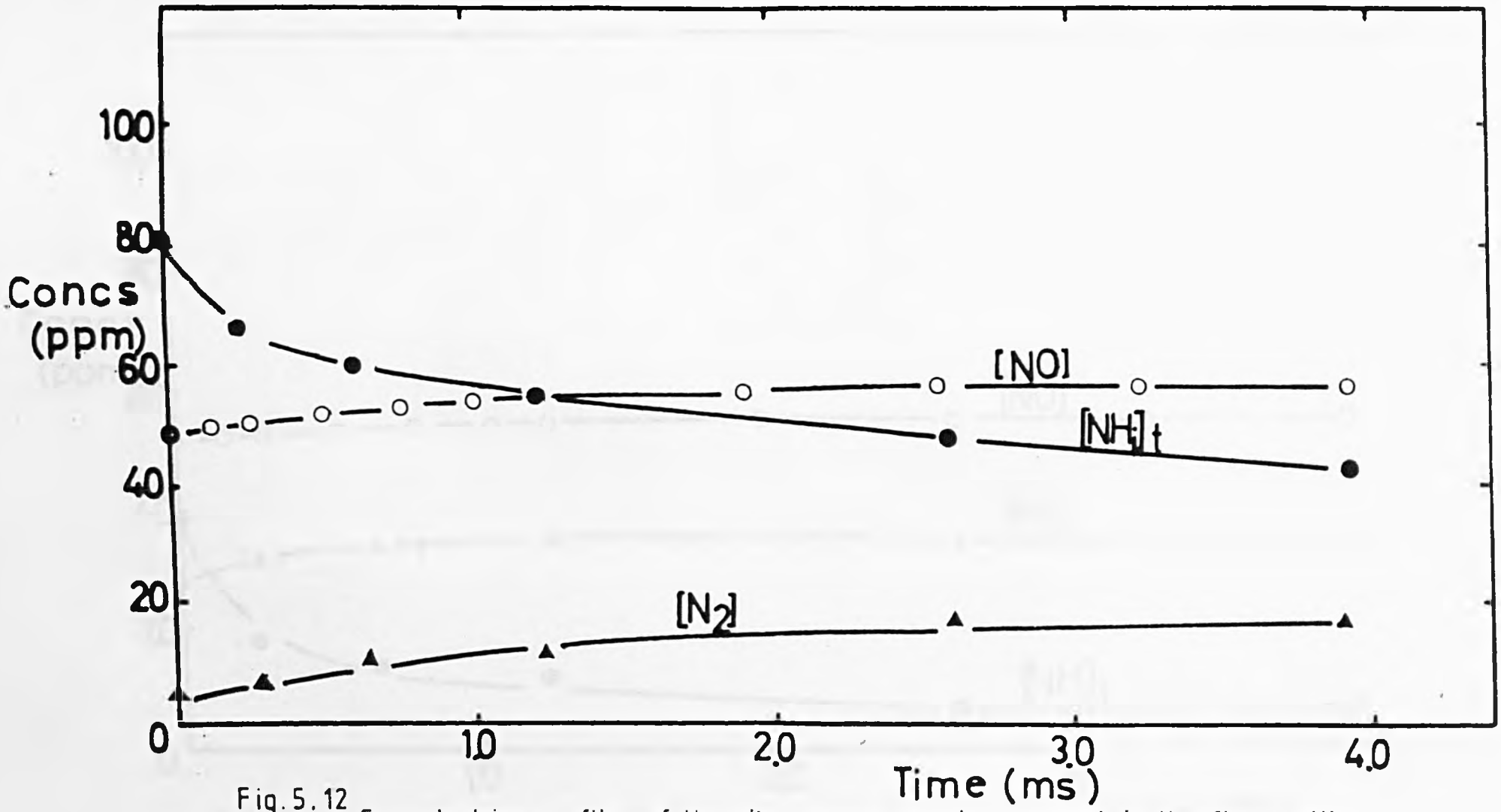

Fig. 5.12 Concentratrion profiles of the nitrogeneous species present in the flame with $[H_2]/[O_2]/[Ar] = 2.5/1./10.5$ and $[NH_3]_o = 125$ ppm.

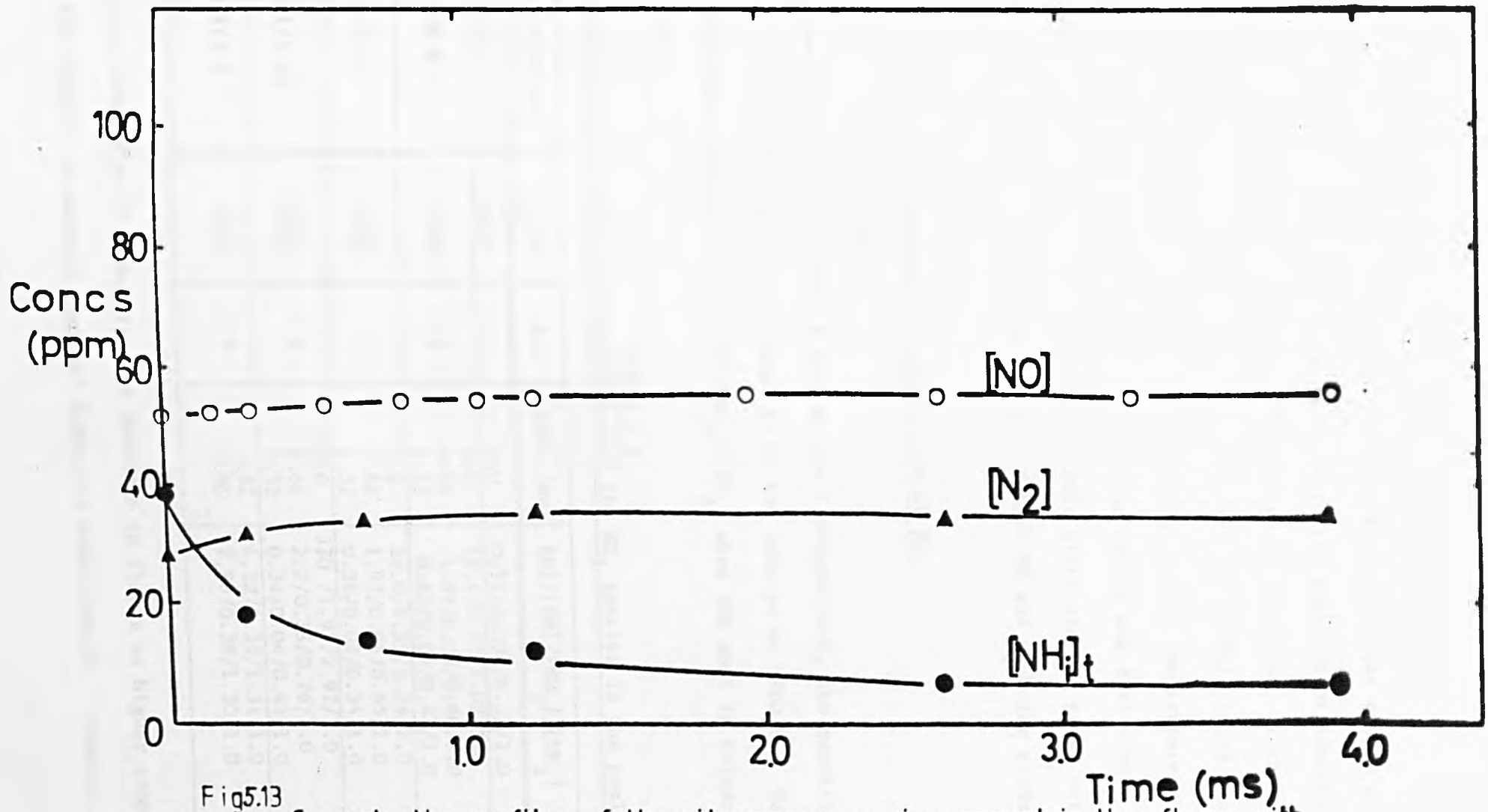

Fig5.13 Concentration profiles of the nitrogeneous species present in the flame with $[H_2]/[O_2]/[Ar] = 2.5/1/8.9$ and $[NH_3]_o = 125$ ppm

$$[N_2]_{(1)} < [N_2]_{(2)} < [N_2]_{(3)} .$$

In section 5.1.2, it was seen that in the same flame [NO] was always bigger than $[NH_i]_t$ and the amount of N_2 increased with the addition of ammonia. This same behaviour appears when the temperature is increased, at the same level of added ammonia (see Figs. 5.2, 5.12 and 5.13). This could mean that one or other NH_i species becomes more reactive at higher temperatures. The other high temperature flames, i.e. between 2030 K and 2635 K have similar concentration profiles, and hence their plots are not given here.

It thus results in increased amounts of both NO and N_2 being produced from NH_i species.

5.4 Discussion of a mechanism of production of NO.

5.4.1 Introduction.

Because the flames with T ≠ 1900 K were hydrogen-rich, the reactions involved in the NH_i pool are expected to be the same as at 1900 K. Table 5.4 below gives values for $[N]/[NH]/[NH_2]/[NH_3]$ when the pool is balanced completely.

Table 5.4
Relative equilibrium concentrations of the NH_i species in the pool.

$[H_2]/[O_2]/[Ar]$	T_{ad}(K)	No.	Time (ms)	$[N]/[NH]/[NH_2]/[NH_3]$
2.5/1/10.5	1822	1	0.0	0.11/0.009/0.21/1.0
2.5/1/8.9	1986	3	0.0	13.4/0.23/1.02/1.0
			0.66	1.89/0.08/0.60/1.0
			1.32	0.62/0.04/0.41/1.0
3.5/1/7.0	2030	5	0.0	32.0/0.35/1.26/1.0
			0.66	1.97/0.06/0.55/1.0
			1.32	0.36/0.03/0.34/1.0
3.18/1/6.49	2151	8	0.0	370 /1.93/2.97/1.0
			0.66	2.2/0.13/0.76/1.0
			1.32	0.34/0.04/0.43/1.0
2.74/1/3.5	2635	9	1.32	4.22/0.35/1.31/1.0
			3.95	2.98/0.28/1.30/1.0

Table 5.4 shows that N atoms are more dominant in flames at higher temperatures. Only for flame 1 is ammonia dominant along its whole length. However, in the

other flames, although $[N]_e$ is very high in the reaction zone, it nevertheless decays very fast downstream. Actually, in all but flame 9, ammonia becomes the dominant species just after 10 mm from the reaction zone, (i.e., 1.3 ms). Only in the very hot flame, i.e. 9, do N atoms become dominant throughout the whole flame. In this flame, as γ was not measured, a value of 1.0 after 10 mm from the reaction zone was assumed, quite justifiably on account of the very high temperature. Even if $\gamma > 1$ as [N] is proportional to γ^3, NH $\propto \gamma^2$ and $NH_2 \propto \gamma$, the dominance of N atoms is more pronounced. Table 5.1 showed $[N]/[NH]/[NH_2]/[NH_3]$ for flames at 1900 K. The concentrations of N atoms and NH_3 are then comparable in the reaction zone, with higher [N] for richer flames. An increase of temperature yields an increase of [N] and differences between [N] and $[NH_3]$ in Table 5.4 are more obvious than in Table 5.1.

To determine the actual concentration of N atoms, the same procedure as in section 5.2.1 is now followed. The temperatures of flames 1, 3, 5 and 8 are not very much different from 1900 K. Only 9 has a temperature which is 700 K above 1900 K. Consequently, the same values for the rate constants assumed for k_3, k_5, k_6 and k_7 were used. Only the equilibrium constant for (3) was calculated for the various flame temperatures and with it the rate constants for the reverse of (3). The table below shows values for k_{-3} at the temperatures of the flames studied.

Temperature (^oK)	$K_{3(H,H_2)}$	$K_{3(OH,H_2O)}$	k_{-3} ml molecule^{-1}s^{-1}	k_{-3a} ml molecule^{-1}s^{-1}
1822	776	9100	6.8×10^{-15}	2.9×10^{-15}
1986	398	4700	1.3×10^{-14}	5.5×10^{-15}
2030	339	4000	1.6×10^{-14}	6.3×10^{-15}
2151	219	2600	2.4×10^{-14}	1.0×10^{-14}
2635	64.6	760	8.2×10^{-14}	3.4×10^{-14}

The values of k_{-3} and k_{-3a} at 1900 K were respectively 1.0×10^{-14} and 4.1×10^{-15} ml molecule^{-1}s^{-1}. A steady state on N atoms was again assumed, yielding eq. (I). Its terms appear in Table 5.5 below. All the other reactions considered unimportant at 1900 K were not included here, for the same reasons.

Table 5.5

Values for the 'rates of reaction' and [N]/[NH] in the reaction zone of flames at various temperatures.

	'Rates or reaction' (s^{-1})				
Designation	1	3	5	8	9(*)
k_{-3} [H_2]	1.05×10^3	1.10×10^3	8.20×10^3	9.90×10^3	2.70×10^4
k_{-3a} [H_2O]	1.80×10^3	3.50×10^3	4.30×10^3	4.40×10^3	5.30×10^3
k_5[NH]	5.00	125	354	29.6	240
k_5[NH_2]	114	553	1.28×10^3	19.3	898
$k_6 \gamma$ [OH]$_e$	4.90×10^4	2.70×10^5	3.80×10^5	11.4×10^5	13.7×10^5
k_7[NO]	5.40×10^3	5.00×10^3	1.00×10^4	2.90×10^3	3.00×10^3
$k_{3a} \gamma$ [OH]$_e$	2.35×10^4	1.32×10^5	1.90×10^5	5.50×10^5	6.30×10^5
$k_3 \gamma$ [H]$_e$	2.40×10^3	1.40×10^4	1.10×10^4	5.60×10^4	7.00×10^4
[N]/[NH]	2.4	2.7	4.3	4.7	1.7
([N]/[NH])$_e$	12.9	65.5	20.7	53.5	8.5
[N]/[N]$_e$	0.19	0.04	0.21	0.09	0.20

Remarks: (*) - These values are for 10 mm from the reaction zone.

The concentrations of NH and NH_2 were also estimated assuming equilibrium for them. For the flames hotter than 1900 K, the left hand side of eq. (I) was dominated by the term $k_{3a} \gamma$ [OH]$_e$ [NH]. As for the right hand side of eq. (I), the term $k_6 \gamma$ [OH]$_e$ in Table 5.5 is more than 10 times bigger than the others, so that [N]/[NH] in these particular flames is given by:

$$\sigma = [N]/[NH] = (k_{3a} \gamma [OH]_e)/(k_6 \gamma [OH]_e) = k_{3a}/k_6 \qquad (X)$$

The values for [N]/[NH] in the case of flames at 1900 K were given by eq. (II) and thus dependent upon γ and [NO]. However, eq. (X) gives [N]/[NH] independent of γ and [NO]. Actually, this is a particular case of eq. (II) i.e., $\sigma = (k_3 \gamma [H]_e + k_{3a} \gamma [OH]_e)/(k_6 \gamma [OH]_e + k_{-3} [H_2] + k_7[NO])$, where the concentrations of H atoms, H_2 and NO are much lower than those in flames at 1900 K. This makes the terms $k_3 \gamma[H_e]$ in the numerator of eq. (II) and $k_{-3}[H_2] + k_7[NO]$ in the denominator too small to be significant. The following table compares the values of σ in the reaction zone for various flames, obtained using eqs. (II) and (X) respectively:

	Flame designation				
	1	3	5	8	9(*)
σ_1	0.47	0.52	0.50	0.52	0.50
σ_2	0.49	0.49	0.49	0.49	0.49

Remarks:

σ_1 - the value of σ obtained from eq. (II)

σ_2 - the value of σ obtained from eq. (X)

(*) - these values are for 10 mm from the reaction zone.

As one can see from the above table, the error in taking σ_2 instead of σ_1 is less than 6% for the reaction zone and tends to decrease with decreasing values of γ. Accordingly, eq. (X) was used instead of eq. (II) for those flames burned at temperatures different from 1900 K.

Now we can also see if the steady state is quickly established in the reaction zone. Neglecting the consumption of NO, $\frac{d[N]}{dt} = (k_{3a}[OH])[NH] - (k_6[OH])[N$ and this is as shown below for each flame:

flame 1 : 1.35×10^5 [NH] - 3.7×10^4 [N] ,

flame 3 : 7.20×10^5 [NH] - 2.7×10^5 [N] ,

flame 5 : 1.70×10^6 [NH] - 11.4×10^5 [N] ,

flame 8 : 5.3×10^6 [NH] - 11.3×10^5 [N]

all in the reaction zone, and

flame 9 : 2.3×10^6 [NH] - 14.2×10^5 [N]

at 10 mm from the reaction zone. Using the definition of section 5.2.1, the relaxation times are, 2 7, 4, 0.9, 0.9 and 0.7 μs, respectively, compared with a residence time in the reaction zone of around 20 μs. The steady state is thus established within the reaction zone, as in flames at 1900 K. Values for $[N]/[N]_e$ are also presented in Table 5.5. These were determined by the same procedure as those in Table 5.3. In flames 1, 3, 5, 8 and 9, the amount of N atoms is also much lower than that predicted for an equilibrated pool. This agrees with the conclusions drawn for flames at 1900 K, and with observations made by Kaskan & Hughes (1973), which have been already discussed in section 5.2.1.

The same procedure for testing reaction schemes as that used in flames at 1900 K will now be followed in this study. However, the value of σ in these flames is that predicted by eq. (X).

5.4.2 Observations in flames at various temperatures.

The observations described at the beginning of section 5.4 will now be checked against different kinetic schemes for the formation and disappearance of nitric oxide. Three of these schemes were represented in section 5.3 by eq. (IV) for reactions (8) and (10), eq. (V) for (9) and (10) and (XI), derived below, for steps (6) and (7), and checks of the experimental measurements are given in Figs. 5.14 to 5.21. Again, only those plots showing reasonable fits to a model will be shown. As reactions (3) and (7) are not very important in determining σ, compared to the other terms in eq. (I), eq. (VI) can be simplified to:

$$\frac{[H_2]^2 \tau \, d[NO]/dt}{K_1 K_2 \gamma^2 [H]_e^2 [NH_i]_t [NO]} = k_{3a} \frac{\gamma [OH]_e}{[NO]} - k_7 \qquad (XI)$$

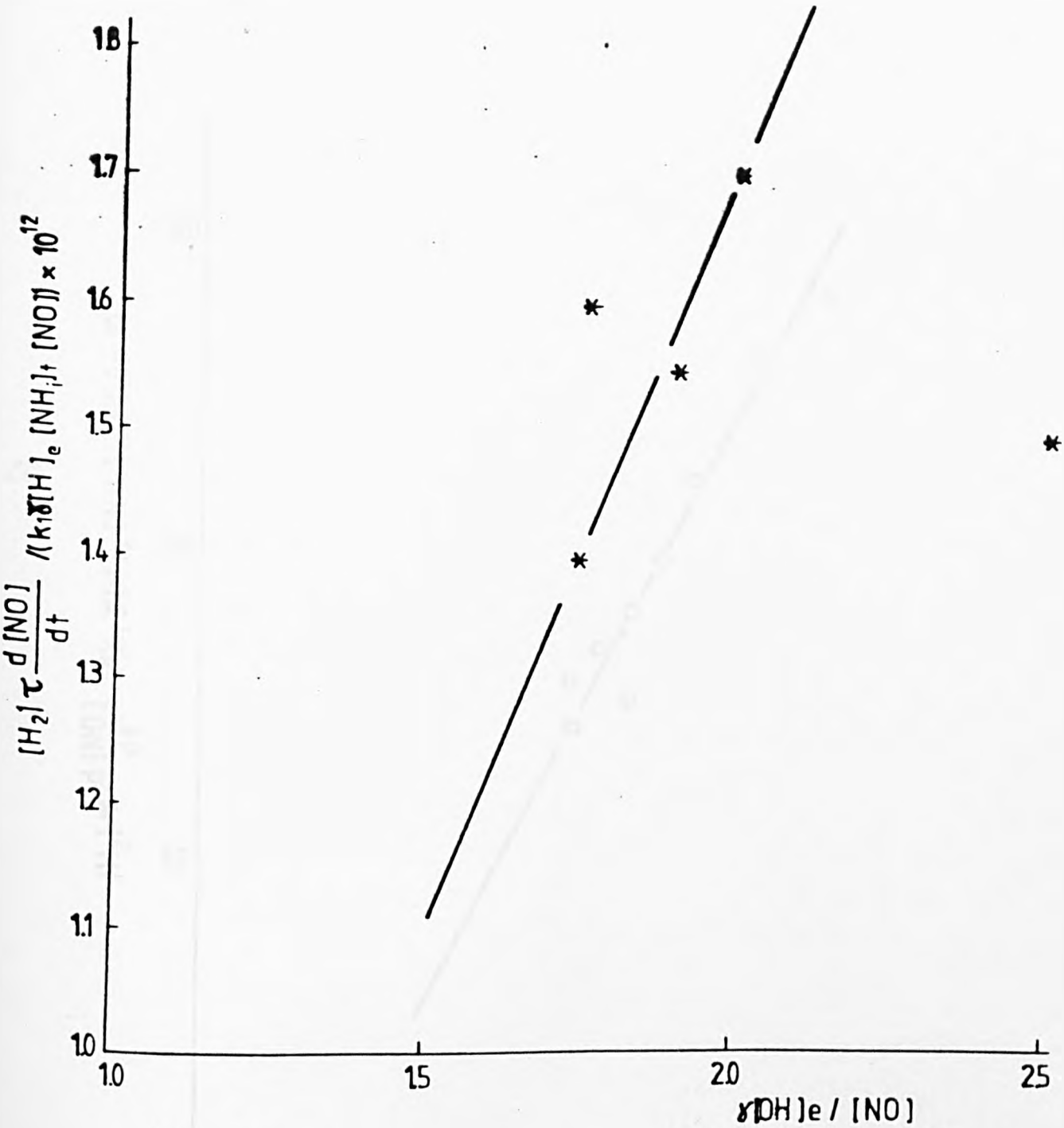

Fig. 5.14 Plot to check the mechanism

$NH_2 + OH \rightarrow NO + H + H_2$

$NH_2 + NO \rightarrow N_2 + H_2O$

in flame 1 at 1822 K

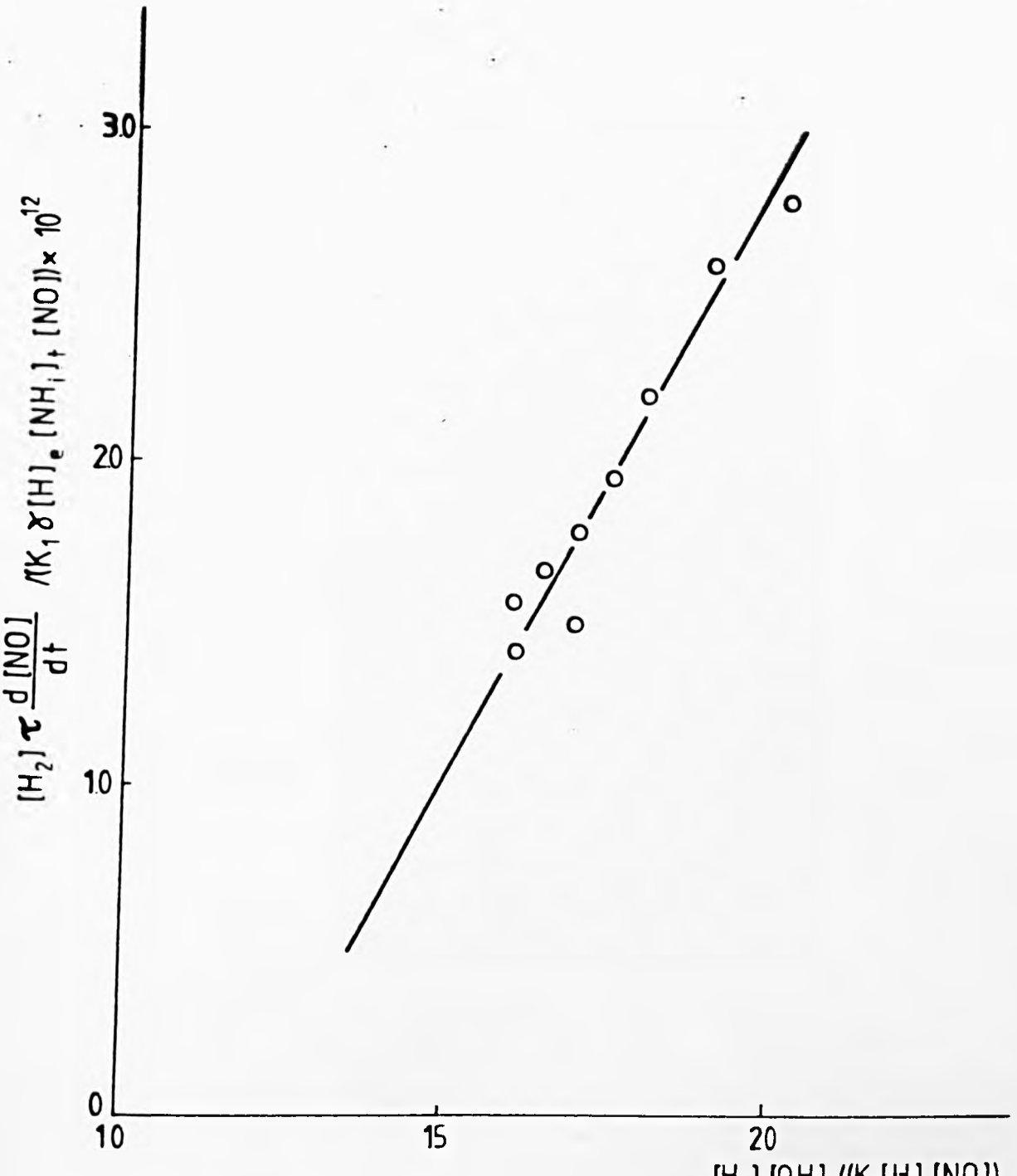

Fig. 5.15

Plot to check the mechanism

$NH_2 + OH \rightarrow NO + prods$

$NH_2 + NO \rightarrow N_2 + prods.$

in flame 1 at 1822 K

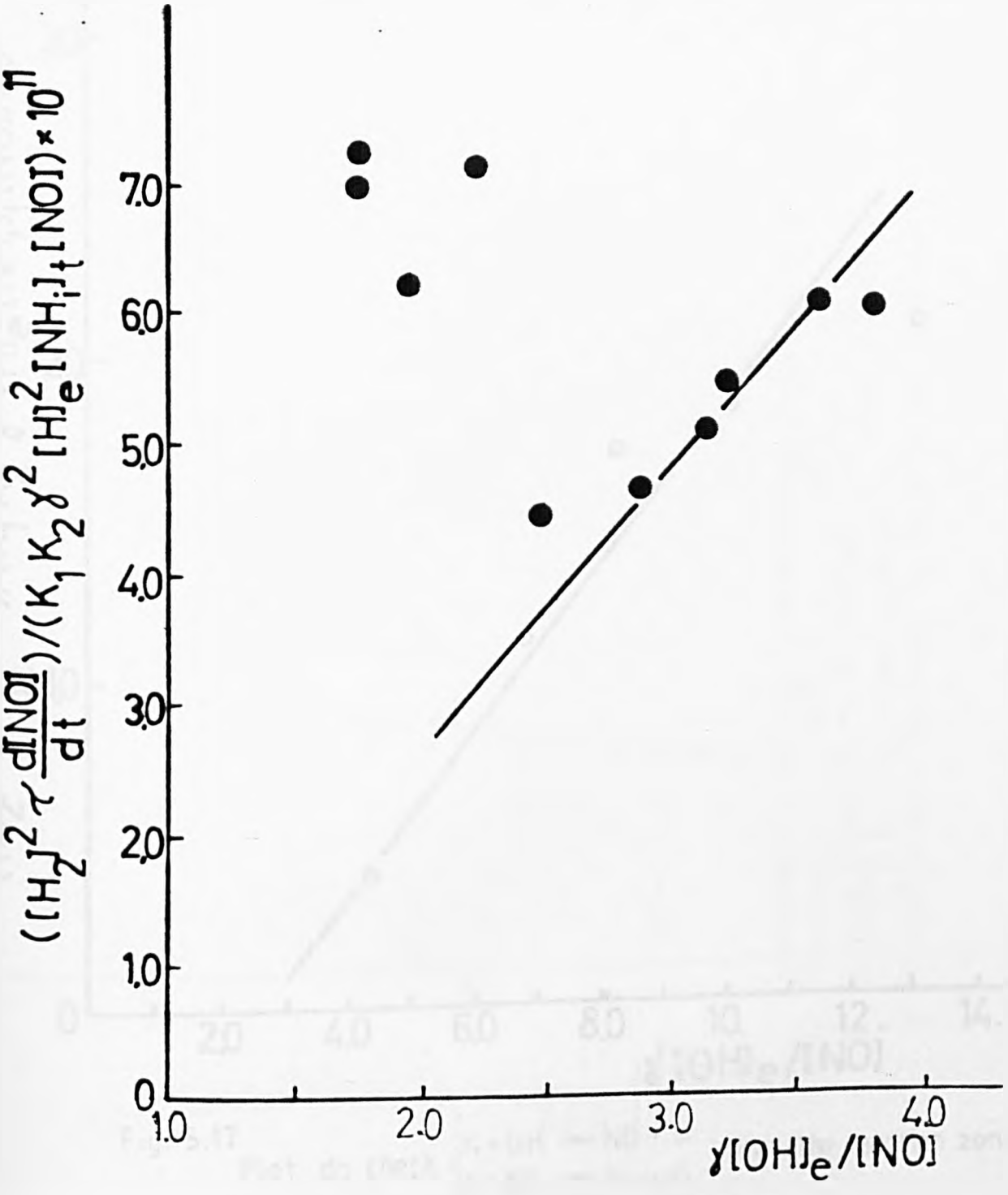

Fig. 5.16 Pic: to check $\begin{cases} N + OH \rightarrow NO + H \\ N + NO \rightarrow N_2 + O \end{cases}$ with eq. (XI) in flame 1

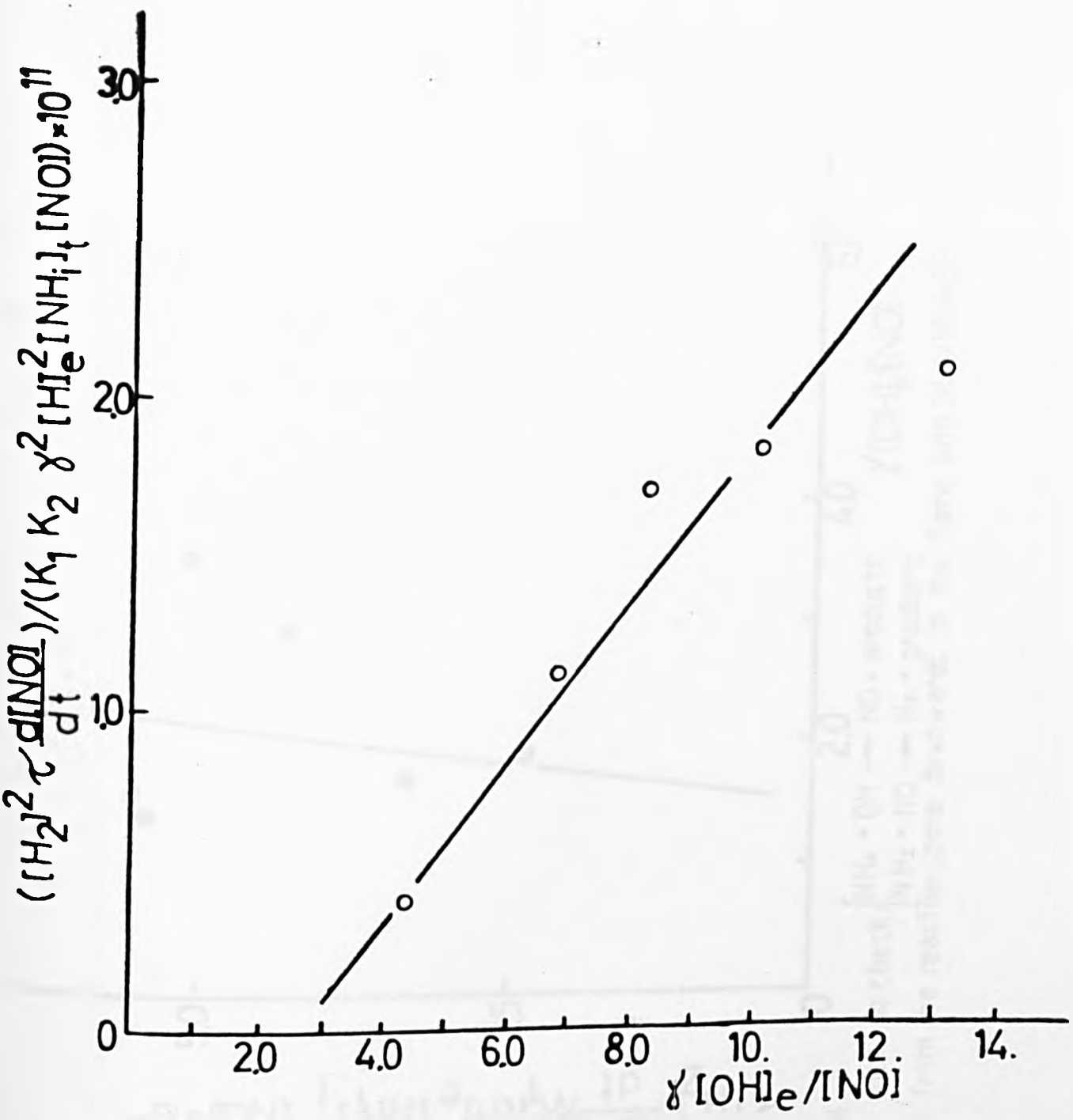

Fig. 5.17 Plot do check $\begin{cases} N + OH \rightarrow NO + H \\ N + NO \rightarrow N_2 + O \end{cases}$ near the reaction zone in the flame with $[H_2]/[O_2] = 3.5$ at 2030K

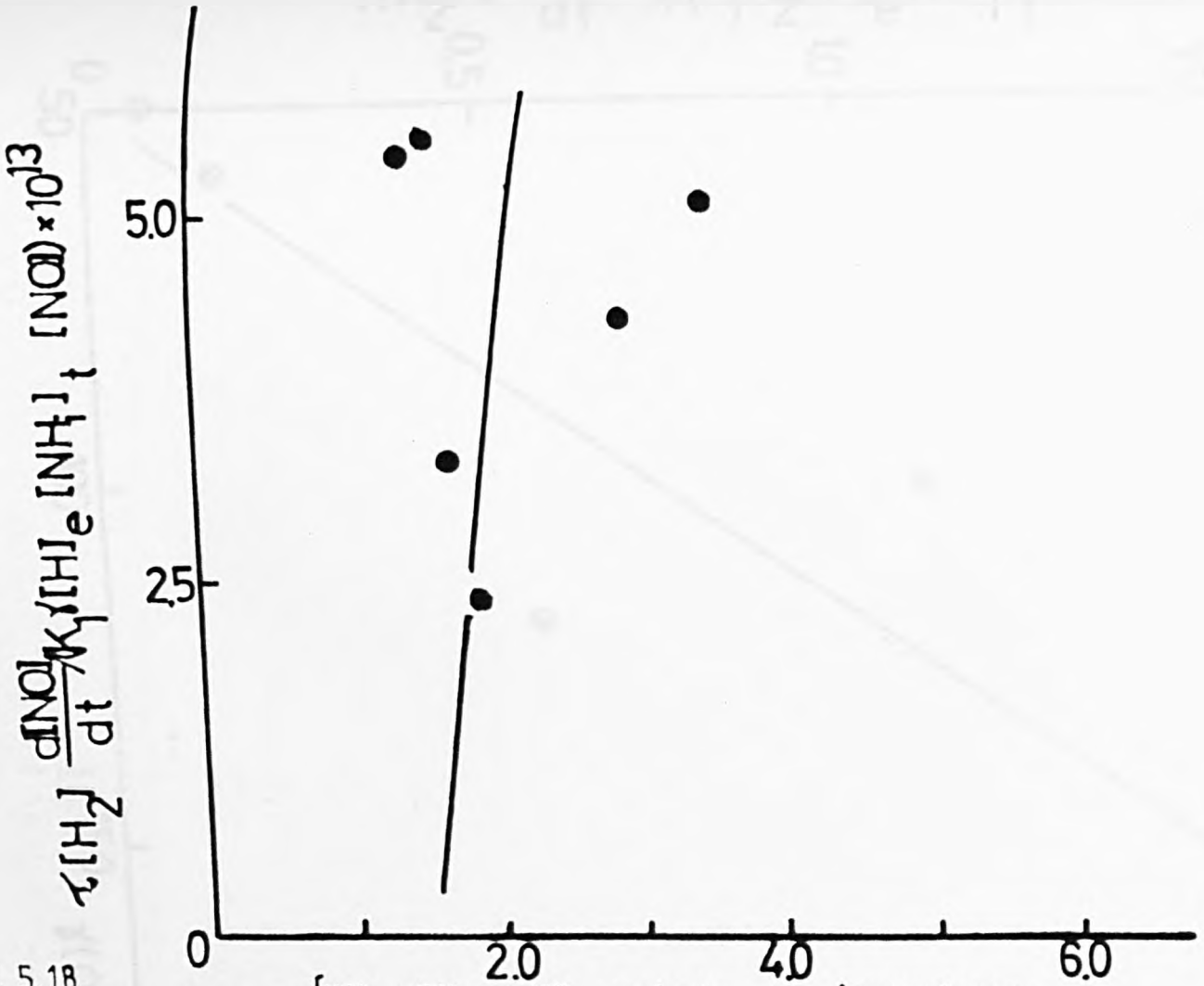

Fig. 5.18

Plot do check $\begin{cases} NH_2 + OH \rightarrow NO + \text{products} \\ NH_2 + NO \rightarrow N_2 + \text{products} \end{cases}$

at 10 mm from the reaction zone downwards in the flame with $[H_2]/[O_2]=3.5$ at 2030 K

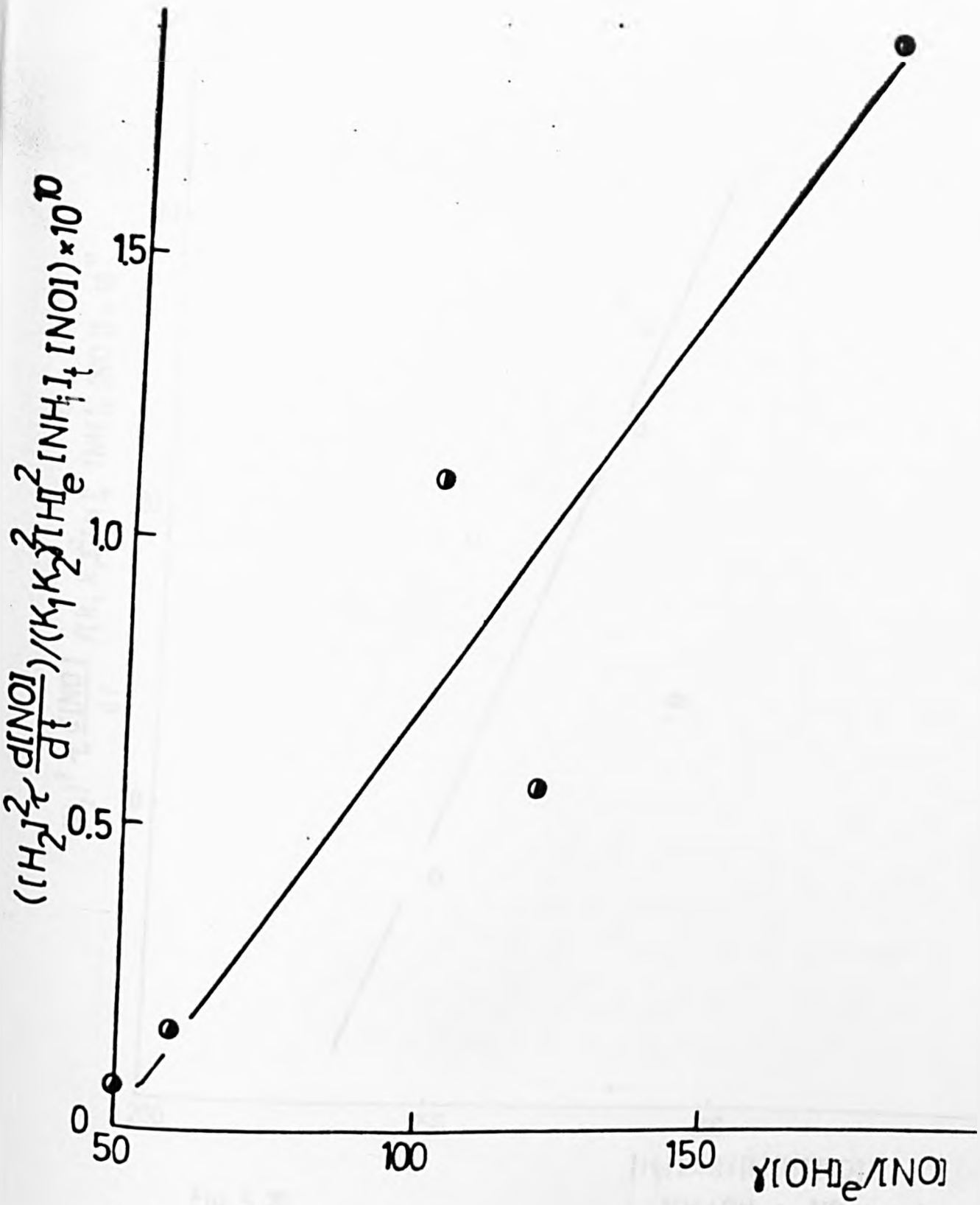

Fig. 5.19

Plot to check the mechanism $N + OH \rightarrow NO + H$, $N + NO \rightarrow N_2 + O$ for the flame with $[H_2]/[O_2] = 3.18$ and 2151 K and $[NH_3]_O = 125$ ppm

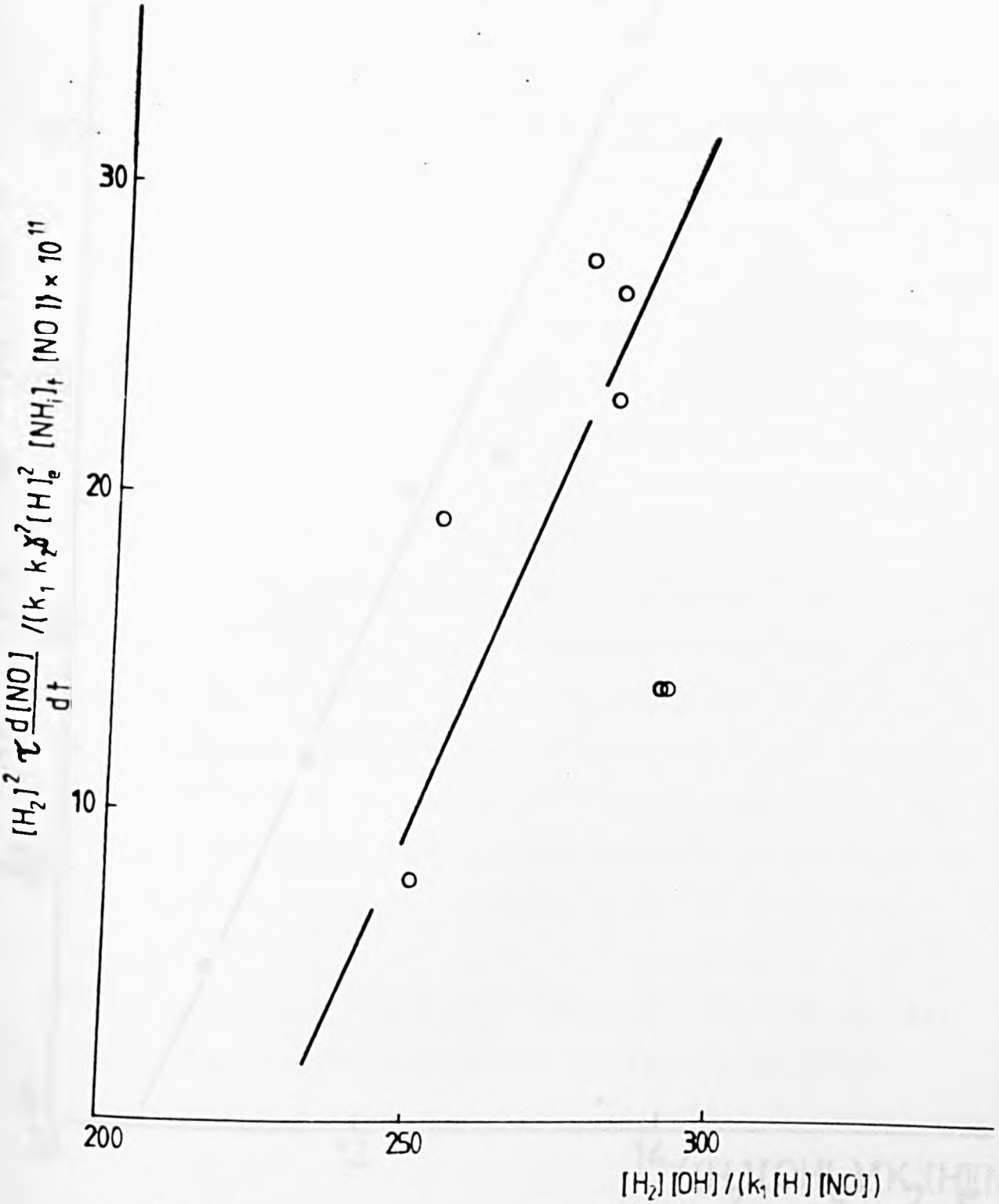

Fig. 5.20 Plot to check the mechanism $NH_2 + OH \rightarrow NO + prods$
$NH + NO \rightarrow N_2 + prods$
for the flame with $[H_2]/[O_2] = 3.18$ at 2151 k and $[NH_3]_o = 125$ ppm

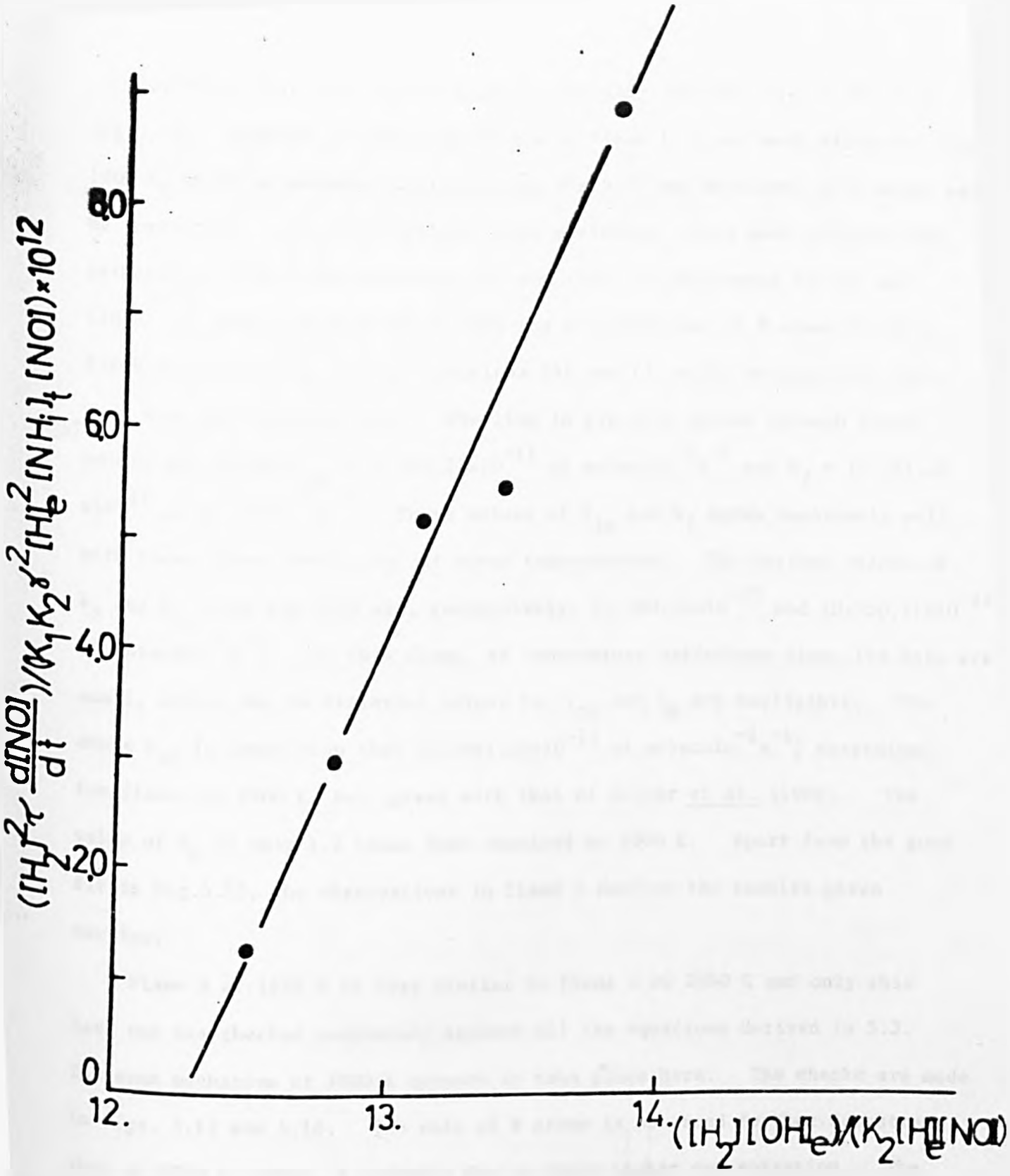

Fig. 5.21

Plot to check $\begin{cases} NH_2 + OH \rightarrow NO + \text{products} \\ NH + NO \rightarrow N_2 + \text{products} \end{cases}$

in the flame with $[H_2]/[O_2] = 2.74$ and 2635K and $[NH_3]_o = 125$ ppm

Of Figs. 5.14 to 5.16 for flame 1, possibly the best fit is shown in Fig.5.15. However, as the temperature of flame 1 is not much different from 1900 K, where no evidence corroborating Fig.5.15 was obtained, this might well be fortuitous. Fig.5.14 will be taken seriously, since much evidence was gathered at 1900 K for reactions (8) and (10), in preference to (9) and (10). It should also be noted that the concentration of N atoms in this flame is very small, so that reactions (6) and (7) might be important only very near the reaction zone. The line in Fig.5.16 passes through these points and yields $k_{3a} = (2.4\pm1.2)\times10^{-11}$ ml molecule^{-1}s^{-1} and $k_7 = (2.3\pm1.2)\times10^{-11}$ ml molecule^{-1}s^{-1}. These values of k_{3a} and k_7 agree remarkably well with those found previously, at other temperatures. The derived values of k_8 and k_{10} from Fig.5.14 are, respectively, $(1.2\pm0.3)\times10^{-12}$ and $(0.7\pm0.2)\times10^{-12}$ ml molecule^{-1}s^{-1}. In this flame, as temperature variations along its axis are small, errors due to different values for γ_{OH} and γ_H are negligible. The above k_{10} is lower than that $\left((4.6\pm1.0)\times10^{-12}\right.$ ml molecule^{-1}s^{-1}) determined for flames at 1900 K, but agrees with that of Silver et al. (1980). The value of k_8 is only 1.2 times that obtained at 1900 K. Apart from the good fit in Fig.5.15, the observations in flame 1 confirm the results given earlier.

Flame 3 at 1986 K is very similar to flame 5 at 2030 K and only this last one was checked completely against all the equations derived in 5.3. The same mechanism at 1900 K appears to take place here. The checks are made in Figs. 5.17 and 5.18. The role of N atoms is observed further downstream than at 1900 K, which is probably due to their higher concentration. The line in Fig.5.17 yields k_{3a} and k_7, respectively, of $(2.5\pm1.3)\times10^{-12}$ and $(8.0\pm4.0)\times10^{-12}$ ml molecule^{-1}s^{-1}, which are lower than those found in flame 1 (i.e., 2.4×10^{-11} and 2.3×10^{-11} ml molecule^{-1}s^{-1}, respectively). Downstream, Fig.5.18 presents a reasonably good fit for NH_2 being the important NH_i

species. The values of k_8 and k_{10} emerging are, respectively $(7.5\pm2.3)\times10^{-13}$ and $(1.2\pm0.3)\times10^{-12}$ ml molecule^{-1}s^{-1}. The value of k_8 is lower than that obtained at 1900 K. Taking into account temperature variations along a flame, both k_{3a} and k_8 should be slightly larger due to the differences in γ_H and γ_{OH}.

The observations in flame 8 at 2151 K will be discussed now. Fig.5.19 checks eq. (XI) with the experimental measurements up to 6 mm from the reaction zone. This shows a reasonable fit to a straight line. The values of k_{3a} and k_7 determined from the slope and intercept, respectively, are $(1.4\pm0.9)\times10^{-12}$ ml molecule^{-1}s^{-1} and $(6.4\pm3.5)\times10^{-11}$ ml molecule^{-1}s^{-1}. The value of k_{3a} is about ten times smaller than that quoted in section 5.2.1, but similar to that obtained in flame 5 at 2030 K. However, the value of k_7 obtained is about ten times larger than that derived above and 2.4 times the value of 2.7×10^{-11} found in the literature. However, taking into consideration that γ_{OH} might well be lower than γ_H, k_{3a} would become larger with a lower k_7. Fig.5.20 checks eq. (XII), given below, with the experimental measurements:

$$\frac{[H_2]^2\ \tau\ d[NO]/dt}{K_1K_2\ \gamma^2[H]_e^2\ [NH_i]_t\ [NO]} = k_8\ \{([H_2][OH])/(K_2[H][NO])\} - k_{11} \quad . \quad \text{(XII)}$$

This represents the scheme: $NH_2 + OH \rightarrow NO +$ products and $NH + NO \rightarrow N_2 + OH$. A tolerable straight line is obtained in Fig.5.20. The values of k_8 and k_{11} are respectively, $(7.0\pm2.5)\times10^{-13}$ and $(1.7\pm1.0)\times10^{-10}$ ml molecule^{-1}s^{-1}. The value of k_8 appears to agree with those determined previously, at other temperatures. The value of k_{11} seems too big compared to those quoted either by Kaskan & Hughes (1973) or Gordon et al. (1971), which were 4×10^{-12} and 4×10^{-11} ml molecule^{-1}s^{-1} respectively. However, as temperature variations along the flame appear to be quite high, and the fact

that γ_{OH} might be lower than γ_H, one might have to reduce the abcissa in Fig.5.20, so that k_{11} is equally lowered. Take e.g. $\gamma_{OH} = 0.5\ \gamma_H$, the average value for $([H_2][OH]/(K_2[H][NO])$ is 150, so that $k_{11} = 9.7 \times 10^{-11}$ ml molecule^{-1}s^{-1}, agreeing better with that of Gordon et al. (1971).

Fig.5.21 shows the only good fit for flame 9 with $[H_2]/[O_2] = 2.74$ at 2635 K. This also suggests reactions (8) and (11) at a distance of 10 mm from the reaction zone. The calculations in this flame involve some slight uncertainty, because γ was not measured, but was taken as 1.0 after 10 mm from the reaction zone, which is probably a very good approximation. The values of k_8 and k_{11} determined from the slope and intercept, are $(6.3 \pm 6.3) \times 10^{-12}$ and $(7.8 \pm 7.8) \times 10^{-11}$ ml molecule^{-1}s^{-1}, respectively. As in the other flames, if $\gamma_{OH} < \gamma_H$, a lower k_{11} is likely to be obtained. The value of k_{11} is, in fact, comparable to k_7 and agrees better with the value reported by Gordon et al. (1971). The value of k_8 appears large compared to those obtained at other temperatures. This could be due to the fact that γ was taken as 1.0. The term γ^2 in the ordinate would lower the value of k_8 considerably, since γ is larger nearer the reaction zone, i.e. those points farthest away from the origin. As a check, let us take γ_H at a distance of 10 mm from the reaction zone to be 2.0 and 1.0 at 30 mm. The value of k_8 would turn out to be 2.4×10^{-12} ml molecule^{-1}s^{-1} and $k_{11} = 3.0 \times 10^{-11}$ ml molecule^{-1}s^{-1}. These are 0.38 times lower than those determined above. Actually, they would become even lower if $\gamma > 2$ at 10 mm.

In the following section, some conclusions will be drawn from the observations in all flames with only ammonia added.

5.5 Conclusions on the production of NO in the ammonia flames.

The main conclusions will be given in Chapter 8. Here only an attempt is made to summarize the observations in flames with ammonia added at various temperatures.

The adiabatic temperature of the flames used in this study varied from 1822 K to 2635 K. The sudden appearance of NO in the reaction zone can be explained by reactions involving N atoms such as $N + OH \rightarrow NO + H$, which occur simultaneously with $N + NO \rightarrow N_2 + O$. The concentration of N atoms was determined considering a steady state, in which reactions (3), (3a), the reverse of (3), (6) and (7) are the most important. According to equilibrium calculations, N atoms are in fact dominant in the reaction zone with the exception of flame 1 at 1822 K. However, consideration of the steady state led to the conclusion that the NH_i pool was depleted of N atoms. This is in agreement with some other investigators (Kaskan & Hughes 1973, Caralp 1979). Downstream of the reaction zone N atoms do not appear to play a role in the production or disappearance of NO. There the species forming NO are NH_2 and OH radicals in $NH_2 + OH \rightarrow NO + H + H_2$. The experimental measurements lead to a more complicated scheme for the disappearance of NO. In flames with temperatures up to 2030 K, reaction (10): $NH_2 + NO \rightarrow N_2 + H_2O$ seems to be responsible for the disappearance of NO, whilst at higher temperatures, $NH + NO \rightarrow N_2 + OH$ fits the measurements better. An important factor appears to be the relative amount of each NH_i species.

The rate constants found at various temperatures are tabulated below:

Table 5.6

Various rate constants obtained at different temperatures.

Reaction	Rate constant	Temperature (K)	Value for k_x (ml molecule^{-1} s^{-1})
$NH + H \rightarrow N + H_2$	k_3	1900	$(6.2\pm5.0)\times10^{-12}$
		1822	$(2.4\pm1.2)\times10^{-12}$
$NH + OH \rightarrow N + H_2O$	k_{3a}	1900	$(3.1\pm2.0)\times10^{-11}$
		2030	$(2.5\pm1.3)\times10^{-12}$
		2151	$(1.4\pm0.9)\times10^{-12}$
$N + OH \rightarrow NO + H$	k_6	1900	$(5.0\pm5.0)\times10^{-10}$

$N + NO \rightarrow N_2 + O$	k_7	1822	$(2.3\pm1.2)\times10^{-11}$
		2030	$(8.0\pm4.0)\times10^{-12}$
		2151	$(6.4\pm3.5)\times10^{-11}$
$NH_2 + OH \rightarrow NO + prod$	k_8	1822	$(1.2\pm0.3)\times10^{-12}$
		1900	$(9.7\pm2.0)\times10^{-13}$
		2030	$(7.5\pm2.3)\times10^{-13}$
		2151	$(7.0\pm2.5)\times10^{-13}$
		2635	$(6.3\pm6.3)\times10^{-12}$
$NH_2 + NO \rightarrow N_2 + H_2O$	k_{10}	1822	$(1.4\pm0.4)\times10^{-12}$
		1900	$(4.6\pm1.0)\times10^{-12}$
		2030	$(1.2\pm0.3)\times10^{-12}$
$NH + OH \rightarrow N_2 + OH$	k_{11}	2151	$(1.7\pm1.0)\times10^{-10}$
		2635	$(7.8\pm5.0)\times10^{-11}$

From the above table, the uncertainties in the rate constants k_3, k_{3a}, k_6 and k_{11} are high, being around a factor of 2. In section 5.2.3 the values for k_3 and k_{3a} at 1900 K were calculated from the slope of the broken line in Fig.5.8, based on the assumption that $k_{3a} = 5k_3$. This gave $k_3 = 6.2\times10^{-12}$ ml molecule^{-1} s^{-1} and $k_{3a} = 3.1\times10^{-11}$ ml molecule^{-1}s^{-1}. The value of k_3 assumed in section 5.2.1 was 5.3×10^{-12} ml molecule^{-1}s^{-1}. It appears that the two values of k_3 agree fairly well. Table 5.6 gives values for k_{3a} at various temperatures. These values were employed in the plot of ℓn k_{3a} against 1/T, given in Fig.5.22. This plot gives $k_{3a} = (1.1\pm0.6)\times10^{-11}$ ml molecule^{-1}s^{-1} at 1900 K. Using this value in the slope of the broken line in Fig.5.8 one obtains $k_3 = (8.0\pm6.0)\times10^{-12}$ ml molecule^{-1}s^{-1}, which is 1.5 times greater than 5.3×10^{-12} ml molecule^{-1}s^{-1} assumed in section 5.2.1. Hence, the ratio k_{3a}/k_3 is 1.4 not 5 as assumed in section 5.2.3. These new values of $k_3 = 8.0\times10^{-12}$ and $k_{3a} = 1.1\times10^{-11}$, both in ml molecule^{-1}s^{-1} appear to fit better the experimental observations at 1900 K and they do not seem to alter conclusions on the mechanism of both formation and disappearance of NO in the reaction zone discussed above. These values are also in fairly

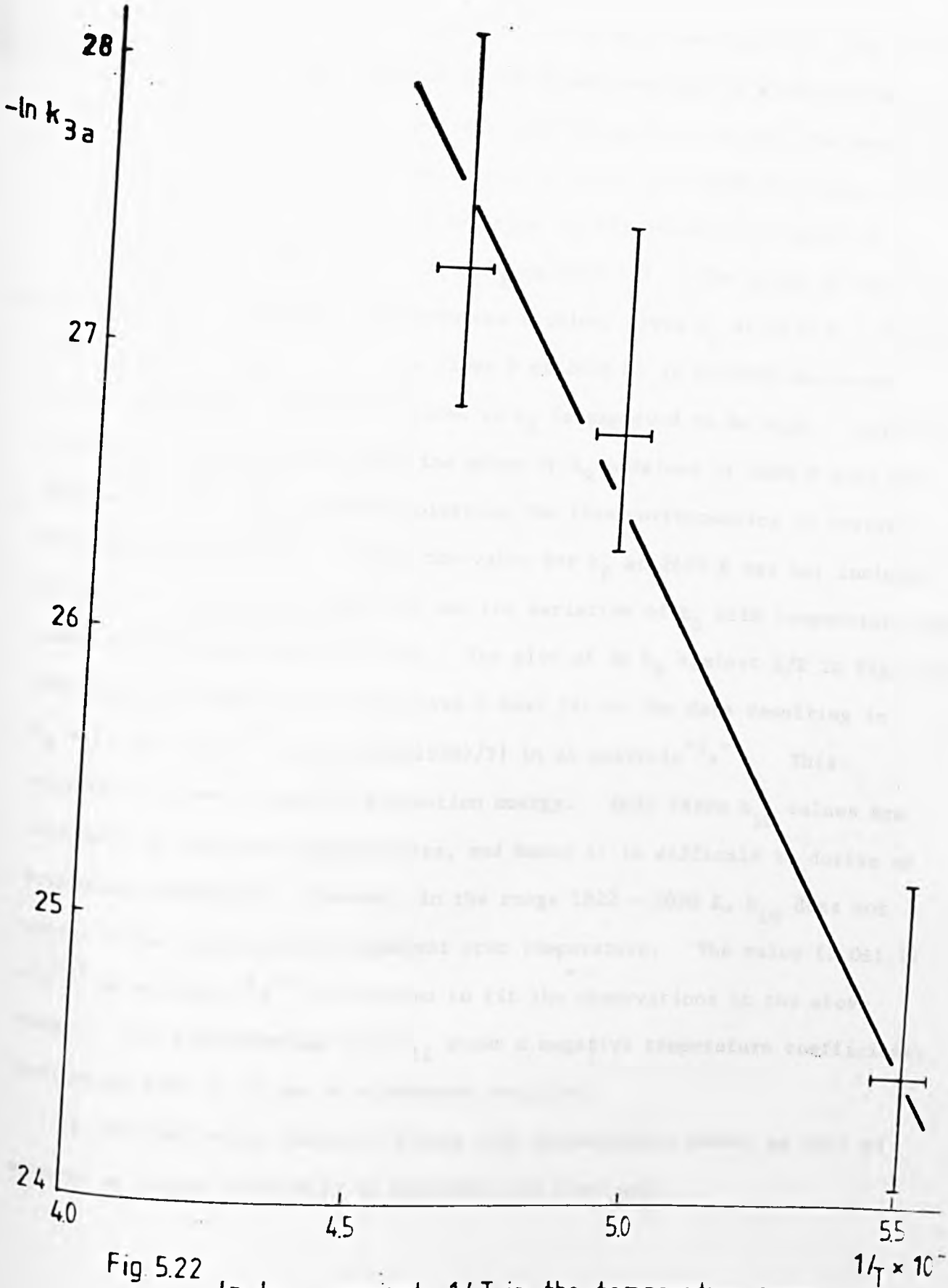

Fig. 5.22 . ln k_{3a} against 1/T in the temperature range 1822 - 2151 K

good agreement with those found in the literature (i.e. $k_3 = 5.3 \times 10^{-12}$ ml molecule^{-1} s^{-1} and $k_{3a} = 2.6 \times 10^{-11}$ ml molecule^{-1}s^{-1}) and quoted in section 5.2.1. The value of k_6 was determined using somewhat insufficient data and is different by one order of magnitude from those in the literature (Campbell & Thrush 1968, Haynes 1977). The value of k_7 appears to agree within a factor of 2 with the value of 2.7×10^{-11} ml molecule^{-1}s^{-1} found in the literature and discussed in section 5.2.1.

Fig.5.23 presents a plot of ℓn k_8 against 1/T. The slope of the line in Fig.5.21, presented in the previous section, gives k_8 at 2635 K. However, due to the uncertainty in γ for flame 9 at 2635 K, as already discussed in the same section, the error related to k_8 is expected to be high. Actually, this agrees with the fact that the value of k_8 obtained at 2635 K does not follow the variation of other points on the line corresponding to several different temperatures. Hence the value for k_8 at 2635 K was not included in the set of points in Fig.5.23 and the variation of k_8 with temperature was taken in the range 1822 - 2151 K. The plot of ℓn k_8 against 1/T in Fig.5.23 produces a straight line which gives a best fit to the data resulting in $k_8 = (3.0 \pm 1.2) \times 10^{-14} \exp\{(6650 \pm 1950)/T\}$ in ml molecule^{-1}s^{-1}. This expression gives a negative activation energy. Only three k_{10} values are available at different temperatures, and hence it is difficult to derive an Arrhenius expression. However, in the range 1822 - 2030 K, k_{10} does not appear to be significantly dependent upon temperature. The value $(2.0 \pm 1.1) \times 10^{-12}$ ml molecule^{-1}s^{-1} is believed to fit the observations in the above range. It is interesting that k_{11} shows a negative temperature coefficient, indicating that it is not an elementary reaction.

In the following chapters, flames with hydrocarbons added, as well as ammonia or nitric oxide will be described and discussed.

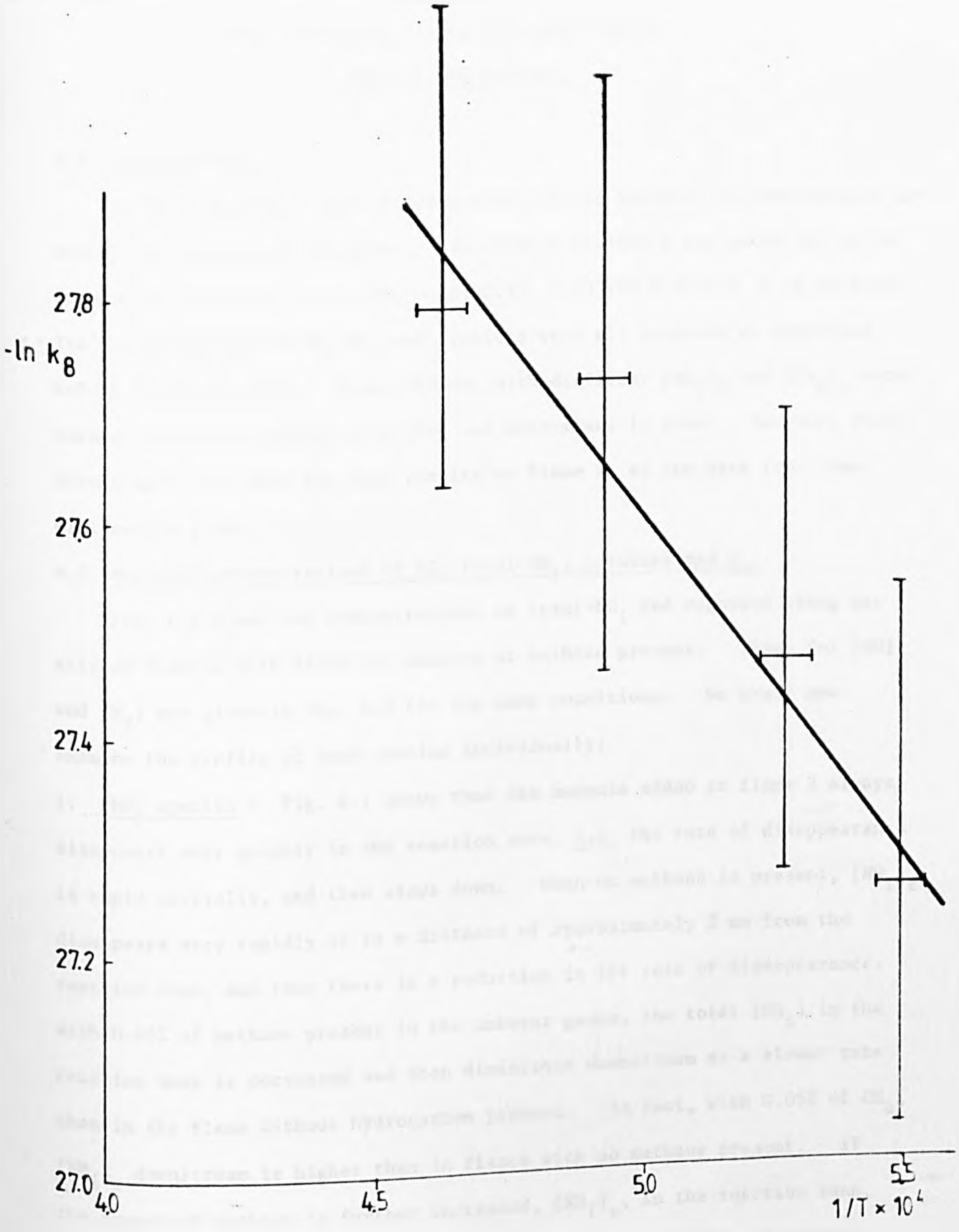

Fig. 5.23 $\ln k_\varepsilon$ against 1/T in the range 1822 - 2635 K

Chapter 6.

Observations in flames with addition of ammonia and methane.

6.1 Introduction.

In this chapter, a very brief account of the addition of both methane and ammonia to flames will be given. To flame 2 at 1900 K was added 615 p.p.m. of ammonia, together with 0.05, 0.15, 0.25, 0.50 and 0.70 vol. % of methane. The concentrations of NO, NH_i and cyanides were all measured as described before in Chapter III. Other flames, with different $[NH_3]_0$ and $[CH_4]_0$ were burned, but unfortunately only [NO] was determined in them. However, these flames gave very much the same results as flame 2, so the data from them will not be given.

6.2 Measured concentrations of NO, total-NH_i, cyanides and N_2.

Fig. 6.1 shows the concentrations of total-NH_i and cyanides along the axis of flame 2 with different amounts of methane present. Those for [NO] and $[N_2]$ are given in Fig. 6.2 for the same conditions. We shall now examine the profile of each species individually:

1. NH_i species - Fig. 6.1 shows that the ammonia added to flame 2 always disappears very quickly in the reaction zone, i.e. the rate of disappearance is rapid initially, and then slows down. When no methane is present, $[NH_i]_t$ disappears very rapidly up to a distance of approximately 2 mm from the reaction zone, and then there is a reduction in the rate of disappearance. With 0.05% of methane present in the unburnt gases, the total $[NH_i]$ in the reaction zone is decreased and then diminishes downstream at a slower rate than in the flame without hydrocarbon present. In fact, with 0.05% of CH_4, $[NH_i]_t$ downstream is higher than in flames with no methane present. If the amount of methane is further increased, $[NH_i]_t$, in the reaction zone, as well as downstream, decreases and its disappearance follows a pattern

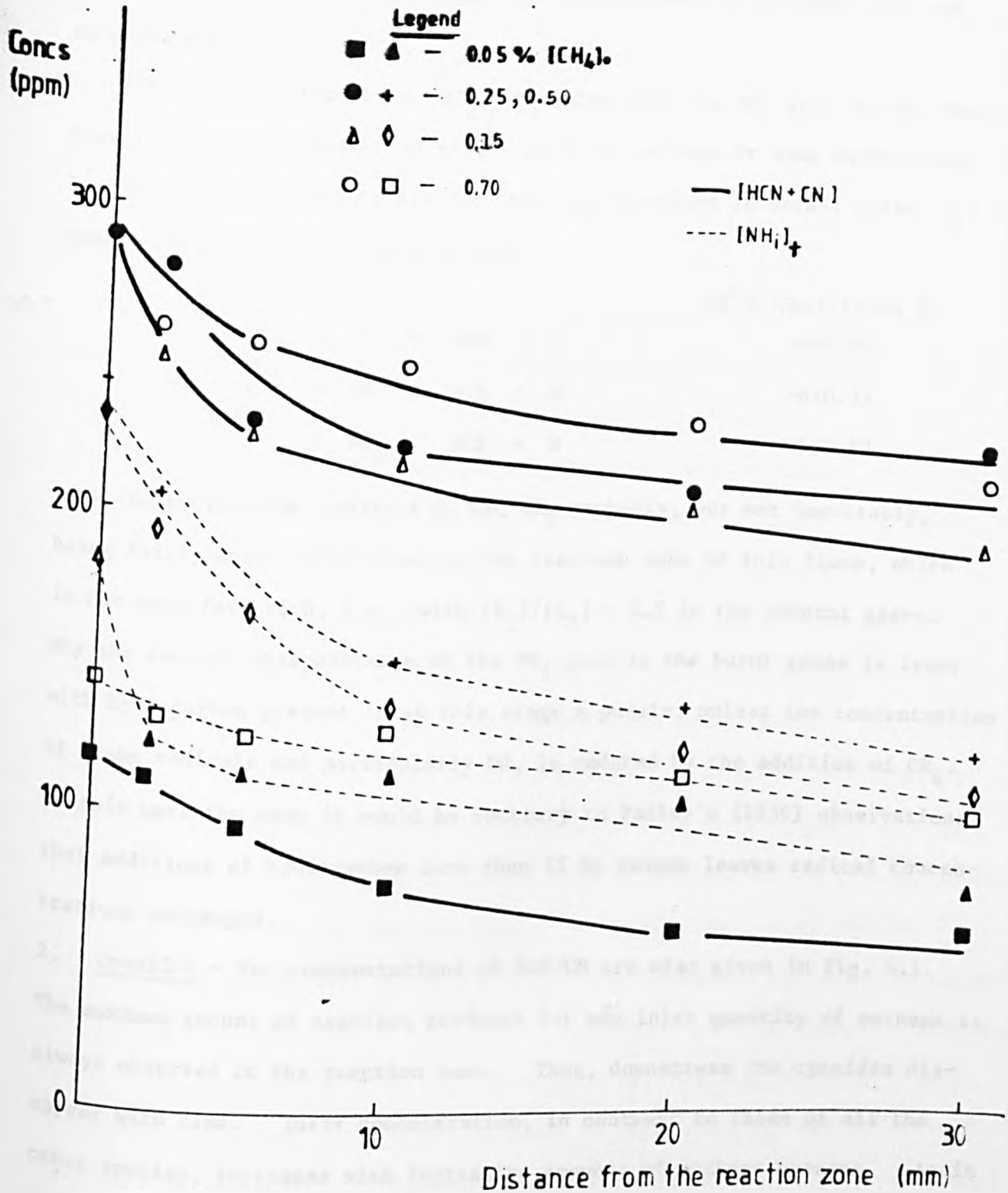

Fig. 6.1

Concentration profiles of NHi and HCN+CN species in flame 2 at 1900 K and $[NH_3]_o = 615$ ppm.

parallel to that with 0.05% of methane. However, the total amount of NH_i species present in the burnt gases is not observed to be lower than $[NH_i]_t$ with no methane present.

It is clear from these $[NH_i]_t$ profiles that the NH_i pool in the reaction zone is being depleted by an attack on it by methane or some hydrocarbon fragment. The possibilities for this are discussed in detail below, but some candidates which spring to mind are:

					ΔH^o(kJ/mol)(1900 K)
CH_2	+ N	→	HCN	+ H	-499.93
CH	+ NH	→	HCN	+ H	-610.31
C	+ NH_2	→	HCN	+ H	-519.30

with the hydrocarbon radicals C, CH, CH_2 probably, but not inevitably, being fairly short-lived close to the reaction zone of this flame, which is not very fuel-rich, i.e., with $[H_2]/[O_2] = 2.5$ in the unburnt gases. Why the rate of disappearance of the NH_i pool in the burnt gases is lower with hydrocarbon present is at this stage a puzzle, unless the concentration of flame radicals and particularly OH, is reduced by the addition of CH_4. If this were the case it would be contrary to Padley's (1959) observations that additions of hydrocarbon less than 1% by volume leaves radical concentrations unchanged.

2. Cyanides - The concentrations of HCN/CN are also given in Fig. 6.1. The maximum amount of cyanides produced for any inlet quantity of methane is always observed in the reaction zone. Then, downstream the cyanides disappear with time. Their concentration, in contrast to those of all the other species, increases with increasing amounts of methane present. Again the profiles for [HCN + CN] in Fig. 6.1 are not far from being parallel to one another. These [cyanide] profiles seem to be roughly in accord with the above idea of HCN or CN being formed in or very close to the reaction

zone by a hydrocarbon fragment attacking some NH_i species. The reactions consuming the cyanides, of course, remain to be identified.

3. Nitric oxide - Fig.6.2 shows that almost all the NO is formed in the reaction zone with or without methane present. In the reaction zone, [NO] decreases as $[CH_4]$ in the unburnt gases is increased. This could be due to a hydrocarbon fragment attacking NO in the reaction zone, possibly by a process such as NO + CH → HCN + O or CNO + H. After the reaction zone, [NO] increases with time and the curves representing [NO] are almost parallel for different inlet concentrations of methane. This means d[NO]/dt in the burnt gases is not very sensitive to the addition of methane. Fig.6.1 showed that $[NH_i]$ also was not much changed by varying the hydrocarbon concentration, which suggests that most of the NO in the burnt gases comes from a step such as $NH_2 + OH \rightarrow NO + H + H_2$ as discussed in the previous chapter.

4. Molecular nitrogen - The profiles for this species are also given in Fig.6.2. The amount of N_2 formed depends upon the quantity of methane added, but much more markedly than for the formation of nitric oxide. Little of the nitrogen is formed in the reaction zone when $[CH_4]_0$ is above 0.05% and in fact most is produced immediately downstream. Its concentration decreases with increasing $[CH_4]_0$ and at 0.25% and 0.5% of methane in the unburnt gases, no N_2 is detected in the reaction zone. At concentrations of methane greater than 0.25% by volume, all the N_2 is formed downstream and increases in amount up to 10 mm away from the reaction zone, depending upon the amount of methane added. At distances greater than 10 mm from the reaction zone its rate of appearance decreases. It should be borne in mind that $[N_2]$ was calculated by a mass balance on the nitrogenous species present and not measured experimentally, so that errors in $[N_2]$ can be considerable. The value of $[N_2] = 0$ in the reaction zone for large amounts of CH_4 present is a puzzle. One might expect N_2 to be formed by $NH_i + NO \rightarrow N_2$ + products at a rate proportional

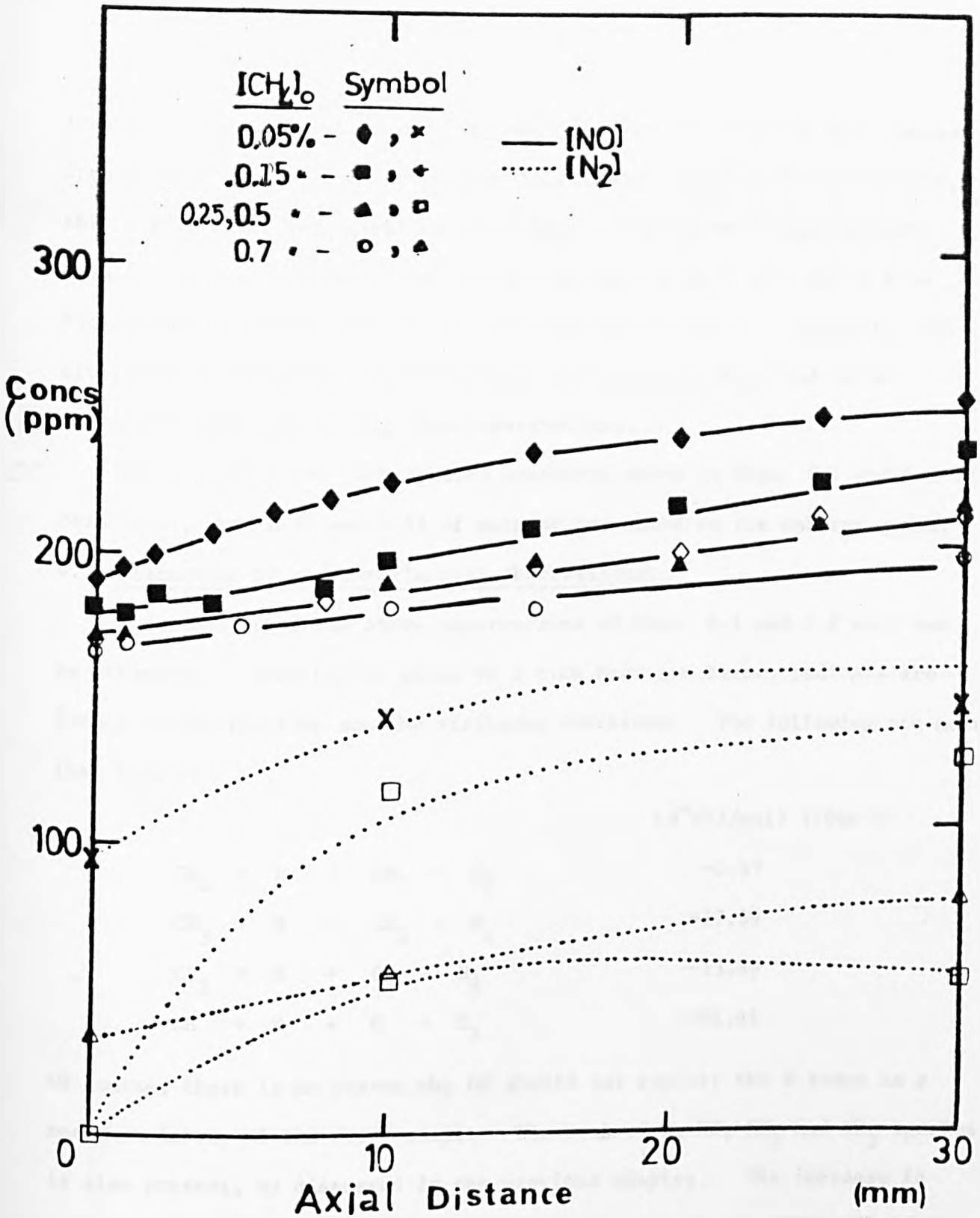

Fig. 6.2 Concentration profiles of NO and N_2 in flame 2 with 615 ppm of ammonia added

to $[NH_i]$ [NO]. Since the product $[NH_i]$ [NO] in the reaction zone changes from 5.95×10^4 $(ppm)^2$ with no methane to 2.61×10^4 $(ppm)^2$ with 0.70% of it, this hardly seems sufficient to cause $[N_2]$ to fall from 90 ppm to zero. Equally, it seems unlikely that a reaction such as $N_2 + CH \rightarrow HCN + N$ is fast enough to reduce $[N_2]$ in the reaction zone to zero. Certainly, the difficulty of measuring concentrations, particularly $[N_2]$, has to be remembered when considering these observations.

Every profile for each species presented above in Figs. 6.1 and 6.2 is coincident, when 0.25 and 0.5% of methane are added to the unburnt gases.

6.3 Discussion of the experimental observations:

A discussion of the above observations of Figs. 6.1 and 6.2 will now be attempted. When CH_4 is added to a rich hydrogen flame, radicals are formed in the reaction zone by stripping reactions. The following are more than likely:

	ΔH^o(kJ/mol) (1900 K)
$CH_4 + H \rightarrow CH_3 + H_2$	-0.47
$CH_3 + H \rightarrow CH_2 + H_2$	+17.59
$CH_2 + H \rightarrow CH + H_2$	-13.89
$CH + H \rightarrow C + H_2$	-101.41

Of course, there is no reason why OH should not replace the H atoms as a reactant in any of the above steps. The pool of N, NH, NH_2 and NH_3 species is also present, as discussed in the previous chapter. The increase in concentration of cyanides with the amount of methane in the flame, has been seen to be in line with the hydrocarbon or one of its derivatives reacting with a nitrogenous species, such as NH_i, and to a lesser extent NO. This is confirmed by $[NH_i]_t$ in the reaction zone being lowered by the progressive addition of methane.

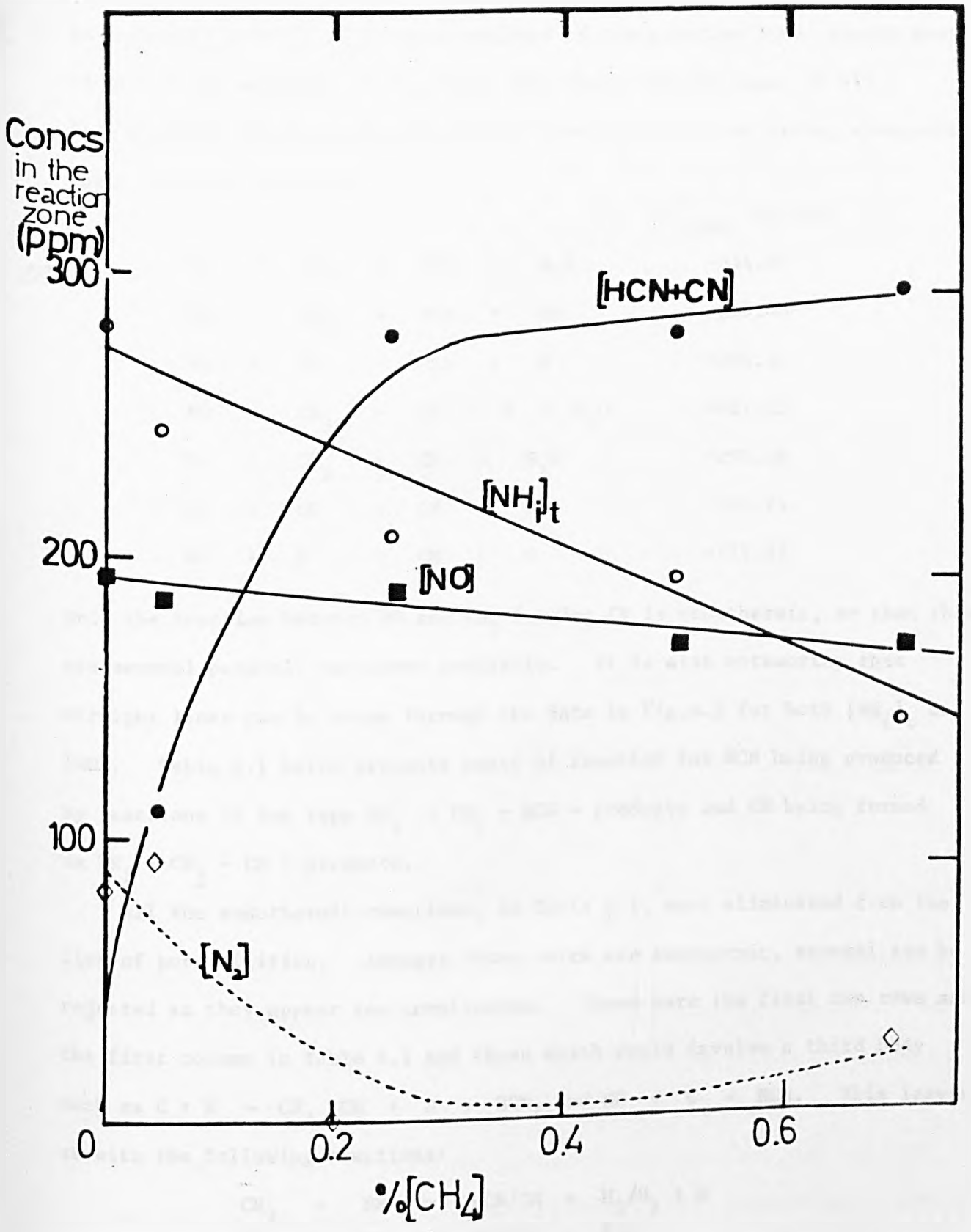

Fig. 6.3 Concentrations in the reaction zone of NO, HCN + CN, N_2 and NH_3 species against the amount of hydrocarbon present in the unburnt gases.

Figure 6.3 shows the values of $[NH_i]_t$, [HCN + CH], [NO] and $[N_2]$ in the reaction zone plotted against the percentage of CH_4 in the burner supplies. As indicated before, $[N_2]$ and [cyanides] in the reaction zone respond most of all to the addition of CH_4, with [NO] there varying least of all. Some possible reactions forming HCN/CN from NO are listed below, along with their heats of reaction:

								ΔH^o_{1900} (kJ/mol)
NO	+	CH_3	→	HCN	+	H_2O		-344.41
NO	+	CH_2	→	HCN	+	OH		-299.45
NO	+	CH	→	HCN	+	O		-294.54
NO	+	CH_3	→	CN	+ H +	H_2O		+181.13
NO	+	CH_2	→	CN	+	H_2O		-290.19
NO	+	CH	→	CN	+	OH		-213.74
NO	+	C	→	CN	+	O		-121.32

Only the reaction between NO and CH_3 forming CN is endothermic, so that there are several possible processes available. It is also noteworthy that straight lines can be drawn through the data in Fig.6.3 for both $[NH_i]_t$ and [NO]. Table 6.1 below presents heats of reaction for HCN being produced by reactions of the type $NH_i + CH_j \rightarrow$ HCN + products and CN being formed in $NH_i + CH_j \rightarrow$ CN + products.

All the endothermic reactions, in Table 6.1, were eliminated from the list of possibilities. Amongst those which are exothermic, several can be rejected as they appear too complicated. These were the first two rows and the first column in Table 6.1 and those which could involve a third body such as C + N → CN, CH + N → HCN, and NH + C → HCN. This leaves us with the following reactions:

CH_2	+	NH	→	HCN/CN	+	H_2/H_2	+ H
CH	+	NH	→	HCN/CN	+	H/H_2	
C	+	NH	→	CN	+	H	

$$CH_3 + N \rightarrow HCN/CN + H_2/H_2 + H$$

$$CH_2 + N \rightarrow HCN/CN + H/H_2$$

$$CH + N \rightarrow CN + H$$

as likely possibilities.

Table 6.1

ΔH^o at 1900 K for reaction between NH_i and hydrocarbon radicals, in kJ/mol (Data are taken from Janaf Tables, 1973). The numbers quoted in space 1 are for HCN as product, those under 2 are for CN as product.

1 \ 2	CH_3	CH_2	CH	C
NH_3	+352.23 / +280.41	+334.63 / -192.17	-105.20 / -177.03	-3.79 / -529.33
NH_2	+362.27 / -163.27	-109.04 / -182.14	-95.16 / -620.69	-447.47 / -519.30
NH	-81.05 / -152.22	-98.65 / -205.78	-538.48 / -609.65	-437.07 / -961.94
N	+43.21 / -482.32	-428.10 / -501.20	-414.23 / -939.75	-766.53 / ---

As mentioned above, the decrease of $[NH_i]_t$ on the addition of methane could be explained by reactions between hydrocarbon radicals and NH_i species. In addition, the presence of methane could well give rise to the formation of species such as OCN and HOCN, which could take part in reactions such as OCN + H → NH + CO etc. to yield NH_i species. The species, OCN and HOCN, are detected by the ammonia electrode, admittedly with reduced sensitivity. However, OCN and HOCN are expected to yield NH_i most probably close to the

reaction zone and so the presence of OCN or HOCN is not much of a complication. The disappearance of cyanides is discussed in the next paragraph. The rate of disappearance of the NH_i species just after the reaction zone was found to be lower with methane present than without it. This could be explained by an additional process forming NH_i species, but this will be dealt with also in the next paragraph, where the disappearance of cyanides is considered.

The disappearance of cyanides cannot produce NH_i directly because the back reactions of those presented in Table 6.1 are very endothermic. The decrease in concentration of the cyanides along the flame axis also cannot be due to $HCN + N \rightarrow N_2 + CH$ or $CN + NO \rightarrow CO + N_2$, because, as Fig. 6.3 shows, $[N_2]$ decreases when [cyanides] increase. A study of the thermodynamics of possible reactions accounting for the disappearance of cyanides with the consequent formation of NH_i or NO is presented below:

Table 6.2

Enthalpy changes of reactions involving CN or HCN disappearance at 1900 K.

Reactions	ΔH^{o}_{1900K} (kJ/mol)
$CN + H_2O \rightarrow HOCN + H$	-3.59
$HCN + OH \rightarrow HOCN + H$	-49.01
$HCN + H_2O \rightarrow HOCN + H_2$	+13.55
$HOCN + H \rightarrow NH_2 + CO$	-77.09
$HOCN + H_2O \rightarrow NH_3 + CO_2$	-10.24
$OCN + H_2 \rightarrow HOCN + H$	-40.18
$CN + CO_2 \rightarrow OCN + CO$	+8.90
$CN + OH \rightarrow OCN + H$	-80.64
$CN + OH \rightarrow NO + CH$	+213.74
$OCN + H \rightarrow NH + CO$	-127.67
$OCN + H \rightarrow NO + CH$	+294.39
$OCN + H_2 \rightarrow NH_2 + CO$	-117.27

There are some endothermic reactions amongst those shown above, and these can be rejected for the production of NO. It does seem that cyanides disappear to form OCN or HOCN, which on reaction with H, H_2 or H_2O produce NH_i species rather than NO.

The reaction HCN + H → HNC + H is likely to be rapid and balanced. Also, considering the reaction HCN + H → CN + H_2 (ΔH^o_{1900} = 17.14 kJ/mol) with an equilibrium constant K, and k_f and k_r as rate constants for the forward and reverse reactions, respectively, the rate of disappearance of HCN is

$$-d[HCN]/dt = k_f[HCN][H] - k_r [CN] [H_2]$$

According to Albers (1977) k_r is $(6\pm2)\times10^{13}$ exp [-(22.2 ± 2.5 kJ/mol)/RT] ml $mol^{-1}s^{-1}$. This agrees quite well with the value found by Robertson and Pease (1942) at 687 K, i.e. $k_r < 2\times10^{-11}$ ml $molecule^{-1}s^{-1}$. Therefore with $k_r = 2.4\times10^{11}$ ml $molecule^{-1}s^{-1}$ and K = 0.0257, $k_f = 6.2\times10^{-13}$ ml $molecule^{-1}s^{-1}$ and hence $-d[HCN]/dt = 3.8\times10^{3}[HCN] - 5\times10^{6}$ [CN] for flame 2 with $[H_2]/[O_2]$ = 2.5. The relaxation time for the interconversion of HCN and CN derived from the above expression is 0.2 μs which is much lower than the residence time in the reaction zone of 20 μs. This means that HCN and CN constitute an equilibrated "pool".

The disappearance of HCN and CN can be dealt with in terms of a parameter θ, defined as $\theta = [HCN]/[CN] = [H_2]/(\gamma[H]_e K)$. This gives $\theta_e = [H_2]/([H]_e K)$ at equilibrium, i.e. $\gamma = 1$. The total concentration of the cyanide pool equals $\{[HCN] + [CN]\} = [CN](1+\theta)$. One possible route for the consumption of the cyanide pool was seen above to be

$$CN + OH \rightarrow OCN + H \qquad (12)$$

If this is the rate determining step:

$$-d[HCN + CN]/dt = k_{12}[CN][OH]$$

$$= k_{12} \frac{[\text{cyanides}][OH]}{(1+\gamma^{-1}\theta_e)}$$

Since $\theta_e \cong 10^4$ and $\gamma^{-1}\,\theta_e >> 1$, one obtains

$$-d\,\ell n\,[\text{cyanides}]/dt = k_{12}\,\gamma^2\,[OH]_e/\theta_e.$$

Integration of this equation from the reaction zone (t = 0) to a general point in the burnt gases yields

$$\ell n[HCN + CN] = k_{12}[OH]_e\,\gamma/(b\,\theta_e) + \ell n[HCN + CN]_{R.Z.} - k_{12}[OH]_e\,\gamma_o/(b\,\theta_e)$$

where $\gamma^{-1} = \gamma_o^{-1} + bt$, and $\gamma_o = [H]/[H]_e$ in the reaction zone. The experimental observations test this equation in Fig. 6.4, where the points nearest the reaction zone are those with highest [cyanides]. A straight line with a positive slope (as predicted by the above equation) can be drawn through the data. The slope yields $k_{12} = (3.2 \pm 1.0)\times 10^{-10}$ ml molecule^{-1}s^{-1} which agrees with the value, 1.0×10^{-10} ml molecule^{-1}s^{-1} found by Morley (1975) at 2000 K.

Alternatively, if the rate-determining step is HCN + OH → products with a rate coefficient k_{13}, a similar procedure produces:

$$d\,\ell n[\text{cyanides}] = \left(k_{13}[OH]_e/b\right)\,d\gamma/\gamma$$

or

$$\ell n\,\frac{[HCN + CN]}{[HCN + CN]_{R.Z.}} = k_{13}\left([OH]_e/b\right)\,\ell n\,(\gamma/\gamma_o)$$

<u>i.e.</u>

$$\ell n\,[HCN + CN] = k_{13}\,([OH]_e/b)\,\ell n\,\gamma + \ell n[HCN + CN]_{R.Z.} - k_{13}\,[OH]_e\,\ell n\,\gamma_o/b.$$

The measured values of ℓn [cyanides] are plotted against $\ell n\gamma$ in Fig. 6.5, using the magnitudes of γ given in Chapter 4. The points nearest the reaction zone are those with highest [cyanides]. Three straight lines are drawn in Fig. 6.5 through the points representing 0.05%, 0.25%, 0.5% and 0.7% of methane in the unburnt gases. These lines appear to fit the experimental observations reasonably and the slopes are positive as predicted by

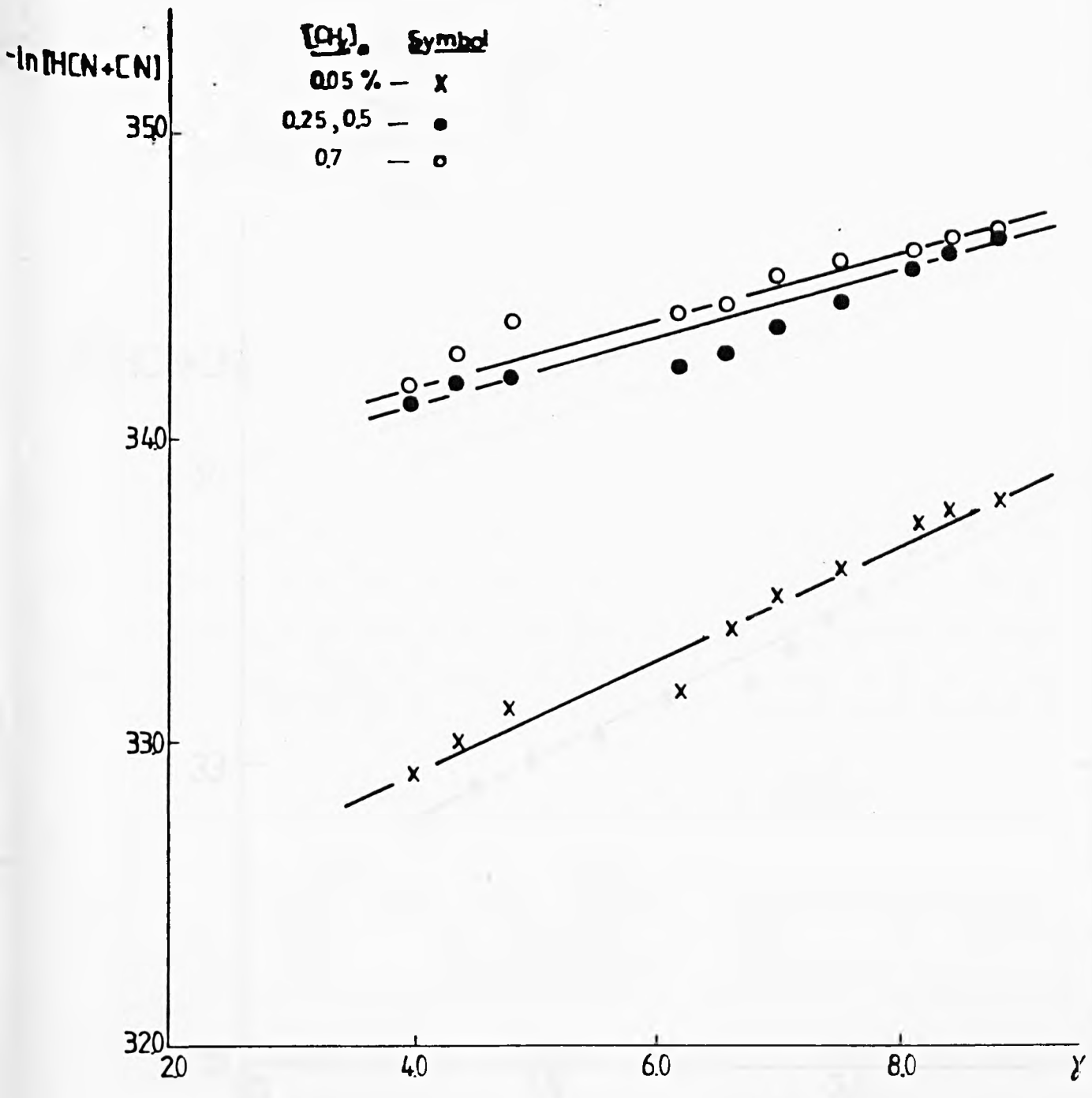

Fig 6.4 Plot to check CN + OH → products

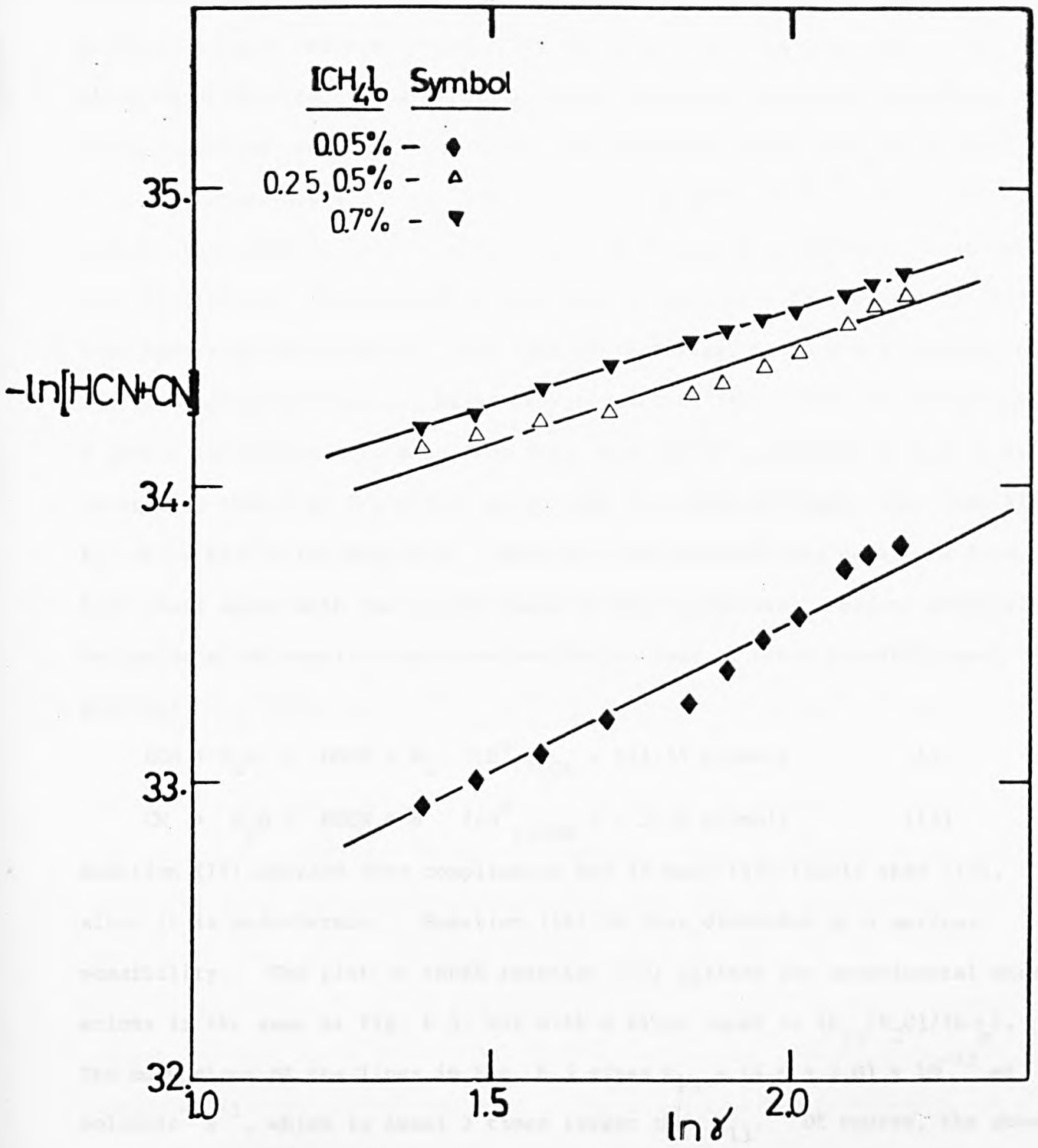

Fig. 6.5 $\ln [HCN+CN]$ against $\ln \gamma$ for the flame with $[H_2]/[O_2] = 2.5$ and 615 ppm of ammonia added to the unburnt gases.

the above theoretical equation. The line passing through the points for 0.05% of methane has a slightly different slope than the other two. The above equation predicts parallel lines for different additions of methane. Using an average value for the slope, the magnitude of $k_{13}[OH]_e/b$ is 0.76 ± 0.24. From this $k_{13} = (1.75 \pm 1.5)\times10^{-13}$ ml molecule^{-1}s^{-1}, which is smaller than that (1.7×10^{-12} ml molecule^{-1}s^{-1}) quoted by Fenimore (1978) but for 1300–1800 K. Haynes (1977) predicted a value of $(3.3 \pm 0.3)\times10^{-13}$ for k_{13} over the range 1950–2380 K. The fact is that Figs. 6.4 and 6.5 suggest that the consumption of cyanides might be via reaction (13), (12) or indeed both. A choice is difficult to make from Figs. 6.4 and 6.5, although it has to be recognised that Fig. 6.4 with γ as abcissa is a more stringent test than Fig. 6.5 where $\ell n\gamma$ is the abscissa. Moreover, the derived rate constants from both plots agree with the values found in the literature. Before attempting to decide which reaction operates,one has to look at other possibilities, such as:

$$HCN + H_2O \rightarrow HOCN + H_2 \quad (\Delta H^o_{1900K} = +13.55 \text{ kJ/mol}) \qquad (14)$$

$$CN + H_2O \rightarrow HOCN + H \quad (\Delta H^o_{1900K} = -3.59 \text{ kJ/mol}) \qquad (15)$$

Reaction (14) appears very complicated and is much less likely than (15), since it is endothermic. Reaction (14) is thus discarded as a serious possibility. The plot to check reaction (15) against the experimental observations is the same as Fig. 6.5, but with a slope equal to $(k_{15}[H_2O]/(b\,\theta_e)$. The mean slope of the lines in Fig. 6.5 gives $k_{15} = (4.8 \pm 2.0) \times 10^{-13}$ ml molecule^{-1}s^{-1}, which is about 3 times larger than k_{13}. Of course, the above value of k_{15} indicates that a more likely set of products for CN reacting with H_2O molecules are HCN + OH,with a rate constant of 7.3×10^{-11} ml molecule^{-1}s^{-1} (Miyauchi 1977). The above values for the rate constants might be slightly in error because of temperature variations along the flame and a consequent error in assuming $\gamma_{OH} = \gamma_H$. However, in this flame, in

which $[H_2]/[O_2]$ = 2.5, γ_{OH} is not expected to be much different from γ_H. The question of which of three reactions is responsible for attacking the CN/HCN pool and ultimately producing NO is finally dealt with in the next chapter.

6.4 Conclusions on a mechanism for the production of NO in flames with ammonia and hydrocarbon present simultaneously.

Some conclusions from the discussion given in the previous sections are:

1. Hydrocarbon radicals attack nitrogenous species NH_i (particularly NH and N atoms) in a flame forming cyanides.

2. The disappearance of the cyanide pool is complicated and at this stage it is not possible to identify the reaction responsible with any certainty.

3. The intermediate species and products of the oxidation of the cyanide pool are likely to include HOCN and OCN. It is probable that cyanides do not form NO, N_2 or even NH_i in one single step.

4. The production of NO and N_2 appears to be through the same reactions with and without the hydrocarbon present. The amount of NO was seen to decrease with increasing additions of the hydrocarbon. This is thought to be mainly due to the depletion of NH_i species in the pool when NH_i species react with the hydrocarbon and its radicals.

5. The production of NO in richer flames with various amounts of ammonia present, as well as in flames with higher temperature, appears to be in agreement with the above conclusion. One possible overall mechanism for the appearance of NO is given below

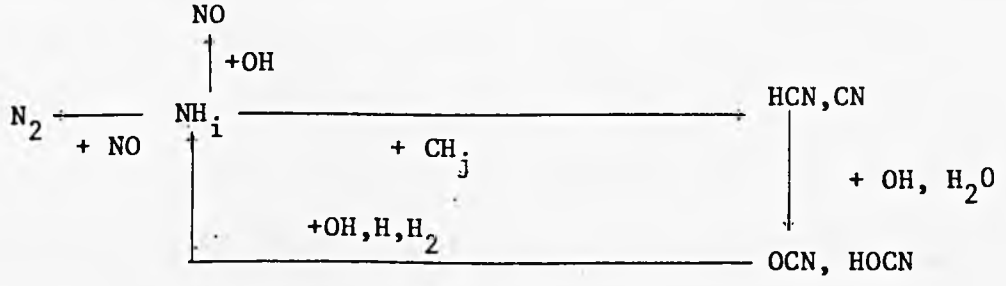

In the following chapter, flames with nitric oxide added both alone and in the presence of hydrocarbons will be dealt with. The brief investigation given in this chapter presents guidelines for the study of flames with NO added, hoping that a better elucidation of a mechanism of production of NO from fuel-nitrogen can be made.

Chapter 7.

Observations in flames with additions of both hydrocarbons and NO.

7.1 Introduction.

The experimental observations in flames with nitric oxide added alone and together with a hydrocarbon will be described and discussed in this chapter. The flames used in this work were designated 2, 4, 6 and 7 in Table 4.1 and in Table C1 of Appendix C. Their adiabatic temperatures were all 1900 K. Different amounts of NO were added to the unburnt gases and, for each of these values of $[NO]_0$ several quantities of hydrocarbon were also added. The type of hydrocarbon added to each unburnt gas mixture was also varied. Measurements of [NO], $[NH_i]_t$ and [HCN + CN] were made by the techniques already explained in Chapter 3.

Firstly, flames with only NO added to the unburnt gases will be discussed in Section 7.2. This will be followed by a study of flames with additions of both nitric oxide and hydrocarbons.

7.2 Discussion of the experimental observations in flames with only nitric oxide present as additive.

The concentrations of NO and total-NH_i species were measured when no hydrocarbon was added to a flame. The measurements obtained in all the flames showed the same general behaviour. Since there were no hydrocarbons present, cyanides were not expected and so were not measured. The total concentration of NH_i species was measured to be zero. The fact that there are no NH_i species present in the burnt gases means that processes, such as $NO + H \rightarrow N + OH$, $H + HNO \rightarrow NH + OH$, $H + NO \rightarrow NH + O$, $NO + H_2 \rightarrow NH + OH$ do not occur, even in very hydrogen-rich flames.

In addition, the amount of NO measured along each flame axis was constant in the burnt gases and approximately the same as that calculated from $[NO]_0$

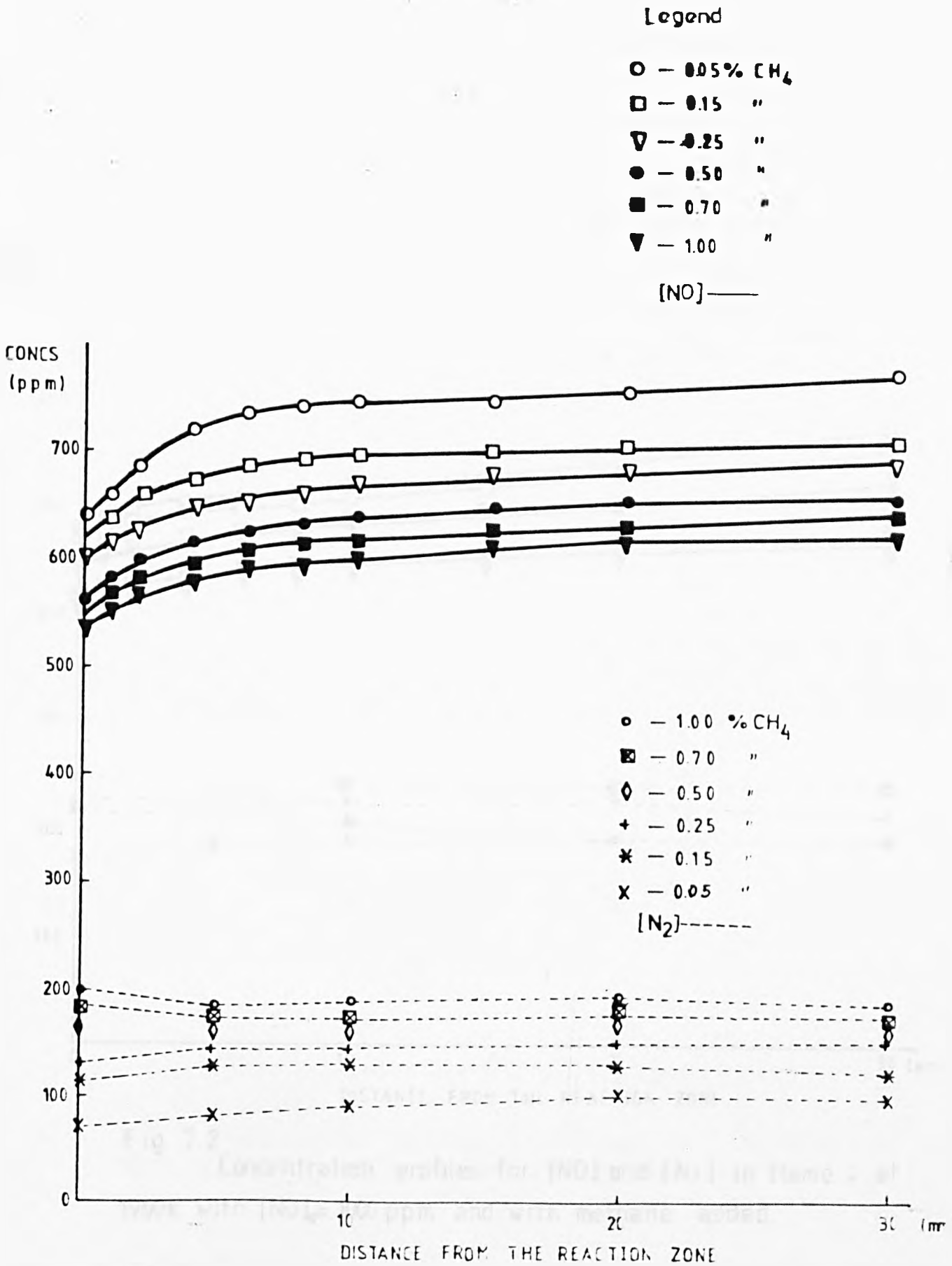

Fig. 7.1. Concentration profiles por [NO] and [N_2] in flame 2 with $[NO]_o$ = 1000 ppm, at 1900 K, and with methane added.

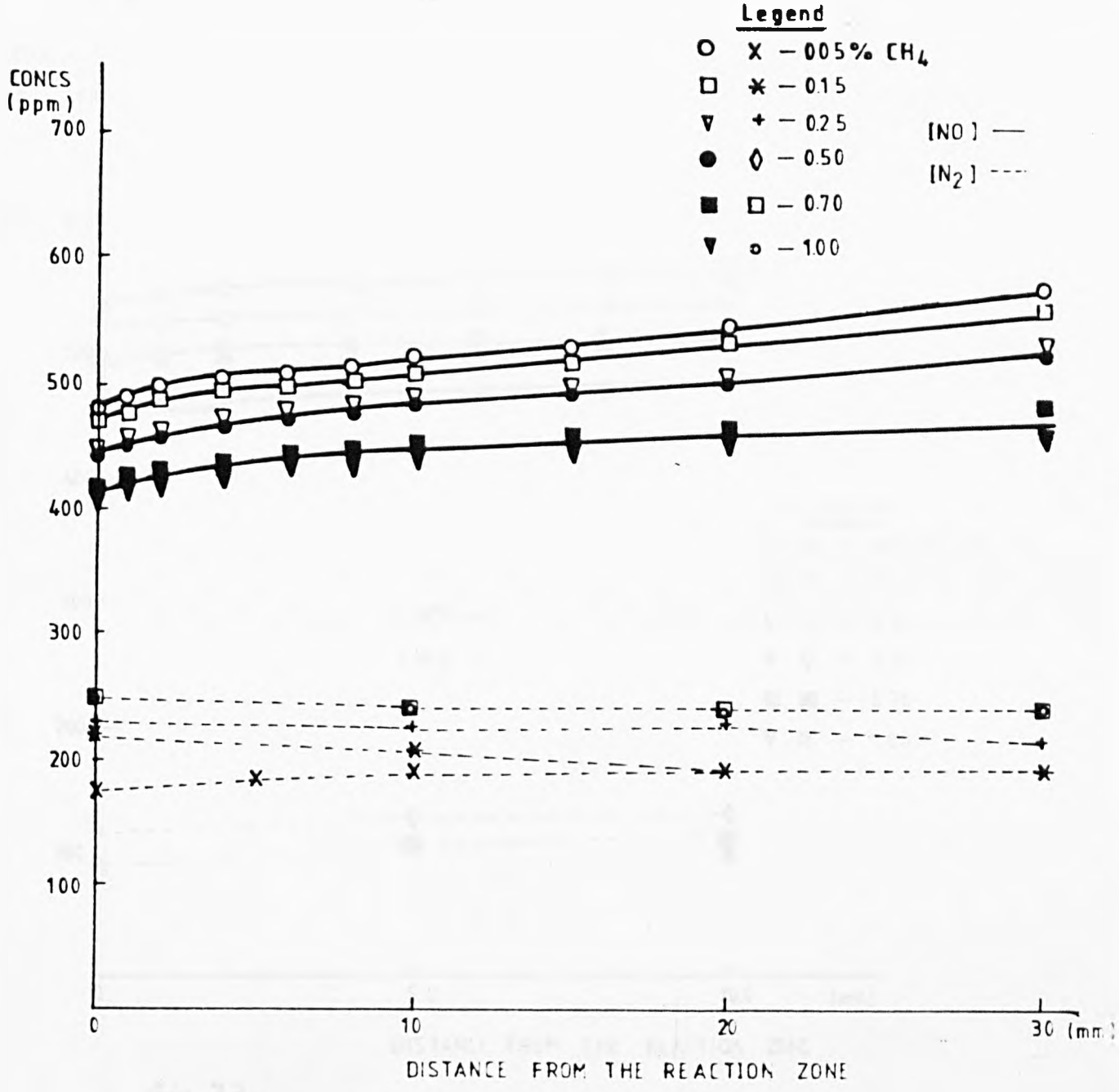

Fig. 7.2 Concentration profiles for [NO] and [N_2] in flame 2 at 1900K with $[NO]_o$= 1000 ppm and with methane added.

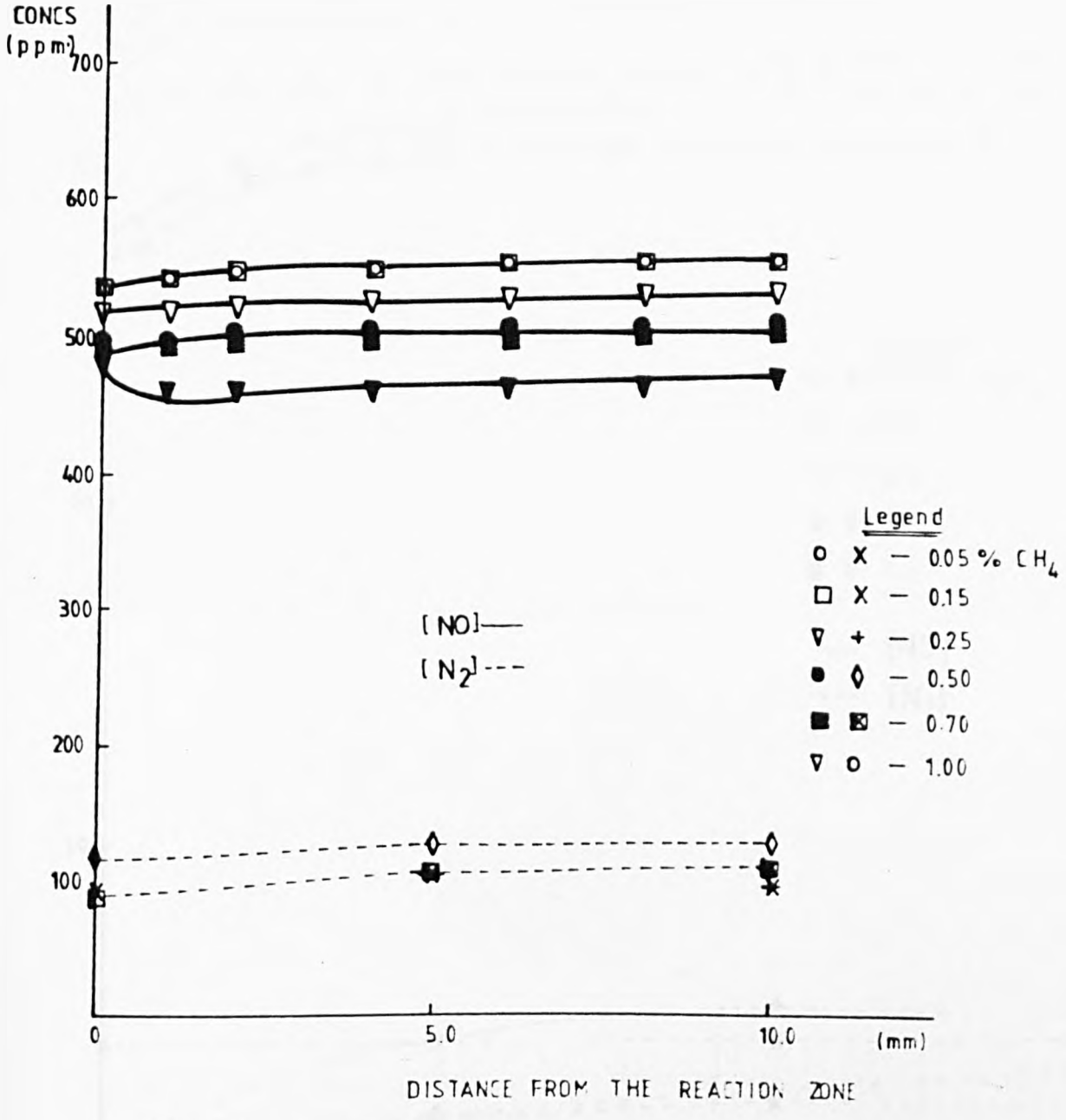

Fig. 7.3 Concentration profiles for [NO] and [N_2] in flame 7 at 1900 K with $[NO]_o$ = 1000 ppm and, with methane added.

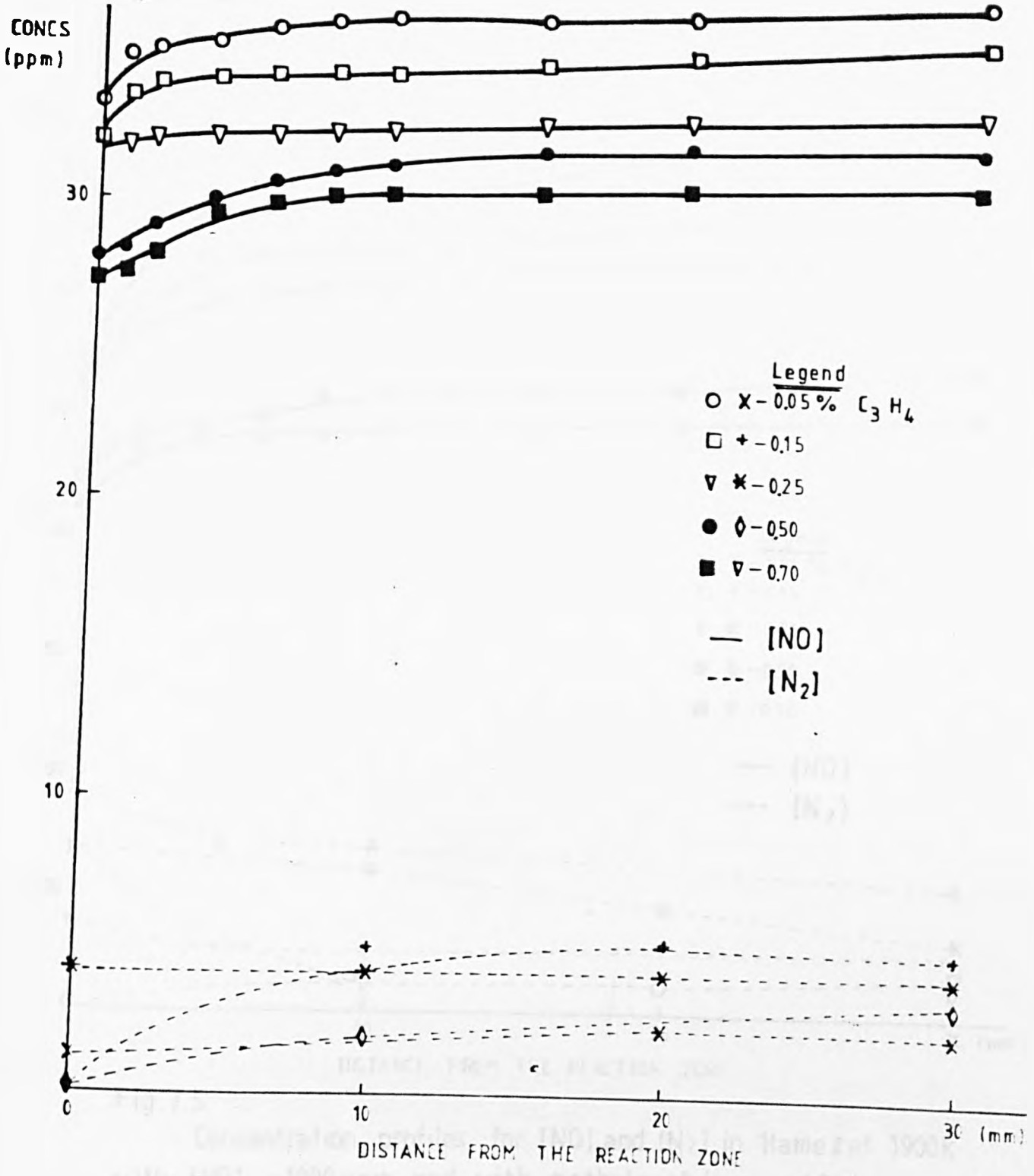

Fig. 7.4 Concentration profiles for [NO] and [N_2] in flame 2 at 1900K with $[NO]_o$ = 90 ppm and the Hydrocarbon added is methylacetylene.

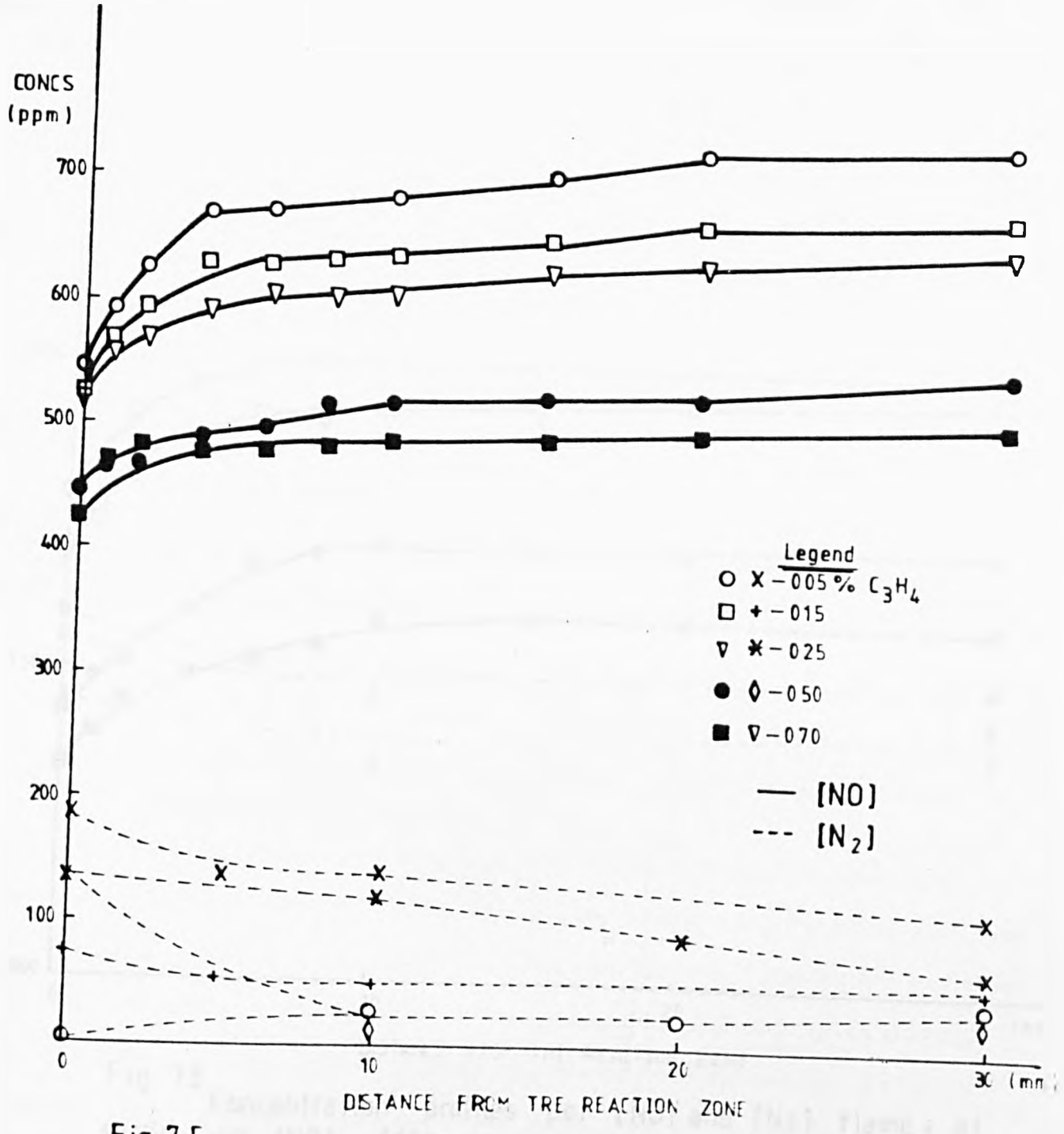

Fig. 7.5

Concentration profiles for [NO] and [N_2] in flame 2 at 1900K with $[NO]_b$ = 1000 ppm and with methylacetylene added

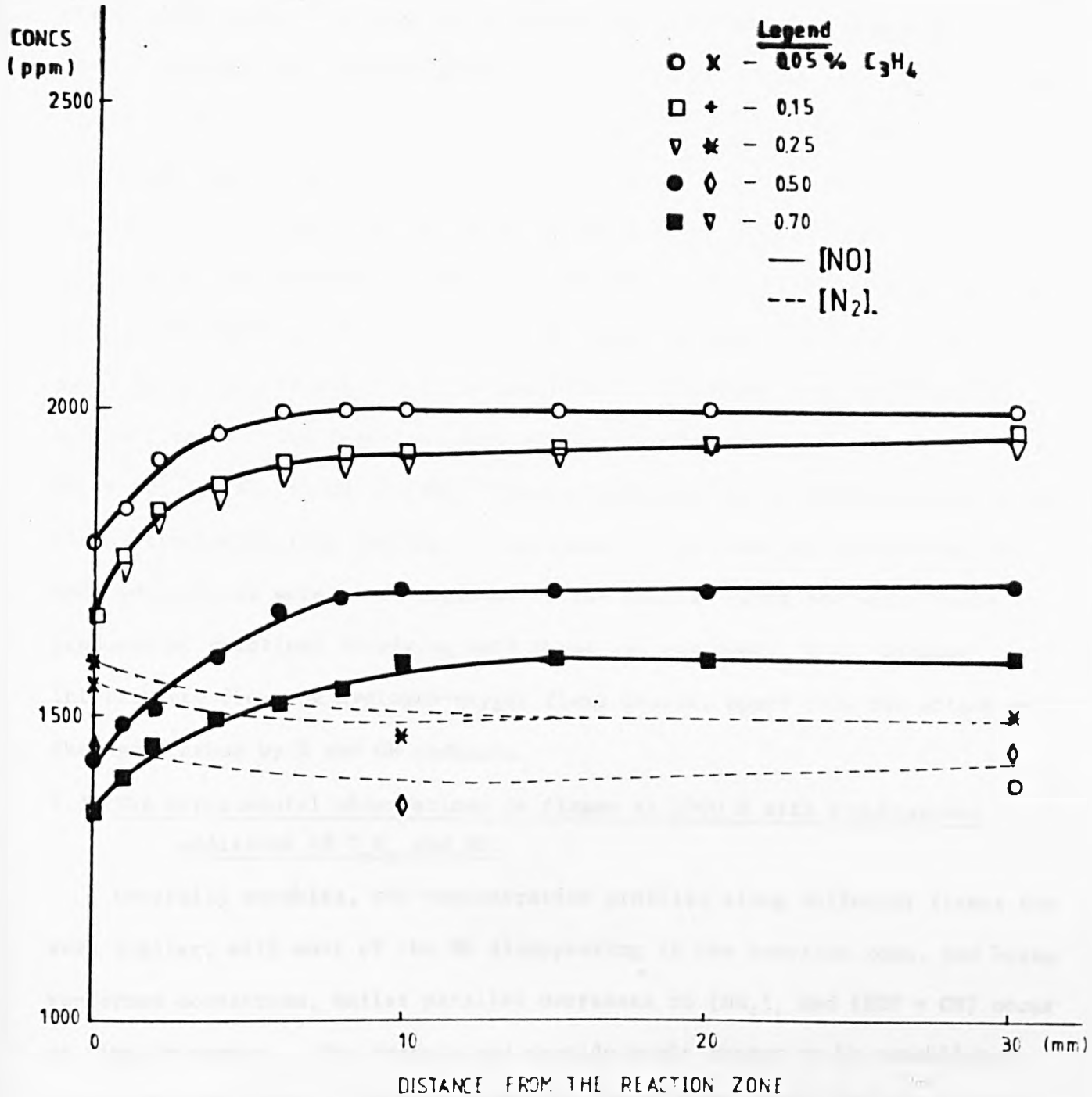

Fig. 7.6 Concentration profiles por [NO] and [N_2] flame 2 at 1900 K with $[NO]_o$ = 5000 ppm and with methylacetylene added

by assuming that there was complete combustion, and NO did not undergo reaction of any kind. Such an observation is in line with Bulewicz and Sugden's (1964) early work. In and very close to the reaction zone (i.e., up to about 3 mm from the reaction zone), in flames 4 and 7 with $[H_2]/[O_2]$ = 3.5 and 5.0, [NO] measured was slightly lower (by up to 4%) than that predicted by the unreacted input of NO. In flame 2 with $[H_2]/[O_2]$ = 2.5, [NO] was always constant, corresponding to the total amount of NO present. Therefore,the decrease in concentration of NO in the two richer flames could be due to either radical overshoot in the vicinity of the reaction zone causing NO to give small quantities of e.g., N atoms and this could become more important in richer flames. The reactions between nitric oxide and hydrogen

$NO + H_2 \rightarrow NH + OH$ or HNO + H were considered to be insignificant in the flames studied in this chapter. Consequently, the species formed when NO and hydrocarbons were added together to the unburnt gases are most likely produced by reactions involving only these two compounds, i.e., without interference from the hydrogen-oxygen flame itself, apart from the attack on the hydrocarbon by H and OH radicals.

7.3 The experimental observations in flames at 1900 K with simultaneous additions of C_nH_m and NO.

Generally speaking, the concentration profiles along different flames are very similar, with most of the NO disappearing in the reaction zone, and being re-formed downstream, whilst parallel decreases in $[NH_i]_t$ and [HCN + CN] occur as time increases. The ammonia and cyanide pools appear to be established in the reaction zone. In this study six flames were chosen for the concentration profiles to be measured; hence variations in the amounts of all the nitrogenous species present with the $[H_2]/[O_2]$ ratio or with the amount of NO added or even with the type of hydrocarbon could be assessed. The [NO] and $[N_2]$ profiles are given in Figs. 7.1 to 7.6 and those for $[NH_i]_t$ and [HCN + CN] in Figs. 7.7 to 7.12. The various cases will now be considered:

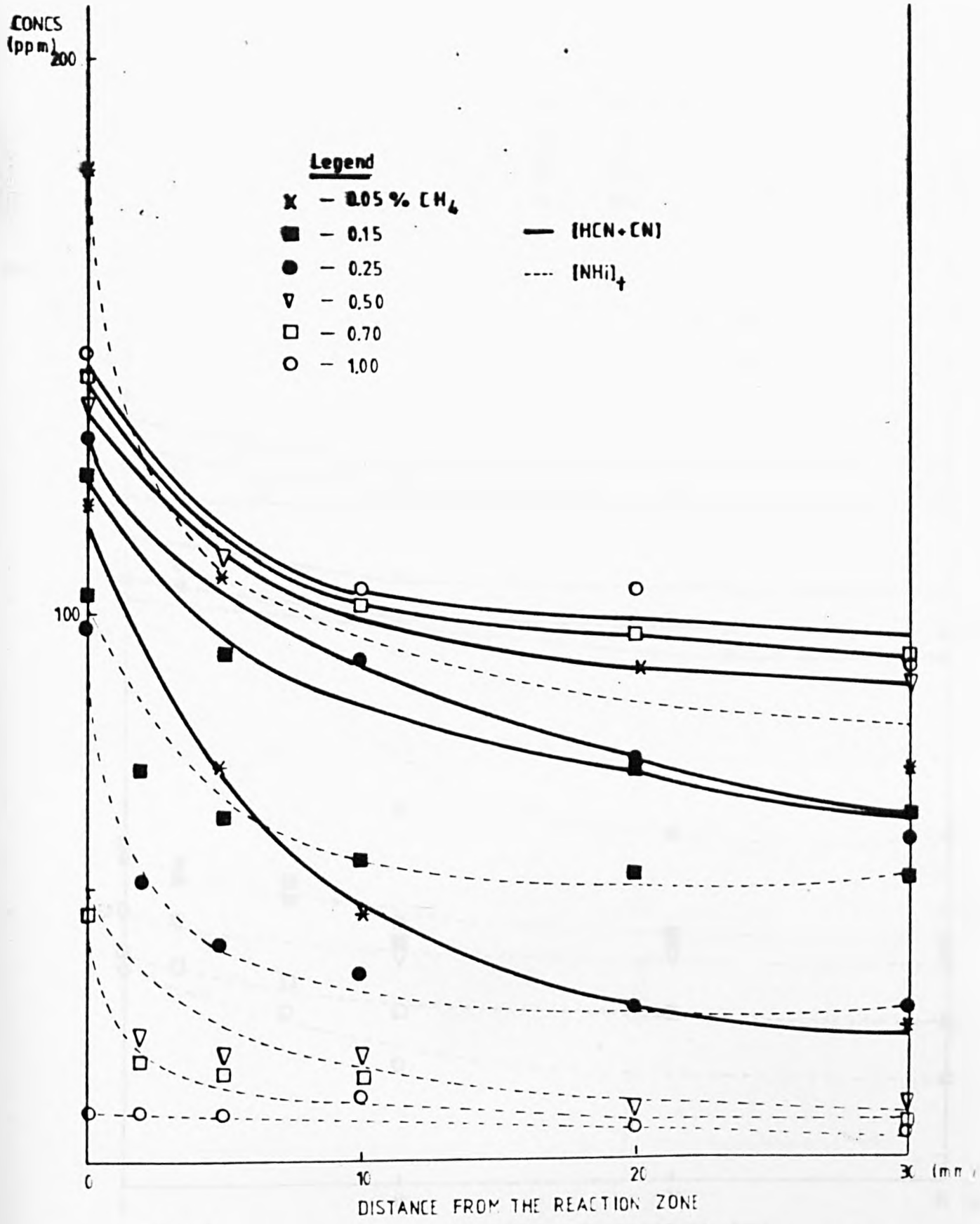

Fig. 7.7

Concentration profiles of NHi and cyanides for flame, 2 at 1900K and 1000 ppm of NO added with various amounts of methane

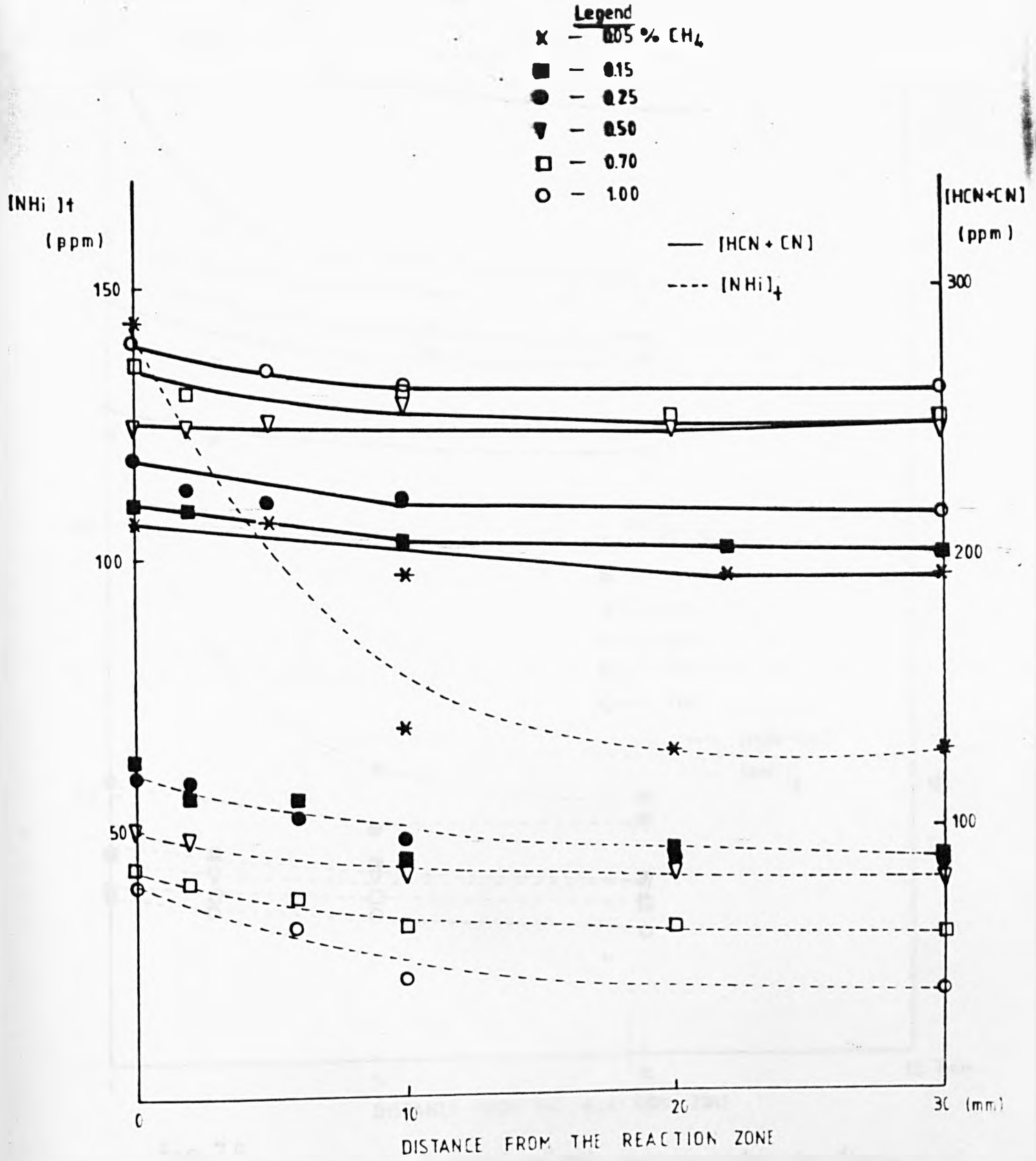

Fig. 7.8 Concentration profiles of NHi and cyarides for flame 4 at 1900 K and 1000 ppm of NO added together with various amounts of methane.

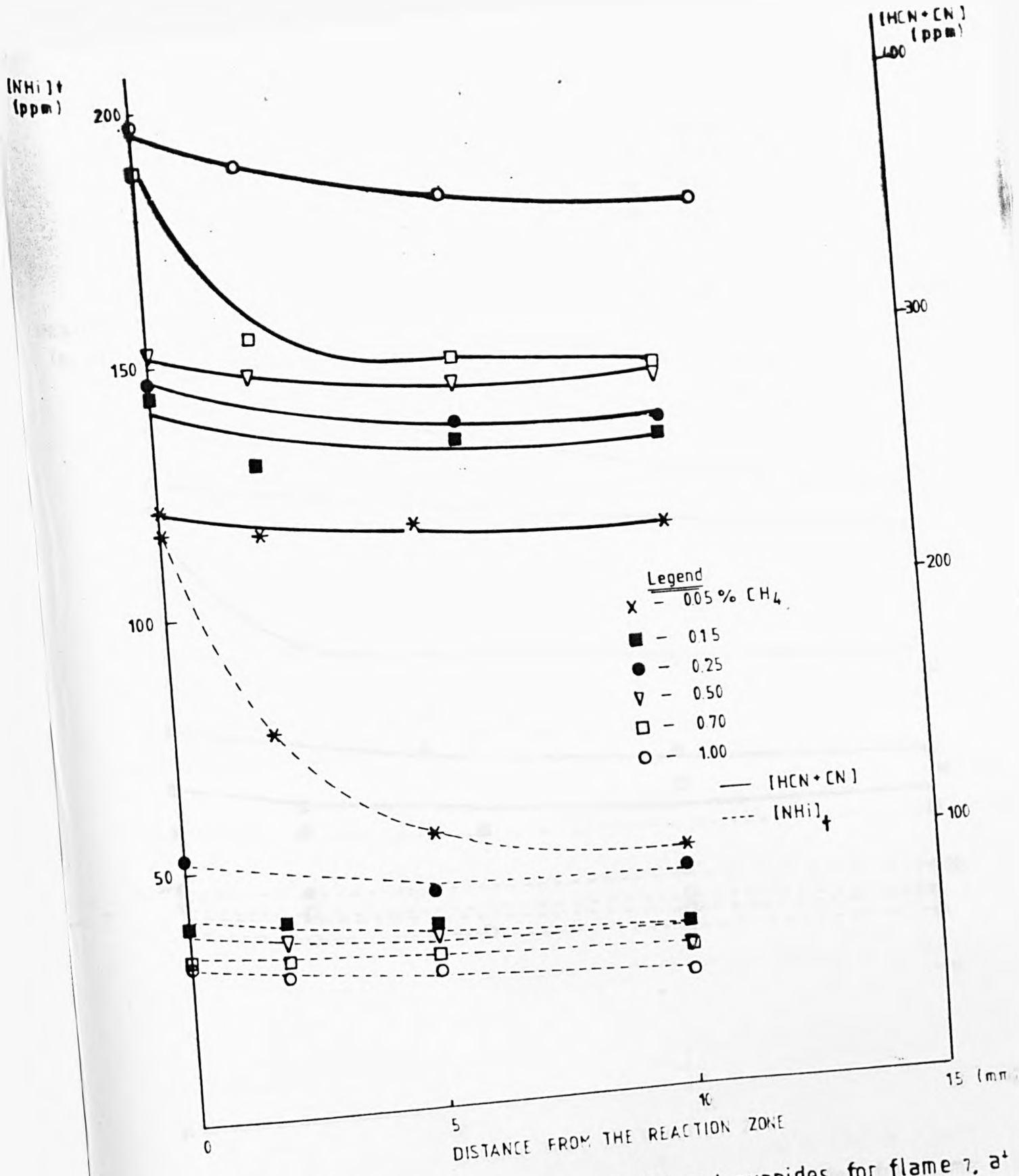

Fig. 7.9 Concentration profiles of NHi and cyanides for flame 7, at 1900K with $[NO]_o$ = 1000 ppm and methane added

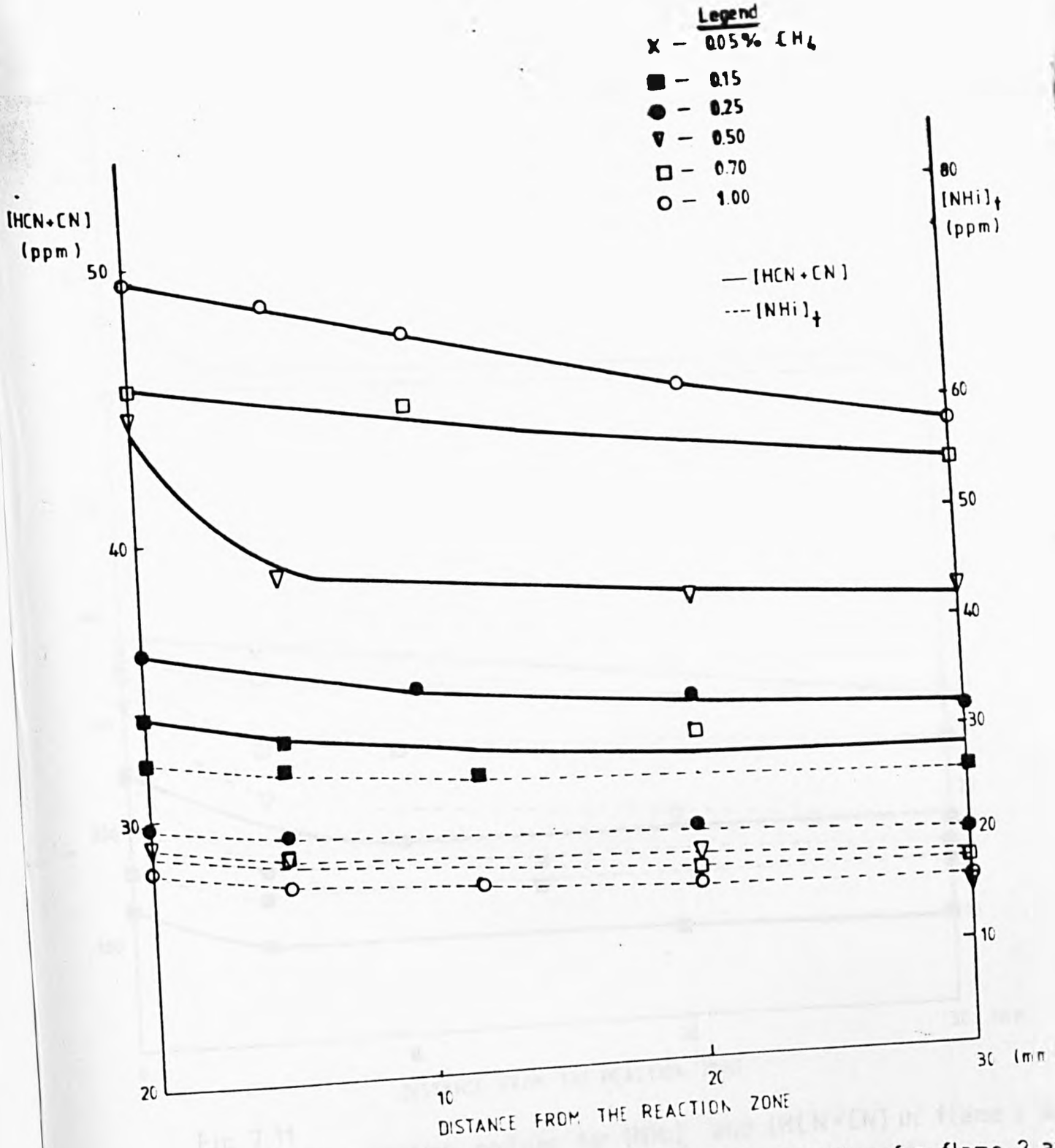

Fig. 7.10 Concentration profiles of NHi and cyanides for flame 2 at 1900K and 90 ppm of NO added with methylacetylene

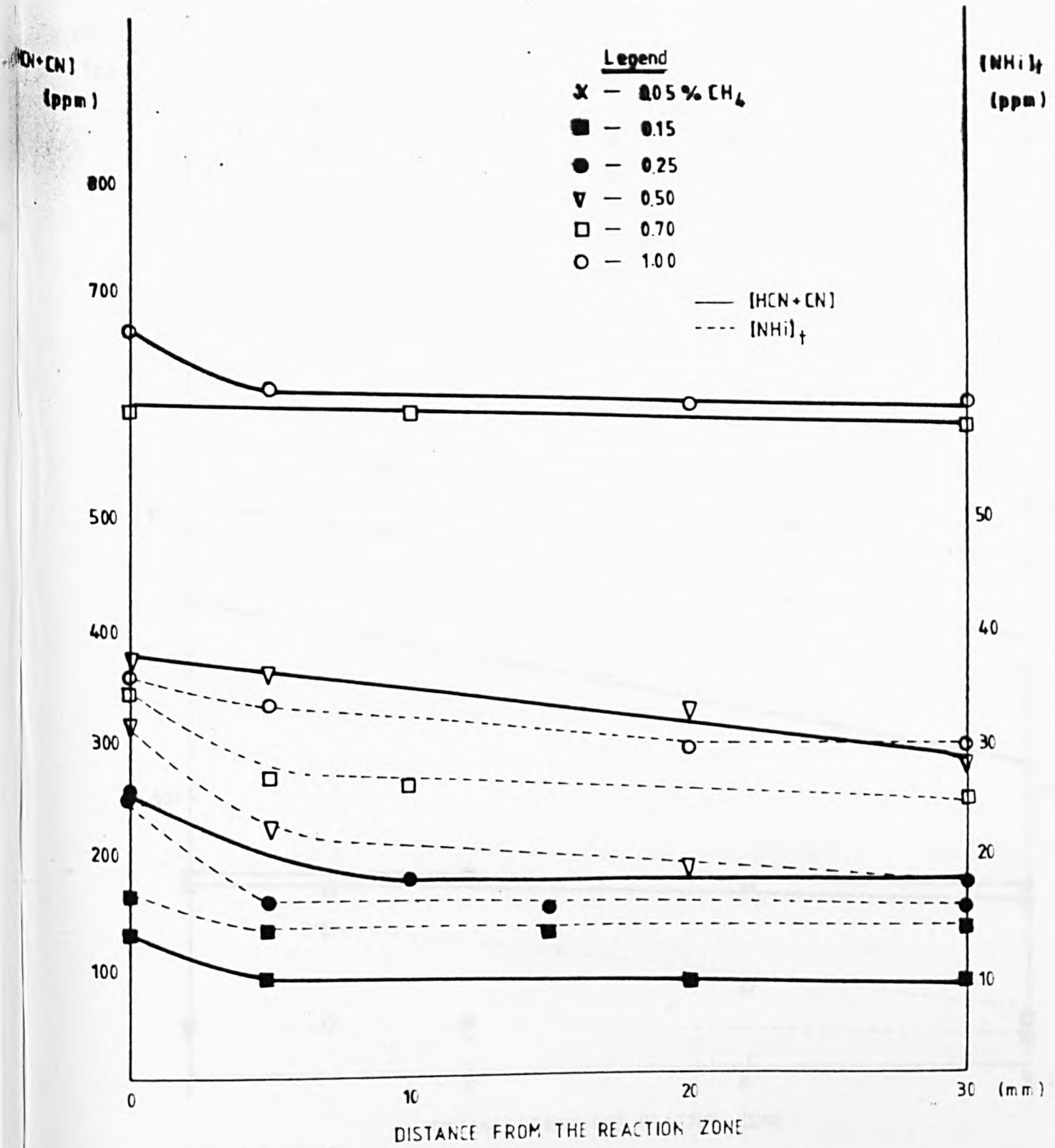

Fig. 7.11 Concentration profiles for $[NHi]_t$ and [HCN+CN] in flame 2 and $[NO]_o$ = 1000 ppm at 1900K, and with methylacetylene added.

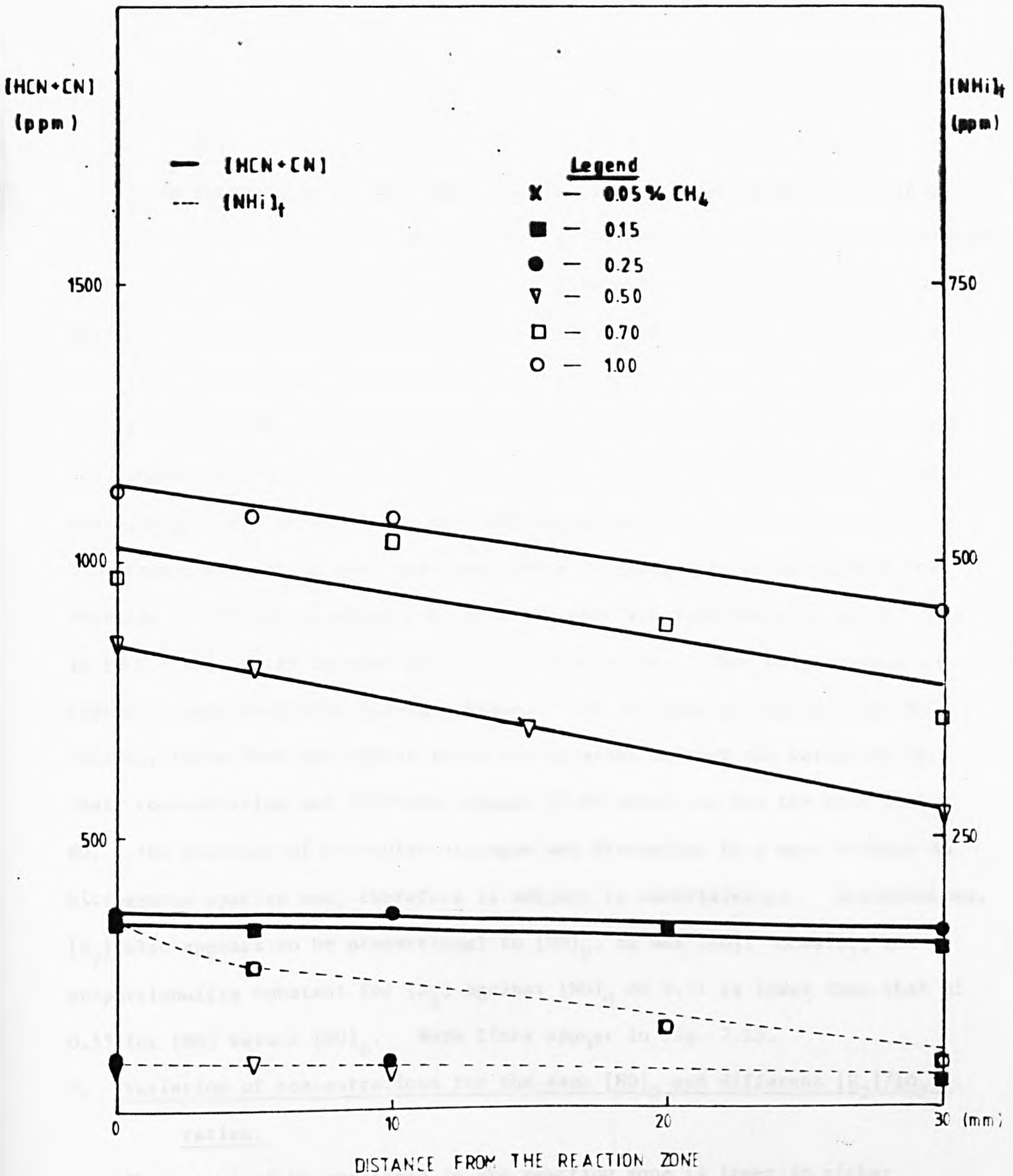

Fig. 7.12 Concentration profiles for $[NHi]_t$ and [HCN+CN] in flame 2 at 1900K and $[NO]_o$ = 5000 ppm with methylacetylene added.

1. Variation of concentrations for the same $[H_2]/[O_2]$ ratio and different $[NO]_0$.

It is interesting to note that the fraction of NO unreacted and that of N_2 formed in relation to the total amount of NO added, both in the reaction zone, is roughly constant in this first case. This means that the amount of NO measured is proportional to the total quantity of NO added. This is shown in Fig.7.13. Also, the concentration of NO generally increases with time, whilst those of NH_i and cyanides decrease. The amount of N_2 does not follow one single pattern like the other species NO, NH_i and HCN. However, in some cases, e.g. in flames with methylacetylene added [NO] decreases until about 1 mm from the reaction zone and then starts to rise. In parallel with the decrease in [NO] up to about 1 mm from the reaction zone there is an increase in [HCN + CN], which is then followed by a decrease. This only appears to happen in very fuel-rich hydrogen flames. In the case of cyanides and NH_i species, there does not appear to be any relation between the variation of their concentration and the total amount of NO added, as was the case with NO. The quantity of molecular nitrogen was determined by a mass balance on nitrogenous species and, therefore is subject to uncertainties. Nevertheless, $[N_2]$ also appears to be proportional to $[NO]_0$, as was [NO]; however, the proportionality constant for $[N_2]$ against $[NO]_0$ of 0.21 is lower than that of 0.55 for [NO] versus $[NO]_0$. Both lines appear in Fig. 7.13.

2. Variation of concentrations for the same $[NO]_0$ and different $[H_2]/[O_2]$ ratios.

The amount of NO unreacted in the reaction zone is lower in richer hydrogen flames. This suggests that the consumption of NO by a hydrocarbon radical is greater when there is some hydrogen present. In a parallel way, the concentrations of cyanides increase with $[H_2]/[O_2]$. However, the profiles for $[NH_i]_t$ and $[N_2]$ do not follow such a consistent pattern.

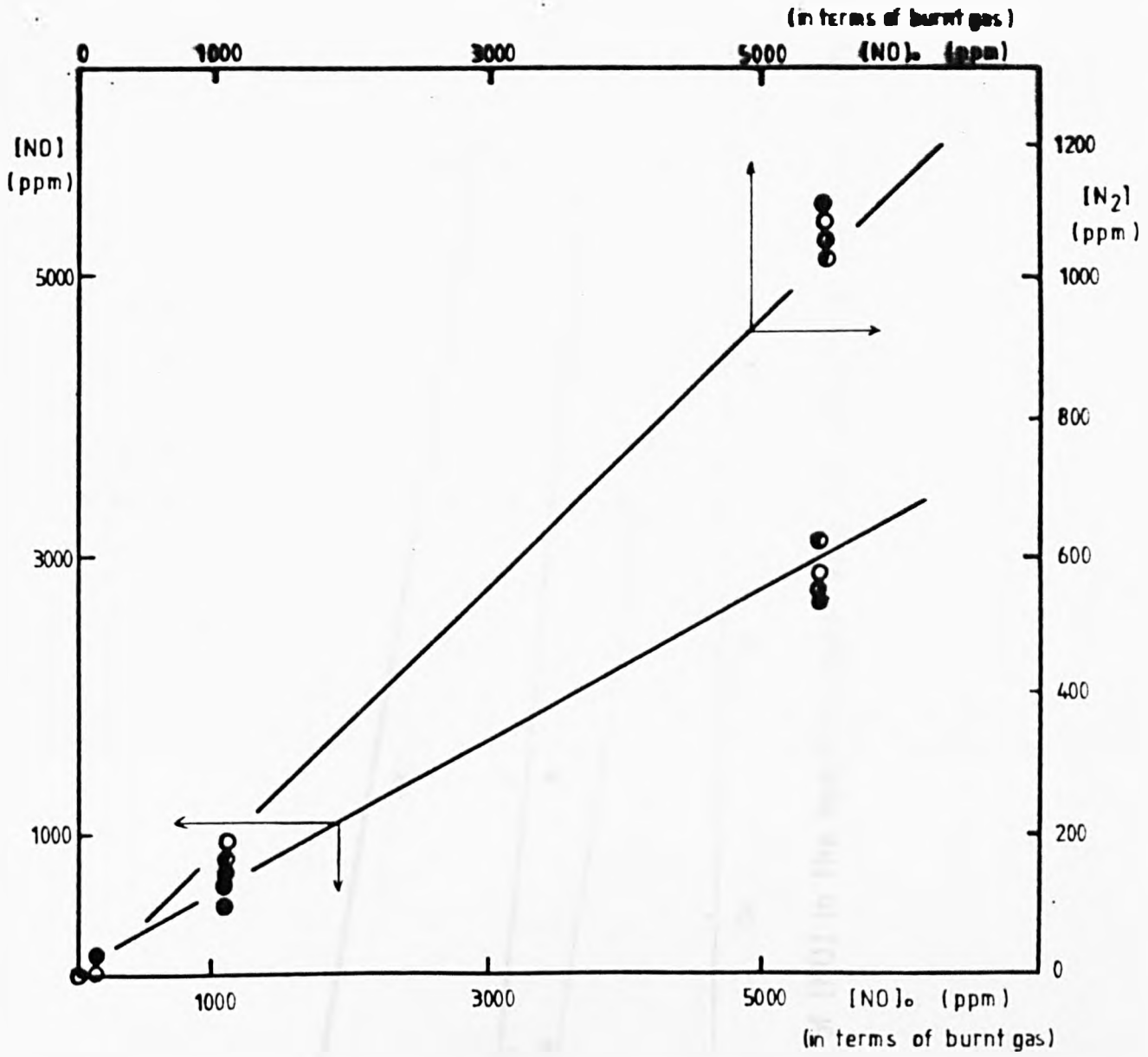

Fig. 7.13 Variation of [NO] and [N_2] with [NO]$_o$ in the reaction zone of flames with nitric oxide and hydrocarbon added together

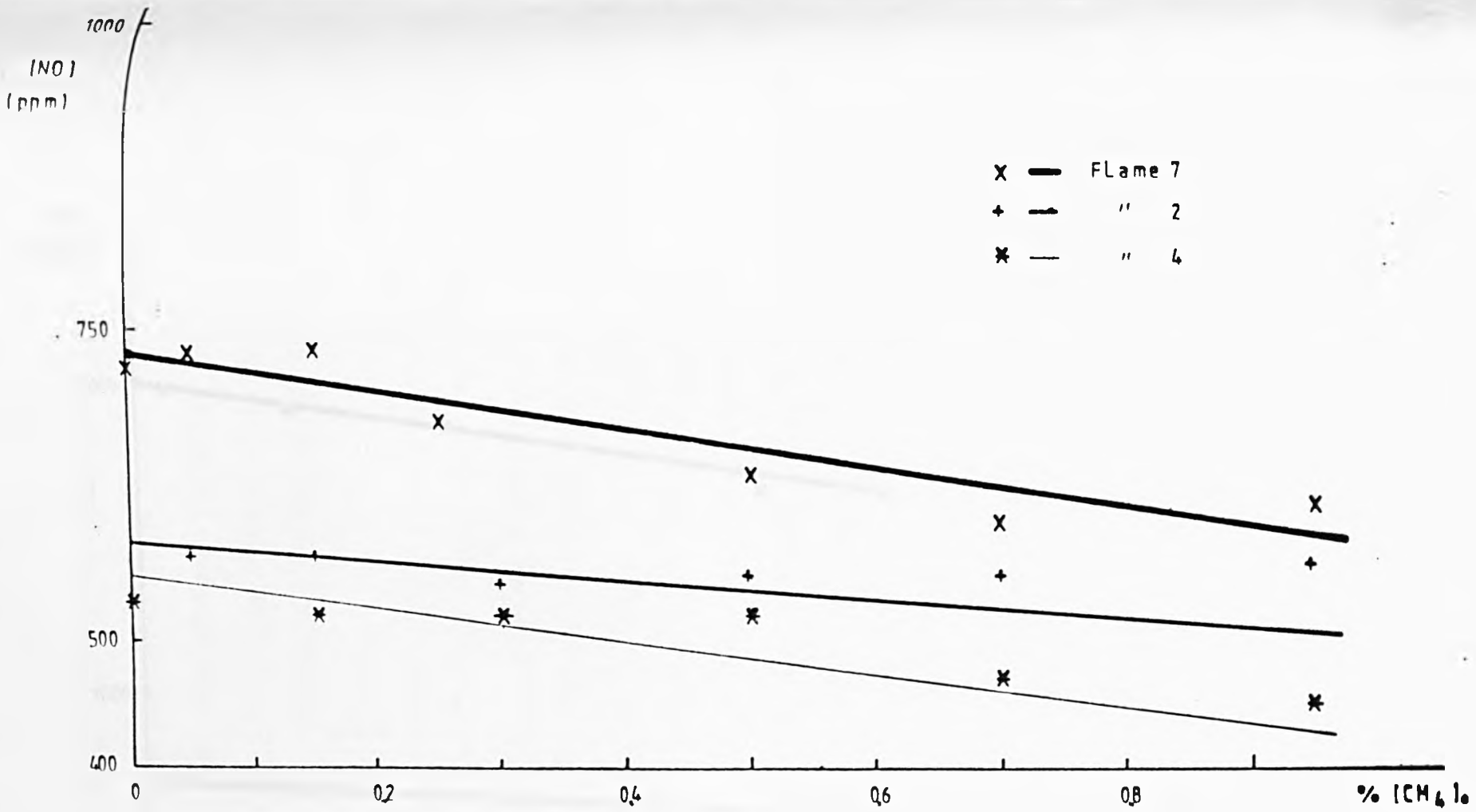

Fig. 7.14

Variation of [NO] in the reaction zone with the amount of methane in the unburnt gases

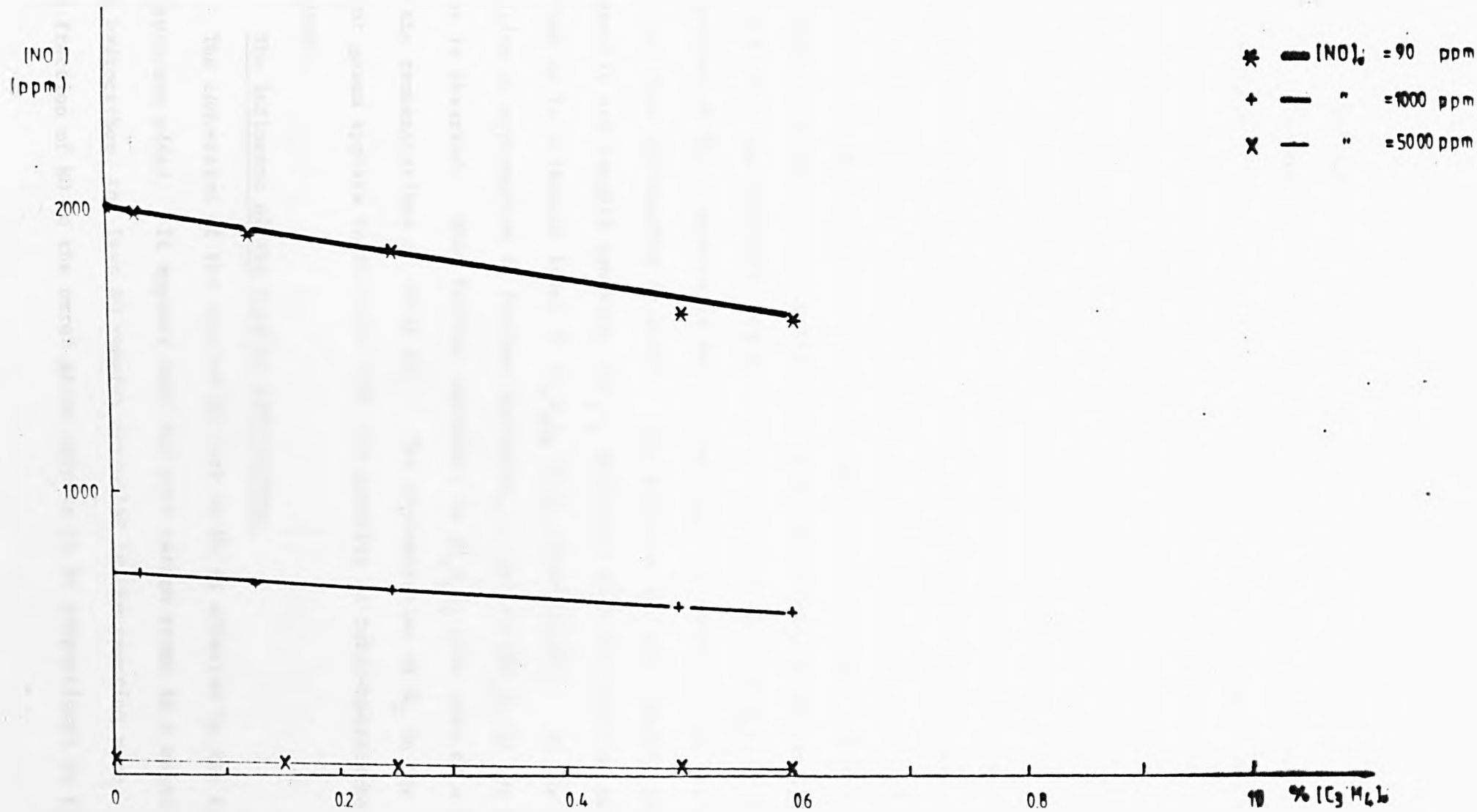

Fig. 7.15

Variation of [NO] in the reaction zone with amount of methylacetylene added for flame 2 at 1900 K.

3. Variation of concentrations for the same $[H_2]/[O_2]$ ratio and $[NO]_0$ and different amounts of hydrocarbons added.

In this case, the amount of NO in the reaction zone decreases with increasing concentration of added hydrocarbon $[C_nH_m]_0$. Downstream all the concentration profiles for each flame are parallel. Actually, [NO] in the reaction zone always appears to be proportional to the amount of hydrocarbon added. Some of the plots illustrating this observation are in Figs. 7.14 and 7.15. However, $[NH_i]_t$ did not depend linearly on $[C_nH_m]_0$, as in flames with ammonia added, described and discussed in the previous chapter. Only [NO] is linear in $[C_nH_m]_0$, independently of the type of hydrocarbon. The slope of these lines appears to depend upon both the total amount of NO added and the $[H_2]/[O_2]$ ratio for each type of hydrocarbon. This is shown in Figs. 7.16 and 7.17 for methane and methylacetylene, respectively. Unlike [NO], the quantity $\{[HCN] + [CN]\}$ increases with $[C_nH_m]_0$. The behaviour of NH_i - species is not as consistent as those of both the cyanides and NO, when hydrocarbon is added. The profiles are also roughly parallel. Generally and roughly speaking, $[NH_i]_t$ decreases with the addition of hydrocarbon up to a certain level of $[C_nH_m]_0$ (i.e. about 0.25%). If the concentration of hydrocarbon is further increased, a rise in $[NH_i]_t$ in the reaction zone is observed. Even further increases in $[C_nH_m]_0$ give rise to a reduction in the concentrations of total NH_i. The concentration of N_2 in the burnt gases appears to increase with the quantity of total-hydrocarbon present.

4. The influence of the type of hydrocarbon.

The conversion of the reacted NO back to NO is affected by the type of hydrocarbon added. It appears that the more carbon atoms in a molecule of the hydrocarbon, the less NO remains unreacted in the reaction zone. In fact, the fraction of NO in the burnt gases appears to be proportional to this

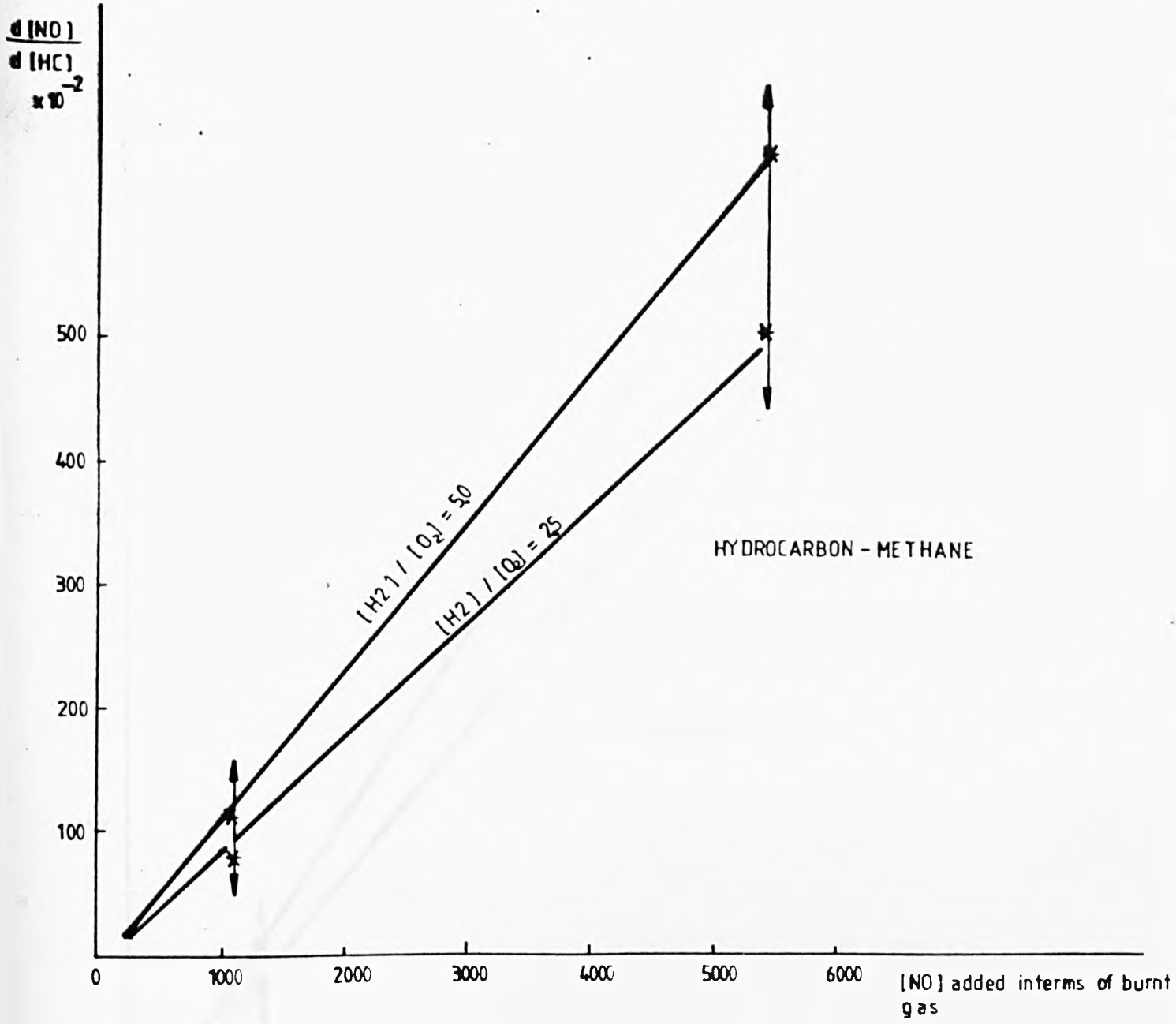

Fig. 7.16

Variation of $\frac{d[NO]}{d[HC]}$ with the amount of nitric oxide added to flames with different $[H_2] / [O_2]$ ratios and with methane present.

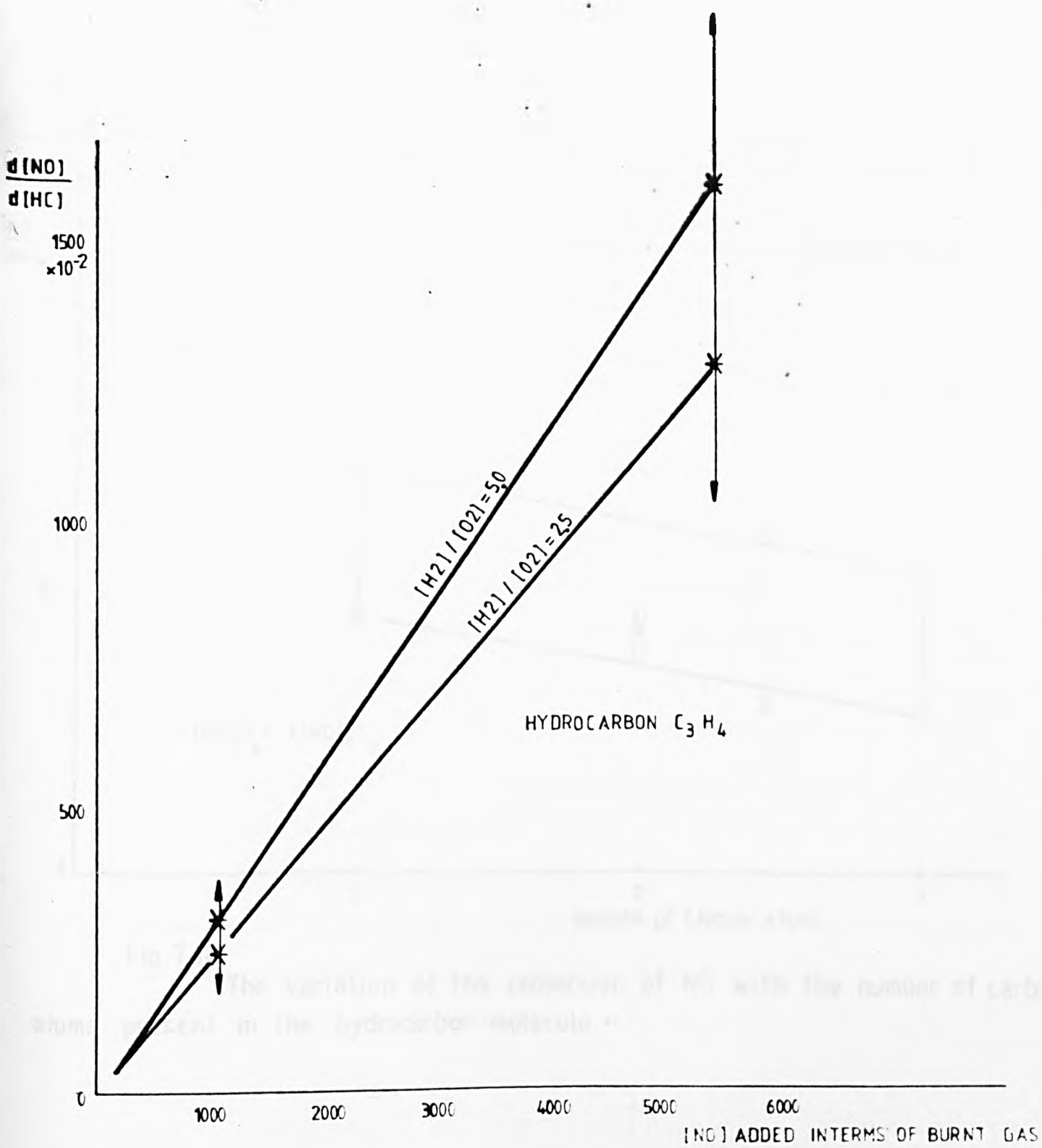

Fig. 7.17 Variation of $\frac{d[NO]}{d[HC]}$ with $[NO]_o$ added to flames with different $[H_2]/[O_2]$ ratios and with methylacetylene.

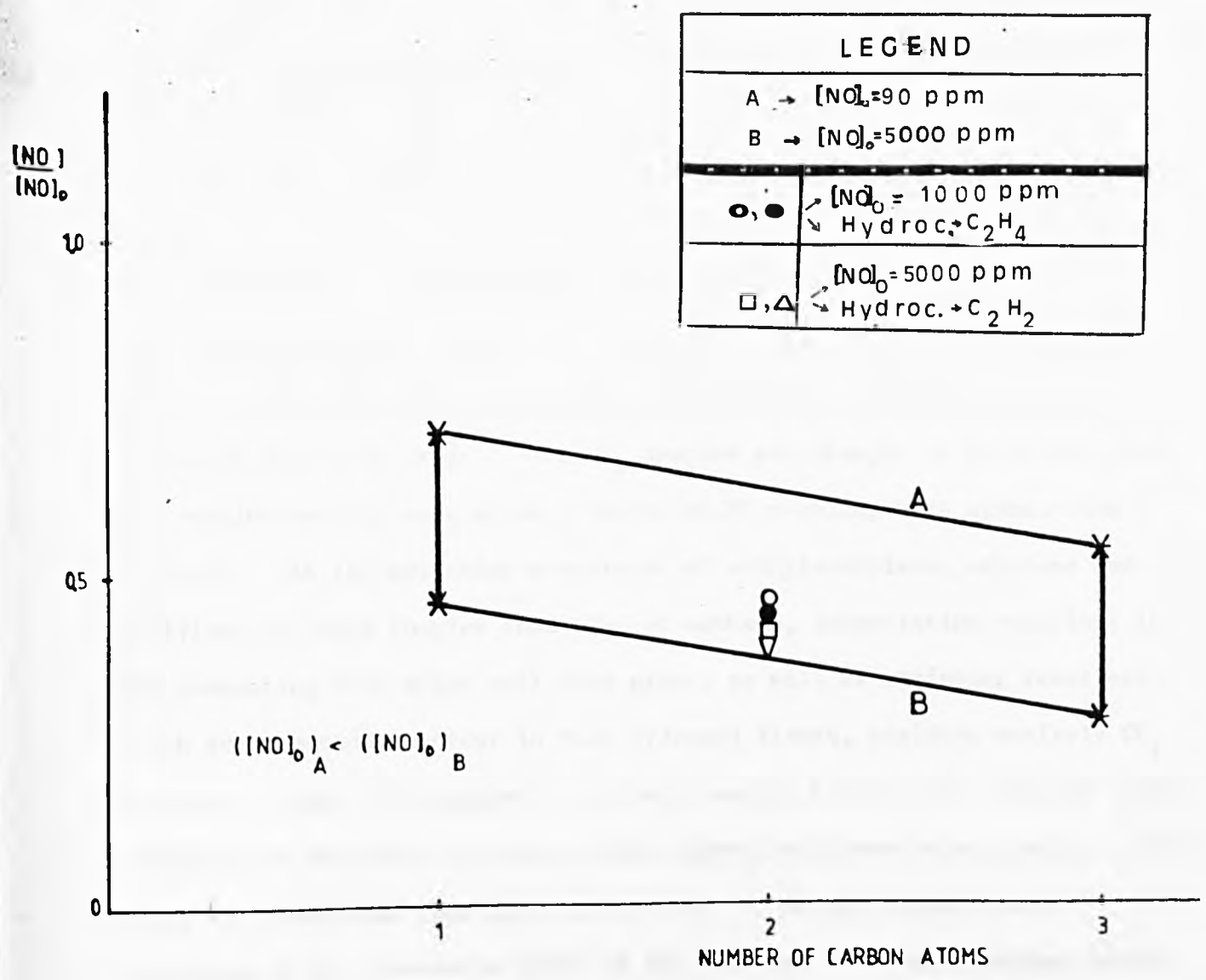

Fig. 7.18 The variation of the conversion of NO with the number of carbon atoms present in the hydrocarbon molecule.

number of carbon atoms, in addition to its dependence on $[NO]_0$. This is shown in Fig. 7.18. This is analogous to the attack of hydrocarbon radicals on N_2 as found by Hayhurst & Vince (1980) in studies on "prompt NO".

7.4 The formation and decay of the cyano-pool.

The identification of the reactions of methane and CH_i radicals with NH_i and NO has already been discussed in Chapter 6. In the last chapter flames had ammonia added and the attack of the hydrocarbon appeared to be more effective on the NH_i-pool. Here, NO was added to the unburnt gases of various flames and the attack of the hydrocarbon is expected to be more effective on nitric oxide. The NH_i species are thought to be formed after the cyanide pool is made up as a result of NO reacting with hydrocarbon radicals. As the molecular structures of methylacetylene, ethylene and acetylene are more complex than that of methane, dissociation reactions in the preheating zone might well take place, as well as stripping reactions, which are expected to occur in rich hydrogen flames, yielding entirely CH_i radicals. Fig. 7.18 suggests a proportionality between the fraction of NO converted in the reaction zone and the number of carbon atoms present. This might well mean that reactions such as CH_i + NO are taking place. According to the discussion given in the previous chapter, reactions which are likely to occur, on the grounds of being exothermic and not too complicated as a mechanism, have values of i in CH_i ranging from 0 to 3:

$$NO + CH_3 \rightarrow HCN + H_2O$$

$$NO + CH_2 \rightarrow HCN + OH$$

$$NO + CH \rightarrow HCN + O$$

$$NO + CH_2 \rightarrow CN + H_2O$$

$$NO + CH \rightarrow CN + OH$$

$$NO + C \rightarrow CN + O$$

The reaction of NO with CH_3 forming CN is endothermic.

A brief preliminary discussion of the decay of the cyano-pool has already been given in Chapter 6. In flames with nitric oxide added instead of ammonia, once the cyanides are formed, their decay is expected to be via the same reactions because of similar temperatures and $[H_2]/[O_2]$ ratios. In this chapter, plots of the observations as ℓn [cyanides] against γ and ℓn γ are given, as in Figs. 6.4 and 6.5. The former plot checks reaction (12) of the previous chapter, the latter both (13) and (15). Unfortunately, the measurements were not sufficient to yield conclusive answers on the rate-determining step for the disappearance of cyanides. More data that was gathered with flames to which NO was added also at 1900 K, will now be discussed in more detail.

Two ways for the decay of the cyano-pool may occur. One involves reactions of direct conversion of cyanides to nitric oxide and the other is through the formation of nitrogenous intermediates which will then react forming NO and N_2. This last mechanism has been proposed by several investigators (Haynes 1977, Morley 1976,1978, Fenimore 1978). The cyanide pool contains HCN and CN species which could react as shown below:

$$CN + OH \rightarrow CH + NO \quad (\Delta H^{o}_{1900} = +213.8 \text{ kJ/mol})$$

$$HCN + OH \rightarrow CH_2 + NO \quad (\Delta H^{o}_{1900} = +300 \text{ kJ/mol})$$

The first reaction was already ruled out in Chapter 6 on the grounds of its high endothermicity. However, both of the above reactions are not likely to occur, because they need rearrangements in the structure of the molecules, which would make them out to be very slow mechanisms to be of importance. Also, the fact that the flame discussed in Chapter 6 showed that $-\frac{dx_{HCN}}{dt} > \frac{dx_{NO}}{dt}$, (where x represents the conversion) reinforced the idea that a direct conversion of the cyanides into NO does not seem correct.

In the flames where nitric oxide was added to the unburnt gases, the formation of both cyanides and NH_i species was observed, as already discussed in previous sections of this chapter. This actually means that the NH_i species are formed after NO is consumed by the hydrocarbon in the reaction zone which is believed to yield first HCN and CN. This is in line with what was found by other investigators (Fenimore 1978, Haynes 1977, Morley 1976, 1978).

Plots of the observations taking ℓn [cyanides] against γ and $\ell n\ \gamma$ were given in Figs. 6.4 and 6.5. The former plot also checks reaction (12) of the previous chapter, i.e.

$$CN + OH \rightarrow OCN + H \qquad (12)$$

and the equivalent one,

$$HCN + H_2O \rightarrow HOCN + H_2 \ . \qquad (14)$$

The latter checks the following reactions:

$$HCN + OH \rightarrow HOCN + H \ , \qquad (13)$$

$$CN + H_2O \rightarrow HOCN + H \ . \qquad (15)$$

Figures 7.19 to 7.24 illustrate some of the plots,but not all of the measurements are shown. In fact, all of them present tolerable fits of straight lines. The slope in every case was transformed to give k_{12}, k_{13} and k_{15}, the values of which are tabulated in Table 7.1, together with those found for flames with ammonia added. The values of k_{14} were not determined because this reaction is expected to be far more complicated than the other steps, involving breakage of more than one bond which does not make it a likely candidate.

Table 7.1

Values for k_{12}, k_{13} and k_{15} determined from flames at 1900 K with $[NO]_0$ of 90, 1000 and 5000 ppm, and different hydrocarbons with amounts ranging from 0.05 to 1% in the unburnt gases.

Flame Designation	Temp. (K)	$[NO]_0$	Hydrocarbon	k_{12}	k_{13}	k_{15}
2	1900	1000	CH_4	$(5.7\pm3.3)\times10^{-10}$	$(4.5\pm2.1)\times10^{-13}$	$(1.5\pm0.7)\times10^{-12}$
		5000	CH_4	$(1.2\pm0.9)\times10^{-10}$	$(1.0\pm0.7)\times10^{-13}$	$(3.3\pm2.3)\times10^{-13}$
4	1900	1000	CH_4	$(5.6\pm2.0)\times10^{-11}$	$(1.2\pm0.5)\times10^{-13}$	$(4.1\pm1.7)\times10^{-13}$
		5000	CH_4	$(1.9\pm1.3)\times10^{-11}$	$(1.5\pm0.6)\times10^{-13}$	$(5.1\pm2.0)\times10^{-13}$
7	1900	90	CH_4	$(5.0\pm2.5)\times10^{-12}$	$(1.5\pm0.8)\times10^{-14}$	$(6.6\pm3.5)\times10^{-14}$
		1000	CH_4	$(8.0\pm3.5)\times10^{-12}$	$(5.0\pm3.0)\times10^{-14}$	$(2.2\pm1.3)\times10^{-13}$
		5000	CH_4	$(6.0\pm3.0)\times10^{-12}$	$(1.3\pm0.8)\times10^{-14}$	$(5.7\pm4.1)\times10^{-14}$
2	1900	90	C_3H_4	$(7.5\pm5.0)\times10^{-11}$	$(8.0\pm6.0)\times10^{-14}$	$(2.6\pm2.0)\times10^{-13}$
		1000	C_3H_4	$(1.0\pm0.8)\times10^{-10}$	$(1.1\pm0.8)\times10^{-13}$	$(4.3\pm3.1)\times10^{-13}$
		5000	C_3H_4	$(8.0\pm6.0)\times10^{-11}$	$(1.0\pm0.8)\times10^{-13}$	$(3.9\pm3.1)\times10^{-13}$
4	1900	90	C_3H_4	$(2.3\pm1.0)\times10^{-10}$	$(6.5\pm5.0)\times10^{-14}$	$(2.2\pm1.7)\times10^{-13}$
		1000	C_3H_4	$(9.0\pm5.6)\times10^{-11}$	$(3.2\pm2.0)\times10^{-14}$	$(1.1\pm0.6)\times10^{-13}$
		5000	C_3H_4	$(3.0\pm2.0)\times10^{-11}$	$(1.0\pm0.8)\times10^{-13}$	$(3.4\pm2.7)\times10^{-13}$
7	1900	90	C_3H_4	$(8.5\pm5.0)\times10^{-12}$	$(3.0\pm2.0)\times10^{-14}$	$(1.3\pm0.9)\times10^{-13}$
		1000	C_3H_4	$(1.6\pm1.0)\times10^{-11}$	$(5.1\pm4.0)\times10^{-14}$	$(2.2\pm0.7)\times10^{-13}$
		5000	C_3H_4	$(1.6\pm1.0)\times10^{-11}$	$(5.0\pm4.0)\times10^{-14}$	$(2.2\pm1.7)\times10^{-13}$
7	1900	90	C_2H_2	$(1.2\pm1.1)\times10^{-11}$	$(3.0\pm2.0)\times10^{-14}$	$(1.3\pm0.9)\times10^{-13}$
2(*)	1900	$[NH_3]_0$ 615	CH_4	$(3.2\pm1.0)\times10^{-10}$	$(1.7\pm1.5)\times10^{-13}$	$(4.8\pm2.0)\times10^{-13}$

(* - Remarks - The values quoted are for the flame indicated, but with ammonia added to the unburnt gases).

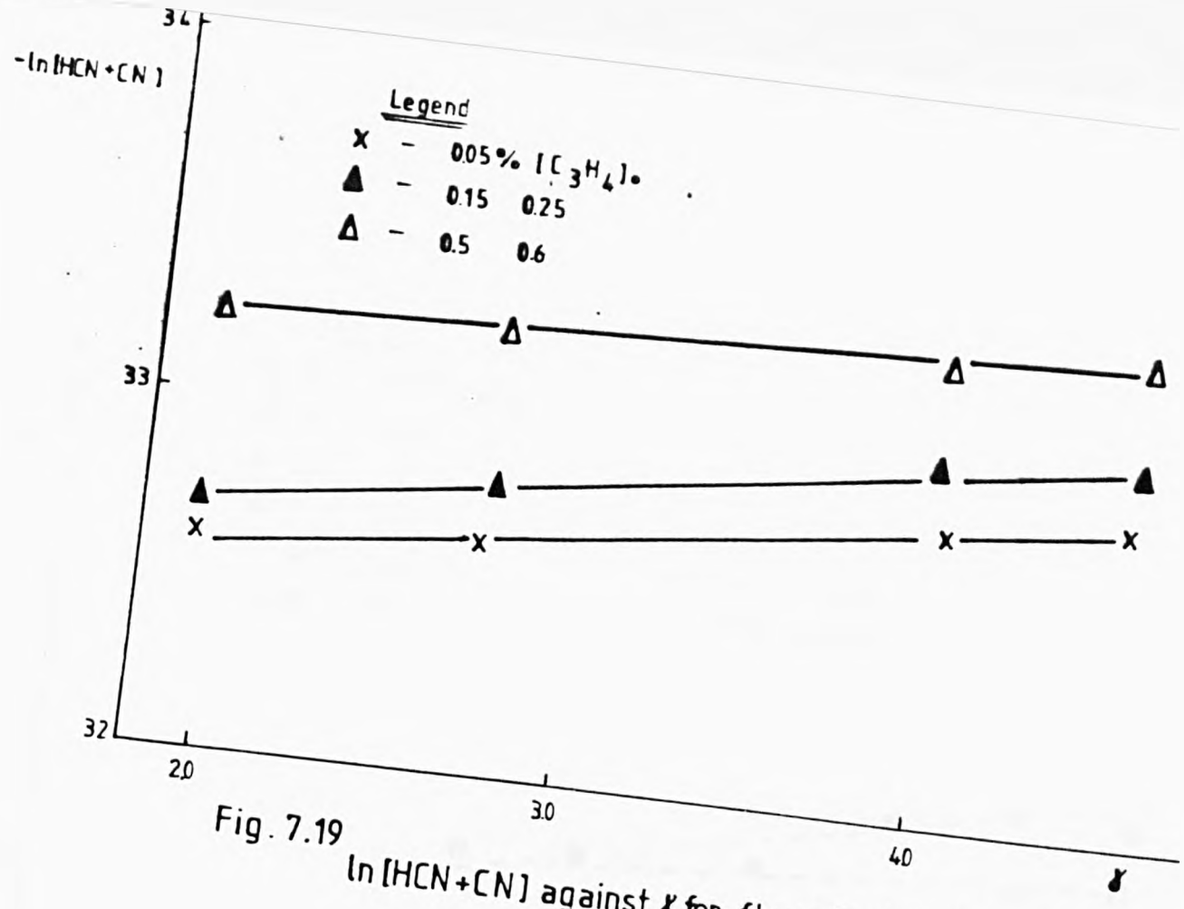

Fig. 7.19 ln [HCN+CN] against γ for flame 7 with $[NO]_o$ = 90 ppm

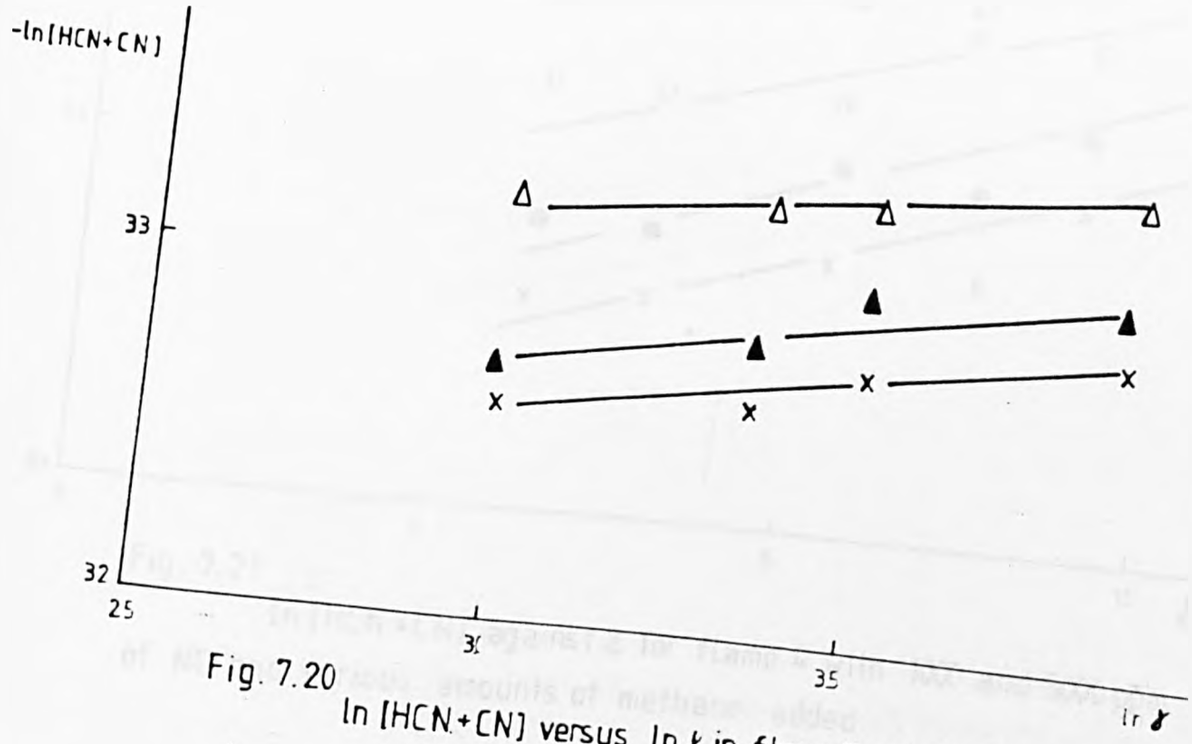

Fig. 7.20 ln [HCN+CN] versus ln γ in flame 7 with $[NO]_o$=90 ppm

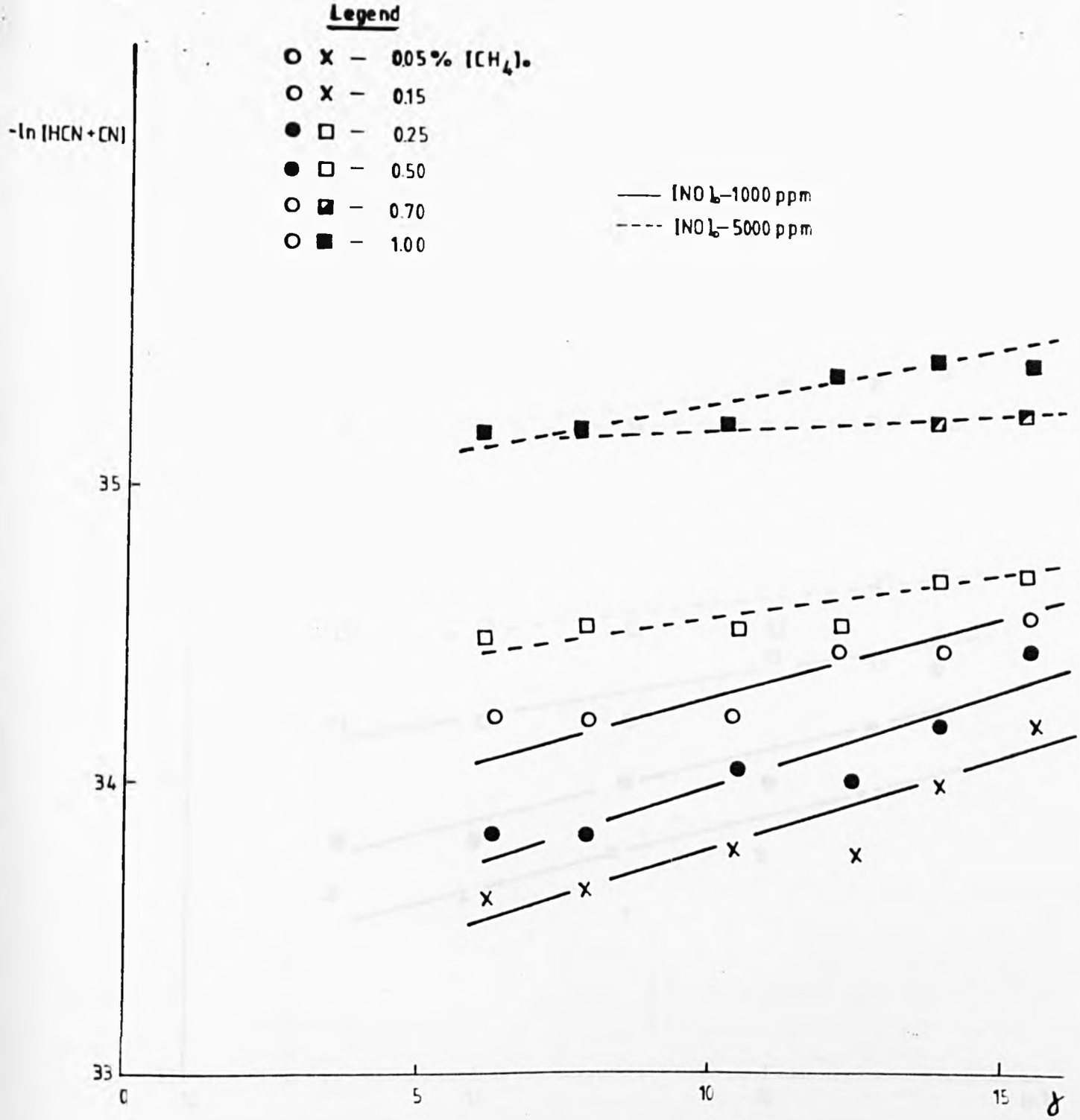

Fig. 7.21

ln [HCN + CN] against γ for flame 4 with 1000 and 5000 ppm of NO and various amounts of methane added.

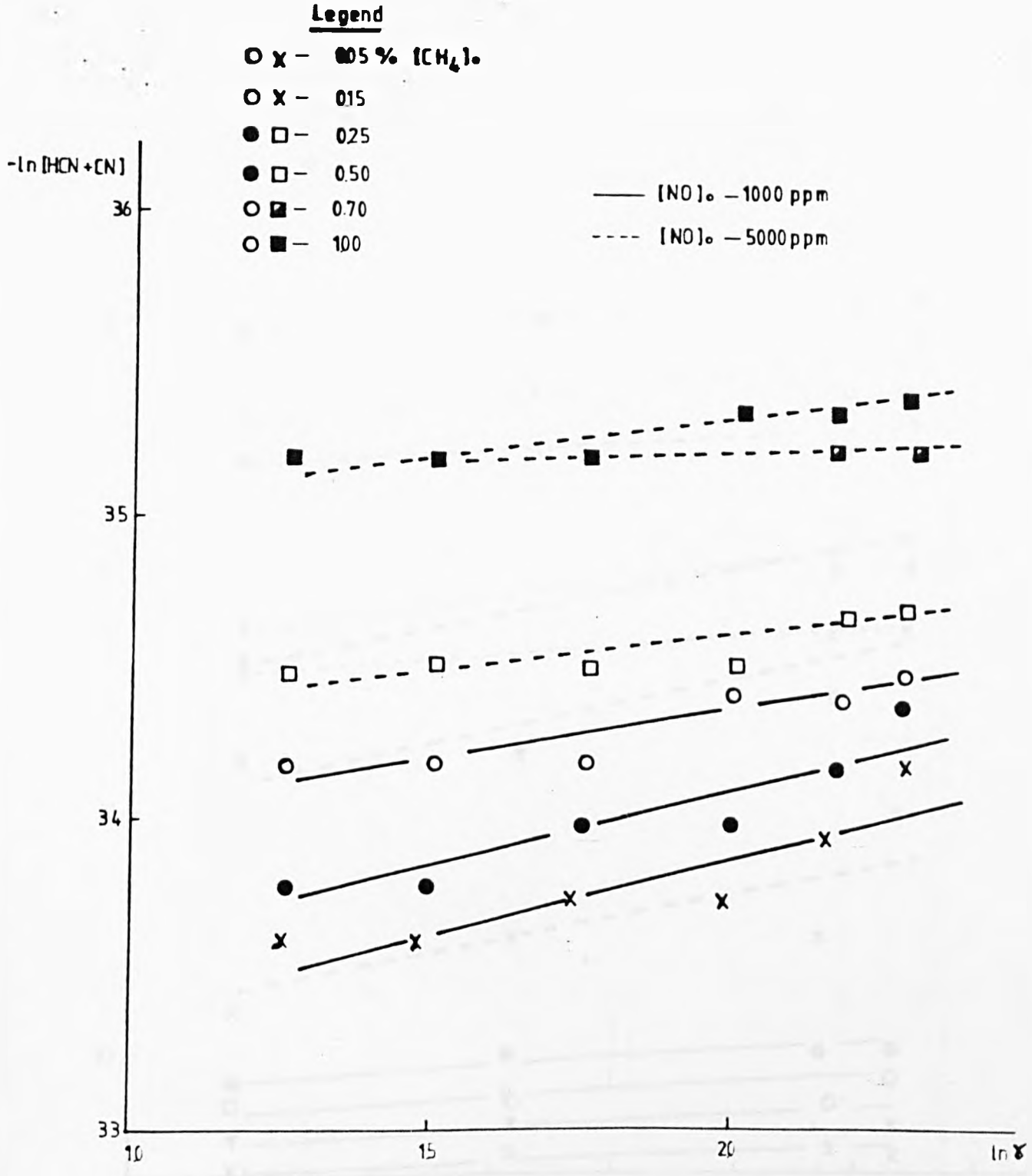

Fig. 7.22 ln [HCN+CN] against ln γ for flame 4 at 1900K with 1000 and 5000 ppm of NO and various amounts of methane added

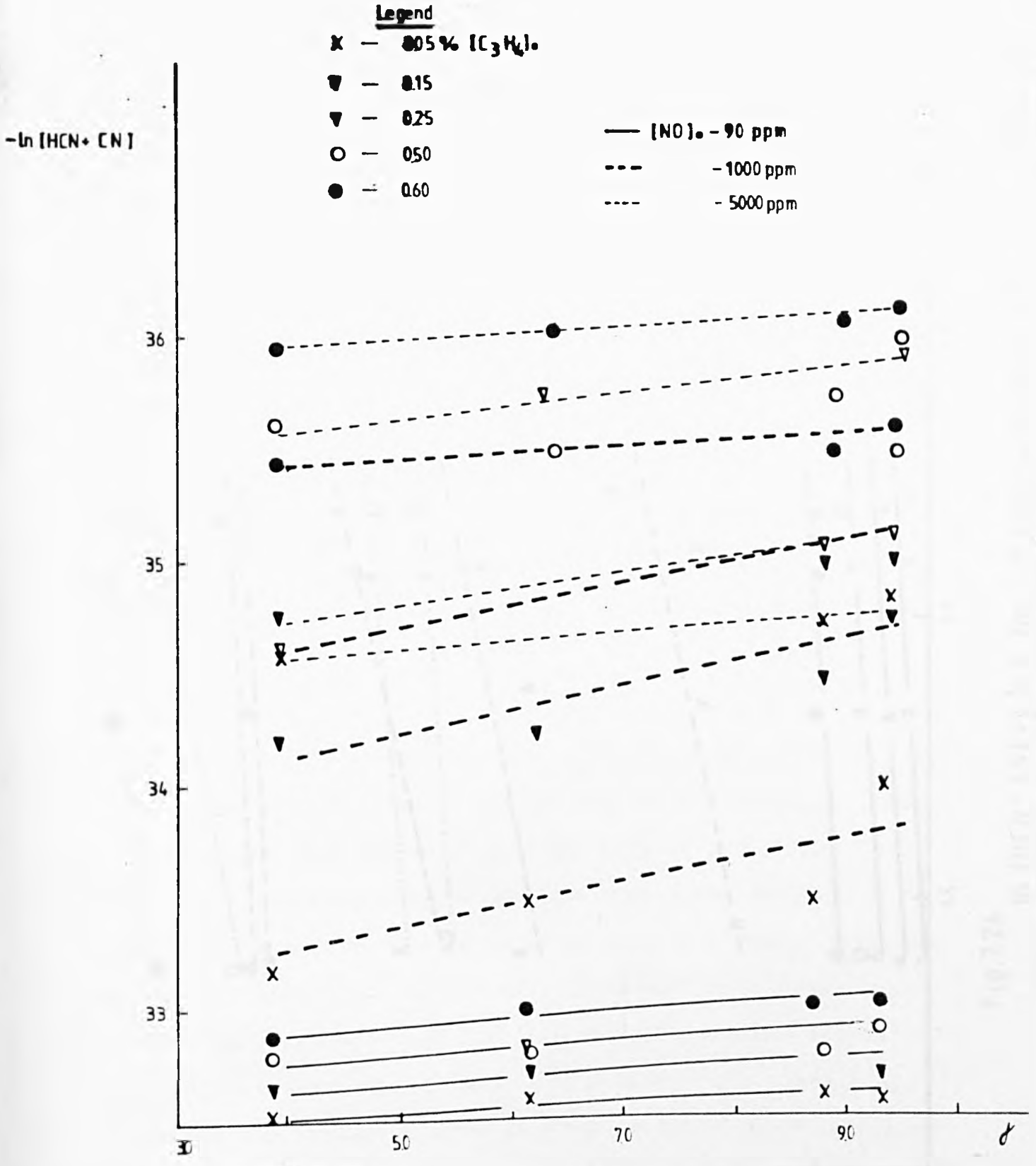

Fig. 7.23 ln [HCN+CN] against γ for flame 2, [NO]o of 90, 1000 and 5000 ppm and with various amounts of methylacetylene added.

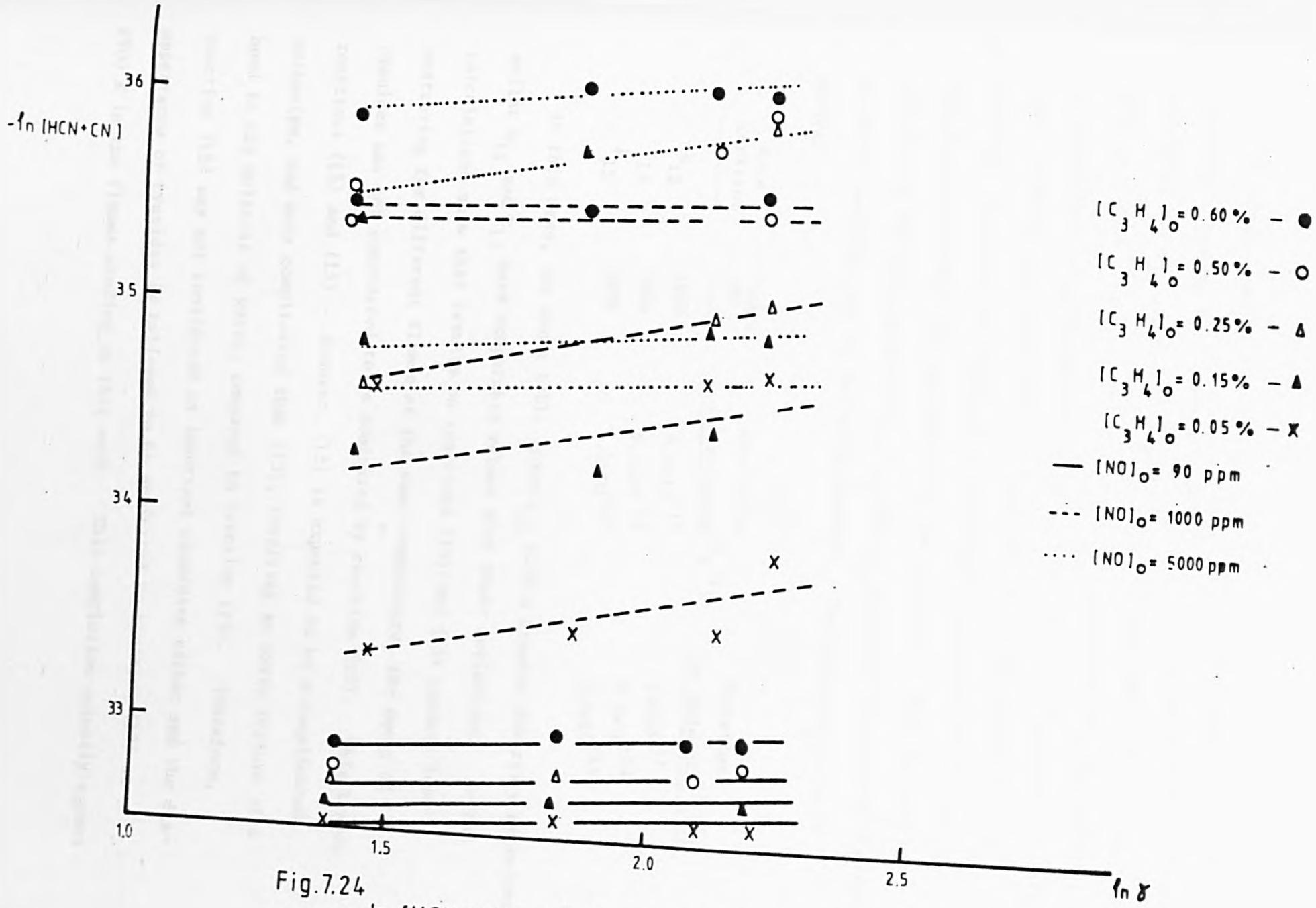

Fig. 7.24 ln [HCN + CN] vs. ln γ for flame 2 with [NO]o of 90, 1000 and 5000 ppm and various amounts of methylacetylene added

A possible mechanism for the disappearance of the cyano-pool may now be discussed, looking at the best fit of the measurements for a rate constant. Actually, all the plots, i.e. Figs. 6.4 and 6.5 and Figs. 7.19 to 7.24 give tolerable straight lines with the same errors affecting the ordinates and slightly lower ones for abcissae with $\ell n Y$ than with Y. Therefore, in this case, a statistical study done on the scattering of the different rate constants obtained, was believed to yield some conclusions on the rate-determining step for the consumption of the cyanides. This was done by calculating the mean value of k_{12}, k_{13} and k_{15} given in Table 7.1 by standard deviation and relating the deviation factors. The following table is derived:

Rate Constant	Temp. (K)	Mean value (ml molecule^{-1} s^{-1})	Deviation (ml molecule^{-1} s^{-1})
k_{12}	1900	9.8×10^{-11}	14×10^{-11}
k_{13}	1900	9.5×10^{-14}	9.7×10^{-14}
k_{15}	1900	3.3×10^{-13}	3.2×10^{-13}

In this case, the above table shows k_{12} with a greater diversity of values whilst k_{13} and k_{15} have comparable values with their deviations. As the calculations show that results on reactions (13) and (15) present less scattering for different flames at the same temperature, the decay of cyanides was not considered to be dominated by reaction (12). This leaves reactions (13) and (15). However, (15) is expected to be a complicated mechanism, and more complicated than (13), involving an extra rupture of a bond in the molecule of water, compared to reaction (13). Therefore, reaction (15) was not considered an important candidate either and the disappearance of cyanides is believed to be dominated by reaction (13) at 1900 K in the flames studied in this work. This conclusion actually agrees

with results given by other investigators (Haynes 1977, Fenimore 1978, Morley 1976, 1978). Summarizing their findings at temperatures below 2300 K, the decay of cyanides appears to occur through the following reaction:

$$HCN + OH \rightarrow \ldots \rightarrow HNCO + H \rightarrow NH_i + CO,$$

which is reaction (13) of this work. The mechanism, at higher temperatures, i.e. above 2300 K, is then thought to change to,

$$HCN + H = H_2 + CN$$

$$CN + OH \rightarrow NCO + H \rightarrow \ldots \rightarrow NH_i + CO.$$

In the study carried out by Fenimore (1978), in which comparable amounts of HCN or of HNCO were added to the same flame, no HCN was formed from added HNCO and most of the HCN added appeared in the burnt gases. Fenimore's flames were free of hydrocarbons and had temperatures in the range 1700-2400 K. Also, this study agrees with theirs in the following terms: (i) HCN and CN are not believed to produce NO directly and (ii) the consumption of cyanides at the temperature of 1900 K is most likely via (13).

Let us discuss now the value of k_{13}. The value of 9.5×10^{-14} ml molecule^{-1} s^{-1} is most likely on the lower side, since temperature variations were not taken into account when $\gamma_{OH} = [OH]/[OH]_e$ and $\gamma_H = [H]/[H]_e$ were assumed equal. As γ_{OH} could be as low as half the values quoted as in flame 7, k_{13} might possibly reach twice the value shown in Table 7.1 for this case. In turn, the addition of NO to flames is also known to affect the magnitude of γ (Bulewicz & Sugden 1964) but only in flames with $[NO]_0$ of at least 5000 ppm can this occur. In this case, as seen in Chapter 4, the value of b could be as high as 2.5 times that of $[NO]_0 = 0$ ppm. The concentrations of H and OH radicals would consequently be increased and the rate constants derived would also be larger. Actually, the values of k_{13}, presented in Table 7.1, appear to be consistent with the above discussion. Finally,

taking k_{13} given in the same table, corrected in accordance with the above discussion, the following rate coefficient of reaction (13) is proposed: $k_{13} = 2.3 \times 10^{-13}$ ml molecule^{-1}s^{-1}, correct to a factor of 2. The value of k_{13} agrees with that of 3.3×10^{-13} ml molecule^{-1}s^{-1} quoted by Haynes (1977) below 2300 K, and also with values proposed by Morley (1980), which are 3.5 to 7.6×10^{-13} ml molecule^{-1}s^{-1} in the range 1790-2000 K. Unfortunately, it was not possible to extend the studies on the decay of the cyano-pool to other temperatures in this work, so that an activation energy could be derived as well as the dependence of the dominance of either step (12) or (13) upon temperature could be checked.

Although the presence of OCN and HOCN species was not checked in this study, there is evidence for the existence of OCN species in hydrocarbon flames from the spectra of negative ions (Hayhurst & Kittelson 1978). Consequently the disappearance of the cyanide pool can be interpreted by a mechanism such as:

$$CN + H_2(O) = HCN + H(O)$$

$$HCN + OH \rightarrow \begin{matrix} H \\ \diagdown \\ CN \\ \diagup \\ HO \end{matrix} \xrightarrow[+M]{} HOCN + H + M \qquad (13)$$

$$HOCN + H = OCN + H_2$$

$$OCN + H \rightarrow CO + NH$$

where the second step is slow compared to the others and hence the rate-determining one. Phillips (1978) studied the dependence of the rate constant for the removal of OH by HCN on pressure and outlined a general mechanism in line with other workers which follows the scheme given above. The species OCN + HOCN were quite possibly detected to some extent in this work, along with the NH_i species and measured by the NH_3 electrode. However, it is not possible to determine the value of [HOCN + OCN] from the electrode measurements.

The same overall mechanism for the production of NO as that suggested at the end of Chapter 5 is proposed here.

Chapter 8.

Final conclusions about a mechanism of production of NO in hydrogen-rich flames with fuel-nitrogen and hydrocarbons.

The production of NO in hydrogen-rich flames at 1900 K was investigated with either ammonia or NO added, with and without hydrocarbon. Flames with temperatures ranging from 1822 K to 2635 K, with ammonia added alone were also studied. Some conclusions are:

1. Nitric oxide does not react in hydrogen flames with $[H_2]/[O_2]$ ranging from 2.5 to 5.0 at 1900 K in line with Bulewicz & Sugden (1964).

2. Cyanides are formed by nitrogenous species reacting with hydrocarbon radicals. In this study the nitrogenous species involved were mainly NH_i (with i most likely equal to 0, 1 or 2) and NO; the hydrocarbon radicals were CH_i. More experimental work with other types of hydrocarbon is needed, for more unequivocal conclusions. However, the fact that CH_i is believed to react with nitrogenous species like NH_i and NO to form CN and HCN also agrees with conclusions drawn by several other investigators (Hayhurst & Vince 1977, Morley 1976, Miyauchi *et al.* 1977, Blauwens *et al.* 1977, Benson 1977).

3. In this work, the consumption of cyanides was studied at 1900 K. The following reaction appears to be involved:

$$HCN + OH \rightarrow HOCN + H \qquad (13)$$

with $k_{13} = 2.3 \times 10^{-13}$ ml molecule^{-1}s^{-1}, correct to a factor of 2. This value agrees with that reported by Haynes (1977). Recently, Morley (1980) found that k_{13} varied from 3.5 to 7.6×10^{-13} ml molecule^{-1}s^{-1}, for temperatures between 1790 - 2000 K. Those values also appear to agree with k_{13} determined in this work.

4. A pool of NH_i species is most likely produced from the cyanide pool via $HOCN \rightarrow OCN \xrightarrow{+H} NH + CO$. These NH_i species are formed in a complicated sequence of steps.

5. In the range 1822 - 2635 K, the NH_i pool was shown to be consumed via reactions such as (6), (7), (8), (10) and (11). Reactions (6) and (7), i.e.

$$N + OH \rightarrow NO + H \qquad (6)$$

$$N + NO \rightarrow N_2 + O \ , \qquad (7)$$

explain the rapid formation of nitric oxide in the reaction zone and very near it. The rate constant for reaction (6) could not be determined accurately with the data available, but it agreed to within a factor of 2 with those in the literature (Haynes 1977, Campbell & Thrush 1969, Bowman 1975). The value of k_7 is only 1.2 times that found in the literature, i.e. 2.7×10^{-11} ml molecule^{-1}s^{-1} and this is expected to be on the low side as already discussed in Chapter 5. The N atoms participating in reactions (6) and (7) appear to be formed in:

$$NH + H \rightleftharpoons N + H_2 \qquad (3)$$

$$NH + OH \rightleftharpoons N + H_2O \qquad (3a)$$

The rate constants obtained could not be determined with any accuracy either, but they appeared to agree with those in the literature (Westley 1979), to within a factor of 2.

An important factor, besides temperature, which decides the rate-determining step in the formation and disappearance of NO is the concentration of each NH_i species.

Values for several rate constants of a variety of reactions were determined, and are listed below:

Reaction	No.	Rate constants (ml molecule^{-1}s^{-1})	Temperature(K)
$N + OH \rightarrow NO + H$	6	$(5.0\pm5.0)\times 10^{-10}$	1900
$N + NO \rightarrow N_2 + O$	7	$(3.2\pm2.5)\times 10^{-11}$	1900 - 2151
$NH + H \rightarrow N + H_2$	3	$(8.0\pm6.0)\times 10^{-12}$	1900
$NH + OH \rightarrow N + H_2O$	3a	$(1.1\pm0.6)\times10^{-11}$	1822 - 2151
$NH + NO \rightarrow N_2 + OH$	11	$(1.0\pm0.9) \times 10^{-10}$	2151 - 2635
$NH_2 + OH \rightarrow NO + H + H_2$	8	$(3.0\pm1.2)\times10^{-14}\exp[(6650\pm1950)/T]$	1822 - 2635
$NH_2 + NO \rightarrow N_2 + H_2O$	10	$(2.0\pm1.0)\times 10^{-12}$	1822 - 2030

The rate constants for reactions (3), (3a), (6) and (11) have large errors. Reaction (8) appears to have a negative activation energy. Unfortunately, this value cannot be compared with one from the literature. Reaction (10) was found by Silver et al. (1980) to have a negative activation energy. However, in this work k_{10} did not appear to be strongly dependent upon temperature within the range 1822-2030 K. The value of k_{10} obtained here, however, agrees with that of Silver et al. (1980) at 1200 K. Fenimore (1978) also did not find k_{10} strongly dependent upon temperature and quoted 8.3×10^{-12} ml molecule^{-1} s^{-1} for it, which is about 4 times higher than the one shown in the above table.

6. The NH_i-pool appeared to have a lower concentration of N atoms than that determined for a balanced pool. This is in agreement with studies carried out by other investigators although under different conditions (Kaskan & Hughes 1973, Caralp 1978).

7. The addition of hydrocarbons to flames with either NO or ammonia present did not appear to change the rates of appearance of NO. In these flames, probably the same kinetic scheme takes place as in flames without hydrocarbon.

8. The amount of NO formed in flames with hydrocarbon appeared to be proportional to the amounts of hydrocarbon and nitrogenous additive added and also to the number of carbon atoms present in the molecule of the hydrocarbon. This agrees with related findings on "prompt NO" obtained by Hayhurst & Vince (1977).

References

Albers, E.A., Hoyermann, K., Schacke, H., Schmatjko, K.J., Wagner, H.G., Wolfram, J. (1975) XVth Combustion Symposium, 765.

Allen, J.D. (1973) J.Inst. Fuel 46, 123.
Allen, J.D. (1975) Comb. and Flame, 24, 133.
Amin, H. (1977) Comb. Sc. Tech. 15, 31.

Ay, J.H., Sichel, M. (1976) Comb. and Flame 26, 1.

Bachmaier, F., Eberius, K.H., Just, T. (1973) Comb. Sc. Tech. 7, 77.

Bartok, W., Crawford, A.R., Manny, E.H., Piegari, G.J. (1972) Paper presented at American Flame Days (Am. Flame Res. Committee), Chicago, Sept. 6-7.

Baulch, D.L., Drysdale, D.D. (1973) Evaluated Kinetic Data for High Temperature Reactions, vol.2, Butterworths, London.

Bilger, R.W. (1975) Report No. PURDU-CL-02, Combustion Lab., Purdue University, Indiana.

Blair, D.W., Bartok, W., Wendt, J.O.L., Lilley, D.G. (1977) XVth Combustion Symposium, 475.

Blauwens, J., Smets, B., Peeters, J. (1977) XVIth Combustion Symposium, 1055.

Blyholder, G., Allen, M.C. (1965) J. Phy. Chem. 69, 3998.

Boden, J.C., Thrush, B.A. (1968) Proc.Roy.Soc. A305, 107.

Bowman, B.R., Pratt, D.T., Crowe, C.T. (1973) XIVth Combustion Symposium, 819.

Bowman, C.T., Seery, D.J. (1975) Comb. and Flame 25, 397.

Bowman, C.T. (1975) Prog. Energy Comb., vol.1, 33.

Bowman, C.T. (1971) Comb. Sc. Tech., vol.3, 37.

Braun, W., McNesby, J.R., Bass, A.M. (1967) J.Chem.Phys. 46, 2071.

Brown, T.D., Mitchel, E.R., Lee, G.K. (1973) Ist European Combustion Symposium, 487.

Bulewicz, E.M., James, C.G., Sugden, T.M. (1956) Proc. Roy. Soc. A235, 89.

Bulewicz, E.M., Sugden, T.M. (1964) Proc. Roy. Soc. A277, 143.

Burdett, N.A., Hayhurst, A.N. (1977) XVIth Combustion Symposium, 903.

Campbell, I.M., Thrush, B.A., T.F.S. (1968), 64, 1265.

Cernansky, N.P. (1976) AIAA Paper No. 76-139, XIVth Aerospace Sciences Meeting, Washington DC, Jan. 26-28.

Cernansky, N.P., Sawyer, R.F. (1975) XVth Combustion Symposium, 1039

Clough, R.N., Thrush, B.A. (1967) Trans. Farad. Soc. 63, 915.

Dechaux, J.C., de Soete, G.G. (1975) Second European Combustion Symposium, 278.

De Soete, G. (1972) Rev. Inst. Fran. Petrole, vol.27, 913.

De Soete, G. (1975) XVth Combustion Symposium, 1093.

Duxbury, J., Pratt, N.H. (1975) XVth Combustion Symposium, 843.

Eberius, H., Just, T., Rittwagen, H. (1975) Second European Combustion Symposium, 272.

Enrich, R., Hency, M.C. (1968) Arch. Environ. Hlth. 17, 860.

England, C., Houseman, J., Teixeira, D.P. (1973) Comb. and Flame 20, 439.

Fenimore, C.P. (1971) XIIIth Combustion Symposium, 373.

Fenimore, C.P. (1972) Comb. and Flame 19, 289.

Fenimore, C.P. (1975) Comb. and Flame 25, 85.

Fenimore, C.P. (1976) Comb. and Flame 26, 249.

Fenimore, C.P. (1976) XIIIth Combustion Symposium, 373.

Fenimore, C.P. (1978) XVIIth Combustion Symposium, 171.

Fenimore, C.P., Jones, G.W. (1957) J. Phys. Chem. 61, 654.

Fenimore, C.P., Jones G.W. (1961) J.Phys. Chem. 65, 298.

Ferguson, R.E. (1957) Comb. and Flame 1, 431.

Fisher, R.C. (1977) Comb. and Flame 30, 143.

Flagan, R.C., Galant, S., Appleton, J.P. (1974) Comb. and Flame 22, 299.

Flower, W.L., Hanson, R.K., Kruger, C.H. (1975) XVth Combustion Symposium, 823.

Fontijn, A., Sabadell, A.J., Ronco, R.J. (1970) Anal. Chem. 42, 575.

Gay, R.L., Young, W.S., Knuth, E.L. (1975) Comb. and Flame 24, 391.

Gaydon, A.G., Wolfhard, H.G. (1970) Flames, their Structure, Radiation and Temperature, 3rd edition, Chapman and Hall, London.

Gordon, S., Mulac, W., Nangia, P. (1971) J. Phys. Chem. 75, 2087.

Gouldin, F.C. (1974) Comb. Sci. Tech. 9, 17.

Green, J.A., Sugden, T.M. (1963) IXth Combustion Symposium, 607.

Greeves, G., Khan, I.M., Onion, G. (1977) XVIth Combustion Symposium, 321.

Halstead, C.J., Jenkins, D.R., Sugden, T.M. (1973) IFRF Paper, Italy

Hayhurst, A.N., Telford, N.R. (1970) Comb. and Flame 14, 303.

Hayhurst, A.N., McLean, H.A. (1974) Nature, 251.

Hayhurst, A.N., Telford, N.R. (1977) Comb. and Flame 28, 67.

Hayhurst, A.N., Kittelson, D.B. (1977) Comb. and Flame 28, 301.

Hayhurst, A.N., Vince, I.M. (1977) Nature, 266, 524.

Hayhurst, A.N., Vince, I.M. (1980) Prog. Energy Combust. Sci., 6, 35.

Haynes, B.S. (1977)[1] Comb. and Flame 28, 81.

Haynes, B.S. (1977)[2] Comb. and Flame 28, 113.

Haynes, B.S., Iverach, D., Kirov, N.Y. (1975) XVth Combustion Symposium, 1103.

Heap, M.P., Lowes, T.M., Walmsley, R. (1972) IFRF Doc.No. 09/a/7, IJmuiden.

Heberling, P.V. (1977) XVIth Combustion Symposium, 159.

Hershey, H.C., Zakin, J.L., Simha, R. (1967) Ind. Eng. Chem. (Fund.) 6, 413.

Hilliard, J.C., Weinberg, F.J. (1976) Nature 259, 556.

Homer, J.B., Sutton, M.M. (1973) Comb. and Flame 20, 71.

Iverach, D., Kirov, N.Y., Haynes, B.S. (1973) Comb. Sci. Tech. 8, 159.

Iverach, D., Haynes, B.S., Kirov, N.Y. (1973) XIVth Combustion Symposium,767.

James, C.G., Sugden, T.M. (1955) Proc. Roy. Soc. 227, 312.

JANAF Thermochemical Tables (1974) National Bureau of Standards, Washington (3rd edition).

Jenkins, D.R., Sugden, T.M. (1959) Flame Emission and Atomic Absorption Spectrometry 1, 151, J.A. Dean & T.C. Rains, Dekker, New York.

Jensen, D.E., Jones, G.A. (1978) Comb. and Flame 32, 1.

Jones, R.E. (1973) NASA TECH. Memo. X-68256.

Jones, W.P. (1975) Comb. Sci. Tech. 10, 93.

Jonke, A.A., Carls, E.L., Jarry, R.L., Anastasia,L.J., Haas, M., Pavlik, J.R., Murphy, W.A., Schoffstoll, C.B. (1969) Argonne Nat. Lab. rep. ANL/ES/-CEN-100/.

Kaskan, W.E., Hughes, D.E. (1973) Comb. and Flame 20, 381.

Lefebvre, A.H. (1975) XVth Comb. Symposium, 1169.

Livesey, L.B., Roberts, A.L., Williams, A. (1971) Comb. Sci. Tech. 4, 9.

Lyonn, R.K., Benn, D.J. (1978) XVIIth Combustion Symposium, 66.

Malte, P.C., Pratt, D.T. (1974) Comb. Sci. Tech. 9, 221.

Malte, P.C., Pratt, D.T. (1975) XVth Combustion Symposium, 1061.

Malte, P.C., Schmidt, S.C., Pratt, D.T. (1977) XVIth Combustion Symposium, 145.

Martin, F.J., Dederick, P.K. (1977) XVIth Combustion Symposium, 191.

McEwan, M.J., Phillips, L.F. (1975) Chemistry of the Atmosphere.

Merryman, E.L., Levy, A. (1975) XVth Combustion Symposium, 1073.

Millikan, R.C. (1962) J. Phys. Chem. 66, 794.

Miyauchi, T., Mori, Y., Imamura, A. (1977) XVIth Combustion Symposium, 1073.

Monat, J.P., Hanson, R.K., Kruger, C.H. (1978) XVIIth Combustion Symposium, 142.

Morley, C. (1975) Second European Symposium, 285.

Morley, C. (1976) Comb. and Flame 27, 189.

Moss, J.B., Bray, K.N.C. (1975) Second European Combustion Symposium, 315.

Müller, F.J., Bottendahl,U., Rörtgen, H. (1975) Second European Combustion Symposium, 297.

Mulvihill, J., Phillips, L.F. (1975) XVth Combustion Symposium, 1113.

Muzio, L.J., Arand, J.K., Teixeira, D.P. (1977) XVIth Combustion Symposium, 199.

Myerson, A.L. (1975) XVth Combustion Symposium, 1085.

NBS Special Publication (1977) 513.

Padley, P.J. (1959) Ph.D. Thesis, University of Cambridge.

Padley, P.J., Sugden, T.M. (1958) Proc. Roy. Soc. A248, 248.

Peeters, J., Lambert, J.F., Hertoghe, P., Van Tiggelen, A. (1971) XIIIth Combustion Symposium, 321.

Peeters, J., Mahnen, G. (1973) XIVth Combustion Symposium, 133.

Peeters,J., Vinckier, C. (1975) XVth Combustion Symposium, 969.

Pereira, F.J. (1975) Ph.D. Thesis, University of Sheffield.

Perkins, H.C. (1974) Air Pollution, McGraw Hill.

Peters, B.D., Borman, G.L. (1973) Comb. Sci. Tech. 7, 159.

Phillips, L.F. (1978) Chem. Phys. Letters, 57, 4, 538.

Rentzepis, P.M., Cottereau, M.J. (1975) Second European Combustion Symposium, 448.

Robinson, E., Robbins, R.C. (1970) J. Air Poll. Control Assoc., 20, 303.

Rose, J.W., Cooper, J.R. (1977) Technical Data on Fuel (7th Edition). British National Committee, World Energy Conference, London.

Sadakata, M., Beer,J.M. (1977) XVIth Combustion Symposium, 93.

Safrany, D.R. (1969) Progress in Reaction Kinetics, 6, 1.

Safrany, D.R., Reeves, R.R., Harteck, P.P. (1964) J.Am.Chem.Soc., 86, 3160.

Sakai, Y., Miyazaki, H., Mukai, K. (1973) SAE Paper 730154.

Sakai, Y., Kunii, K., Sasaki, M., Kakuta,N., Aihara, H. (1976) I.Mech.E. C247/76, 55.

Saltzman, B.E. (1954) Anal. Chem. 26, 1949.

Sarofim, A.F., Flagan, R.C. (1976) Progr.Energy Comb. Sci. 2, 1.

Sarofim, A.F., Pohl, J.H. (1973) XIVth Combustion Symposium, 739.

Sawyer, R.F. (1972) AGARD Advisory Report No. 40.

Shahed, S.M., Newhall, H.K. (1971) Comb. and Flame 17, 2.

Shaw, J.T. (1973) J. Inst. Fuel, 170.

Shaw, H. (1972) Am. Flame Days, Chicago, Sep. 6-7.

Schofield, K. (1967) Planet Space Sci. 15, 643.

Shelef, M., Otto, K., Gandhi, H. (1968) J. Catal. 12, 361.

Shy, M.M., Creason, J.P.,Pearlman, M.E., McClain, K.E., Benson F.B., Young, M.M., (1970) J. Air Pol. Control Assoc. 20, 539.

Siewert, R.M. (1975) Comb. and Flame 25, 273.

Silver, J.A., Gosewski, C.M., Kolb, C.E. (1980) ARI-RR-216.

Solymosi, F.,Kiss, J. (1975) XVth Combustion Symposium, 1233.

Sternling, C.V., Wendt, J.O.L. (1974) AIChE J. 20, 81.

Sugden, T.M., Bulewicz, E.M., Demerdache, A. (1971) Symposium on Chemical Reactions in the upper Atmosphere, Chapter 6, 89.

Tabaczynski, R.J., Klomp, E.D. (1974) Soc. of Automotive Eng. Paper 741.

Takagi, T., Fujii, K., Ogasawara, M. (1973) Fuel 52, 294.

Tagaki, T., Fujii, K., Ogasawara, M. (1974) Fuel 53, 114.

Takagi, T., Ogasawara, M., Fujii, K., Daizo, M. (1975) XVth Combustion Symposium, 1051.

Tagaki, T., Ogasawara, M., Daizo, M., Tatsumi, T. (1977) XVIth Combustion Symposium, 181.

Takagi, T., Tatsumi, T., Ogasawara, M. (1979) Comb. and Flame 35, 17.

Telford, N.R. (1969) Ph.D. Thesis, University of Cambridge.

Thompson, D., Brown, T.D., Beer, J.M. (1972) Comb. and Flame 19, 69.

Turner, D.W., Siegmund, C.W. (1972) Am. Flame Days, Chicago, Sept. 6-7.

Vince, I.M. (1978) Ph.D. Thesis, University of Sheffield.

Wendt, J.O.L., Ekmann, J.M. (1975) Comb. and Flame 25, 355.

Westenberg, A.A., Raezer, S.D., Fristrom, R.M. (1957) Comb. and Flame 1, 467.

Westley, F. (1979) NBSIR-79-1941.

Yamagishi, K., Nozawa, M., Yoshie, T., Tokumoto, T., Kakegawa, Y. (1975) XVth Combustion Symposium, 1157.

Yanagi, T. (1977) Comb. and Flame 28, 33.

Zel'dovich, Y.B. (1946) Acta Physicochim. USSR 21, 577.

APPENDIX A.

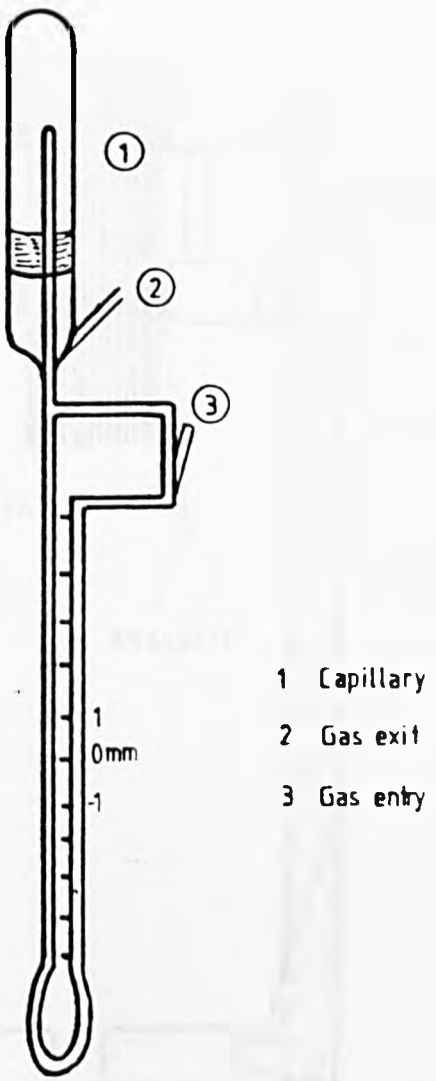

Fig. 1

Schematic diagram of the flow meter used to measure the supply of gas to the burner

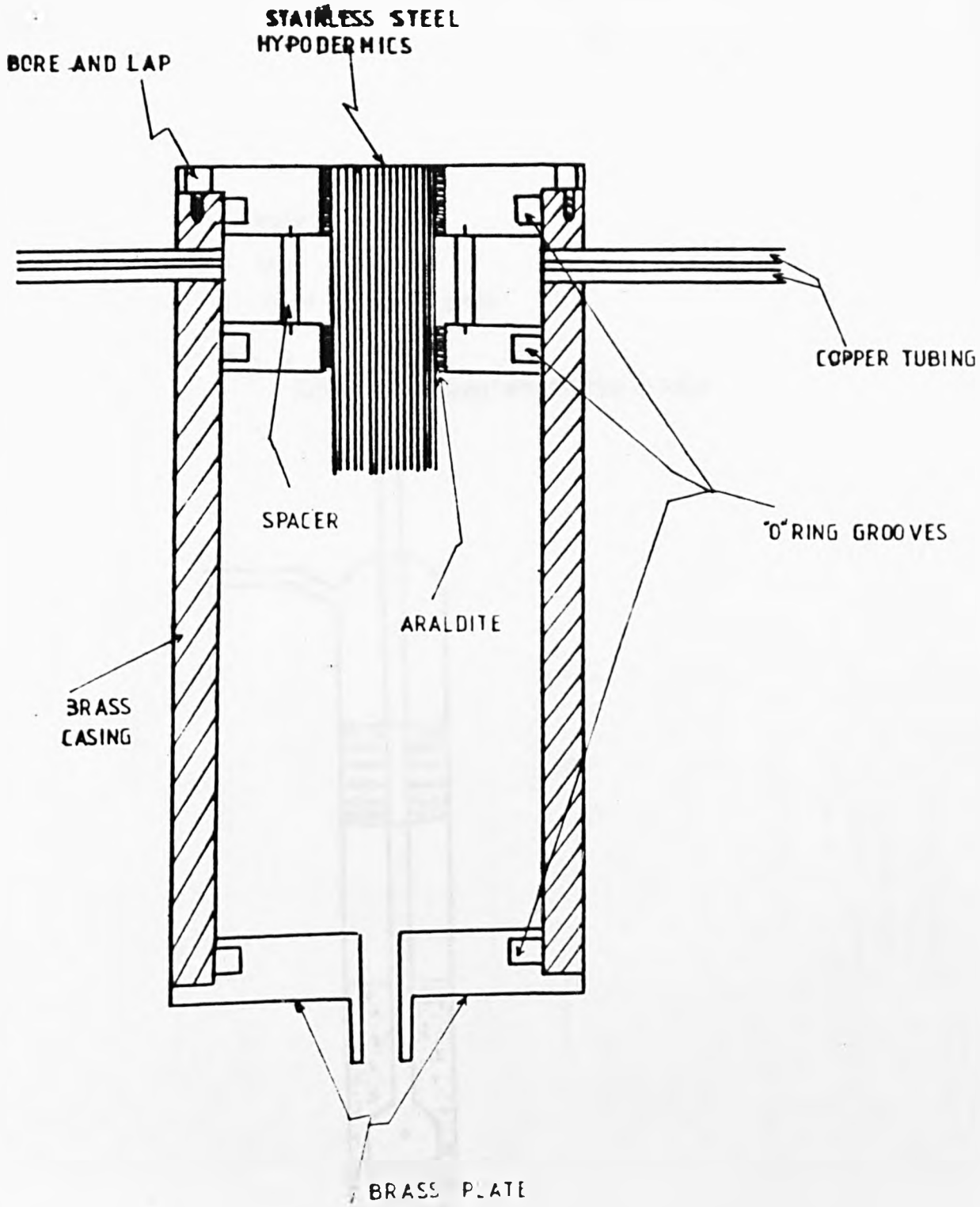

Fig. 2

Vertical cross section of the burner

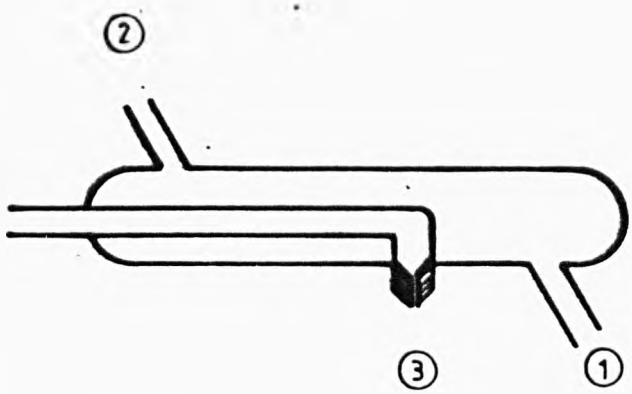

1 Water inlet

2 Water outlet

3 Tip of the quartz probe

Fig. 3
Schematic diagram of the probe

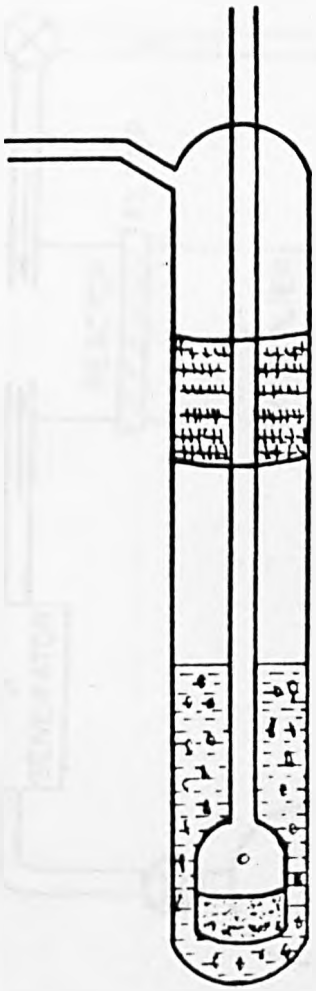

Fig. 4
Schematic diagram of the gas bubbler

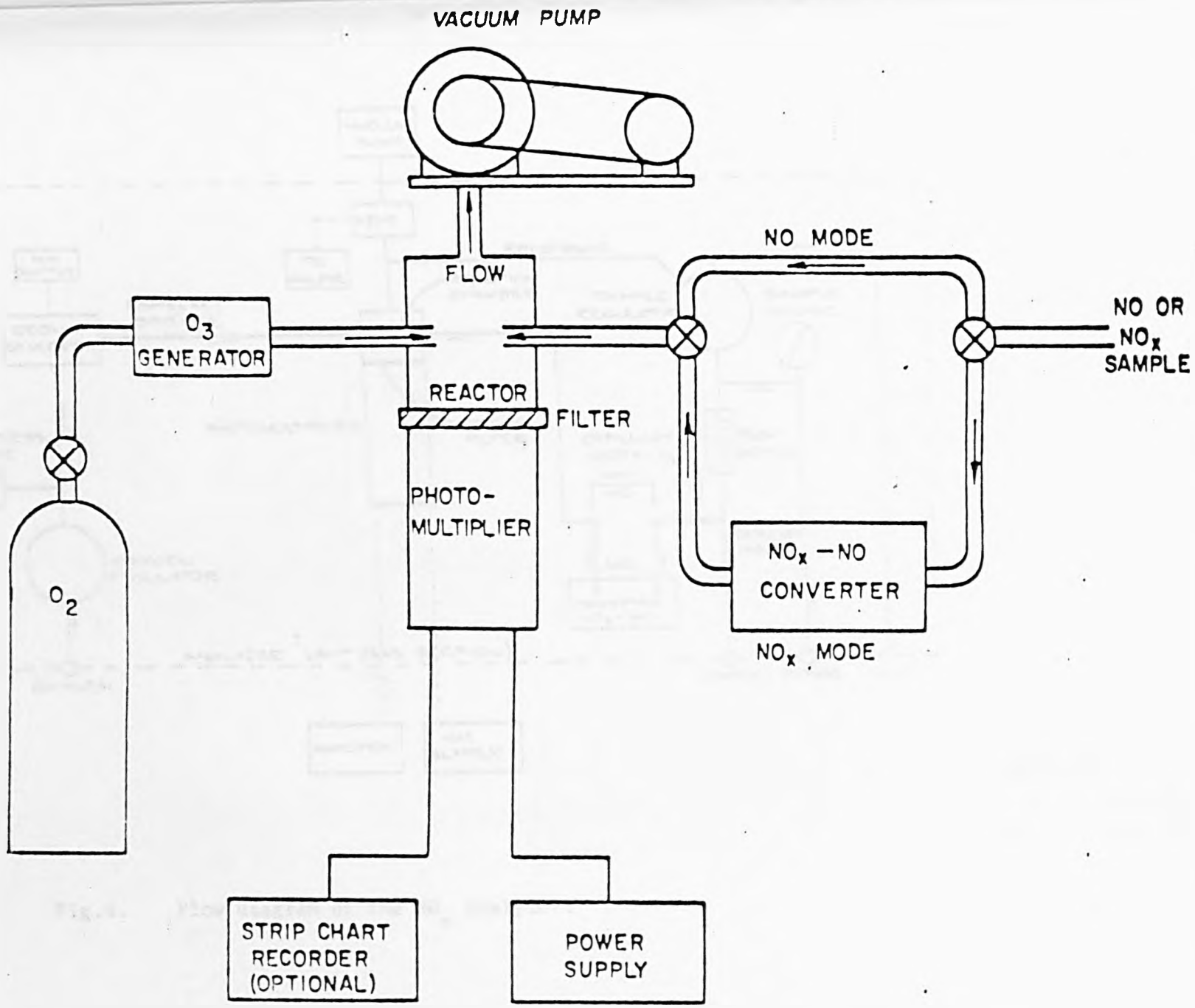

Fig.5. Schematic diagram of the NO_x Analyser (Teco Model 10A).

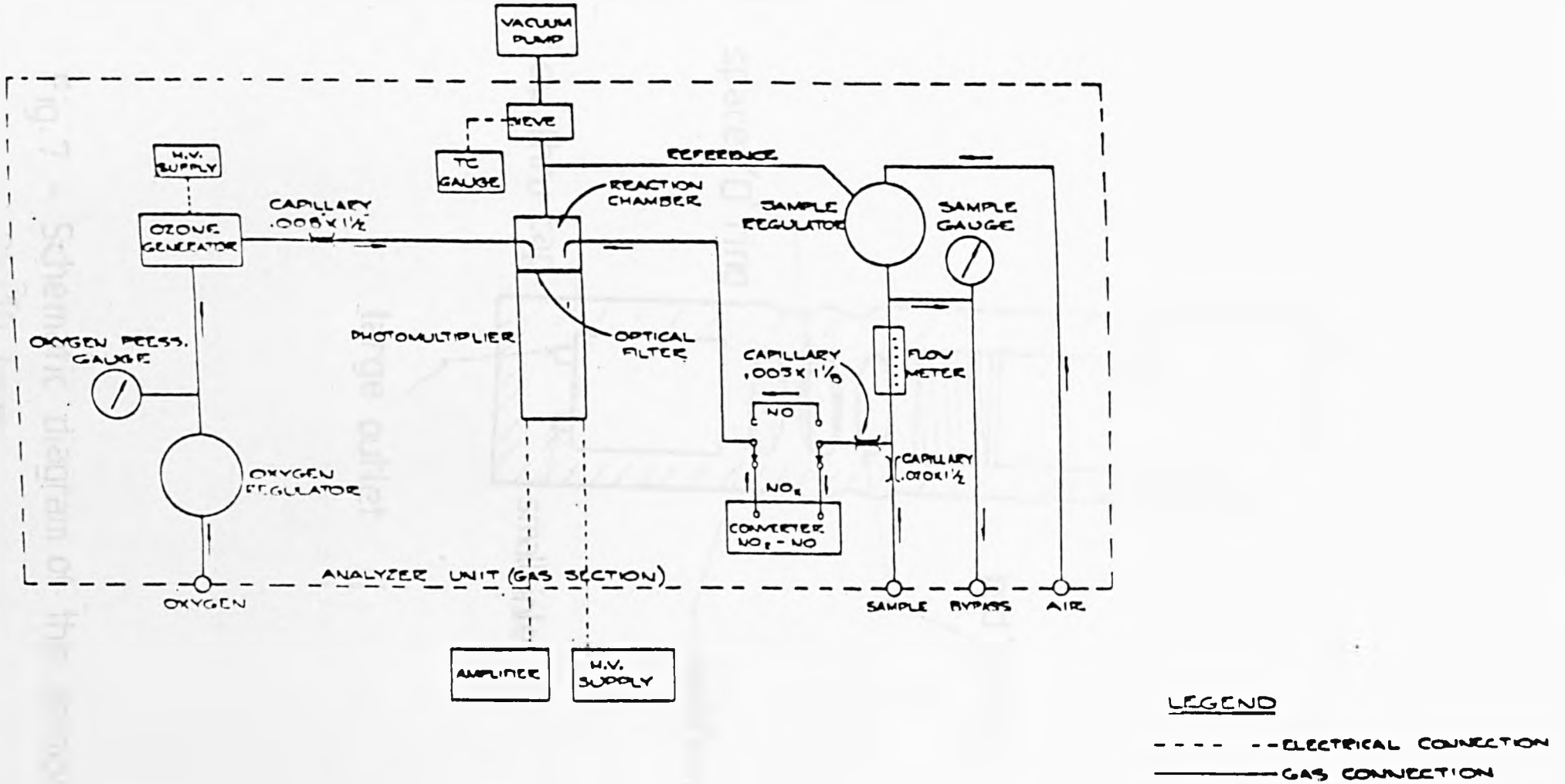

Fig.6. Flow diagram of the NO_x Analyser.

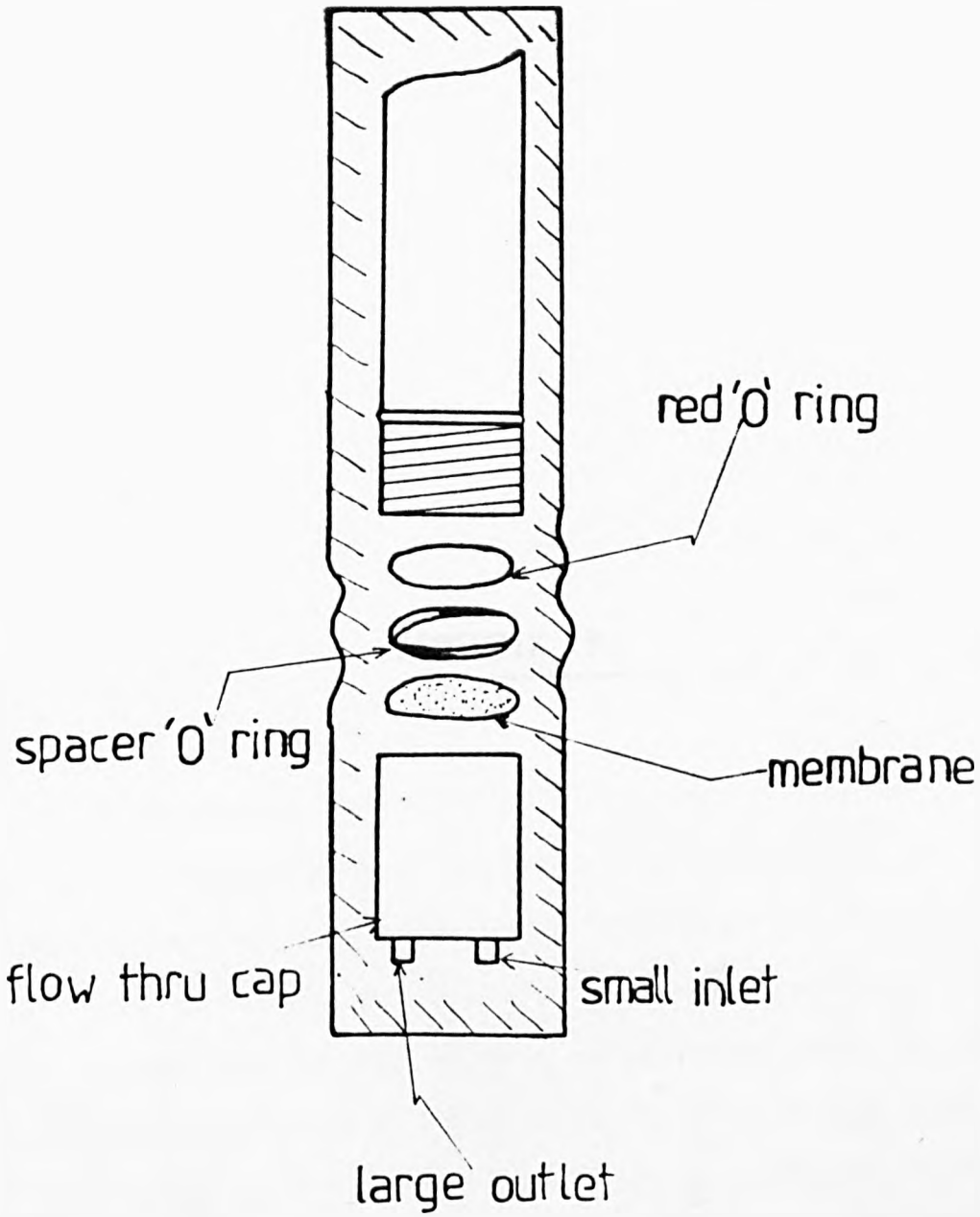

Fig. 7 - Schematic diagram of the ammonia electrode 95-10 type

APPENDIX B.

Appendix B.

The concentrations of cyanides and ammonia in the burnt gases were obtained from the amounts of these species found in fixed volumes of alkaline solutions using ion selective electrodes.

Calling m the concentration of the species in the solution, expressed in terms of molarity, the number of moles will be vm, where v is the volume of solution in litres. Assuming that the burnt gases behave as an ideal gas, the total number of moles bubbled through the solution equals PVt/RT, where P is the pressure just before the solution in atm, V is the volumetric flow rate at the same point, t is the time taken by the burnt gas to go through the solution, T is the absolute temperature which is taken as being the same as that of the solution and, R is the gas constant. Therefore, the concentration of either ammonia or cyanides is calculated using the relation $(RTvm)/(PVt) \times 10^6$ ppm.

As there was some condensation in the sampling line, corrections were also made to every measurement taking this into account. Calling Q the measured volumetric sampling flow rate, which does not include the amount of water vapour condensed, any species' concentration is proportional to 1/Q. If y_{H_2O} is the mole fraction of water in the burned gases and the saturated vapour pressure of water at the sampling temperature (i.e. room temperature, 15° C) is 16 mm Hg, the amount of water vapour condensed can be calculated from $(y_{H_2O} - 16/760)$. Thus, the total flow rate of gas is given by $Q/[1-(y_{H_2O} - \frac{16}{760})] = Q/(1.021-y_{H_2O})$. Therefore, all the concentrations have to be reduced by a factor of $(1.021-y_{H_2O})$, i.e., in the case of $[NH_i]_t$ or [HCN + CN] is:

$$\frac{RTvm}{PVt} (1.021 - y_{H_2O}) \times 10^6 \text{ in ppm.}$$

As an example, take the flame with $[H_2]/[O_2]/[Ar] = 3.5/1/7.0$ and $[NH_3]_0 = 525$ ppm. The molarity of the solution for NH_i was 8.1×10^{-5} M in the reaction zone; the temperature of the same was 290 K; the volume of KOH solution was 0.02 ℓt; the pressure on the sampling line, 0.96 atm; the flow rate equalled 1.24 cm^3/s and the gas bubbled through the solution for 150 s. Substituting this in the above equation gives $[NH_i]_t$ equal to 178 ppm for $y_{H_2O} = 0.1929$.

Appendix C.

TABLE C1.

List of the flames studied and their additives.

Flame Designation	$[NH_3]_0$ (ppm)	$[NO]_0$ (ppm)	Type of hydrocarbon	$[C_nH_m]_0$ (%)
1	125	-	-	-
2	50	-	-	-
	125	-	-	-
	615	-	CH_4	0.0;0.05;0.15;0.25; 0.50;0.70
	-	1000	CH_4	0.0;0.05;0.15;0.25; 0.50;0.70;1.00
	-	5000	CH_4	0.0;0.05;0.15;0.25; 0.50;0.70;1.00
	-	90	C_3H_4	0.05;0.15;0.25; 0.50;0.60
	-	1000	C_3H_4	0.05;0.15;0.25; 0.50;0.60
	-	5000	C_3H_4	0.05;0.15;0.25 0.50;0.60
3	125	-	-	-
4	50	-	-	-
	125	-	-	-
	525	-	-	-

Table C1(Cont.)

Flame Designation	$[NH_3]_0$ (ppm)	$[NO]_0$ (ppm)	Type of hydrocarbon	$[C_nH_m]_0$ (%)
4	-	1000	CH_4	0.0;0.05;0.15;0.25; 0.50;0.70;1.00
	-	5000	CH_4	0.0;0.05;0.15;0.25; 0.50;0.70;1.00
	-	90	C_3H_4	0.05;0.15;0.25; 0.50;0.60
	-	5000	C_3H_4	0.05;0.15;0.25; 0.50;0.60
5	525	-	-	-
6	50	-	-	-
	125	-	-	-
	515	-	-	-
	-	90	CH_4	0.0;0.15;0.25;0.50; 0.70;1.00
	-	1000	CH_4	0.0;0.15;0.25;0.50; 0.70;1.00
	-	5000	CH_4	0.0;0.15;0.25;0.50; 0.70;1.00
7	-	90	C_3H_4	0.05;0.15;0.25; 0.50;0.60
	-	1000	C_3H_4	0.05;0.15;0.25; 0.50;0.60
	-	5000	C_3H_4	0.05;0.15;0.25; 0.50;0.60

Table C1 (Concl.)

Flame Designation	$[NH_3]_0$ (ppm)	$[NO]_0$ (ppm)	Type of hydrocarbon	$[C_nH_m]_0$ (%)
8	90	-	-	-
9	90	-	-	-
7	-	90	C_2H_4	0.05;0.15;0.25; 0.50;0.70

with

1 - $[H_2]/[O_2]/[Ar]$ = 2.5/1/10.5

2 - $[H_2]/[O_2]/[Ar]$ = 2.5/1/9.7

3 - $[H_2]/[O_2]/[Ar]$ = 2.5/1/8.9

4 - $[H_2]/[O_2]/[Ar]$ = 3.5/1/8.2

5 - $[H_2]/[O_2]/[Ar]$ = 3.5/1/7.0

6 - $[H_2]/[O_2]/[Ar]$ = 4.0/1/7.43

7 - $[H_2]/[O_2]/[Ar]$ = 5.0/1/5.97

8 - $[H_2]/[O_2]/[Ar]$ = 3.18/1/6.49

9 - $[H_2]/[O_2]/[Ar]$ = 2.74/1/3.5

Appendix D.

A computer program was developed for calculating rates of reaction. This program is shown at the end of this appendix together with tables for different flames. The rates of reaction were determined by the first derivative of the variation of concentration with time. For this, a polynomial had to be first fitted to the experimental observations. A second order polynomial was fitted to strips of five experimental points (Hershey, 1967). The value of the polynomial of the mid-point was always taken as the new ordinate to fit another polynomial to the same "strip". Original ordinates and final calculated ones from the polynomials are also shown in the tables referred to above.

This computer program is only worthwhile using when the number of points is greater than five. However, in the study carried out in this work, some species concentrations were only measured at five or six distances from the reaction zone. In these cases, the calculation of the rates of reaction was made manually by determining the slope of the tangent to the point on the curve which gives the concentration as a function of time. The slope is equal to the rate required. This method is known as the process of the slope tangent to the point. In this case, errors are also expected to be higher. In the following, a listing of the program used and tables with rates of reaction for different flames are given, where the concentrations, measured and calculated by the polynomials, are shown.

```
      MASTER SMODIF
C     X REPRESENTS TIME IN MILLISECONDS
C     Y REPRESENTS CONVERSION TO NO
      DIMENSION X(11),Y(11),YY(11),S(4),O(3),D(11)
      READ(1,880)MM
      DO 450 L=1,MM
      READ(1,830)RFLAME,RNH3T,RADT
      READ(1,850)(X(J),YY(J),J=1,11)
      D0 3 K=1,11
3     Y(K)+YY(K)
      DO 400 NI=1,6
      WRITE(2,500)
      DO 290 J=1,7
100   DO 5 K=1,4
5     S(K)=0.0
      DO 8 M=1,3
8     O(M)=0.0
      DO 180 I=J,J+4
150   S(1)=S(1)+X(I)
      S(2)=S(2)+X(I)**2
      S(3)=S(3)+X(I)**3
      S(4)=S(4)+X(I)**4
      O(1)=O(1)+Y(I)
      O(2)=O(2)+X(I)*Y(I)
      O(3)=O(3)+(X(I)**2)*Y(I)
180   CONTINUE
200   A1=(S(2)*S(4))-(S(3)**2)
      A2=(S(2)*S(3))-(S(1)*S(4))
      A3=(S(1)*S(3))-(S(2)**2)
      A4=(5.0*S(4))-(S(2)**2)
      A5=(S(1)*S(2))-(5.0*S(3))
      A6=5.0*S(2)-(S(1)**2)
      A=(O(1)*A1+O(2)*A2+O(3)*A3)/(5.0*A1+S(1)*A2+S(2)*A3)
      B=(O(1)*A2+O(2)*A4+O(3)*A5)/(5.0*A1+S(1)*A2+S(2)*A3)
      C=(O(1)*A3+O(2)*A5+O(3)*A6)/(5.0*A1+S(1)*A2+S(2)*A3)
      K=J+2
      RMIDOR=A+B*X(K)+C*X(K)*X(K)
      IF(K.EQ.3)GO TO 210
      GO TO 250
210   D(1)=2.0*C*X(1)+B
      D(2)=2.0*C*X(2)+B
      WRITE(2,700)RFLAME,RADT,RNH3T,X(1),YY(1),D(1),X(2),YY(2),D(2)
250   D(K)=2.0*C*X(K)+B
      WRITE(2,820)X(K),YY(K),RMIDOR,D(K)
      Y(K)=RMIDOR
      IF(K.EQ.9)GO TO 260
      GO TO 270
260   D(10)=2.0*C*X(10)+B
      D(11)=2.0*C*X(11)+B
      WRITE(2,825)X(10),YY(10),D(10),X(11),YY(11),D(11)
270   CONTINUE
290   CONTINUE
400   CONTINUE
450   CONTINUE
500   FORMAT(//,//,//,5X,'[H2]/[O2]',6X,'[AR]/[O2]',6X,'[NH3]T',6X,'TIME
     1',11X,'[NO]/[NH3]T',11X,'(D[NO]/DT)/[NH3]T',/,35X,'(PPM)',6X,'(MSE
     2C)',6X,'MEASURED',3X,'CALCULATED',9X,'(MSEC-1)')
700   FORMAT(//,8X,F3.1,11X,F4.2,10X,F5.1,7X,F5.3,8X,F5.3,5X,'-',18X,F7
     14,//,9X,',,',13X,',,',12X,',,',8X,F5.3,8X,F5.3,5X,'-',18X,F7.4)
820   FORMAT(/,9X,',,',13X,',,',12X,',,',8X,F5.3,8X,F5.3,5X,F5.3,14X,F7.
     14)
825   FORMAT(/,9X,',,',13X,',,',12X,',,',8X,F5.3,8X,F5.3,5X,'-',18X,F7.4
     1,//,9X,',,',13X,',,',12X,',,',8X,F5.3,8X,F5.3,5X,'-',18X,F7.4)
830   FORMAT(3F0.0)
850   FORMAT(11(2F0.0))
880   FORMAT(I1)
900   STOP
```

Table D1

Rates of Reaction in Flame 1.

$[H_2]/[O_2]$	$[Ar]/[O_2]$	$[NH_3]_t$ (ppm)	Time (mS)	$[NO]/[NH_3]_t$ Measured	$[NO]/[NH_3]_t$ Calculated	$(d[NO]/dt)/[NH_3]_t$ (ms^{-1})
2.5	10.50	135.0	0.000	0.389	-	0.0589
			0.132	0.399	-	0.0528
			0.263	0.404	0.404	0.0458
			0.526	0.413	0.413	0.0320
			0.789	0.421	0.421	0.0259
			1.053	0.427	0.427	0.0214
			1.316	0.431	0.431	0.0173
			1.974	0.441	0.440	0.0132
			2.632	0.447	0.448	0.0121
			3.287	0.456	-	0.0117
			3.947	0.463	-	0.0114

Table D2

Rates of Reaction in Flame 2.

$[H_2]/[O_2]$	$[Ar]/[O_2]$	$[NH_3]_t$ (ppm)	Time (mS)	$[NO]/[NH_3]_t$ Measured	$[NO]/[NH_3]_t$ Calculated	$(d[NO]/dt)/[NH_3]_t$ (ms^{-1})
2.5	9.70	54.4	0.000	0.394	-	0.1399
			0.132	0.413	-	0.1219
			0.263	0.431	0.427	0.1041
			0.526	0.450	0.448	0.0696
			0.789	0.463	0.463	0.0463
			1.053	0.472	0.471	0.0318
			1.316	0.481	0.476	0.0211
			1.974	0.489	0.487	0.0161
			2.632	0.496	0.496	0.0161
			3.287	0.506	-	0.0171
			3.947	0.519	-	0.0181

Table D2 (Cont.)

$[H_2]/O_2]$	$[Ar]/[O_2]$	$[NH_3]_t$ (ppm)	Time (mS)	$[NO]/[NH_3]_t$ Measured	$[NO]/[NH_3]_t$ Calculated	$(d[NO]/dt)/[NH_3]_t$ (ms^{-1})
2.5	9.70	135.0	0.000	0.395	-	0.0604
			0.132	0.404	-	0.0529
			0.263	0.413	0.410	0.0455
			0.526	0.419	0.419	0.0313
			0.789	0.426	0.426	0.0243
			1.053	0.431	0.431	0.0197
			1.316	0.437	0.435	0.0163
			1.974	0.444	0.445	0.0123
			2.632	0.452	0.451	0.0089
			3.287	0.456	-	0.0058
			3.947	0.459	-	0.0026

Table D2 (Cont.)

$[H_2]/[O_2]$	$[Ar]/[O_2]$	$[NH_3]_t$ (ppm)	Time (mS)	$[NO]/[NH_3]_t$ Measured	$[NO]/[NH_3]_t$ Calculated	$(d[NO]/dt)[NH_3]_t$ (ms^{-1})
2.5	9.70	665.0	0.000	0.305	-	0.0419
			0.132	0.308	-	0.0423
			0.263	0.316	0.315	0.0427
			0.526	0.327	0.326	0.0470
			0.789	0.338	0.339	0.0433
			1.053	0.353	0.352	0.0370
			1.316	0.359	0.357	0.0259
			1.974	0.368	0.368	0.0149
			2.632	0.376	0.376	0.0125
			3.287	0.383	-	0.0112
			3.947	0.391	-	0.0099

Table D3

Rates of Reaction in Flame 3.

$[H_2]/[O_2]$	$[Ar]/[O_2]$	$[NH_3]_t$ (ppm)	Time (mS)	$[NO]/[NH_3]_t$		$(d[NO]/dt)/[NH_3]_t$ (ms^{-1})
				Measured	Calculated	
2.5	8.90	135.0	0.000	0.411	-	0.0608
			0.132	0.419	-	0.0493
			0.263	0.426	0.425	0.0379
			0.526	0.430	0.429	0.0210
			0.789	0.433	0.433	0.0199
			1.053	0.439	0.440	0.0186
			1.316	0.446	0.444	0.0169
			1.974	0.452	0.452	0.0116
			2.632	0.459	0.459	0.0097
			3.287	0.465	-	0.0084
			3.947	0.470	-	0.0070

Table D4

Rates of Reaction in Flame 4.

$[H_2]/[O_2]$	$[Ar]/[O_2]$	$[NH_3]_t$ (ppm)	Time (mS)	$[NO]/[NH_3]_t$ Measured	$[NO]/[NH_3]_t$ Calculated	$(d[NO]/dt)/[NH_3]_t$ (ms^{-1})
3.5	8.20	54.4	0.000	0.427	-	0.0766
			0.132	0.436	-	0.0625
			0.263	0.446	0.444	0.0484
			0.526	0.451	0.450	0.0311
			0.789	0.455	0.457	0.0291
			1.053	0.468	0.467	0.0281
			1.316	0.473	0.473	0.0240
			1.974	0.484	0.482	0.0138
			2.632	0.488	0.489	0.0129
			3.287	0.497	-	0.0143
			3.947	0.508	-	0.0157

Table D4 (Cont.)

$[H_2]/[O_2]$	$[Ar]/[O_2]$	$[NH_3]_t$ (ppm)	Time (mS)	$[NO]/[NH_3]_t$ Measured	$[NO]/[NH_3]_t$ Calculated	$(d[NO]/dt)/[NH_3]_t$ (ms^{-1})
3.5	8.20	135.0	0.000	0.373	-	0.0684
			0.132	0.382	-	0.0600
			0.263	0.392	0.389	0.0516
			0.526	0.400	0.400	0.0358
			0.789	0.408	0.407	0.0254
			1.053	0.413	0.412	0.0192
			1.316	0.416	0.416	0.0151
			1.974	0.426	0.425	0.0125
			2.632	0.432	0.432	0.0113
			3.287	0.439	-	0.0104
			3.947	0.446	-	0.0095

Table D4 (Cont.)

$[H_2]/[O_2]$	$[Ar]/[O_2]$	$[NH_3]_t$ (ppm)	Time (mS)	$[NO]/[NH_3]_t$ Measured	$[NO]/[NH_3]_t$ Calculated	$(d[NO]/dt)/[NH_3]_t$ (ms^{-1})
3.5	8.20	570.0	0.000	0.314	-	0.1044
			0.132	0.332	-	0.0070
			0.263	0.342	0.339	0.0696
			0.526	0.351	0.350	0.0380
			0.789	0.358	0.359	0.0288
			1.053	0.364	0.365	0.0227
			1.316	0.373	0.369	0.0172
			1.974	0.377	0.378	0.0122
			2.632	0.386	0.386	0.0097
			3.287	0.390	-	0.0075
			3.947	0.395	-	0.0054

Table D5

Rates of Reaction in Flame 5.

$[H_2]/[O_2]$	$[Ar]/[O_2]$	$[NH_3]_t$ (ppm)	Time (mS)	$[NO]/[NH_3]_t$ Measured	$[NO]/[NH_3]_t$ Calculated	$(d[NO]/dt)/[NH_3]_t$ (ms^{-1})
3.5	7.00	570.0	0.000	0.333	-	0.0984
			0.132	0.351	-	0.0804
			0.263	0.360	0.357	0.0626
			0.526	0.364	0.365	0.0300
			0.789	0.373	0.372	0.0234
			1.053	0.377	0.378	0.0183
			1.316	0.382	0.381	0.0128
			1.974	0.386	0.384	0.0061
			2.632	0.386	0.387	0.0055
			3.287	0.393	-	0.0062
			3.947	0.395	-	0.0069

Table D6

Rates of Reaction in Flame 6.

$[H_2]/[O_2]$	$[Ar]/[O_2]$	$[NH_3]_t$ (ppm)	Time (mS)	$[NO]/[NH_3]_t$ Measured	$[NO]/[NH_3]_t$ Calculated	$(d[NO]/dt)/[NH_3]_t$ (mS^{-1})
4.0	7.43	54.4	0.000	0.447	-	0.1097
			0.132	0.465	-	0.0949
			0.263	0.478	0.474	0.0802
			0.526	0.487	0.489	0.0505
			0.789	0.502	0.501	0.0342
			1.053	0.509	0.506	0.0224
			1.316	0.515	0.509	0.0120
			1.974	0.515	0.514	0.0089
			2.632	0.520	0.520	0.0122
			3.287	0.528	-	0.0167
			3.947	0.542	-	0.0212

Table D6 (Cont.)

$[H_2]/[O_2]$	$[Ar]/[O_2]$	$[NH_3]_t$ (ppm)	Time (mS)	$[NO]/[NH_3]_t$ Measured	$[NO]/[NH_3]_t$ Calculated	$(d[NO]/dt)[NH_3]_t$ ($m s^{-1}$)
4.0	7.43	135.0	0.000	0.381	-	0.0642
			0.132	0.390	-	0.0546
			0.263	0.397	0.396	0.0460
			0.526	0.404	0.404	0.0279
			0.789	0.410	0.410	0.0197
			1.053	0.414	0.414	0.0159
			1.316	0.417	0.417	0.0135
			1.974	0.426	0.426	0.0126
			2.632	0.434	0.434	0.0110
			3.287	0.441	-	0.0092
			3.947	0.446	-	0.0073

Table D6 (Cont.)

$[H_2]/[O_2]$	$[Ar]/[O_2]$	$[NH_3]_t$ (ppm)	Time (mS)	$[NO]/[NH_3]_t$ Measured	$[NO]/[NH_3]_t$ Calculated	$(d[NO]/dt)[NH_3]_t$ (ms^{-1})
4.0	7.43	540.0	0.000	0.340	-	0.1430
			0.132	0.368	-	0.1162
			0.263	0.377	0.375	0.0896
			0.526	0.386	0.357	0.0385
			0.789	0.397	0.395	0.0259
			1.053	0.401	0.399	0.0174
			1.316	0.405	0.402	0.0110
			1.974	0.408	0.408	0.0078
			2.632	0.412	0.412	0.0064
			3.287	0.416	-	0.0051
			3.947	0.419	-	0.0038

Table D7

Rates of Reaction in Flame 8.

$[H_2]/[O_2]$	$[Ar]/[O_2]$	$[NH_3]_t$ (ppm)	Time (mS)	$[NO]/[NH_3]_t$ Measured	$[NO]/[NH_3]_t$ Calculated	$(d[NO]/dt)/[NH_3]_t$ (ms^{-1})
3.2	6.49	99.5	0.000	0.354	-	0.0794
			0.132	0.366	-	0.0736
			0.263	0.377	0.375	0.0677
			0.526	0.388	0.389	0.0560
			0.789	0.405	0.404	0.0476
			1.053	0.416	0.416	0.0398
			1.316	0.424	0.424	0.0298
			1.974	0.438	0.436	0.0188
			2.632	0.445	0.447	0.0148
			3.287	0.457	-	0.0122
			3.947	0.462	-	0.0095